DETECTION FILTERS FOR FAULT-TOLERANT CONTROL OF TURBOFAN ENGINES

by

JERE SCHENCK MESEROLE, JR.

B.S.E., Princeton University (1973)
M.S., Cornell University (1975)

SUBMITTED IN PARTIAL FULFILLMENT
OF THE REQUIREMENTS FOR THE
DEGREE OF

DOCTOR OF PHILOSOPHY

at the

MASSACHUSETTS INSTITUTE OF TECHNOLOGY

June 1981

Signature of Author Signature redacted
Department of Aeronautics and Astronautics
May 1, 1981

Certified by Signature redacted
Jack L. Kerrebrock
Thesis Supervisor

Signature redacted
Wallace E. VanderVelde
Thesis Supervisor

Signature redacted
John J. Deyst
Thesis Supervisor

Accepted by Signature redacted
Harold Y. Wachman
Chairman, Departmental Graduate Committee

I hereby assign my copyright of this thesis to
The Charles Stark Draper Laboratory, Inc.
Cambridge, Massachusetts.

Signature redacted

DETECTION FILTERS FOR FAULT-TOLERANT CONTROL
OF TURBOFAN ENGINES

by

Jere Schenck Meserole, Jr.

Submitted to the Department of Aeronautics & Astronautics
on May 1, 1981 in partial fulfillment of the
requirements for the Degree of Doctor of Philosophy

ABSTRACT

Application of modern electronic control technology to aircraft turbine engines requires new methods of designing highly reliable control systems for stressful environments. A way to reduce the number of redundant components needed is to implement within the microcomputer controllers advanced analytical techniques for detecting, identifying, and accommodating failures. One promising analytical technique is the failure detection filter. The results reported in this dissertation demonstrate that detection filter theory, a linear theory introduced about 10 years ago, can be easily adapted for application to advanced-technology turbofan engines. A suitably simple approach to modeling the nonlinear dynamics of such engines was devised for use in the design of a detection filter for the F100 military engine. This filter was tested on a nonlinear dynamic simulation of that engine, and it proved able to produce readily detectable and identifiable failure signatures for fifteen different sensors, actuators, and internal engine components. The malfunctions that were simulated were biases and scale factor changes; the magnitudes of these malfunctions ranged from 2 to 20 percent of the normal operating ranges of the components that were failed. The testing encompassed various power levels from idle to intermediate, both steady and transient, at sea-level-static inlet conditions. The results demonstrate that the detection filter is a viable technique that can be useful in the development of a fault-tolerant engine controller.

Thesis Supervisor: Dr. Jack L. Kerrebrock
Title: Professor of Aeronautics and Astronautics

Thesis Supervisor: Dr. Wallace E. Vander Velde
Title: Professor of Aeronautics and Astronautics

Thesis Supervisor: Dr. John J. Deyst
Title: Lecturer, Aeronautics and Astronautics

ACKNOWLEDGMENTS

I wish to extend my heartfelt thanks to Professors Jack Kerrebrock and Wallace Vander Velde for the invaluable assistance and guidance they so freely gave me throughout this project. John Deyst and Basil Smith and their staffs at the C. S. Draper Laboratory also provided support and practical suggestions without which this thesis would not have been possible. I also thank the staff of the MIT Gas Turbine Laboratory for teaching me about turbine engines. This research was supported by the Pratt and Whitney Company and the Draper Laboratory under contract F33615-79-C-2082 from the Aeropropulsion Laboratory of the U.S. Air Force.

Publication of this thesis does not constitute approval by the Draper Laboratory, the MIT Gas Turbine Laboratory, the U.S. Air Force, or Pratt and Whitney Aircraft of the findings or conclusions contained herein. It is published for the exchange and stimulation of ideas.

TABLE OF CONTENTS

LIST OF FIGURES

LIST OF TABLES

LIST OF SYMBOLS

A	System dynamics matrix
B	Matrix of input gains
C	Matrix of measurement gains
CSV	Compressor stator vane angle
D	Matrix of filter feedback gains
F	Matrix of event vectors
FIGV	Fan inlet guide vane angle
FS	Scalar failure signal
G	Matrix of basis vectors of the event spaces
I	Identity matrix
K	Scalar gain (subscripted)
K	Matrix used in determining an event space
M	Matrix used in determining an event space
N	Parameter used in failure identification
N_1	Fan speed
N_2	Compressor speed
P	Pressure
P_b	Total pressure in primary burner
P_{t2}	Total pressure at the face of the fan
P_{t6}	Total pressure in the afterburner
Q	Partition of an augmented system matrix
R	Matrix of basis vectors not contained in G
T	Temperature; or transformation matrix
T_{t2}	Total temperature at the face of the fan
T_{t25}	Fan outlet total temperature
T_{t45}	FTIT, fan turbine inlet total temperature
W	A partition of a transformation matrix T or of an augmented system matrix A'
W_f	Fuel flow rate
a_{ij}	An element of A
$\underline{b}_i$	A column of B
$\underline{d}_j$	A column of D
$\underline{e}_i$	A unit basis vector
$\underline{f}$, $\underline{h}$	Event vectors

(Continued)

$\underline{g}$	Event generator
i, j	Subscript variables
k	Subscript variable indicating the time of a measurement sample.
k(t)	Time-varying scalar
ℓ	Dimension of input vector; or a subscript variable.
m	Dimension of measurement vector
n	Dimension of state vector; order of a matrix
n(t), n_k	Arbitrary time-varying scalar
$\underline{q}$	State difference vector
$\underline{r}$	Residual vector
t	Time; or a subscript variable
$\underline{u}$	Input vector
$\underline{v}$	A unit vector specifying a failure direction
$\underline{x}$, $\underline{y}$	State and measurement vectors
$\underline{\hat{x}}$, $\underline{\hat{y}}$	State and measurement vectors of the filter
$\mathcal{f}$, $\mathcal{h}$	Event space
$\mathscr{F}$	Group event space
$\mathscr{R}$	Subspace of $\mathscr{F}$ not contained in the union of $\mathcal{f}$'s
Φ	State transition matrix
Γ	Input transfer matrix
Λ	A diagonal matrix of eigenvalues
$\Psi(s)$	Characteristic polynomial
Π, Θ	Matrices related to G and R
ϕ	Null space
α, β	Scalar parameters
$\underline{\gamma}_i$	A column of Γ
κ, ρ	Scale factors
λ	Eigenvalue
ν	Event order
μ	Superscript variable
σ	Angle
τ	Time constant; or dummy variable of integration.

Chapter I

INTRODUCTION

Aircraft turbofan engines now under development will be built with electronic controllers that will increase engine performance and efficiency, but the use of sophisticated control laws will make these engines vulnerable to failures of the many sensors, actuators, and electronic components in the control system. Because of this vulnerability, the controllers are being designed as best as possible to be fault tolerant--that is, to be able to sustain one or several component malfunctions without loss of capacity to perform essential functions. A complex system such as a turbine engine is made fault tolerant by installing duplicates of critical components, by providing back-up modes of operation for use when nonredundant components fail, and by incorporating in the system various means for automatically detecting and identifying malfunctions so that appropriate compensation can be selected. This thesis concerns adaptation of the detection filter, an analytical method of detecting and identifying failures, for use with microcomputer controllers on advanced-technology turbofan engines.

1.1 EVOLUTION OF FAULT-TOLERANT ELECTRONIC ENGINE CONTROLS

Analytical work on new control laws for use with microcomputer engine controllers began in earnest in the early 1970's (e.g. [5], [6], [34], and [51]). In 1975, at the culmination of the Integrated Propulsion Control System (IPCS) Program [10] [27], an electronic inlet/engine controller was flight-tested in an F-111E aircraft [11]. At about the same time, several investigators tested early approaches to fault-tolerant

control [18] [23] [49]. They used simple steady-state engine models for diagnosis of sensor failures and for estimation of replacement values for failed measurements; because of the simplicity of the models, only failures with large magnitude could be properly identified.

In the mid-1970's, the Navy initiated the Full-Authority Digital Electronic Control (FADEC) Program. This involved separate projects at General Electric [2] and at Pratt and Whitney Aircraft [3] to develop a flight-worthy, engine-mounted controller capable of regulating the numerous actuators on an envisioned variable cycle engine. (Such an engine might have as many as fifteen control inputs.) The Pratt and Whitney FADEC incorporated numerical maps of the steady-state operating points of the engine for identification of sensor failures and for subsequent measurement synthesis. This controller was successfully operated on a prototype F401 engine in an altitude chamber at NASA's Lewis Research Center in 1979. The General Electric FADEC is the first controller to include a dynamic model of the engine for use in failure detection and identification [42]. Both FADEC controllers also have some provision for accommodation of actuator faults.

Concurrent with the FADEC program, an effort was underway to apply multivariable (state-space) control theory to the design of a new control law for the Pratt and Whitney F100 turbofan. Part of this effort was the work by Hackney, Miller, and Small [21] and by Adams, DeHoff, and Hall [1] [14] on developing simplified dynamic engine models. The resulting control law--programmed on a laboratory minicomputer--was tested on a hybrid simulation of the F100 engine [45] and then was used by Lehtinen, DeHoff, and Hackney [29] to run an F100 in an altitude chamber. Rock and DeHoff [37] are continuing the analytical work on engine models and on control system synthesis.

A symposium on propulsion controls was held at the Lewis Research Center in May, 1979 [33]. The symposium highlighted the requirements for reliable engine systems, particularly for fault-tolerant capabilities throughout the control system--in the microcomputers, the actua-

tors, and the sensors. The need for accurate, yet simple, dynamic engine models was emphasized.

Recently, Behbehani [9] completed an investigation of identifying sensor failures by an analytical procedure known as the generalized likelihood ratio (GLR) technique. He tested the method on sensor failures induced in a simulation of the NASA Quiet, Clean, Short-Haul, Efficient Engine (QCSHEE).

Two government-financed programs on control system reliablity are currently in progress. The Sensor Failure Detection System Program, contracted by NASA to Pratt and Whitney and to Systems Control, Inc., involves investigation of several advanced detection and identification techniques, including GLR, banks of Kalman filters, and failure-sensitive filters. The best ones will be tested on a simulation of the F100 [28]. The Full-Authority, Fault-Tolerant Electronic Engine Control (FAFTEEC) Program, contracted to Pratt and Whitney's Government Products Division and to Draper Laboratory, Inc., by the Air Force Aero-Propulsion Lab, is aimed more generally at the design of reliable microprocessor controllers. The reliablity required for each component and the number of redundant components needed are being investigated [31]. The research presented in this thesis is part of the FAFTEEC program and complements the work in the Sensor Failure Detection Program.[1]

1.2 THE DETECTION FILTER

The simplest method of failure detection is comparison of the performance of two similar components; a discrepancy signals a failure. Identification of which of the two has failed is made by comparing each to a third component. This voting procedure is simple, but the redundant components may be costly, heavy, or bulky. The advent of microcomputers makes feasible other methods of failure detection and identification [52], many that substitute computer calculation of the expected behavior of the components in a system for one or more levels of redundancy.

[1] Detection filters are not being investigated in that program.

Among them is the failure detection filter, a technique for simultaneously monitoring many diverse components, including sensors, actuators, and dynamic elements of the system.

The detection filter incorporates a linear, dynamic model of the system and compares the system's performance to the model's predictions. Figure 1.1 is a block diagram of this arrangement. The model receives the same control inputs as the system; thus the outputs of the model normally match those of the system. But when a component fails, whether it be a sensor, an actuator, or a dynamic component, the match breaks down, signaling a failure.

Reference models are commonly used in failure detection; what distinguishes the detection filter from other techniques is its manner of identifying which component has failed. The filter residuals, which are the differences between the model's predictions and the system's measurements, are fed back to the model's input in a manner that forces the model to respond to particular mismatches in such a way that just one residual or a specific combination of residuals appears. The particular residual or combination of residuals corresponds to the component that has failed. In other words, the residuals are filtered back through the model in a such way that when one of the components monitored by the detection filter fails, the vector that the residuals form in the residual space--the vector space comprising all possible residuals--is fixed in direction. This is illustrated in Figure 1.2. The direction of the residual vector corresponds to the failed component, although sometimes not uniquely. In most circumstances the direction is independent of the manner of failure; thus, when designing a detection filter, one is not required to hypothesize numerous failure modes. This and the unidirectional characteristic of the residual vector constitute important advantages of the detection filter technique.

The structure of the detection filter is similar to that of the Kalman filter and other linear filters and observers. The feedback gain

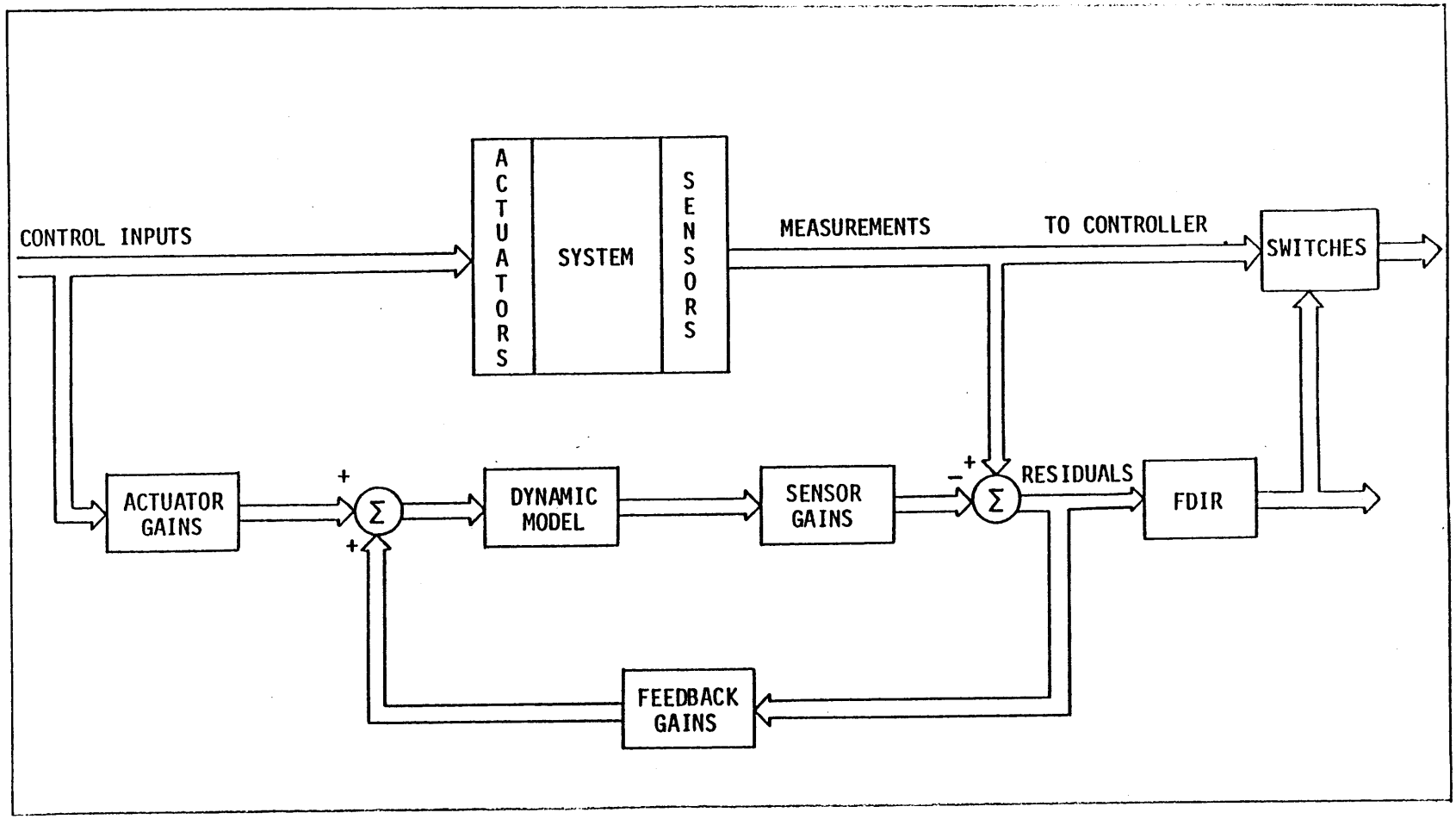

Figure 1.1. Structure of a detection filter.

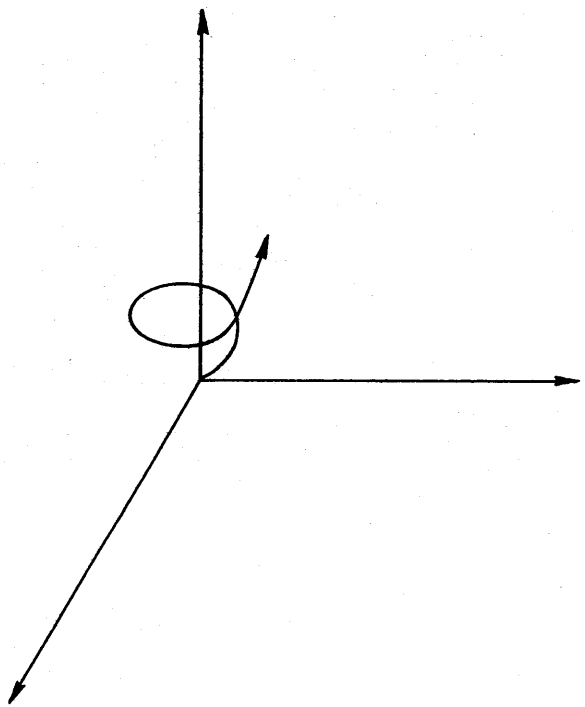

UNCONSTRAINED RESIDUALS
FROM A CONVENTIONAL LINEAR FILTER

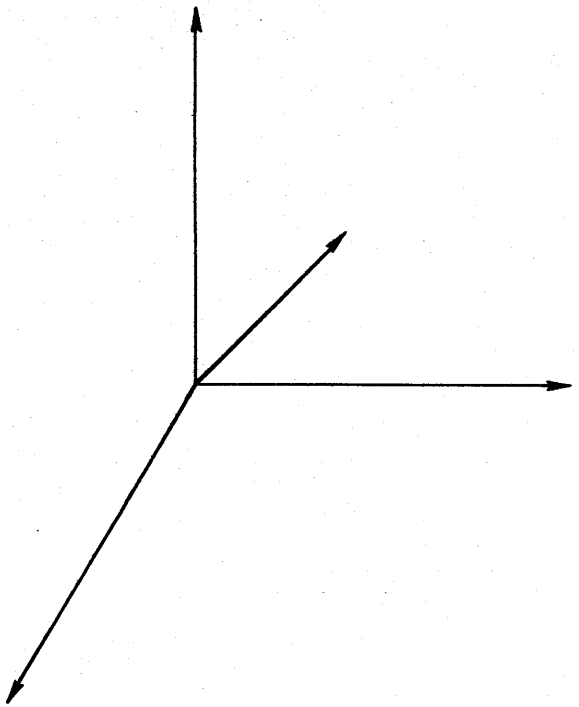

CONSTRAINED RESIDUALS
FROM A DETECTION FILTER

Figure 1.2. Residuals from an arbitrary linear filter and a detection filter.

matrices are markedly different, however. For example, the Kalman filter uses the modeled relationships among the system components to relate noisy measurements to one another in order to optimize its estimate of the state of the system; the detection filter uses the modeled relationships to decouple the predictions of the measurements from each other so that when a failure causes a residual, that residual does not propagate through the filter. The Kalman filter will also produce a residual when a component malfunctions, but this residual usually will not be fixed in direction. Furthermore, as optimal state estimators, Kalman filters suppress all residuals, regardless of their cause. Detection filters, on the other hand, are not designed to attenuate residuals much, and they highlight residuals produced by failures by holding these residuals fixed in direction.

A detection filter can also be used as a state estimator, but the requirements for failure detection prevent it from being made an optimal one. On the whole, though, this combination of functions yields a useful property: following a failure, those estimates not involved in the unidirectional failure signature remain accurate. Furthermore, if appropriate compensation is made following failure identification, the detection filter resumes normal operation. For example, disconnecting a failed sensor will eliminate the failure signature; then the filter's estimate of what the lost measurement ought to be can be substituted for that measurement.

The concept of the detection filter was devised by Beard [4]; his work presents the theory covering linear, deterministic, time-invariant, continuous systems. Jones [23] reformulated the theory in vector space notation (Beard used matrix algebra) and extended the development to both sampled-data and stochastic systems. He showed that the theory developed by Beard is not, except in special circumstances, strictly valid for sampled-data systems, but that when the sampling rate is sufficiently rapid, satisfactory detection filters can be constructed using that theory. Vander Velde [47] and Gerard [19] have applied the deterministic theory to designing a detection filter for a computer-controlled guideway vehicle. They presented

a design procedure condensed from Beard's and Jones's theses and, as well, a computer program that implements it.

1.3 OUTLINE OF THIS STUDY

Chapter 2 presents the salient aspects of detection filter theory and a comprehensive method for designing the filters. Some of the material is similar to the discussion by Vander Velde and Gerard; much of it has been condensed directly from Jones's work and reorganized for application. Several procedural aids derived from experience with the F100 problem have been added, and a few comments on what parts of the theory appear to be most useful in practice have been included. In Chapter 3 the design steps are applied to an example that is an analogy to a gas turbine engine. A more readily implemented approach to detection filter design is presented in Chapter 4. This approach results from the finding that designing a filter for the F100 does not require the generality of the full design procedure. It also appears that the F100 problem may be typical of many applications, so the less complex procedure described here may be adaptable to a variety of systems.

For whatever applications it applies to, including the F100, the simpler procedure is complete and does not require reference to any part of the detailed procedure and theory in Section 2.4 or to the demonstration of it in Chapter 3.

In addition to the simpler design method, Chapter 4 also describes the technique needed to implement detection filters in digital computers, and further, a procedure for analyzing the filter residuals and identifying failures. Chapters 5 and 6 describe the design of a filter for the F100 and the testing of it on an F100 nonlinear dynamic simulation provided by Pratt and Whitney Aircraft. First a low-order linear model is obtained for sea-level-static conditions and maximum power without afterburning. A filter is designed that monitors the six engine sensors, the inlet sensors, the actuator position sensors, the fuel system, and the high-pressure rotor. It is then tested on simulated failures at the full-power point and during transients from that point. In

Chapter 6 the linear model is refined, models for other power points are derived, and they are linked together to extend the range of validity of the filter. Results of tests on failures induced during large transients are presented. Chapter 7 summarizes this investigation and draws conclusions from the results obtained.

Chapter II

DETECTION FILTER THEORY

Detection filter theory is cast in the mathematics of matrices and vector spaces--the tools of state-variable control theory. This chapter presents the theoretical basis of detection filters and the procedure used to design them. The development begins with the formulation of reference models; then there follows a brief example that illustrates the concept on which the operation of detection filters is based. The development continues with descriptions of the various failure models encompassed by the theory, and concludes with a comprehensive method for designing the filters.

2.1 The Structure of Detection Filters

Any system to be monitored by a detection filter must be representable by a linear, time-invariant model with observable dynamics. For now, we shall consider only systems with continuous measurements and inputs.

We represent the system by these linear equations:

$$\begin{aligned} \dot{\underline{x}}(t) &= A\underline{x}(t) + B\underline{u}(t) \\ \underline{y}(t) &= C\underline{x}(t) \end{aligned} \qquad (2\text{-}1)$$

The vector $\underline{x}$ comprises the state variables; $\underline{u}$ is the vector of control inputs; and $\underline{y}$ is the vector of measurements. The dimension of $\underline{x}$ is n, of $\underline{u}$ is 1, and of $\underline{y}$ is m. The triplet of invariant matrices {A,B,C} characterizes the system. This representation is incorporated as a

reference model within the detection filter in the manner shown in Figure 2.1. The state equations of the detection filter are

$$\begin{aligned} \dot{\hat{\underline{x}}}(t) &= A\hat{\underline{x}}(t) + B\underline{u}(t) + D[\underline{y}(t)-\hat{\underline{y}}(t)] \\ \hat{\underline{y}}(t) &= C\hat{\underline{x}}(t) \end{aligned} \tag{2-2}$$

with $\hat{\underline{x}}$ as the state of the reference model, and $\hat{\underline{y}}$ the predicted measurement vector.

The residual vector is the vector composed of the differences between the measurements and the model's predictions of the measurements:

$$\underline{r}(t) = \underline{y}(t) - \hat{\underline{y}}(t) \tag{2-3}$$

The elements of $\underline{r}$ are the observed quantities used for failure detection and identification. We define another vector, $\underline{q}$, to represent the model's prediction of the state:

$$\underline{q}(t) = \underline{x}(t) - \hat{\underline{x}}(t) \tag{2-4}$$

Using Equations (2-1) through (2-4), we can determine the behavior of the residual $\underline{r}$. Differentiating (2-4) yields

$$\dot{\underline{q}}(t) = \dot{\underline{x}}(t) - \dot{\hat{\underline{x}}}(t) \tag{2-5}$$

and substituting (2-1) and (2-2) into (2-5) gives us

$$\begin{aligned} \dot{\underline{q}} &= [A\underline{x} + B\underline{u}] - [A\hat{\underline{x}} + B\underline{u} + D(\underline{y}-\hat{\underline{y}})] \\ &= A(\underline{x}-\hat{\underline{x}}) - D(\underline{y}-\hat{\underline{y}}) \\ &= A(\underline{x}-\hat{\underline{x}}) - DC(\underline{x}-\hat{\underline{x}}) \\ &= [A-DC](\underline{x}-\hat{\underline{x}}) \end{aligned}$$

Finally,

$$\begin{aligned} \dot{\underline{q}}(t) &= [A-DC]\underline{q}(t) \\ \underline{r}(t) &= C\underline{q}(t) \end{aligned} \tag{2-6}$$

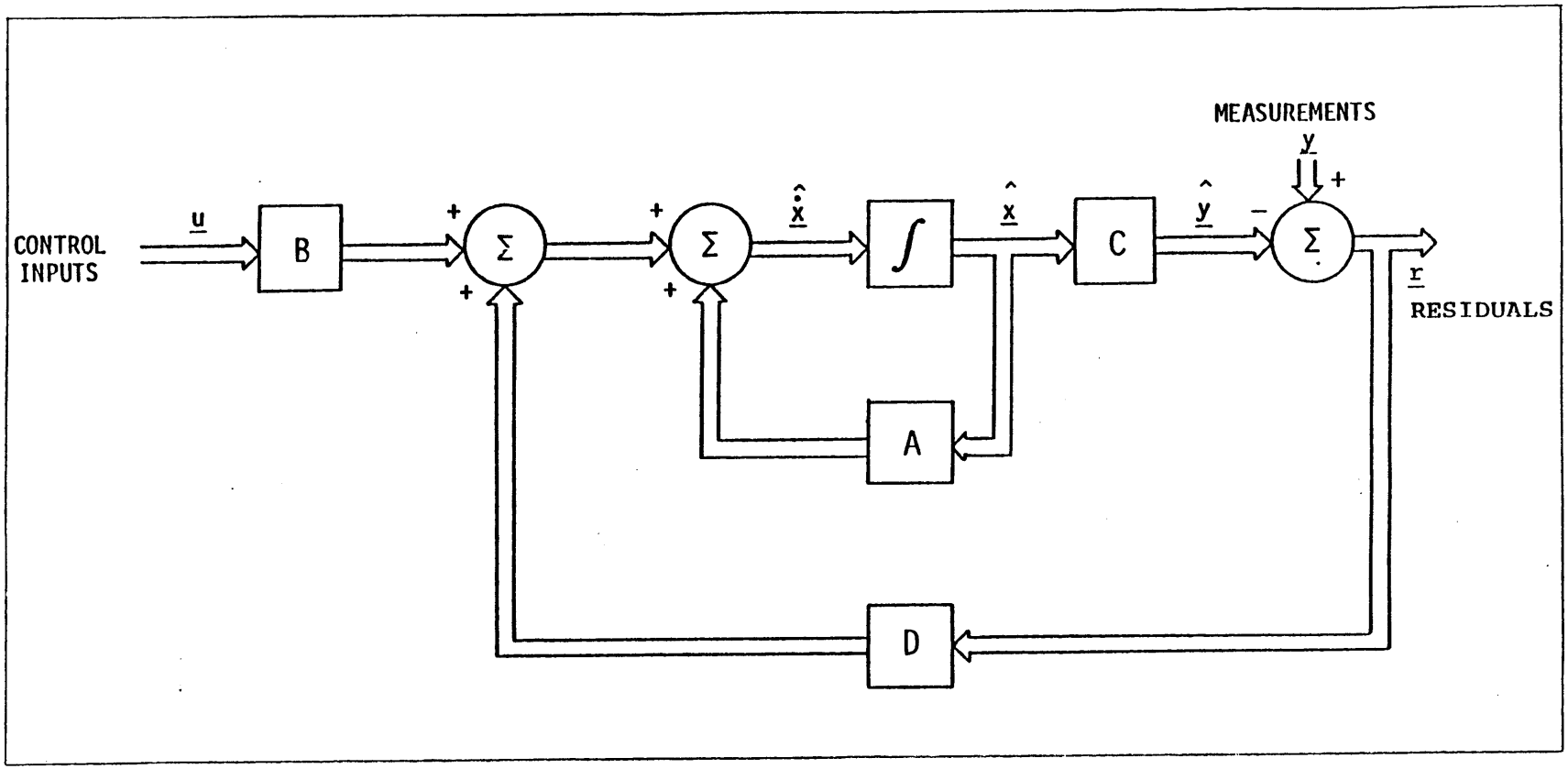

Figure 2.1. Diagram of a detection filter.

Provided that A, B, and C accurately represent the system when it is functioning normally, (2-6) is always valid in the absence of failures.

Proper choice of the feedback matrix D is the object of detection filter design. One requirement is that [A-DC] be such that any deviation $\underline{q}$ introduced by incorrect initial conditions or by spurious noise will die out, allowing $\hat{\underline{x}}(t)$ to track $\underline{x}(t)$. Another is that when any one of a number of selected components of the system fails, a residual appears that has a specific, time-invariant direction in the residual space. An optional requirement is that the residuals caused by sensor failure be confined to unique planes in the residual space. The prominent features of detection filter theory are the proofs that these requirements are compatible and that the directions of the residuals from the various components are independent of the manners in which failures occur.[1]

2.2 EXAMPLE: AN AIR-DRIVEN TURBINE

Although the way detection filters operate is mostly straightforward, their mathematical formulation is abstract. For this reason, the basic idea is presented here first through a simple example. Consider the air-driven turbine shown in Figure 2.2. This simple system consists of a constant-pressure air supply, a pressure regulator, and a small, high-speed turbine. The pressure regulator and the turbine are modeled as linear, first-order mechanisms, as indicated in the block diagram in Figure 2.3. With K_p and K_t representing the gains of the regulator and the turbine, and τ_p and τ_t their time constants, the transfer function of this second-order system is

$$\frac{N(s)}{u(s)} = \frac{K_p}{\tau_p s + 1} \cdot \frac{K_t}{\tau_t s + 1} \qquad (2\text{-}7)$$

[1] This statement does not apply generally to simultaneous failures, though in many circumstances detection filters provide adequate information for identifying the separate components involved should two or more components fail at once.

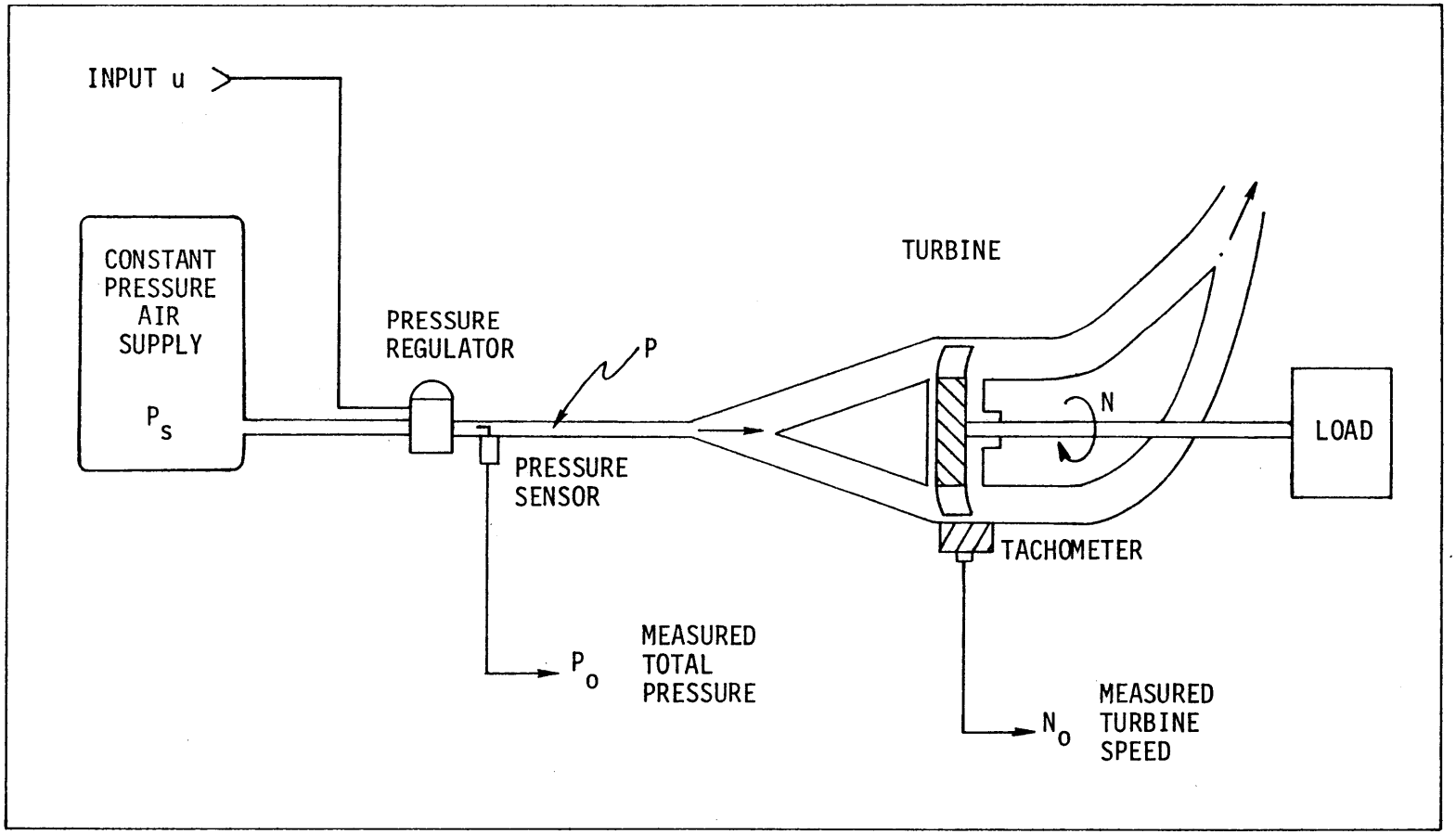

Figure 2.2. Turbine driven by compressed air.

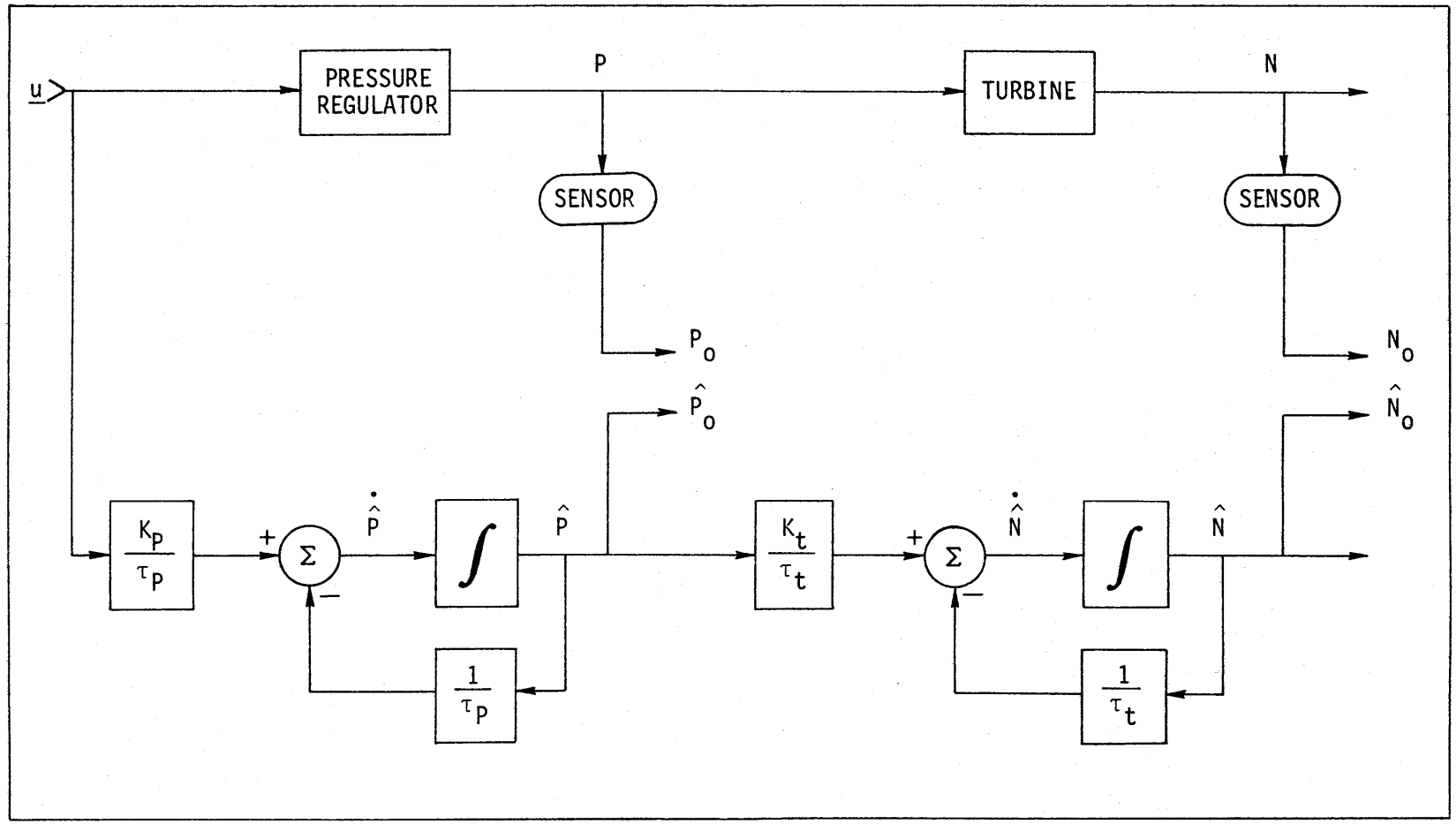

Figure 2.3. Modeling the air turbine system.

where N denotes the speed of the turbine, and u the control input to the pressure regulator. The total pressure, P, downstream of the regulator is equal to K_p times u when the system is in equilibrium.

From Figure 2.2, we see that the dynamics of P and N are described by

$$\dot{P} = 1/\tau_p \, (K_p \cdot u - P) \tag{2-8}$$

$$\dot{N} = 1/\tau_t \, (K_t \cdot P - N) \tag{2-9}$$

Defining [P,N] as the state vector, we can express (2-8) and (2-9) in a single matrix equation:

$$\begin{bmatrix} \dot{P} \\ \dot{N} \end{bmatrix} = \begin{bmatrix} -1/\tau_p & 0 \\ K_t/\tau_t & -1/\tau_t \end{bmatrix} \begin{bmatrix} P \\ N \end{bmatrix} + \begin{bmatrix} K_p/\tau_p \\ 0 \end{bmatrix} u \tag{2-10}$$

The measurement equation is

$$\begin{bmatrix} P_0 \\ N_0 \end{bmatrix} = \begin{bmatrix} 1 & 0 \\ 0 & 1 \end{bmatrix} \begin{bmatrix} P \\ N \end{bmatrix} \tag{2-11}$$

The subscript $_0$ indicates an output of a sensor; here the two sensor outputs are the measurements of P and N.

With (2-10) we now construct a linear filter of the form (2-2):

$$\begin{bmatrix} \dot{\hat{P}} \\ \dot{\hat{N}} \end{bmatrix} = \begin{bmatrix} -1/\tau_p & 0 \\ K_t/\tau_t & -1/\tau_t \end{bmatrix} \begin{bmatrix} \hat{P} \\ \hat{N} \end{bmatrix} + \begin{bmatrix} Kp/\tau_p \\ 0 \end{bmatrix} u + \begin{bmatrix} d_{11} & d_{12} \\ d_{21} & d_{22} \end{bmatrix} \begin{bmatrix} P_0 - \hat{P}_0 \\ N_0 - \hat{N}_0 \end{bmatrix} \tag{2-12}$$

As yet, the d's are unspecified. The residual vector produced by the filter is

$$\begin{bmatrix} r_p \\ r_t \end{bmatrix} = \begin{bmatrix} P_0 - \hat{P}_0 \\ N_0 - \hat{N}_0 \end{bmatrix} \tag{2-13}$$

This linear filter will be a detection filter if d_{11}, d_{12}, d_{21} are chosen such that:

1. The filter is always stable;
2. In the event of a malfunction of the pressure regulator, a discrepancy appears between $\hat{P}_0$ and P_0 but not between $\hat{N}_0$ and N_0, regardless of how the speed of the turbine may vary (we assume for the time being that the pressure transducer and the tachometer are reliable);
3. In the event of turbine malfunction--for example, a quick decrease in efficiency caused by damage to some of the turbine blades--a discrepancy between $\hat{N}_0$ and N_0 appears, but not between $\hat{P}_0$ and P_0.

We shall see that condition (1) sets a lower limit on each of d_{11} and d_{22}, and that conditions (2) and (3) prescribe fixed values for d_{12} and d_{21}.

For this example we can ascertain D by inspection. Let τ_1 and τ_2 be two constants we can specify at will. Suppose we choose D in Equation (2-12) as follows:

$$D = \begin{bmatrix} d_{11} & d_{12} \\ d_{21} & d_{22} \end{bmatrix} = \begin{bmatrix} -1/\tau_p + 1/\tau_1 & 0 \\ K_t/\tau_t & -1/\tau_t + 1/\tau_2 \end{bmatrix} \tag{2-14}$$

A block diagram of this filter is shown in Figure 2.4. After simplification, this diagram reduces to the one in Figure 2.5. From Figure 2.5 it is clear that as long as P_0 is reliable and the turbine is functioning normally, $\hat{N}_0$ will not deviate from N_0, regardless of what happens in the pressure regulator. Likewise, since neither $\hat{N}_0$ nor N_0

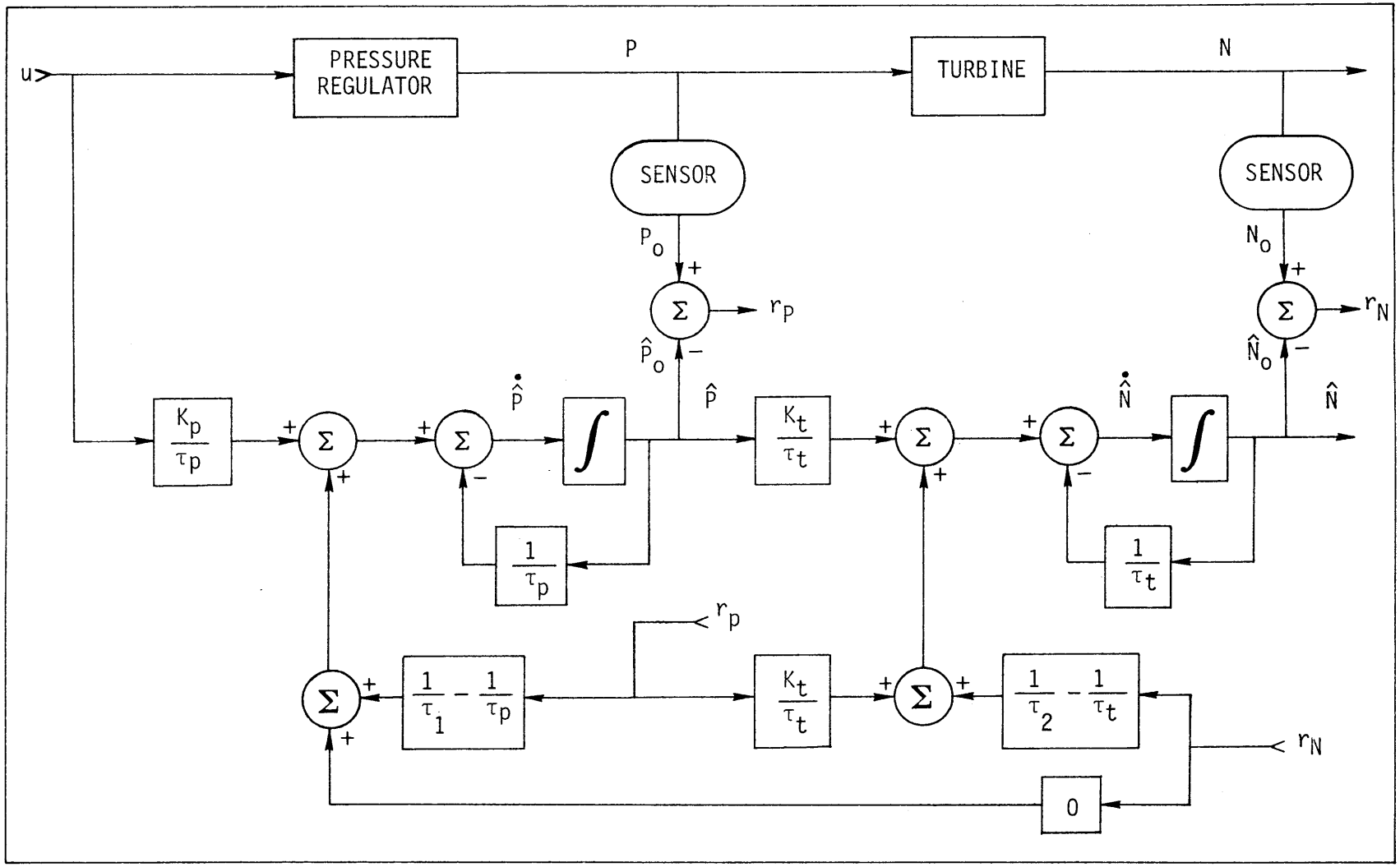

Figure 2.4. Detection filter for the air-driven turbine.

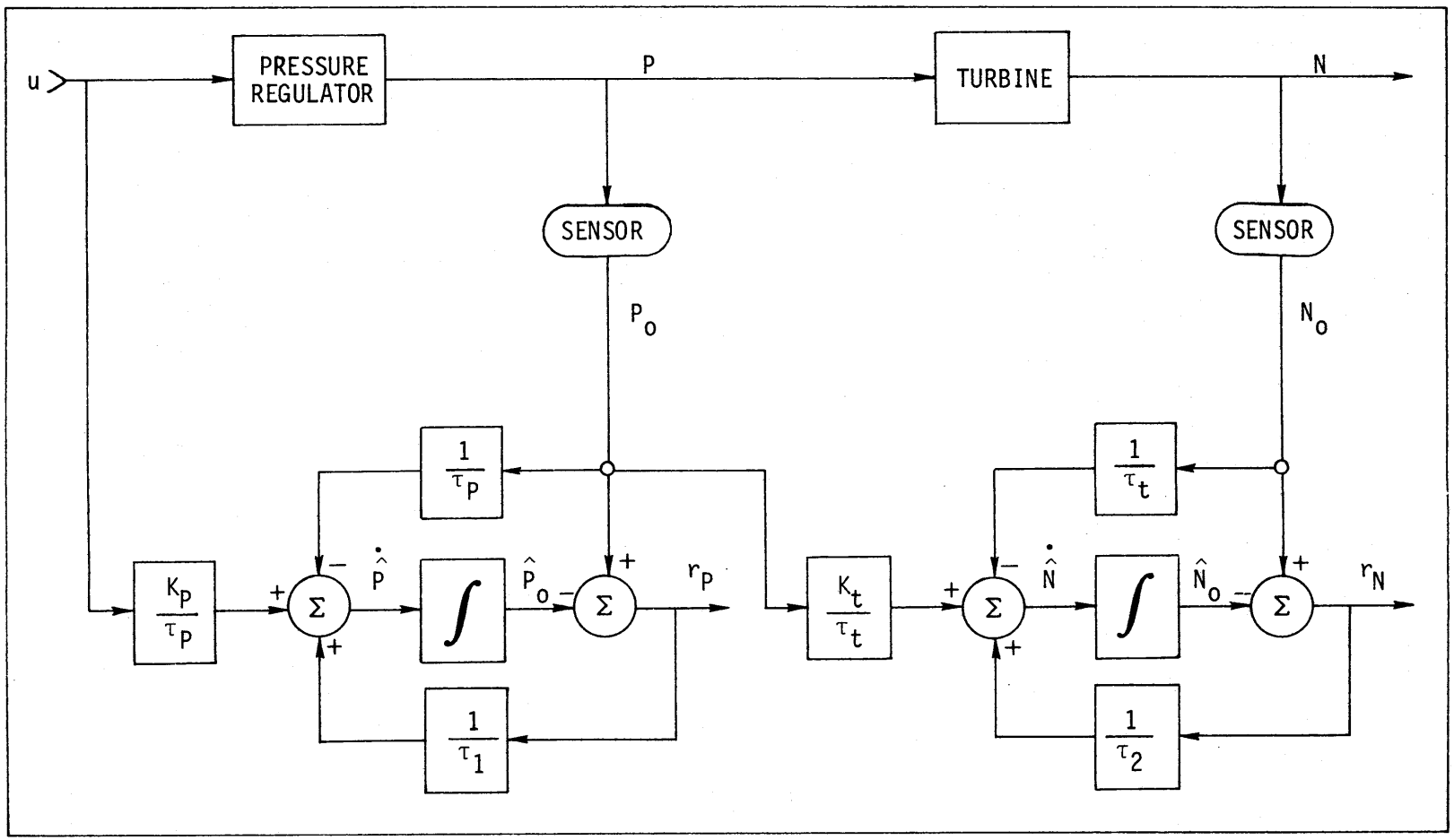

Figure 2.5. Reduced block diagram of the filter.

has any effect on $\hat{P}$, $\hat{P}_0$ will not deviate from P_0 if the turbine malfunctions.

Let us now see what effect τ_1 and τ_2 have on the stability of the filter. Substituting D from (2-14) into (2-12), we find that the behavior of the filter is described by

$$\dot{\hat{P}} = -1/\tau_p \cdot \hat{P} + K_p/\tau_p \cdot u + (-1/\tau_p + 1/\tau_1)(P_0 - \hat{P}_0)$$

$$\dot{\hat{N}} = K_t/\tau_t \cdot \hat{P} - 1/\tau_t \cdot \hat{N} + K_t/\tau_t \cdot (P_0 - \hat{P}_0) + (-1/\tau_t + 1/\tau_2)(N_0 - \hat{N}_0)$$

Since $\hat{P}_0 = \hat{P}$ and $\hat{N}_0 = \hat{N}$, these equations reduce to

$$\begin{aligned} \dot{\hat{P}} &= -1/\tau_1 \cdot \hat{P} + K_p/\tau_p \cdot u + (-1/\tau_p + 1/\tau_1)P_0 \\ \dot{\hat{N}} &= K_t/\tau_t \cdot P_0 - 1/\tau_2 \cdot \hat{N} + (-1/\tau_t + 1/\tau_2)N_0 \end{aligned} \tag{2-15}$$

The residuals r_P and r_N behave according to

$$\begin{aligned} \dot{r}_P &= (\dot{P}_0 - \dot{\hat{P}}_0) = (\dot{P} - \dot{\hat{P}}) = -1/\tau_1(P - \hat{P}) = -1/\tau_1 \cdot r_P \\ \dot{r}_N &= (\dot{N}_0 - \dot{\hat{N}}_0) = (\dot{N} - \dot{\hat{N}}) = -1/\tau_2(N - \hat{N}) = -1/\tau_2 \cdot r_N \end{aligned} \tag{2-16}$$

Thus τ_1 and τ_2 are the time constants associated with the time responses of r_P and r_N. They must, therefore, be positive for the filter to be stable. Their sizes dictate the decay rates of transient residuals and regulate the magnitudes of steady-state residuals caused by malfunctions or any other mismatches between the reference model and the system.

For this example, Equations (2-16) are the equivalent of (2-6). Indeed, $-1/\tau_1$ and $-1/\tau_2$ are the eigenvalues of [A-DC]. Furthermore, any state vector along either the P-axis or the N-axis is an eigenvector of [A-DC]. In other words, the residual r_P created by a regulator failure will not propagate through the model and make r_N nonzero, and conversely, the r_N caused by a turbine malfunction will not affect r_P.

Let us now consider what happens if the pressure transducer fails. From Figure 2.4, it is apparent that P_0 will immediately deviate from $\hat{P}_0$ and that the erroneous P_0 signal will cause $\hat{N}_0$ to deviate from N_0, thus creating a residual vector that could wander throughout the plane spanned by the P_0 and N_0 axes. In this example, this plane is the entire residual space, but even if the dimension of this example were greater, the residual caused by a transducer failure could be made to stay within a single plane. The simplest way to do this would be to assign the same value to $\tau_1, \tau_2, \cdots \tau_n$.

This example illustrates the design of a detection filter for a single-input, single-output system. A filter for a complex system like a turbofan engine cannot be designed so easily; to cope with multiple inputs and outputs and with cross-coupled state variables, we must use the analytical methods prescribed by detection filter theory.

2.3 FAILURE MODELS

In the event of a failure, {A,B,C} and Equation (2-1) no longer model the system correctly, and $\hat{\underline{y}}(t)$ will deviate from $\underline{y}(t)$. By assuming suitable models for failures of the various system components, we can determine the ensuing behaviour of the residual $\underline{r}(t)$. Three general classes of failures will be considered: actuator failures, dynamics changes, and sensor failures.

2.3.1 Actuator Failures

Actuator failures can usually be modeled by changes, sometimes time-varying, in the B matrix. The set of system matrices would then be $\{A, B+\Delta B(t), C\}$. Since each column of B gives the response of the system to the corresponding element of the input vector $\underline{u}(t)$, $\Delta B(t)$ for a failure of an input to the system can frequently be written as[2]

[2]Actuator failures involving changes in actuator dynamics can often be modeled more easily by the dynamics change model described in the next subsection.

$$\Delta B(t) = [\ 0 : \cdots : 0 : \underline{b}_i : 0 : \cdots : 0\ ]\ k(t) \qquad (2\text{-}17)$$

where $k(t)$ is a time-varying scalar and b_i is the column of B corresponding to the input u_i that is altered by the failure.

With the addition of the term from (2-17), the state equation (2-1) becomes

$$\dot{\underline{x}}(t) = A\underline{x}(t) + B\underline{u}(t) + \underline{b}_i\, k(t) \cdot u_i(t) \qquad (2\text{-}18)$$

The failure does not alter the reference model (2-2), so the difference between the state and the prediction of the state behaves according to

$$\dot{\underline{q}}(t) = A[\underline{x}(t) - \hat{\underline{x}}(t)] + \underline{b}_i k(t) \cdot u_i(t) - D[(\underline{y}(t) - \hat{\underline{y}}(t)]$$

$$\dot{\underline{q}}(t) = [A - DC]\underline{q}(t) + \underline{b}_i k(t) \cdot u_i(t) \qquad (2\text{-}19)$$

The vector $\underline{b}_i$ will be called the <u>event vector</u> associated with the i'th actuator. It will not usually be necessary to know $k(t) \cdot u_i(t)$ to identify the failed component, so let us designate this term by $n(t)$, a name which will be used repeatedly for the scalar time function that multiplies the event vector. We have, then,

$$\dot{\underline{q}}(t) = [A - DC]\underline{q}(t) + \underline{b}_i n(t)$$

$$\underline{r}(t) = C\underline{q}(t) \qquad (2\text{-}20)$$

As an example of an actuator failure, suppose the i'th actuator freezes at its zero position, producing no output at all; then $n(t)$ is $-u_i(t)$, and (2-18) becomes

$$\dot{\underline{x}}(t) = A\underline{x}(t) + B\underline{u}(t) - \underline{b}_i u_i(t)$$

The D matrix would be chosen to constrain the response of $\underline{q}(t)$ in (2-20) so that $\underline{r}(t)$ is fixed in direction.

2.3.2 Dynamics Changes

Many changes in the system's dynamics can also be modeled by a single event vector times some scalar function of time. First is a simple state-independent alteration of the derivatives of the state variables, modeled by

$$\dot{\underline{x}}(t) = A\underline{x}(t) + B\underline{u}(t) + \underline{f}n(t) \tag{2-21}$$

with $\underline{f}$ an invariant event vector that tells which elements of $\dot{\underline{x}}(t)$ are altered, and by what relative amounts.

Second, a state-independent change in only one of the state derivatives can be modeled by changes, possibly time-varying, in the corresponding row of A. The event vector is the appropriate unit vector $\underline{e}_i$, and

$$n(t) = \sum_{j=1}^{n} \Delta a_{ij}(t)x_j(t) \tag{2-22}$$

where the $\Delta a_{ij}(t)$'s are the variations in the elements of the i'th row of A. The failure model is

$$\dot{\underline{x}}(t) = A\underline{x}(t) + B\underline{u}(t) + \underline{e}_i n(t) \tag{2-23}$$

A simple example of such a malfunction is a change in the time constant of a hydraulic actuator that has essentially first-order behavior. If x_i is the state variable associated with the actuator, the only nonzero element of the i'th row of A is a_{ii}, and the failure model is

$$\dot{\underline{x}}(t) = A\underline{x}(t) + B\underline{u}(t) + \underline{e}_i \Delta a_{ii}(t)x_i(t) \tag{2-24}$$

Third, when several, or all, of the state derivatives that are driven by any one state variable, say the j'th, are altered in a fixed ratio, the malfunction can be modeled by a nonvarying change in the j'th column of A. This change can be described by the event vector

$$\underline{f} = \sum_i \underline{e}_i \Delta a_{ij} \tag{2-25}$$

The failure model becomes

$$\dot{\underline{x}}(t) = A\underline{x}(t) + B\underline{u}(t) + \underline{f}x_j(t) \tag{2-26}$$

Malfunctions describable in this manner could occur in systems in which the output of one component drives several other components--identical mechanical elements functioning in parallel, for example.

All the failure models presented thus far have the form

$$\begin{aligned} \dot{\underline{x}}(t) &= A\underline{x}(t) + B\underline{u}(t) + \underline{f}n(t) \\ \underline{y}(t) &= C\underline{x}(t) \end{aligned} \tag{2-27}$$

We shall call this the input failure model. It is so named because we shall use it most frequently for malfunctions of the input devices of a system and because the anomalies in dynamic behavior that fit the model are those that can be written as extraneous linear inputs to the system. The residuals generated by failures of the form (2-27) behave according to

$$\begin{aligned} \dot{\underline{q}}(t) &= [A-DC]\underline{q}(t) + \underline{f}n(t) \\ \underline{r}(t) &= C\underline{q}(t) \end{aligned} \tag{2-28}$$

Detection filter theory shows that for any $\underline{f}$ it is possible to find a D such that $\underline{r}(t)$ assumes a fixed direction in response to $\underline{f}n(t)$, whatever n(t) is. Furthermore, for a set of event vectors $\{\underline{f}_1, \underline{f}_2, \cdots \underline{f}_r\}$, often a D can be found such that each $\underline{f}$ is projected to a unique, fixed

residual direction. The conditions that the vectors of a set must satisfy to make this possible are important results in detection filter theory.

2.3.3 Sensor Failures

Sensor failures are modeled in one of two ways, depending on the way the sensors themselves are represented in the reference model. Accordingly, sensors are separated into two groups. The first contains sensors whose outputs are included in the state vector $\underline{x}$, explicitly or implicitly. There may not be any such sensors. The second group contains all other sensors.

The outputs of sensors in the first group have some effect on the derivative of the state vector. They may, but need not, be state variables themselves. Two relatively common circumstances in which a sensor would be modeled this way are 1) when the dynamics of the sensor are significant and must be included in the reference model, and 2) when the designer of a detection filter wishes to include failures of the feedback control system within the coverage of the detection filter. In the latter case, the feedback law--including any dynamics it may have--must be represented in the A matrix, so the measurements involved must either be state variables or be implicit in certain elements of A.

The failures of sensors in the first group we model as changes in A, just as changes in the dynamics of the systems are modeled. Therefore, these sensors fit the input failure model, and an event vector exists for each of them.

Failures of sensors in the second group must be modeled differently and, as a consequence, must be treated differently in the detection filter. Since these sensors are not modeled in the state equation, only in the measurement equation, their failures must be represented by changes in the latter. The changes are simple, though, because all possible failures of any of these sensors can be modeled by one term composed of the appropriate unit vector times a time-varying scalar. For instance, failures of the j'th sensor are modeled by

$$\begin{aligned} \dot{\underline{x}}(t) &= A\underline{x}(t) + B\underline{u}(t) \\ \underline{y}(t) &= C\underline{x}(t) + \underline{e}_j n(t) \end{aligned} \tag{2-29}$$

Here, $\underline{e}_j$ is the j'th unit vector in the residual space, and n(t) is again an arbitrary time function. Since the failure term appears in the measurement equation, we call (2-29) the measurement failure model.

In contrast to the other failures that we have described, those modeled by the measurement failure model produce a residual vector that cannot be held fixed in direction. It can, however, always be constrained to a plane that is uniquely associated with the failed sensor. The measurement vector $\underline{y}(t)$ is fed into the reference model through the term $D[y(t)-\hat{y}(t)]$, so a failure of the j'th sensor, for example, alters the model by the amount

$$\underline{d}_j n(t) = D\underline{e}_j n(t) \tag{2-30}$$

where $\underline{d}_j$ is the j'th column of D. Consequently, the equations for the residuals become

$$\begin{aligned} \dot{\underline{q}}(t) &= [A-DC]\underline{q}(t) - \underline{d}_j n(t) \\ \underline{r}(t) &= C\underline{q}(t) + \underline{e}_j n(t) \end{aligned} \tag{2-31}$$

It is possible to choose D such that the contribution to $\underline{r}(t)$ induced by $\underline{d}_j n(t)$ is unidirectional, but the direction usually will not be $\underline{e}_j$. Therefore, most of the time a detection filter can only be made to constrain the residual generated by such a sensor failure to the plane spanned by $\underline{e}_j$ and $C\underline{d}_j$. Although this behavior is not as easy to identify as a unidirectional signature, it does make the failure signature of the sensor distinctly different from that of the component that the sensor is monitoring. Sensor failures can therefore be distinguished from failures of other parts of the system. A filter can be designed, for

example, such that failures of position sensors on actuators have planar signatures and failures of the actuators themselves have unidirectional signatures.

Note that, in apparent contradiction to the statements in the above paragraph, the failure described by (2-31) would always produce a residual vector constrained to the direction $\underline{e}_j$ if $\underline{d}_j$ were set equal to zero. This means the measurement $y_j(t)$ would not be fed into the filter at all. But in the design of detection filters we are concerned not only with constraining residual vectors to identifiable regions of the residual space, either lines or planes, but also with specifying the eigenvalues of [A-DC]. Making $\underline{d}_j$ equal to zero relinquishes control of what would otherwise be an eigenvalue that could be freely set at the most useful value. Nonetheless, in some circumstances this may be a desirable option.

The next section presents the fundamentals of detection filter theory and the details of the remainder of the design procedure. Not all of this theory, however, is essential to the design of a detection filter for the F100 engine. The necessary background for that task is condensed in Chapter 4. The presentation there does not presuppose an understanding of Section 2.4 or of Chapter 3.

2.4 DETECTION FILTER DESIGN

The design procedure begins with specification of a model of the system. To provide a proper basis for much of the design process, this model must be in the form of Equation (2-1). When the system is nonlinear and a linear model of it is not sufficiently accurate throughout the needed range of operation of the filter, one can treat the system as piecewise linear and vary the model accordingly--this is the approach taken in Chapter 6 with the F100 engine. The specification of a linear model involves choosing an appropriate state vector $\underline{x}$ and determining an accurate set of system matrices {A,B,C}. Choices should be made with the intention of creating the simplest model that will accurately estimate

all of the state variables that would be affected by the anticipated failures. Also, the model must be observable.[3]

2.4.1 Sets of Event Vectors

Once the model is established, one must find the event vector for each component that is to be monitored. This is done as described above in Section 2.3, though sometimes one more step is required. If the event vector $\underline{f}$ for any component is such that

$$C\underline{f} = \underline{0}$$

then that vector must be multiplied by the matrix A repeatedly until the result is nonzero--until the smallest μ is found for which

$$CA^{\mu}\underline{f} \neq \underline{0}$$

Then $A^{\mu}\underline{f}$ becomes the $\underline{f}$ for the component in question, superseding the original.

Occasionally, several components will have the same event vector. Failures of these components will not be distinguishable on the basis of residual direction alone, for when D is chosen so the corresponding $\underline{f}$ yields a unidirectional residual, a failure of any of these components would generate a residual in the same direction. As an aid in describing this situation mathematically, we define the event space of an event

[3] A system is observable if the behavior of every part of the system affects the measured outputs of the system, either directly or indirectly. Formally, {A,B,C} is observable if and only if the rank of the matrix

$$\begin{bmatrix} C \\ CA \\ \vdots \\ CA^{n-1} \end{bmatrix}$$

equals n, the dimension of $\underline{x}$. Jones discussed the consequences of using an unobservable model.

vector $\underline{f}$ as the vector space comprising every vector whose residual would lie solely along $C\underline{f}$ when the detection filter makes the residual from $\underline{f}$ lie solely along $C\underline{f}$. We denote an event space by $\mathcal{f}$. Its dimension is termed the event order of $\underline{f}$ and is written as ν. Every event vector has an event space, even event vectors uniquely associated with single components. Such vectors have one-dimensional event spaces containing only the event vector and scalar multiples thereof. We shall determine a set of basis vectors for each event space and then use these sets to calculate the gain matrix D.

As with any type of filter or state observer, designing suitable dynamics into a detection filter is crucial to successful implementation. The dynamics of a detection filter are characterized by the poles of the filter, which are the eigenvalues of [A-DC]. Thus, to be able to give a filter the dynamics we desire, we would like sufficient freedom in the specification of D that we can alter at will every eigenvalue of [A-DC]. The number of elements of D left unspecified by the requirements for failure identification depends on the number of event vectors and on the relationships among them.

The directions of the event vectors determine, first, whether a detection filter is possible for those vectors together, and, second, whether the dynamics of the filter will be freely adjustable. There may be more event vectors than can be included in the design of a single filter. The first restriction on the vectors is that the vectors $C\underline{f}_1, C\underline{f}_2, C\underline{f}_3, \cdots$ must be linearly independent. When several vectors $\underline{f}_1, \cdots \underline{f}_r$ meet this condition, we say they are output separable. This guarantees that 1) the gain matrix D can be chosen so that each $\underline{f}_i$ will yield a residual solely along its projection $C\underline{f}_i$ in the residual space, and 2) there will be ν_i freely alterable eigenvalues of [A-DC] associated with $\underline{f}_i$ and its event space.

Any vectors that are set aside during the assembly of a set of output separable vectors can sometimes be reincluded in the design later in the procedure. With favorable conditions, this can be done merely by assigning the same value to two or more eigenvalues. When one of these

vectors is given a unidirectional residual, we say it is output stationary with $\underline{f}_1, \cdots \underline{f}_r$; when several vectors are given unidirectional residuals, in unique directions, we call them mutually output stationary with $\underline{f}_1, \cdots \underline{f}_r$.

A minor constraint on eigenvalue assignment is that whenever a complex eigenvalue is associated with a particular event space, its complex conjugate must be also. With this constraint understood, we shall say the eigenvalues of [A-DC] are assignable when the set of event vectors selected allows free choice of each of these eigenvalues. (We shall not consider any equality constraints introduced by the option of output stationarity as making the eigenvalues involved "unassignable.")

When might some eigenvalues not be assignable? If the number s of output separable vectors equals the rank of C--the number of independent sensors--then the number of unassignable eigenvalues equals the difference between the dimension of the model and the sum of the event orders. When there is no difference, the eigenvalues are all assignable. If s is less than the rank of C, then determining if any eigenvalues are unassignable is not always so straightforward. For any particular choice for the model, the set of event vectors chosen determines whether all the eigenvalues will be assignable and, if not, what the unassignable values are. We shall describe any set of output separable vectors that leaves all the eigenvalues freely assignable as nonrestrictive. It is desirable to choose a set that is nonrestrictive, but unassignable eigenvalues, as long as they are negative, do not necessarily impair the performance of the filter.

With one particular class of systems, all possible sets of output separable vectors are nonrestrictive. This occurs whenever the number of independent measurements is the maximum possible, equal to the number of state variables needed to model the system. We shall call a system like this fully measured. As the example of the air-driven turbine in Section 2.2 illustrates, the design of detection filters for fully-measured systems is straightforward.

2.4.2 Outline of the Design Procedure

This outline lists the sequence of steps in the design method; the subsections that follow describe the calculations required.

1. Analyze the system and determine the matrices {A,B,C} for a reference model of the form

$$\dot{\underline{x}}(t) = A\underline{x}(t) + B\underline{u}(t)$$

$$\underline{y}(t) = C\underline{x}(t)$$

2. Determine an event vector $\underline{f}$ for each component to be monitored; when necessary, multiply the vector by A successively until an alternate vector is obtained for which $C\underline{f}$ is nonzero.

3. Test the collection of event vectors to see if they are output separable. If not, either delete one or more vectors from the set so the remaining ones are output separable, or arrange the event vectors appropriately into two or more sets. In the latter case, a separate detection filter may be required for each set, pending the results of Step (7).

   Choose one set of output separable vectors, $\{\underline{f}_1, \cdots \underline{f}_s\}$, and continue.

4. Determine the event order ν of each $\underline{f}$, and compute basis vectors for each event space. When an event space is one-dimensional--which may frequently be the case--the only basis vector is the event vector itself.

5. Determine whether $\{\underline{f}_1, \cdots \underline{f}_s\}$ is nonrestrictive. When $s = \text{rank}[C]$, there will be $n - \sum \nu_i$ unassignable eigenvalues. If there are none, then $\{\underline{f}_1, \cdots \underline{f}_s\}$ is nonrestrictive; otherwise, the set is restrictive, and one of the following options must be chosen:

   a) Accept all the unassignable eigenvalues.

   b) Try a different set of output separable vectors.

c) Install more sensors in the system.

d) Delete from the set sufficiently many vectors to eliminate any unacceptable eigenvalues.

e) Expand the reference model with additional state variables so $\{\underline{f}_1, \cdots \underline{f}_s\}$ becomes nonrestrictive. This is always possible (the proof is given by Jones).

f) Separate $\{\underline{f}_1, \cdots \underline{f}_s\}$ into nonrestrictive subsets; design a detection filter for each subset.

Let $\{\underline{f}_1, \cdots \underline{f}_t\}$, denote the set selected in this step; whether or not it is nonrestrictive.

6. For the set $\{\underline{f}_1, \cdots \underline{f}_t\}$, derive the equations that D must satisfy. These equations are based on the sets of basis vectors assembled in Step (4) and contain as parameters the assignable eigenvalues of [A-DC].

7. Look for event vectors that can be made output stationary with $\underline{f}_1, \cdots \underline{f}_t$. These will be vectors that are not output separable with $\underline{f}_1, \cdots \underline{f}_t$ and that can be made to have fixed residual directions which are linear combinations of the directions $C\underline{f}_1, \cdots C\underline{f}_t$.

   When the system is fully measured (i.e., when rank[C] = n), all the eigenvalues of [A-DC] can be made equal, which makes all vectors output stationary and makes D independent of $\underline{f}_1, \cdots \underline{f}_t$.

8. Assign the free eigenvalues of [A-DC]. Frequently, the best approach will be to assign the same value to all them, for this is the simplest approach and this maximizes the number of output stationary vectors. The value chosen should usually be somewhat more negative than the important eigenvalues of A.

   This completes the specification of the feedback matrix D.

2.4.3 Output Separable Event Vectors

Several event vectors $\underline{f}_1, \cdots \underline{f}_s$ are output separable if and only if the vectors $C\underline{f}_1, \cdots C\underline{f}_i$ are linearly independent. The requirement for linear independence of the $C\underline{f}_i$'s restricts the number of event vectors in a set of output separable vectors to the number of independent measurements available--in other words, s must be less than or equal to the rank of C. When a detection filter is designed to give each $\underline{f}$ in $\{\underline{f}_1, \cdots \underline{f}_s\}$ a unidirectional residual, the directions of the residuals will be the directions of $C\underline{f}_1, \cdots C\underline{f}_s$, respectively.

Although linear independence of $C\underline{f}_1, \cdots C\underline{f}_s$ guarantees the existence of a detection filter for $\underline{f}_1, \cdots \underline{f}_s$, a stronger condition is needed if the filter is to be workable in practice. Suppose that the independence condition is met, but that $C\underline{f}_i$ and $C\underline{f}_j$, say, lie nearly in the same direction--that is, they are barely independent. Then in order for the detection filter to distinguish between them, it must weight heavily those residuals that would most show the slight differences between $C\underline{f}_i$ and $C\underline{f}_j$. In other words, the matrix D, which multiplies the residual vector, must have some large elements. If the reference model is accurate, then this presents no problem; but most often the reference model is approximate, and the modeling inaccuracies are accentuated by the large gains in D. Obviously, the less accurate the model is, the more difficult is the task of distinguishing between failures whose signatures point in similar directions. A filter designed to do so will be overly sensitive to modeling errors.

Thus the degree of output separability is important. One should design the reference model and choose the event vectors so the failure directions are as well-separated as possible. There is a simple measure of their separation that is useful in this task. Suppose there are m independent measurements, and suppose m output separable event vectors are chosen, the maximum number possible. Form $C\underline{f}_1, \ldots C\underline{f}_s$ and normalize them so they are each of length one. The absolute value of the determinant of the m x m matrix with the normalized $C\underline{f}$'s as its columns will be

between zero and one [36]. When the $C\underline{f}$'s are orthogonal, the value will be one, and when one or more is nearly a linear combination of the others, the value will be nearly zero. It appears that for the detection filter to perform well, this determinant should be two-tenths or more in absolute value.

2.4.4 Event Spaces

As previously defined, the event space $\underline{f}$ is composed of the vectors representing all conceivable failures, single or multiple, real or fictitious, that would induce a unidirectional residual along $C\underline{f}$, given that the detection filter is designed to monitor for the failure represented by $\underline{f}$. In essence, $\underline{f}$ is the event vector for any failure modeled by a vector in the event space of $\underline{f}$.

The mathematical definition of event space is

$$\mathcal{f} = \mathcal{f}_0 + \mathcal{f}_1$$

where $\mathcal{f}_1$ is the one-dimensional vector space containing all scalar multiples of $\underline{f}$, including $\underline{f}$, and $\mathcal{f}_0$ is the largest vector subspace (of the n-dimensional state space) for which

i) $\overline{C}\mathcal{f}_0$ contains only the zero vector.

ii) $\overline{A}\mathcal{f}_0$ belongs to $\mathcal{f}$.

The symbols $\overline{A}$ and $\overline{C}$ designate the linear operators corresponding to the matrices A and C.

An event space $\mathcal{f}$ is completely described by any set of vectors that forms a basis for it. The number of vectors required equals the dimension of $\mathcal{f}$, which was named the event order ν. A particular set of basis vectors is used in computing the feedback matrix D; that set is

$$\{\underline{g},\ A\underline{g},\ \cdots,\ A^{\nu-1}\underline{g}\} \qquad (2\text{-}34)$$

where $\underline{g}$ is a vector called the event generator of $\mathcal{f}$. This vector is found by solving

$$
\begin{aligned}
C\underline{g} &= \underline{0} \\
CA\underline{g} &= \underline{0} \\
&\vdots \\
CA^{\nu-2}\underline{g} &= \underline{0} \\
CA^{\nu-1}\underline{g} &= C\underline{f}
\end{aligned}
\qquad (2\text{-}35)
$$

subject to the constraint that $\underline{f}$ be expressible as a linear combination of the vectors in (2-34):

$$\underline{f} = \alpha_1\underline{g} + \alpha_2 A\underline{g} + \cdots + \alpha_{\nu-1}A^{\nu-2}\underline{g} + \alpha_\nu A^{\nu-1}\underline{g} \qquad (2\text{-}36)$$

This last equation is merely a statement that $\underline{f}$ is in its own event space. The α's are arbitrary scalars--it is only necessary that $\underline{g}$ be such that a set of α's exists for which (2-36) is satisfied. Comparing (2-36) with (2-35), we see that α_ν must always equal one, so whenever ν equals one, $\underline{g}$ is simply $\underline{f}$.

Equations (2-35) and (2-36) depend on the value of ν, but there is no explicit equation that gives that value. A formal procedure for finding ν was developed by Beard and is presented below, but that procedure is involved and is not usually needed. Most often ν equals one, and seldom does it exceed two or three. The reason for this is that the reference model is usually constructed with as few state variables and as many measurements as possible, which tends to minimize the event orders. Usually as many event vectors as there are measurements are selected, and from the definition of event spaces it follows that the sum of the event orders will never exceed the order of the reference model. As a result, one can often determine each ν by careful examination of the reference model. Alternatively, one can use Equations (2-35) themselves to find ν:

If there exists no g for which

$$C\underline{g} = \underline{0}$$

$$CA\underline{g} = C\underline{f}$$

then $\nu = 1$ and $\underline{g} = \underline{f}$. If such a $\underline{g}$ exists, then $\nu \geq 2$. If then there exists no $\underline{g}$ for which

$$C\underline{g} = \underline{0}$$

$$CA\underline{g} = \underline{0}$$

$$CA^2\underline{g} = C\underline{f}$$

then $\nu = 2$. If such a $\underline{g}$ exists, then $\nu \geq 3$, and one more equation from (2-35) must be tried.

When ν is known, if (2-35) specifies $\underline{g}$ completely, then (2-36) will be satisfied automatically. This is usual; rarely does (2-35) leave any freedom in the specification of any of the elements of $\underline{g}$. When it does, (2-36) eliminates the freedom and yields a unique solution for $\underline{g}$.

The method presented by Beard for determining ν proceeds in the following manner. First form the matrix

$$A' = A - D'C \tag{2-37}$$

with D' arbitrarily chosen to zero out as many columns of A' as possible. This makes the ensuing calculations easier, with no loss in generality. Then calculate

$$C' = C - C\underline{f}[(C\underline{f})^T(C\underline{f})]^{-1}(C\underline{f})^TC \tag{2-38}$$

$$K = A' - A'\underline{f}[(C\underline{f})^T(C\underline{f})]^{-1}(C\underline{f})^TC \tag{2-39}$$

$$M = \begin{bmatrix} C' \\ C'K \\ C'K^2 \\ \cdot \\ \cdot \\ C'K^{n-1} \end{bmatrix} \tag{2-40}$$

The event space of $\underline{f}$ is the null space of M; that is, $\mathscr{f}$ is the largest subspace that satisfies

$$\overline{M}\mathscr{f} = \emptyset$$

where $\overline{M}$ is the linear operator corresponding to M. The event order ν is the dimension of the null space of M and is given by

$$\nu = n - \text{rank}[M]$$

The rank of M can usually be determined by inspection; if not, one should resort to a numerical technique such as the orthogonal reduction procedure to find both $\mathscr{f}$ and ν from M.[4].

2.4.5 Restrictive Sets

By definition, $\{\underline{f}_1, \cdots \underline{f}_s\}$ is nonrestrictive if after D is constrained to make the residual associated with each $\underline{f}$ unidirectional, there remains sufficient freedom in the construction of D that the eigenvalues of [A-DC] can be specified at will, except for the constraint that both members of any complex pair of eigenvalues be assigned together to the same event space. One way of determining if a set is nonrestrictive is to skip to Step (6) and calculate the elements of D. With low-order systems, this approach is effective. Usually any unassignable eigenvalues become readily apparent, and should they be unacceptable, the filter is easily redesigned.

Another approach is to determine beforehand whether any unassignable eigenvalues exist, and, if so, what they are. These eigenvalues depend on A and $\{\underline{f}_1, \ldots \underline{f}_s\}$ only, so this can be done prior to calculating D. To do this we first find the dimension ν' of what is called the group event space $\mathscr{F}$ of $\{\underline{f}_1, \ldots \underline{f}_s\}$. That space is defined in the same way as each $\mathscr{f}$ is, with $\mathscr{F}_1$ and $\mathscr{F}_0$ in place of $\mathscr{f}_1$ and $\mathscr{f}_0$. The procedure for

[4]This procedure is described by Beard [4], Jones [24], and Gerard [20].

finding ν' is the same as the formal one for finding an event order. Form the n x s matrix F by inserting $\underline{f}_1, \cdots \underline{f}_s$ as its columns:

$$F = [\underline{f}_1 : \underline{f}_2 : \cdots \underline{f}_s] \tag{2-41}$$

Then form the nm x s matrix M' in the same manner M in (2-40) was formed, but with $\underline{f}$ replaced by F. The group event space is the null space of M', and the group event order ν' is given by

$$\nu' = n - \text{rank}[M']$$

The number of unassignable eigenvalues is

$$\nu_0 = \nu' - \sum \nu_i$$

When the number of event vectors equals the number of independent measurements--that is, when s equals the rank of C--then ν' equals the state dimension n.

When there are unassignable eigenvalues, they are associated with a subspace of $\mathscr{F}$ of dimension ν_0. This subspace, designated as $\mathscr{R}$, is that part of $\mathscr{F}$ that is not contained in any of the event spaces of $\underline{f}_1, \ldots \underline{f}_t$. By comparing $\mathscr{F}$ with the event spaces, one can find a set of basis vectors for $\mathscr{R}$. Then with those vectors, one can calculate the unassignable eigenvalues. Let R be the n x ν_0 matrix with those vectors as its columns, and let the basis vectors of all the event spaces (from (2-34)) be collected as the columns of a matrix G. Then the unassignable eigenvalues of [A-DC] are the eigenvalues of the ν_0 x ν_0 matrix Π that is part of the solution of

$$AR = [R : G] \begin{bmatrix} \Pi \\ \\ 0 \end{bmatrix} \tag{2-42}$$

This equation is just a statement that $\bar{A}\mathscr{R}$ is in $\mathscr{F}$, which follows from the definition of $\mathscr{F}$.

2.4.6 Augmenting the State Space

It is always possible to make unassignable eigenvalues assignable by adding one or more dummy variables to the state vector. This increases the dimension of the A matrix, which, at the cost of increased computational complexity, allows one to freely specify part of A. The object is to choose the new elements of A to enlarge the dimensions of the appropriate event spaces so that the sum of the event orders equals the group event order. Several additional state variables may be required to make up each deficit of one in the sum of the event orders. Each additional variable enlarges the group order by one and usually only a single event order by one. Eventually the next new variable will increase two event orders by one, thereby decreasing the deficit by one.

The form of the augmented A, B, and C matrices is:

$$A' = \begin{bmatrix} A & W \\ 0 & Q \end{bmatrix} \tag{2-43}$$

$$B' = \begin{bmatrix} B \\ 0 \end{bmatrix} \tag{2-44}$$

$$C' = [C : 0] \tag{2-45}$$

Many different choices of W and Q will eliminate an unassignable eigenvalue; which one is best for a given application may well be determined by what else the designer might wish to accomplish with the expanded A matrix. Jones presented an explicit procedure for obtaining a suitable [W,Q] pair from the solution $[\Pi,\Theta]$ of (2-42). Alternatively, one can approach the problem as follows: Start by making Q a diagonal matrix with arbitrary dimension and arbitrary diagonal elements. Then use Equations (2-35) and (2-36) to specify the conditions W must satisfy

to enlarge the appropriate event spaces. The necessary dimension of Q will become apparent, and generally there will be some freedom in the choice of its elements.

2.4.7 Calculating the Gain Matrix D

The expression that specifies D is derived from the event generators that were determined in Step (4). To each event generator we assign a set of numbers, real or complex,[5] which we wish to be eigenvalues of [A-DC]. We write the set as $\{\lambda_1, \cdots \lambda_\nu\}$, where, as before, ν is the event order. With each set we then form a polynomial Ψ in the complex variable s, as follows:

$$\Psi(s) = \prod_{j=1}^{\nu} (s-\lambda_j) = s^\nu + p_\nu s^{\nu-1} + \cdots + p_2 s + p_1 \qquad (2\text{-}46)$$

The λ's, then, are the roots of the characteristic equation formed by setting $\Psi(s)$ equal to zero. That they will also be poles of the detection filter we shall ensure by using $\Psi(s)$ in the calculation of D.

For each $\underline{f}$ we wish to specify appropriate conditions on D so we attain two objectives--first that the residual created by any of the failures represented by $\underline{f}$ is unidirectional along $C\underline{f}$, and second that the numbers $\lambda_1, \cdots \lambda_\nu$ are roots of the equation

$$\text{Det } [(A-DC) - sI] = 0 \qquad (2\text{-}47)$$

Regarding the first condition, recall from (2-6) that following a malfunction representable by the input failure model, the residual vector behaves according to

$$\dot{\underline{q}}(t) = [A-DC]\underline{q}(t) + \underline{f}n(t) \qquad (2\text{-}48a)$$

$$\underline{r}(t) = C\underline{q}(t) \qquad (2\text{-}48b)$$

[5] Both members of a complex pair must be included in the same set.

We must choose D such that the $\underline{q}(t)$ induced by $\underline{f}$, according to (2-48a), always stays within $\mathcal{f}$, because only the vectors within $\mathcal{f}$ will when propagated by the filter yield an $\underline{r}(t)$ that lies solely along $C\underline{f}$.

The region of the state space that the $\underline{q}(t)$ generated by $\underline{f}$ will propagate into is the subspace spanned by[6]

$$\{\underline{f},\ [A-DC]\underline{f},\ [A-DC]^2\underline{f},\ [A-DC]^3\underline{f},\ \cdots\} \tag{2-49}$$

The elements of D are chosen so that (2-49) spans only the event space of $\underline{f}$, no less, nor no more.[7] The first ν vectors in (2-49),

$$\{\underline{f},\ [A-DC]\underline{f},\ [A-DC]^2\underline{f},\ \cdots\ [A-DC]^{\nu-1}\underline{f}\}, \tag{2-50}$$

will form a basis for $\mathcal{f}$, and the remaining vectors in (2-49), being members of $\mathcal{f}$, will be linear combinations of these first ones. Recall that

---

[6]For those unfamiliar with the use of vector spaces in control theory, consider writing (2-48a) as

$$d\underline{q} = [A-DC]\underline{q}\cdot dt + n(t)\cdot\underline{f}\cdot dt$$

From this, one can form a progression that approximates the response of $\underline{q}$ to an impulse in $n(t)\cdot\underline{f}$ at $t = 0$:

$$\begin{aligned}
d\underline{q}_1 &= n_0\cdot\underline{f}\cdot dt \\
d\underline{q}_2 &= [A-DC]n_0\underline{f}\cdot dt \\
d\underline{q}_3 &= [A-DC][n_0\underline{f}+(A-DC)n_0\underline{f}]\cdot dt \\
&= [A-DC]n_0\underline{f}\cdot dt + [A-DC]^2 n_0\underline{f}\cdot dt \\
d\underline{q}_4 &= [A-DC]n_0\underline{f}\cdot dt + [A-DC]^2 n_0\underline{f}\cdot dt + [A-DC]^3 n_0\underline{f}\cdot dt \\
&\ \ \vdots
\end{aligned}$$

[7]This ensures that the dimension of the space spanned by (2-49) will be ν, thereby guaranteeing just enough control over [A-DC] for one to specify each of the ν eigenvalues in $\{\lambda_1, \cdots \lambda_\nu\}$.

in the section on event spaces we established another basis for $\mathcal{f}$, namely

$$\{\underline{g},\ A\underline{g},\ A^2\underline{g},\ \cdots\ A^{\nu-1}\underline{g}\} \tag{2-51}$$

Using (2-35) we rewrite this basis as

$$\{\underline{g},\ [A\text{-}DC]\underline{g},\ [A\text{-}DC]^2\underline{g},\ \cdots\ [A\text{-}DC]^{\nu-1}\underline{g}\} \tag{2-52}$$

This does not change the basis vectors; (2-51) and (2-52) are identical sets. For our first condition to be upheld, just as $[A\text{-}DC]^{\nu}\underline{f}$ must be a linear combination of the vectors in (2-50), so must $[A\text{-}DC]^{\nu}\underline{g}$ be a linear combination of the vectors in (2-52), since $\underline{g}$ belongs to $\mathcal{f}$. Expressing this statement as an equation, we have

$$[A\text{-}DC]^{\nu}\underline{g} = \alpha_1\underline{g} + \alpha_2[A\text{-}DC]\underline{g} + \cdots + \alpha_{\nu}[A\text{-}DC]^{\nu-1}\underline{g} \tag{2-53}$$

where the α's may be any scalars whatever.

To achieve our second objective, we now require that the set $\{-\alpha_1, \cdots -\alpha_{\nu}\}$ be equal to the set of polynomial coefficients $\{p_1,\ p_2, \cdots p_{\nu}\}$ from (2-46); that is, we require D to satisfy

$$-[A\text{-}DC]^{\nu}\underline{g} = p_1\underline{g} + p_2[A\text{-}DC]\underline{g} + \cdots + p_{\nu}[A\text{-}DC]^{\nu-1}\underline{g} \tag{2-54}$$

A result in linear algebra known as the Cayley-Hamilton Theorem ensures that $\lambda_1, \cdots \lambda_{\nu}$ will then be roots of (2-47). This theorem states that every square matrix satisfies its own characteristic equation. That equation for an n x n matrix M is

$$\Psi(s) = s^n + p_n s^{n-1} + \cdots p_2 s + p_1 = 0 \tag{2-55}$$

so the theorem says

$$\Psi(M) = M^n + p_n M^{n-1} + \cdots p_2 M + p_1 = \underline{0} \tag{2-56}$$

In calculating D, we specify a set of polynomials $\{\Psi_1(s), \cdots \Psi_t(s)\}$ corresponding to the set of event vectors $\{\underline{f}_1, \cdots \underline{f}_t\}$, and then we require for each Ψ_i in turn that

$$\Psi_i(\text{A-DC}) = \underline{0} \tag{2-57}$$

Thus we have

$$\Psi_0(\text{A-DC}) \cdot \Psi_1(\text{A-DC}) \cdot \cdots \Psi_t(\text{A-DC}) = \underline{0} \tag{2-58}$$

where $\Psi_0(\text{A-DC})$ is a polynomial whose roots are the unassignable eigenvalues of [A-DC] (if there are any) and if t is less than the rank of C, the eigenvalues of [A-DC] that can yet be assigned by exercising the remaining freedom in the choice of D that would exist in this case. Equation (2-58) is a statement of the Cayley-Hamilton Theorem for [A-DC]: we have set the conditions on D so that the characteristic equation of [A-DC], (2-47), is factorable into the form

$$\Psi_0(s) \cdot \Psi_1(s) \cdot \cdots \Psi_t(s) = 0 \tag{2-59}$$

Equation (2-57) applied to each Ψ_i, i=1,2,...t, yields the equations that are to be solved for D. To obtain a more detailed version of (2-57), we write it in the form of (2-56),

$$[\text{A-DC}]^{\nu} + p_{\nu}[\text{A-DC}]^{\nu-1} + \cdots + p_2[\text{A-DC}] + p_1 = 0 \tag{2-60}$$

multiply by $\underline{g}$, expand the powers, and then use (2-35) to obtain

$$A\underline{g} - DC\underline{f} = -p_1\underline{g} - p_2A\underline{g} \cdots - p_{\nu}A^{\nu-1}\underline{g} \tag{2-61}$$

Note that whenever the event order of $\underline{f}$ is one, (2-61) reduces to

$$[\text{A-DC}]\underline{f} = \lambda\underline{f} \tag{2-62}$$

Hence, in that case the condition on D is that f be an eigenvector of [A-DC] and λ be the corresponding eigenvalue.

In summary, to solve for D, assign to every event vector in $\{\underline{f}_1, \cdots \underline{f}_t\}$ a set of numbers $\{\lambda_1, \cdots \lambda_{\nu_i}\}$, then calculate the coefficients of the polynomial $\Psi_i(s)$ by using

$$\Psi(s) = \prod_{j=1}^{\nu} (s-\lambda_j) = p_1 + p_2 s + \cdots + p_\nu s^{\nu-1} + s^\nu \qquad (2\text{-}63)$$

and write the equation

$$DC\underline{f} = p_1\underline{g} + p_2 A\underline{g} + \cdots + p_\nu A^{\nu-1}\underline{g} + A^\nu \underline{g} \qquad (2\text{-}64)$$

After values for the λ's have been assigned, simultaneously solve all of the equations (2-64) for D. When the number of event vectors equals the number of independent measurements, this specifies every element of D.

2.4.8 D for Sensor Failures

We derived Equation (2-64) for failures representable by the input failure model, but it can usually be used also with the measurement failure model. It may, however, become nonlinear. If one wishes failures of the j'th sensor to yield a residual that is constrained to the plane spanned by $\underline{e}_j$ and $C\underline{d}_j$, then $\underline{d}_j$ must be made an event vector of the detection filter. But $\underline{d}_j$ is not known beforehand as are the $\underline{f}$'s. In three situations that occur frequently, this difficulty can be overcome.

First, if one of the other event vectors, say $\underline{f}_i$, is such that $C\underline{f}_i$ equals $\underline{e}_j$, then $\underline{d}_j$ is fully specified by (2-64) applied only to $\underline{f}_i$, irrespective of what the other $\underline{f}$'s are. That will be so when $\underline{f}_i$ is associated with an actuator whose position is measured by the j'th sensor. In that case, $DC\underline{f}_i$ is simply D times $\underline{e}_j$, which is $\underline{d}_j$. Thus $\underline{d}_j$ can easily be found and then inserted into (2-64) as an event vector itself.

Second, if from the structure of the reference model one can determine the likely event order of $\underline{d}_j$, then it may be possible to write (2-64) as a nonlinear equation that can be solved numerically. For example, if the event order of $\underline{d}_j$ can only be one, then

$$\underline{g}_i = \underline{f}_i = \underline{d}_i$$

and with $\underline{d}_i$ substituted for $\underline{f}$, (2-64) becomes

$$DC\underline{d}_j = p_1\underline{d}_j + A\underline{d}_j$$

This nonlinear equation must be solved simultaneously with the equations obtained with the other event vectors. Most likely, the solution will require use of a computer algorithm that solves systems of nonlinear equations.

Third, one can sometimes make $\underline{d}_j$ output stationary with the $\underline{f}$'s, thereby avoiding the problems attendent with making $\underline{d}_j$ be one of the $\underline{f}$'s. This is the preferred solution, particularly since it may be possible to make several, perhaps all, of the columns of D output stationary at once by assigning the same value to many, or all, of the assignable eigenvalues of [A-DC]. The next section describes the procedure for making vectors output stationary.

2.4.9 Output Stationarity

In Step (5), the set $\{\underline{f}_1, \cdots \underline{f}_t\}$ was assembled either as a nonrestrictive group of event vectors or as a restrictive one that yields acceptable eigenvalues; it may be both possible and desirable to add to this set one or more events that are not output separable with $\underline{f}_1, \cdots \underline{f}_t$. As mentioned before, to do this we must make the additional vectors mutually output stationary with $\{\underline{f}_1, \cdots \underline{f}_t\}$. For that to be possible, these vectors must meet the requirements set out below. Whether it is desirable or not depends on the constraints that will be incurred. Some of the

freedom in eigenvalue selection is sacrificed when making a vector output stationary, because at least two sets of eigenvalues, say $\{\lambda_1,\cdots\lambda_{\nu_i}\}$ and $\{\lambda_1,\cdots\lambda_{\nu_j}\}$, must be set equal to one another (or partially so if one is larger than the other). Also, when ν_j is unequal to ν_i, the unmatched eigenvalues become unassignable.

First we determine which of the additional event vectors taken one at a time can be made output stationary. The condition a vector $\underline{h}$ must satisfy if it is to produce a unidirectional residual from a filter designed for $\{\underline{f}_1,\ldots\underline{f}_t\}$ is that [A-DC]$\underline{h}$ be contained in the event space $\mathcal{h}$ of $\underline{h}$, that is, that

$$[A-DC]\underline{h} \ \varepsilon \ \mathcal{h} \tag{2-65}$$

The event space of $\underline{h}$ is found the same way the event spaces $\mathcal{f}$ of the $\underline{f}$'s are found, and (2-65) is the same condition that when applied to all the $\underline{f}$'s specifies what D must be, except for the choice of eigenvalues for [A-DC]. This choice can sometimes be made so (2-65) is satisfied.

For example, suppose that the event orders of $\underline{h}$, $\underline{f}_1$, and $\underline{f}_2$ are all equal to one and that $\underline{h}$ is a combination of $\underline{f}_1$ and $\underline{f}_2$:

$$\underline{h} = \alpha_1\underline{f}_1 + \alpha_2\underline{f}_2 \tag{2-66}$$

Then

$$\begin{aligned}[A-DC]\underline{f}_1 &= \lambda_1\underline{f}_1 \\ [A-DC]\underline{f}_2 &= \lambda_2\underline{f}_2\end{aligned} \tag{2-67}$$

and

$$\begin{aligned}[A-DC]\underline{h} &= [A-DC][\alpha_1\underline{f}_1 + \alpha_2\underline{f}_2] \\ &= \alpha_1\lambda_1\underline{f}_1 + \alpha_2\lambda_2\underline{f}_2\end{aligned} \tag{2-68}$$

The one-dimensional event space of $\underline{h}$ consists of all scalar multiples of $\underline{h}$, so $[A-DC]\underline{h}$ will lie in that space if and only if λ_1 and λ_2 are equal. Then (2-68) becomes

$$\begin{aligned}[A-DC]\underline{h} &= \alpha_1\lambda\underline{f}_1 + \alpha_2\lambda\underline{f}_2 \\ &= \lambda(\alpha_1\underline{f}_1 + \alpha_2\underline{f}_2) \\ &= \lambda\underline{h} \end{aligned} \tag{2-69}$$

In general, to determine if any particular vector $\underline{h}$ can be made output stationary, proceed as follows: Write the vector $C\underline{h}$ as a linear combination of $C\underline{f}_1, \cdots C\underline{f}_t$, and collect in a set I the indices of the $\underline{f}$'s needed in this linear combination. Then write

$$\underline{h} = \sum_{i\in I} \alpha_i\underline{f}_i + \underline{\xi} \tag{2-70}$$

where $\underline{\xi}$ satisfies $C\underline{\xi} = \underline{0}$, and none of the α's are zero. Thus,

$$[A-DC]\underline{h} = \sum_{i\in I} \alpha_i[A-DC]\underline{f}_i + A\underline{\xi} \tag{2-71}$$

Equations (2-70) and (2-71) present three possibilities:

1. The vector $\underline{\xi}$ is zero or is contained in the union[8] of the $\mathscr{f}$'s:$i\in I$. Then the definition of an event space implies that $\underline{\xi}$ is entirely within the union of the $\mathscr{f}$'s:$i\in I$. We know, too, that $A\underline{\xi}$ must lie in that union. Furthermore, the freedom to choose the eigenvalues of [A-DC] can be used to make the right-hand side of (2-71) lie anywhere at all in that union, which means that (2-65) can be satisfied. If all the event orders ν_i:$i\in I$ are equal, then (2-65) is satisfied whenever all

[8]The union of several vector spaces is the space spanned by the collection of the basis vectors of those spaces.

the sets of eigenvalues $\{\lambda_1, \cdots \lambda_{\nu_i}\}: i \in I$ are equal. (It is not necessary that the λ's within each set be equal.) If the ν_i's are not equal, then Equations (2-70) and (2-71) force some of the λ's to take specific values. Let ν_{min} specify the smallest of the ν_i's; then in each set $\{\lambda_1, \cdots \lambda_{\nu_i}\} : i \in I$, $\nu_i - \nu_{min}$ of the λ's will be so specified. The remaining portions of the sets are constrained only to be equal, as before.

2. The vector $\underline{\xi}$ is not in the union of the $\mathcal{f}$'s:$i \in I$, but $A\underline{\xi}$ is in the union of $\mathcal{h}$ with that union. This can occur only if $\{\underline{f}_1, \cdots \underline{f}_t\}$ is a restrictive set. Once again (2-65) can be satisfied, and if $A\underline{\xi}$ is either entirely in $\mathcal{h}$ or entirely in the union of the $\mathcal{f}$'s:$i \in I$, it can be satisfied the same way as in (1) above. Otherwise, Equations (2-63), (2-64), and (2-71) must be used together to find which values of the λ's will make $\underline{h}$ output stationary--simply making the sets equal will not do so.

3. The vector $A\underline{\xi}$ does not lie in the union of $\mathcal{h}$ and the $\mathcal{f}$'s:$i \in I$. No choice of the λ's can make $\underline{h}$ output stationary.

Mutual output stationarity of several event vectors $\underline{h}_1, \cdots \underline{h}_v$ is assured, in the two simplest cases, whenever 1) there is no overlap in the sets $\{\underline{f}_i : i \in I_1\}, \cdots \{\underline{f}_i : i \in I_v\}$ used in the linear combinations making up $\underline{h}_1, \cdots \underline{h}_v$, or 2) the sets are identical. If, on the other hand, some of the indicial sets I are intersecting but not identical, stationarity of those additional vectors so related depends on whether or not two of the sets make the same eigenvalue unassignable and require different values for it.

2.4.10 Eigenvalue Assignment

Except for the constraint on complex pairs and the equality requirements introduced by any output stationary vectors, the designer has considerable freedom in choosing the assignable eigenvalues of [A-DC]. Using it

effectively demands awareness of the various factors that influence the performance of the filter. To begin with, the eigenvalues should be negative--or have negative real parts--else the state of the reference model will eventually diverge from the state of the actual system. Large negative values make the model track the measurements closely, and they minimize the size of the residuals caused by malfunctions or by modeling errors. On the other hand, small negative values make transient residuals die out slowly, and they allow steady residuals produced by malfunctions to sustain large magnitudes. Residuals due to high-frequency measurement noise are relatively little affected by the choice of eigenvalues; consequently, the more negative the eigenvalues are, the smaller the signal-to-noise ratio in the residuals is.

In most circumstances, the eigenvalues ought to be somewhat more negative than the corresponding eigenvalues of the system itself. This gives a good compromise between response rate and signal-to-noise ratio. Much of the time, the most practical approach is to choose the same value for all the assignable eigenvalues.

2.5 SUMMARY

The method of detection filter design developed in this chapter comprises procedures for designating the event vectors of failures, for determining whether a set of output separable vectors is nonrestrictive, for testing vectors for output stationarity, and for calculating the gain matrix. Attention was restricted to continuous linear systems.

Chapter 3 illustrates this material with a simple example. The first part of Chapter 4 describes the few modifications that make the design procedure applicable to sampled-data systems. Such systems cannot be monitored exactly, but when the sampling rate is sufficiently high, the deviations from ideal operation are slight. The second and third parts of the chapter present a less general, but more concise, design procedure and a method of processing the residuals for failure diagnosis.

Chapter III

AN EXAMPLE: A STEAM TURBINE

The theory presented in Chapter 2 becomes straightforward when applied to a simple, low-order system. In particular, the physical justification for the definitions of output separable vectors, nonrestrictive sets, and output stationary vectors become apparent. To illustrate each of the aspects of detection filters, we shall design detection filters for four versions of the steam turbine engine described below. The first version is a fully-measured system similar to the air turbine discussed near the beginning of Chapter 2. The design of a detection filter for it demonstrates how to find event vectors, how to calculate the feedback matrix D, and how to make an event vector output stationary. The three other versions are not fully measured, and the construction of detection filters for them shows several circumstances in which an eigenvalue of a filter is unassignable.

The important difference between this example and the one in Section 2.2 is that in this one there are three state variables rather than two. This makes visible several aspects of detection filter design that do not appear with a second-order system. It should be noted that this chapter is intended to illustrate the design procedure--diagnosis of failures is described in Chapter 4 and in the subsequent treatment of the F100 engine.

3.1 THE REFERENCE MODEL

The steam turbine engine of this example is shown schematically in Figure 3.1. The engine is modeled as a third-order system comprising a fuel valve, a boiler, and a turbine. Figure 3.2 shows the block dia-

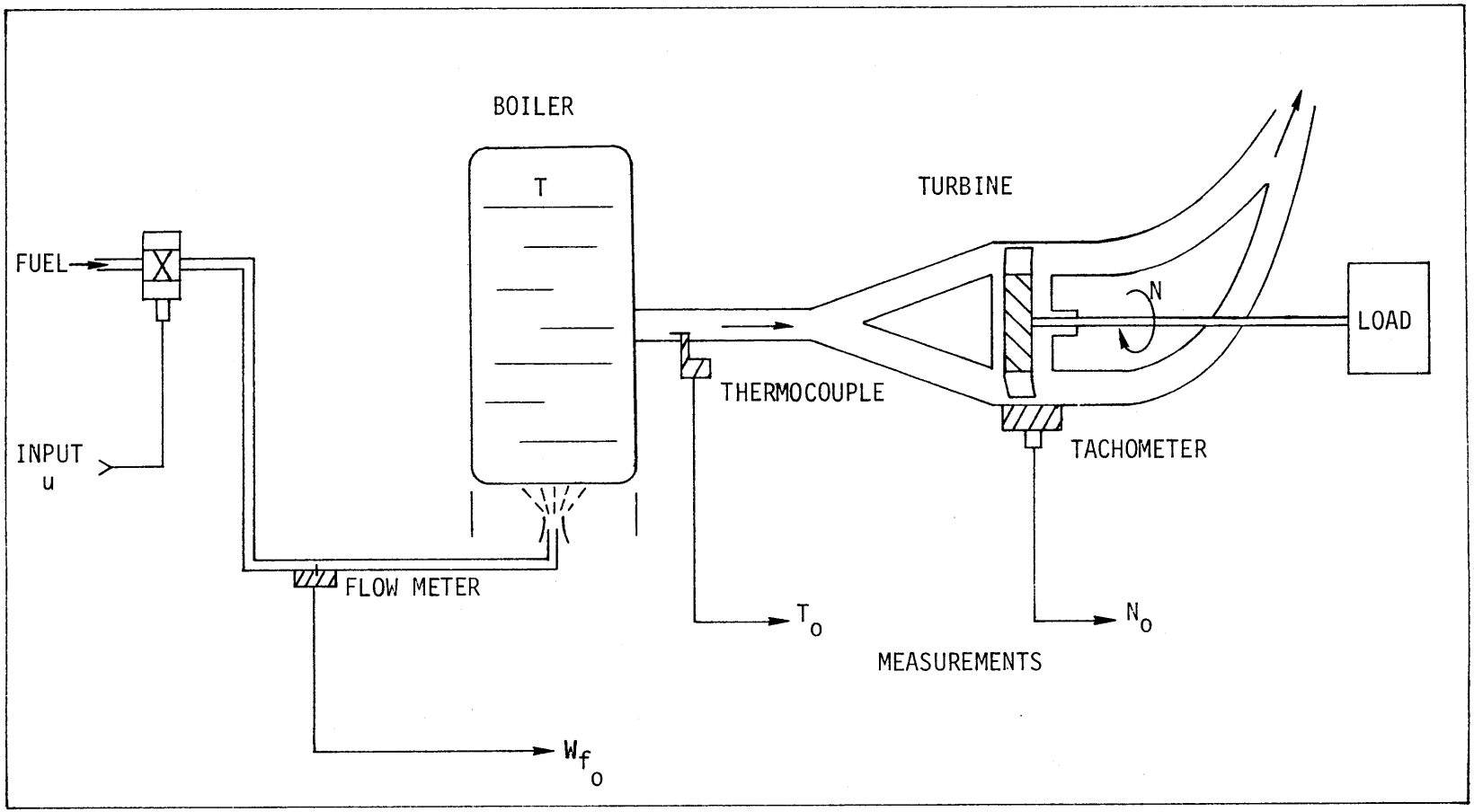

Figure 3.1. A steam turbine engine.

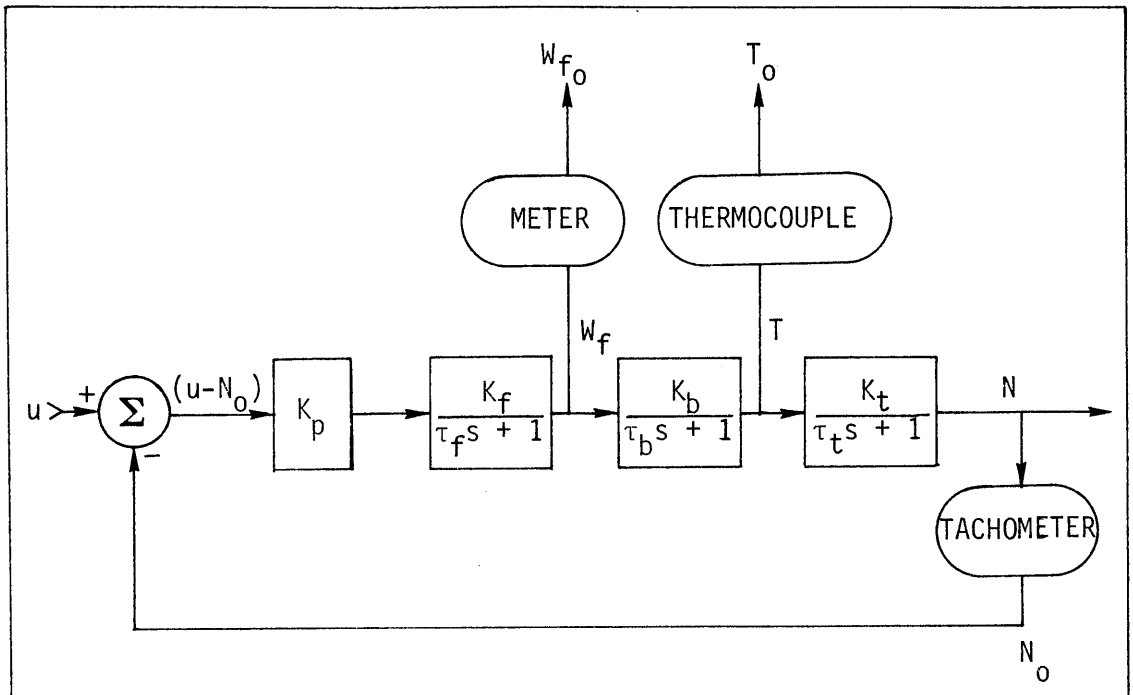

τ_f = Positioning time constant of valve spool

τ_b = Thermal time constant of boiler

τ_t = Acceleration time constant of turbine

u = Reference input

W_f = Fuel flow rate

T = Steam temperature

N = Turbine speed

K_p = Control loop proportional gain

K_f = Scale factor: voltage to flow rate

K_b = Scale factor: flow rate to temperature

K_t = Scale factor: temperature to speed

Figure 3.2. Block diagram of the steam turbine.

gram. The model is a linearization about a steady-state operating point; the dynamics of the major components--the valve, the boiler, and the turbine--are modeled by first-order lags. In this linear model, steady-state values of fuel flow, temperature, and speed are proportional to each other. As shown in the diagram, there are three sensors in the system: a flow meter, a thermocouple, and a tachometer. The tachometer is used in a feedback loop, while the flow meter and the thermocouple just monitor the system. None of the sensors is considered to have any significant dynamics of its own.

To form a convenient state-variable model of the system, we choose the three variables to be the fuel flow W_f, the temperature T, and the measurement N_0 of the turbine speed N. (Here again, the subscript $_0$ denotes the output of a sensor.) The differential equations describing the dynamics of the system as modeled in the diagram in Figure 3.2 are:

$$\frac{d[W_f]}{dt} = 1/\tau \cdot [K_p \cdot K_f \cdot (u - N_0) - W_f] \tag{3-1}$$

$$\frac{d[T]}{dt} = 1/\tau_b \cdot [K_b \cdot W_f - T] \tag{3-2}$$

$$\frac{d[N_0]}{dt} = 1/\tau_t \cdot [K_t \cdot T - N_0] \tag{3-3}$$

Writing (3-1) to (3-3) in the form

$$\dot{\underline{x}} = A\underline{x} + B\underline{u}$$

gives us

$$\frac{d}{dt}\begin{bmatrix} W_f \\ T \\ N_0 \end{bmatrix} = \begin{bmatrix} -1/\tau_f & 0 & -K_p K_f/\tau \\ K_b/\tau_b & -1/\tau_b & 0 \\ 0 & K_t/\tau_t & -1/\tau_t \end{bmatrix} \begin{bmatrix} W_f \\ T \\ N_0 \end{bmatrix} + \begin{bmatrix} K_p K_f/\tau_f \\ 0 \\ 0 \end{bmatrix} u \tag{3-4}$$

Each of the state variables is sensed directly, so the system is fully measured, and the measurement equation is

$$\begin{bmatrix} W_{f0} \\ T_0 \\ N_0 \end{bmatrix} = \begin{bmatrix} 1 & 0 & 0 \\ 0 & 1 & 0 \\ 0 & 0 & 1 \end{bmatrix} \begin{bmatrix} W_f \\ T \\ N_0 \end{bmatrix} \tag{3-5}$$

To make this example easy to work with, we assume the system is a somewhat sluggish one, with parameters as listed in Table 3.1.

TABLE 3.1

Parameters for the steam turbine example.

τ_f	= 0.1 sec	K_f	= 0.25
τ_b	= 1.0 sec	K_b	= 20.0
τ_t	= 0.5 sec	K_t	= 0.10

$K_p = 2.0$

Accordingly, we obtain the following as the A, B, and C matrices:

$$A = \begin{bmatrix} -10 & 0 & -5 \\ 20 & -1 & 0 \\ 0 & .2 & -2 \end{bmatrix} \quad B = \begin{bmatrix} 5 \\ 0 \\ 0 \end{bmatrix} \quad C = \begin{bmatrix} 1 & 0 & 0 \\ 0 & 1 & 0 \\ 0 & 0 & 1 \end{bmatrix} \tag{3-6}$$

The characteristic equation is

$$\text{Det } [sI-A] = 0 \tag{3-7}$$

which expands to

$$(s+10)(s+1)(s+2) - 20 = 0 \qquad (3\text{-}8)$$

The poles of the system--the eigenvalues of A--are

$$\begin{aligned} s_1 &= -10.26 \\ s_{2,3} &= -1.37 \pm 1.42i \end{aligned} \qquad (3\text{-}9)$$

3.2 A DETECTION FILTER FOR A FULLY-MEASURED SYSTEM

The first step in designing a detection filter is ascertaining the types of malfunctions that could occur. Several failures that the steam turbine system would be susceptible to are listed in Table 3.2, categorized

TABLE 3.2

Examples of failures.

Actuators	i) Fuel valve	- Biased output - Hardover failure - Change in K_f - Change in τ_f
Dynamic components	i) Boiler	- Plugged fuel nozzle - Flame out of part or all of burner - Steam leak
	ii) Turbine	- Broken turbine blade - Loss of vane(s) in turbine nozzle - Failed bearing - Change in torque
Sensors	i) Flow meter	- Biased output - Zero or saturation
	ii) Thermocouple	- Change in scale factor - Erratic output
	iii) Tachometer	- Excessive noise

according to component type. The possible failures are listed for illustration only; we shall be concerned just with identifying failed components, not with determining the particular mode of failure.

Any of the failures listed for the valve, the boiler, or the turbine can be represented mathematically by the input failure model (2-27). The failure is expressed by the product of an event vector $\underline{f}$, which is time-invariant, and a scalar function n(t):

$$\dot{\underline{x}}(t) = A\underline{x}(t) + B\underline{u}(t) + \underline{f}n(t) \qquad (2\text{-}27)$$

The event vector for malfunctions of the fuel valve is easily determined by considering the effects of a particular malfunction. Suppose the fuel flow began to vary from the rate appropriate for the given input u; then the time behavior of the flow rate would no longer be represented by (3-1), but by

$$\dot{W}_f(t) = 1/\tau_f\{K_p \cdot K_f \cdot [u(t)-N(t)] - W_f(t)\} + \Delta\dot{W}_f(t) \qquad (3\text{-}10)$$

where $\Delta\dot{W}_f(t)$ is a function describing the dynamics of whatever is causing the deviation in the fuel flow. The state equation describing the system becomes

$$\frac{d}{dt}\begin{bmatrix} W_f \\ T \\ N_0 \end{bmatrix} = A\begin{bmatrix} W_f \\ T \\ N_0 \end{bmatrix} + B\,u + \begin{bmatrix} 1 \\ 0 \\ 0 \end{bmatrix}\Delta\dot{W}_f(t) \qquad (3\text{-}11)$$

Comparing (3-11) with (2-27) we see that the event vector $\underline{f}_f$ for such a time-varying bias in the fuel valve is

$$\underline{f}_f = \begin{bmatrix} 1 \\ 0 \\ 0 \end{bmatrix}$$

and that the time-varying function is

$$n(t) = \Delta\dot{W}_f(t) \tag{3-13}$$

For each of the valve failures listed in Table 3.2, the event vector is $\underline{f}_f$. The scalar n(t) is different for each, but that is unimportant in the design of the filter.

Any change in boiler performance will cause the steam temperature to deviate from its normal value, without changing the fuel flow or the relation between turbine speed and temperature. We model such a malfunction by adding a term to Equation (3-2), so the event vector associated with the boiler is

$$\underline{f}_b = \begin{bmatrix} 0 \\ 1 \\ 0 \end{bmatrix}$$

Similarly, any problem in the turbine that changes the shaft speed while the steam temperature remains the same can be modeled by adding a term to Equation (3-3). The event vector associated with the turbine is

$$\underline{f}_t = \begin{bmatrix} 0 \\ 0 \\ 1 \end{bmatrix}$$

One turbine failure listed in Table 3.2, the loss of one or more vanes in the turbine nozzle, cannot be represented by $\underline{f}_t$ because it causes a temperature change as well as a speed change. Consideration of this circumstance will be deferred until last.

Of the various sensor failures possible in this example, only those of the speed sensor produce a residual that can be constrained to a single line; signatures of the other two can only be constrained to two-dimensional planes. The residual direction for tachometer failures is the same as that for turbine failures, and consequently, on the basis of residual direction alone, failures of the two cannot be distinguished.

We are now at the point of determining the event space and the event generator of each of the event vectors. Knowing the dimension of the event spaces, we will be able to discern immediately whether the event vectors are nonrestrictive. Recall that the event space of an event vector $\underline{f}$ consists of all the state vectors that yield a unidirectional residual along $C\underline{f}$. Our steam turbine is a fully-measured system, so the event space of each of the event vectors consists simply of the event vector and scalar multiples of it. In other words, there are no regions of the state space that are not directly observed by the sensors, and hence there is no possibility that any of the event spaces could have a dimension greater than one. For the same reason, none of the three eigenvalues of [A-DC] is unassignable; thus the set $\{\underline{f}_f, \underline{f}_b, \underline{f}_t\}$ is nonrestrictive. Also, the event orders ν_d, ν_b, and ν_t all equal one.

Let λ_f, λ_b, and λ_t denote the eigenvalues of [A-DC], with λ_f the one associated with $\underline{f}_f$, and so on. As given by (2-46), the polynomial we associate with an event vector is

$$\prod_{j=1}^{\nu} (s-\lambda_j) = s^{\nu} + p_{\nu}s^{\nu-1} + \cdots + p_1 \qquad (2\text{-}46)$$

Applying (2-46) three times, with ν equal to one each time, we have

$$\begin{aligned} (s-\lambda_f) &= s + p_{1_f} \\ (s-\lambda_b) &= s + p_{1_b} \\ (s-\lambda_t) &= s + p_{1_t} \end{aligned} \qquad (3\text{-}16)$$

These yield the identities

$$\begin{aligned} p_{1_f} &= -\lambda_f \\ p_{1_b} &= -\lambda_b \\ p_{1_t} &= -\lambda_t \end{aligned} \qquad (3\text{-}17)$$

For simplicity, let us suppose that the flow meter never fails. Then the only planar residuals will be those induced by failures of the thermocouple. Although identification of these residuals requires additional detection logic, that failure signature is distinguishable from the unidirectional signature of boiler failures. The failure model for the thermocouple is the measurement failure model of Equation (2-29):

$$\begin{aligned} \dot{\underline{x}}(t) &= A\underline{x}(t) + \underline{b}u(t) \\ \underline{y}(t) &= \underline{x}(t) + \begin{bmatrix} 0 \\ 1 \\ 0 \end{bmatrix} n(t) \end{aligned} \tag{3-14}$$

From (2-31), we find that the behavior of the residual $\underline{r}$ is described by

$$\begin{aligned} \dot{\underline{q}}(t) &= [A-DC]\underline{q}(t) - \begin{bmatrix} d_{12} \\ d_{22} \\ d_{32} \end{bmatrix} n(t) \\ \underline{r}(t) &= \underline{q}(t) + \begin{bmatrix} 0 \\ 1 \\ 0 \end{bmatrix} n(t) \end{aligned} \tag{3-15}$$

The residual produced by any failure of the temperature sensor will be constrained to the plane spanned by $[0,1,0]$ and $[d_{12},d_{22},d_{32}]$ if the feedback matrix D is chosen such that the vector $[d_{12},d_{22},d_{32}]$, the second column of D, is an event vector with unidirectional residual. We shall defer further consideration of this until the last step of the design, by which time most of the elements of D will be specified.

We thus have three event vectors that we wish to consider: $\underline{f}_f$, $\underline{f}_b$, and $\underline{f}_t$. The next objective is to determine a D matrix that causes each of these vectors to yield a unidirectional residual. The vectors $C\underline{f}_f$, $C\underline{f}_b$, and $C\underline{f}_t$ are linearly independent, so $\underline{f}_f$, $\underline{f}_b$, and $\underline{f}_t$ are output separable, and we are assured that a single detection filter can detect the failures with which each of them is associated.

The equation that D must satisfy for each $\underline{f}$ is (2-64):

$$DC\underline{f} = p_1\underline{g} + p_2A\underline{g} + \cdots + p_\nu A^{\nu-1}\underline{g} + A^\nu\underline{g} \qquad (2\text{-}64)$$

(Recall that $\underline{g}$ is the event generator of the event space of $\underline{f}$.) In this example, the $\underline{g}$'s are equal to the $\underline{f}$'s, because each of the event spaces is one-dimensional. Applying (2-64) to each $\underline{f}$, we obtain

$$DC\underline{f}_f = -\lambda_f\underline{f}_f + A\underline{f}_f$$

$$DC\underline{f}_b = -\lambda_b\underline{f}_b + A\underline{f}_b$$

$$DC\underline{f}_t = -\lambda_t\underline{f}_t + A\underline{f}_t$$

Rearrangement yields

$$\begin{aligned} [A-DC]\underline{f}_f &= \lambda_f\underline{f}_f \\ [A-DC]\underline{f}_b &= \lambda_b\underline{f}_b \\ [A-DC]\underline{f}_t &= \lambda_t\underline{f}_t \end{aligned} \qquad (3\text{-}18)$$

We find, then, that in this case the criterion for the selection of D is that each of the event vectors be an eigenvector of [A-DC].

Using A and C from (3-6) to solve (3-18) for D in terms of the λ's, we easily find

$$D = \begin{bmatrix} -10-\lambda_f & 0 & -5 \\ 20 & -1-\lambda_b & 0 \\ 0 & .2 & -2-\lambda_t \end{bmatrix} \qquad (3\text{-}19)$$

Then

$$[\text{A-DC}] = \begin{bmatrix} \lambda_f & 0 & 0 \\ 0 & \lambda_b & 0 \\ 0 & 0 & \lambda_t \end{bmatrix} \tag{3-20}$$

Because the steam turbine system is fully measured, the D matrix of (3-19) is similar in structure to the D matrix obtained for the air turbine in Chapter 2 (see Equation (2-13)). The off-diagonal elements are fixed at the values that decouple the state variables of the filter, and the λ's contained in the main diagonal elements become the poles of the filter. They determine the rates at which the components of $\underline{r}$,

$$\begin{aligned} r_f &= W_{f0} - \hat{W}_{f0} \\ r_b &= T_0 - \hat{T}_0 \\ r_t &= N_0 - \hat{N}_0 \end{aligned} \tag{3-21}$$

settle out to steady-state values. The poles also affect the magnitudes of the steady-state values: the more negative the λ's are, the smaller the steady-state values are.

Now that D has been specified except for λ_f, λ_b, and λ_t (or, equivalently, d_{11}, d_{22}, and d_{33}), we resume consideration of the two failures left in abeyance earlier: malfunction of the thermocouple and burn-out of a nozzle vane. It was noted then that $[d_{12},d_{22},d_{32}]$ is the event vector that yields the second failure vector for a thermocouple failure (the first is [0,1,0]), and in the meantime this column of D has been constrained to be

$$\begin{bmatrix} 0 \\ -1-\lambda \\ .2 \end{bmatrix}$$

The failure vector for this is a linear combination of $\underline{Cf}_b$ and $\underline{Cf}_t$. Therefore, since D has been selected such that no residual vector along either $\underline{Cf}_b$ or $\underline{Cf}_t$ propagates into a vector along the other failure direction, $\underline{Cf}_f$, and since the initial residual produced by the failure,

$$\begin{bmatrix} 0 \\ 1 \\ 0 \end{bmatrix} n(t),$$

lies along $\underline{Cf}_b$, the net time-varying residual vector produced by the failure is constrained to the plane spanned by $\underline{Cf}_b$ and $\underline{Cf}_t$, that is, by [0,1,0] and [0,0,1]. In this case, nothing further needs to be done to D to make failures of the thermocouple identifiable. They will be characterized by a residual appearing along $\underline{Cf}_b$, followed immediately by one along $\underline{Cf}_t$.

Burn-out of one or more vanes in the turbine nozzle is an example of a failure whose event vector can be made output stationary with the event vectors upon which the design of the detection filter is based. First, we must determine what this event vector is. Loss of a nozzle vane increases the nozzle area, allowing the steam flow to increase. This in turn results in a decrease in the steam temperature. These two effects have counteracting influences on the turbine speed, but because the fluid-dynamic efficiency of the flow also decreases, the turbine tends to slow down. Suppose if there were no feedback of the turbine speed (and thus no change in fuel flow rate) the system would settle into a new equilibrium with the temperature decreased by 4 percent and the speed decreased by 2 percent. Equations (3-2) and (3-3) would change to

$$\dot{T} = 1/\tau_b \cdot [K_b \cdot W_f - T] - 1/\tau_b \cdot [.04\ K_b \cdot W_f] \qquad (3\text{-}23)$$

$$\dot{N}_0 = 1/\tau_t \cdot [K_t \cdot T - N_0] + 1/\tau_t \cdot [.02\ K_t \cdot K_b \cdot W_f] \qquad (3\text{-}24)$$

The corresponding state equation is

$$\begin{bmatrix} \dot{W}_f \\ \dot{T} \\ \dot{N}_0 \end{bmatrix} = \begin{bmatrix} -1/\tau_f & 0 & -K_p K_f/\tau_f \\ K_b/\tau_b & -1/\tau_b & 0 \\ 0 & K_t/\tau_t & -1/\tau_t \end{bmatrix} \begin{bmatrix} W_f \\ T \\ N_0 \end{bmatrix} + \begin{bmatrix} K_p K_f/\tau_f \\ 0 \\ 0 \end{bmatrix} u + \begin{bmatrix} 0 \\ -.04 K_b/\tau_b W_f \\ .02 K_t K_b/\tau_b \end{bmatrix} \tag{3-25}$$

So the event vector for this failure is

$$\underline{f}_v = k \begin{bmatrix} 0 \\ -.04\ K_b/\tau_b \\ .02\ K_t K_b/\tau_t \end{bmatrix} = k \begin{bmatrix} 0 \\ -.8 \\ .08 \end{bmatrix} \tag{3-26}$$

where k is an arbitrary constant. Choosing $k = 100/8$, we have

$$\underline{f}_v = \begin{bmatrix} 0 \\ -10 \\ 1 \end{bmatrix}$$

We see that $\underline{f}_v$ is a linear combination of $\underline{f}_b$ and $\underline{f}_t$:

$$\underline{f}_v = -10\ \underline{f}_b + \underline{f}_t$$

Therefore, $\underline{f}_v$ satisfies the conditions set forth in Chapter 2 for output stationarity. If λ_b is set equal to λ_t, $\underline{f}_v$ will produce a residual vector that is unidirectional along

$$C\underline{f}_v = \begin{bmatrix} 0 \\ -10 \\ 1 \end{bmatrix}$$

To verify that this is correct, we apply Equation (2-64) to $\underline{f}_v$, using D from (3-19) with $\lambda_b = \lambda_t$:

$$DC\underline{f}_v \stackrel{?}{=} -\lambda_t \underline{f}_v + A\underline{f}_v \qquad (3\text{-}27)$$

$$[A-DC]\underline{f}_v \stackrel{?}{=} \lambda_t \underline{f}_v$$

$$\begin{bmatrix} \lambda_f & 0 & 0 \\ 0 & \lambda_t & 0 \\ 0 & 0 & \lambda_t \end{bmatrix} \begin{bmatrix} 0 \\ -10 \\ 1 \end{bmatrix} \stackrel{?}{=} \lambda_t \begin{bmatrix} 0 \\ -10 \\ 1 \end{bmatrix}$$

$$\begin{bmatrix} 0 \\ -10\lambda_t \\ 1\lambda_t \end{bmatrix} = \begin{bmatrix} 0 \\ -10\lambda_t \\ 1\lambda_t \end{bmatrix}$$

Thus the assertion is correct.

In summary, with D given by

$$D = \begin{bmatrix} -10-\lambda_f & 0 & -5 \\ 20 & -1-\lambda_t & 0 \\ 0 & .2 & -2-\lambda_t \end{bmatrix} \qquad (3\text{-}28)$$

each $\underline{f}$ in $\{\underline{f}_f, \underline{f}_b, \underline{f}_t, \underline{f}_v\}$ produces a unidirectional residual. A failure in any of the corresponding components would be identified by a residual lying solely along the appropriate failure direction. For this example, the λ's should probably be between -5 and -20, unless the measurements are exceptionally free of noise, in which case they could be more negative.

3.3 THREE STATE VARIABLES, TWO SENSORS

Removing the fuel flow meter makes the steam turbine system less than fully measured and complicates the design of a detection filter for it. The state equation of the system remains the same, but the measurement equation changes to

$$\begin{bmatrix} T_0 \\ N_0 \end{bmatrix} = \begin{bmatrix} 0 & 1 & 0 \\ 0 & 0 & 1 \end{bmatrix} \begin{bmatrix} W_f \\ T \\ N_0 \end{bmatrix} \tag{3-29}$$

The dimension of D changes, and the state equation of the filter becomes

$$\begin{bmatrix} \dot{\hat{W}}_f \\ \dot{\hat{T}} \\ \dot{\hat{N}}_0 \end{bmatrix} = \begin{bmatrix} -10 & 0 & -5 \\ 20 & -1 & 0 \\ 0 & .2 & -2 \end{bmatrix} \begin{bmatrix} \hat{W}_f \\ \hat{T} \\ \hat{N}_0 \end{bmatrix} + \begin{bmatrix} 5 \\ 0 \\ 0 \end{bmatrix} u + \begin{bmatrix} d_{11} & d_{12} \\ d_{21} & d_{22} \\ d_{31} & d_{32} \end{bmatrix} \begin{bmatrix} T_0-\hat{T}_0 \\ N_0-\hat{N}_0 \end{bmatrix} \tag{3-30}$$

Suppose we are concerned about the same malfunctions as before. This time not more than two of the event vectors at a time will be output separable. Let us choose the pair $\{\underline{f}_b, \underline{f}_t\}$. The vectors $C\underline{f}_b$ and $C\underline{f}_f$ are easily verified as nonzero and linearly independent and hence, as output separable.

The impact of $\underline{f}_b$ on the design of the detection filter will be different than before, as the event space of $\underline{f}_b$ is no longer one-dimensional. Noting that $C\underline{f}_f$ equals zero and that $CA\underline{f}_f$ is proportional to $C\underline{f}_b$, we conclude that the event vector $\underline{f}_f$ is in the event space of $\underline{f}_b$. The event order of $\underline{f}_b$ is two. Malfunctions of the fuel valve cannot now be distinguished from malfunctions of the boiler by monitoring only the direction of the residual vector.

To find the event generator $\underline{g}_b$ for the event space of $\underline{f}_b$, we use (2-35) to obtain

$$\begin{aligned} C\underline{g}_b &= \underline{0} \\ A\underline{g}_b &= \underline{f}_b \end{aligned} \tag{3-31}$$

The solution is

$$\underline{g}_b = \begin{bmatrix} -.05 \\ 0 \\ 0 \end{bmatrix} \tag{3-32}$$

Let λ_1 and λ_2 denote the two eigenvalues of [A-DC] that will now be associated with $\underline{f}_b$, and let λ_3 be the eigenvalue associated with $\underline{f}_t$ (the event order of $\underline{f}_t$ is still one). Applying Equation (2-46) to each of $\underline{f}_b$ and $\underline{f}_t$, we obtain the two polynomials

$$\begin{aligned} (s-\lambda_1)(s-\lambda_2) &= s^2 + p2_b s + p1_t \\ (s-\lambda_3) &= s + p1_t \end{aligned} \tag{3-33}$$

From (2-64), the two vector equations that determine D are

$$\begin{aligned} DC\underline{f}_b &= p1_b\underline{g}_b + p2_b A\underline{g}_b + A^2\underline{g}_b \\ DC\underline{f}_t &= p1_t\underline{f}_t + A\underline{f}_t \end{aligned} \tag{3-34}$$

The solution for D is

$$D = \begin{bmatrix} .05\lambda_1\lambda_2 + .5(\lambda_1+\lambda_2) + 5 & -5 \\ -(\lambda_1+\lambda_2) - 11 & 0 \\ .2 & -(2+\lambda_3) \end{bmatrix} \tag{3-35}$$

Then

$$[A-DC] = \begin{bmatrix} -10 & -.05\lambda_1\lambda_2 - .5(\lambda_1+\lambda_2) - 5 & 0 \\ 20 & 10 + (\lambda_1+\lambda_2) & 0 \\ 0 & 0 & -\lambda_3 \end{bmatrix} \tag{3-36}$$

Note that unless either λ_1 or λ_2 equals -10, $\underline{f}_b$ is not an eigenvector of [A-DC]. The feedback matrix D has been so specified, however, that any vector that can be written as a linear combination of $\underline{g}_b$ and $\underline{f}_f$ is is projected by [A-DC] into a vector that is also a linear combination of $\underline{g}_b$ and $\underline{f}_b$. All such vectors when projected by C into the residual space lie on $C\underline{f}_b$, which is on the T_0-axis. The reason $[A-DC]\underline{f}_b$ has a component along $\underline{g}_b$ is that the residual $(T_0-\hat{T}_0)$ is multiplied by the gain

$$d_{11} = .05\ \lambda_1\lambda_2 + .5\ (\lambda_1 + \lambda_2) + 5$$

and is fed back to update $\hat{W}_f$.

The fourth event vector, $\underline{f}_v$, can again be made output stationary, but doing so makes one of the eigenvalues of [A-DC] unassignable. This happens because the event orders of $\underline{f}_b$ and $\underline{f}_t$ are no longer equal. For $\underline{f}_v$ to satisfy the relation (3-27),

$$DC\underline{f}_v = -\lambda_3\underline{f}_v + A\underline{f}_v \qquad (3\text{-}37)$$

it is necessary that

$$.05\lambda_1\lambda_2 + .5(\lambda_1+\lambda_2) + 5 = 0 \qquad (3\text{-}38)$$

and

$$-(\lambda_1+\lambda_2) - 11 = -\lambda_3 - 1 \qquad (3\text{-}39)$$

Consequently, if $\underline{f}_v$ is to be output stationary, we must set λ_1 equal to -10, in addition to making λ_2 and λ_3 equal. Thus by including the loss of a nozzle vane in the set of identifiable failures, we force λ_1 to take on the value that makes d_{11} zero, eliminating the feedback of $(T_0-\hat{T}_0)$ to $\hat{W}_f$. This prevents the residual $(T_0-\hat{T}_0)$ from causing a change in itself that would alter the ratio between it and $(N_0-\hat{N}_0)$.

3.4 A RESTRICTIVE SET OF EVENT VECTORS

For this part of the example, we take the steam turbine system as originally described and now use the fuel flow measurement in a feedback loop around the fuel metering valve, as shown in Figure 3.3. For ease of calculation, we assign a gain of one to this loop. The system dynamics are little changed, and if the valve, sensor, and feedback loop are considered a single unit, then the task of failure detection and identification is the same as before. But by separately modeling the sensor and the valve, we can design a detection filter that produces unique unidirectional residuals in reponse both to valve failures and to sensor failures.

To do this, we include the sensor's measurement W_{f0} in the state vector and add the sensor's dynamics to the reference model. Suppose the sensor has a first-order response and is ten times faster than the valve; then the state equation and the output equation become

$$\frac{d}{dt}\begin{bmatrix} W_f \\ W_{f0} \\ T \\ N \end{bmatrix} = \begin{bmatrix} -10 & -2.5 & 0 & -5 \\ 100 & -100 & 0 & 0 \\ 20 & 0 & -1 & 0 \\ 0 & 0 & .2 & -2 \end{bmatrix} \begin{bmatrix} W_f \\ W_{f0} \\ T \\ N \end{bmatrix} + \begin{bmatrix} 5 \\ 0 \\ 0 \\ 0 \end{bmatrix} u \qquad (3\text{-}40a)$$

$$\begin{bmatrix} W_{f0} \\ T_0 \\ N_0 \end{bmatrix} = \begin{bmatrix} 0 & 1 & 0 & 0 \\ 0 & 0 & 1 & 0 \\ 0 & 0 & 0 & 1 \end{bmatrix} \begin{bmatrix} W_f \\ W_{f0} \\ T \\ N \end{bmatrix} \qquad (3\text{-}40b)$$

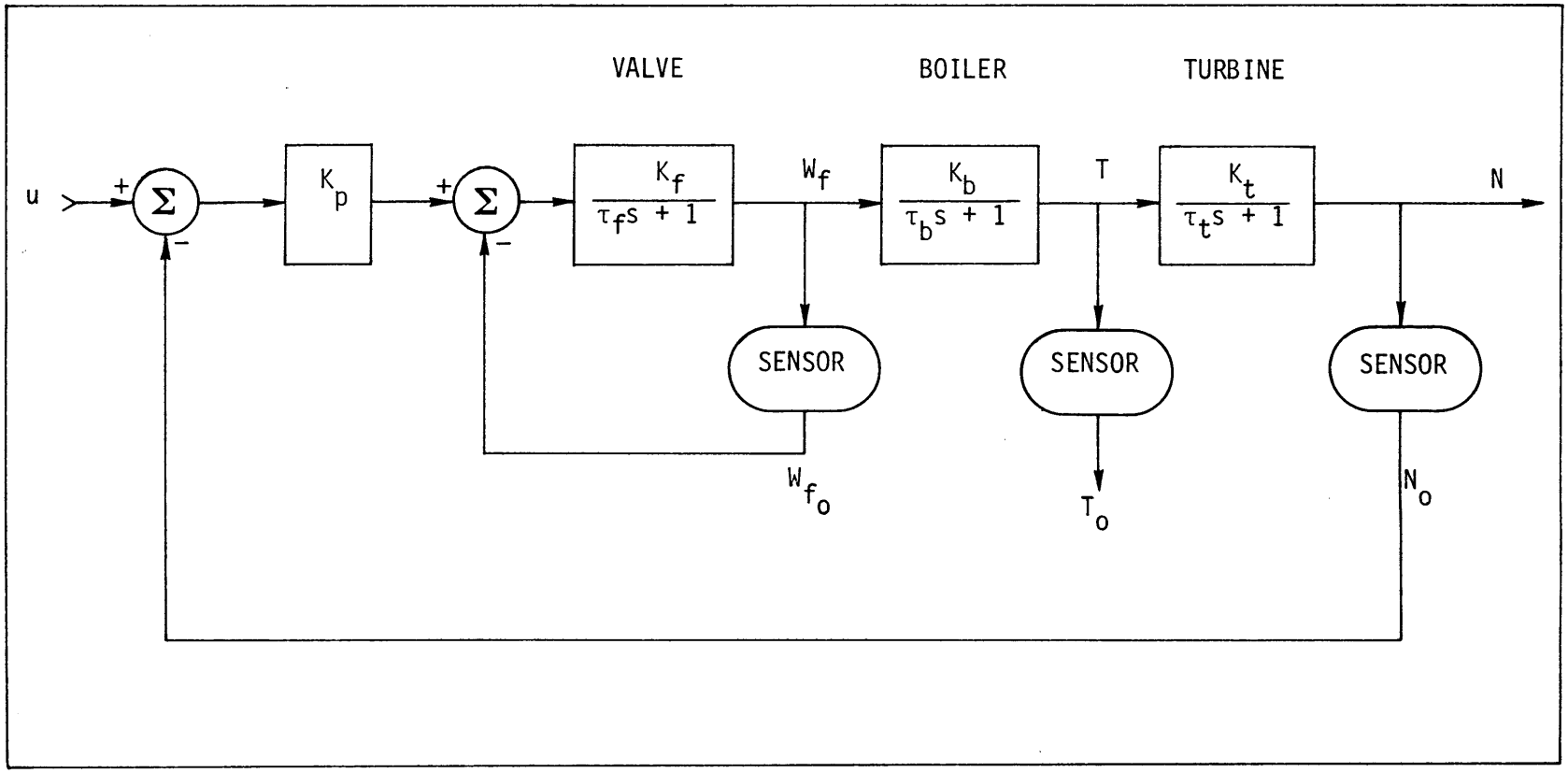

Figure 3.3. The steam turbine system with a fuel control loop.

The event vectors for the valve and the sensor are

$$\underline{f}_f = \begin{bmatrix} 1 \\ 0 \\ 0 \\ 0 \end{bmatrix} \qquad \underline{f}_s = \begin{bmatrix} 0 \\ 1 \\ 0 \\ 0 \end{bmatrix} \tag{3-41}$$

The residual induced by any failure of the sensor will be unidirectional along

$$C\underline{f}_s = \begin{bmatrix} 1 \\ 0 \\ 0 \end{bmatrix}$$

For the valve's event vector, we have $C\underline{f}_f = \underline{0}$, so $\underline{f}_f$ must be replaced by any scalar multiple of $A\underline{f}_f$. That vector is

$$\begin{bmatrix} -10 \\ 100 \\ 20 \\ 0 \end{bmatrix}$$

As the replacement for $\underline{f}_f$, we choose

$$\underline{f}_f = \begin{bmatrix} -.5 \\ 5 \\ 1 \\ 0 \end{bmatrix}$$

The failure vector for $\underline{f}_f$ is

$$C\underline{f}_f = \begin{bmatrix} 5 \\ 1 \\ 0 \end{bmatrix}$$

We now have five event vectors:

$$\underline{f}_s = \begin{bmatrix} 0 \\ 1 \\ 0 \\ 0 \end{bmatrix} \quad \underline{f}_f = \begin{bmatrix} -.5 \\ 5 \\ 1 \\ 0 \end{bmatrix} \quad \underline{f}_b = \begin{bmatrix} 0 \\ 0 \\ 1 \\ 0 \end{bmatrix} \quad \underline{f}_t = \begin{bmatrix} 0 \\ 0 \\ 0 \\ 1 \end{bmatrix} \quad \underline{f}_v = \begin{bmatrix} 0 \\ 0 \\ -10 \\ 1 \end{bmatrix}$$

The three output separable vectors $\underline{f}_s$, $\underline{f}_b$, and $\underline{f}_t$ form a reasonable set on which to base the design of the detection filter. The remaining two,

$\underline{f}_f$ and $\underline{f}_v$, satisfy the conditions for mutual output stationarity; we can accommodate them when we assign the eigenvalues of the filter.

The set $\{\underline{f}_s, \underline{f}_b, \underline{f}_t\}$ is a restrictive one--there will be an eigenvalue of [A-DC] that cannot be altered. Three of the four directions in the state space are spanned by $\{\underline{f}_s, \underline{f}_b, \underline{f}_t\}$; it is the fourth direction, $\underline{e}_1 = [1,0,0,0]$, with which that eigenvalue will be associated. The difficulty is that any vector $k\underline{e}_1$ along this direction is projected by A into a linear combination of $\underline{e}_1$, $\underline{f}_s$, and $\underline{f}_b$, not just of either $\underline{e}_1$ and $\underline{f}_s$ or $\underline{e}_1$ and $\underline{f}_b$:

$$Ak\begin{bmatrix}1\\0\\0\\0\end{bmatrix} = k\begin{bmatrix}-10\\-10\\100\\0\end{bmatrix} = k[-10\underline{e}_1 + 100\underline{f}_s + 20\underline{f}_b]$$

Therefore, $\underline{e}_1$ is not in the event space of either $\underline{f}_s$ or $\underline{f}_b$, and both their event orders equal one. The event order of $\underline{f}_t$ is also one; thus the sum of the three of them is one less than the dimension of the state space. Consequently, there will be one unassignable eigenvalue.

With λ_1, λ_1, and λ_3 denoting the assignable eigenvalues, Equations (2-63) and (2-64) yield

$$\begin{aligned}[A-DC]\underline{f}_s &= \lambda_1\underline{f}_s\\ [A-DC]\underline{f}_b &= \lambda_2\underline{f}_b\\ [A-DC]\underline{f}_t &= \lambda_3\underline{f}_t\end{aligned} \qquad (3\text{-}42)$$

The solution for D is

$$D = \begin{bmatrix}-2.5 & 0 & -5\\ -100-\lambda_1 & 0 & 0\\ 0 & -1-\lambda_2 & 0\\ 0 & .2 & -2-\lambda_3\end{bmatrix} \qquad (3\text{-}43)$$

and

$$[A\text{-}DC] = \begin{bmatrix} -10 & 0 & 0 & 0 \\ 100 & \lambda_1 & 0 & 0 \\ 20 & 0 & \lambda_2 & 0 \\ 0 & 0 & 0 & \lambda_3 \end{bmatrix} \qquad (3\text{-}44)$$

The unassignable eigenvalue is -10, the eigenvalue associated with the time response of the fuel valve.[1] This value is acceptable--it guarantees that the portion of the filter representing the valve will be stable.

The two remaining event vectors, $\underline{f}_f$ and $\underline{f}_v$, can both be made output stationary. As before, to do so with $\underline{f}_v$, simply set $\lambda_3 = \lambda_2$. And with $\underline{f}_f$, we have

$$\underline{f}_f = 5\underline{f}_s + \underline{f}_b - .5\underline{e}_1$$

Because $A\underline{e}_1$ is a linear combination of $\underline{f}_s$, $\underline{f}_b$, and $\underline{f}_f$, $\underline{f}_t$ satisfies the conditions for output stationarity. Thus with all three assignable eigenvalues given the same value, all five vectors in the set $\{\underline{f}_s, \underline{f}_f, \underline{f}_b, \underline{f}_t, \underline{f}_v\}$ generate unidirectional residuals.

3.5 AVOIDING AN UNASSIGNABLE EIGENVALUE

Previously, no matter which three vectors were chosen for the output separable set and which two were subsequently made output stationary, in the end the feedback matrix D would always be the same and one eigenvalue would be -10. If this is unacceptable, we could choose our set of output separable vectors specifically to avoid the unassignable eigenvalue and then refrain from making either of the two remaining event vectors output stationary. We would have to leave them for a second detection filter or for some other detection device.

---

[1] With systems in which the state variables are cross-coupled, not just cascaded, an unassignable eigenvalue will not necessarily be an eigenvalue of the system.

For example, one subset of $\{\underline{f}_s, \underline{f}_f, \underline{f}_b, \underline{f}_t, \underline{f}_t\}$ that is nonrestrictive is $\{\underline{f}_s, \underline{f}_f, \underline{f}_t\}$. The event space of $\underline{f}_f$ is two-dimensional--it is the plane spanned by $\underline{f}_f$ and $\underline{e}_1$--consequently the sum of the event orders of $\underline{f}_s$, $\underline{f}_f$, and $\underline{f}_t$ is four, and there can be no unassignable eigenvalues.

The solution for D is, with λ_0, λ_1, λ_2, and λ_3 denoting the eigenvalues,

$$D = \begin{bmatrix} -2.5 & .05\lambda_0\lambda_2 + .5(\lambda_0+\lambda_2) + 5 & -5 \\ -100-\lambda_1 & 5[-(10+\lambda_0) + \lambda_1 - \lambda_2] & 0 \\ 0 & -(10+\lambda_0) - (1+\lambda_2) & 0 \\ 0 & .2 & -(2+\lambda_3) \end{bmatrix} \tag{3-45}$$

Then

$$[A-DC] = \begin{bmatrix} -10 & 0 & -[.05\lambda_0\lambda_2 + .5(\lambda_0+\lambda_2) + 5 & 0 \\ 100 & \lambda_1 & -5[-(10+\lambda_0) + \lambda_1 - \lambda_2] & 0 \\ 20 & 0 & (10+\lambda_0) + \lambda_2 & 0 \\ 0 & 0 & 0 & \lambda_3 \end{bmatrix} \tag{3-46}$$

The temperature residual, $T_0-\hat{T}_0$, is now fed back to $\hat{W}_f$ and $\hat{W}_{f0}$.

A way of avoiding the unassignable eigenvalue while keeping four event vectors instead of only three is to add another variable to the state vector. With this example, a simple way to do this is to add a duplicate of W_f. This creates a model in which W_f*, the new variable, is the input to W_{f0} and W_f is the input to T. The state equation for this model is

$$\begin{bmatrix} \dot{W}_f \\ \dot{W}_f^* \\ \dot{W}_{f0} \\ \dot{T} \\ \dot{N}_0 \end{bmatrix} = \begin{bmatrix} -10 & 0 & -2.5 & 0 & -5 \\ 0 & -10 & -2.5 & 0 & -5 \\ 0 & 100 & -100 & 0 & 0 \\ 20 & 0 & 0 & -1 & 0 \\ 0 & 0 & 0 & .2 & -2 \end{bmatrix} \begin{bmatrix} W_f \\ W_f^* \\ W_{f0} \\ T \\ N_0 \end{bmatrix} + \begin{bmatrix} 5 \\ 5 \\ 0 \\ 0 \\ 0 \end{bmatrix} u \tag{3-48}$$

The five event vectors are:

$$\underline{f}_s = \begin{bmatrix} 0 \\ 0 \\ 1 \\ 0 \\ 0 \end{bmatrix} \quad \underline{f}_f = \begin{bmatrix} -.5 \\ 0 \\ 5 \\ 1 \\ 0 \end{bmatrix} \quad \underline{f}_b = \begin{bmatrix} 0 \\ 0 \\ 0 \\ 1 \\ 0 \end{bmatrix} \quad \underline{f}_t = \begin{bmatrix} 0 \\ 0 \\ 0 \\ 0 \\ 1 \end{bmatrix} \quad \underline{f}_v = \begin{bmatrix} 0 \\ 0 \\ 0 \\ -10 \\ 1 \end{bmatrix}$$

We find this time that the event orders of $\underline{f}_s$ and $\underline{f}_b$ are both two; consequently, $\{\underline{f}_s, \underline{f}_b, \underline{f}_t\}$ is now a nonrestrictive set. The previously unassignable eigenvalue has been displaced by two assignable ones. Making $\underline{f}_t$ output stationary poses no difficulty; simply assign the same two values to the pairs of eigenvalues associated with $\underline{f}_s$ and $\underline{f}_b$. On the other hand, making $\underline{f}_v$ output stationary requires not only setting the eigenvalue associated with $\underline{f}_t$ equal to one of those of $\underline{f}_b$, but also allowing the other eigenvalue of $\underline{f}_b$ to revert to -10.

Taken together, the various parts of this example illustrate that there are many ways to design a detection filter for a given system. The number of measurements used and the way the reference model is constructed strongly influence the design of the filter.

Chapter IV

METHODS FOR APPLICATION

Thus far the discussion of detection filters has been in the context of systems with continuously measured outputs, but the potential applications are mostly in systems with digital electronic controllers that only take measurements periodically. The following section presents the extension of the material in Chapter 2 needed to fit a detection filter into this context. Then Section 4.2 presents a special case of detection filter design that draws sparingly from the general theory in Chapter 2, but which describes in concise form all that is necessary for designing a detection filter for the F100 engine. The third section describes a technique for interpreting the residuals produced by a detection filter.

4.1 SAMPLED-DATA SYSTEMS

To design a detection filter that is implementable on a microcomputer, we must first formulate the system model in a manner compatible with digital computation. The resulting model is said to be in sampled-data or discrete-time form. The procedure for designing a detection filter for such a model is identical to that used with a continuous-time model. For some types of failures there will be no degradation in performance of the filter, but for others, particularly those that involve changes in the dynamics of the system, the discontinuity in the measurements prevents the filter from keeping failure-induced residuals exactly unidirectional. But when the time interval between measurement samples is small, the deviations in the residuals will be small as well.

4.1.1 Discrete-Time Models

Discrete-time models are readily calculated from continuous-time ones. The form of the continuous-time models we are concerned with is

$$\dot{\underline{x}}(t) = A\underline{x}(t) + B\underline{u}(t) \tag{4-1a}$$

$$\underline{y}(t) = C\underline{x}(t) \tag{4-1b}$$

In a discrete-time model, the differential equation is replaced by a difference equation. If we define $\underline{x}_k$, $\underline{u}_k$, and $\underline{y}_k$ as the state, the input, and the measurement vectors at the sampling times $t_k = k \cdot \Delta t$, $k=0,1,2,3,\cdots$ (with Δt constant), and if we assume that $\underline{u}(t)$ changes only at the times t_k, then the discrete-time model derived from (4-1) has the following form:

$$\underline{x}_{k+1} = \Phi\underline{x}_k + \Gamma\underline{u}_k \tag{4-2a}$$

$$\underline{y}_{k+1} = C\underline{x}_{k+1} \tag{4-2b}$$

The n x n matrix Φ is called the state transition matrix, and Γ, the input transfer matrix.

We obtain Φ and Γ from the solution of (4-1a). As we shall prove, that solution is[1]

$$\underline{x}(t) = \exp(A \cdot t)\, \underline{x}(0) + \int_0^t \exp(A \cdot (t-\tau))\, B\underline{u}(\tau)\, d\tau \tag{4-3}$$

$$\underline{x}(0) = \underline{x}_0 \,, \quad \text{given.} \tag{4-4}$$

---

[1] The exponential of any square matrix M is defined as

$$\exp(M) = I + M + \frac{1}{2}M^2 + \frac{1}{2 \cdot 3}M^3 + \cdots \frac{1}{n!}M^n + \cdots$$

The proof follows from substituting (4-3) into (4-1a): The derivative of (4-3) is

$$\dot{\underline{x}}(t) = \frac{d}{dt}[\exp(A\cdot t)\ \underline{x}(0)] + \int_0^t \frac{d}{dt}[\exp(A\cdot(t-\tau))\ B\underline{u}(\tau)\ d\tau] + [\exp(A\cdot(t-\tau))\ B\underline{u}(\tau)]\Big|_{\tau=t} \tag{4-5}$$

Since A is constant, we have

$$\frac{d}{dt}[\exp(A\cdot t)] = A\ \exp(A\cdot t)$$

and hence,

$$\dot{\underline{x}}(t) = A\ \{\exp(A\cdot t)\ \underline{x}(0) + \int_0^t \exp(A\cdot(t-\tau))\ B\underline{u}(\tau)\ d\tau\} + \exp(0)\cdot B\underline{u}(t) \tag{4-6}$$

The expression in brackets is $\underline{x}(t)$, so (4-6) is equivalent to (4-1a). Thus $\underline{x}(t)$ as given in (4-3) is the solution to (4-1a). We now define $\Phi(t)$ and $\Gamma(t)$ as follows:

$$\Phi(t) \equiv \exp(A\cdot t) \tag{4-7}$$

$$\Gamma(t) \equiv \Psi(t)\ B \tag{4-8}$$

The n x n matrix $\Psi(t)$ is defined by

$$\Psi(t) \equiv \int_0^t \Phi(t-\tau)\ d\tau \tag{4-9}$$

Now, noting that B is constant and that $\underline{u}(\tau)$ is constant over each sampling interval, we substitute Equations (4-7) to (4-9) into (4-3) and set

$$t = \Delta t = t_{k+1} - t_k$$

$$\underline{x}_0 = \underline{x}_k$$

$$\Phi = \Phi(\Delta t)$$

$$\Gamma = \Gamma(\Delta t)$$

to obtain Equation (4-2a).

There are several methods for calculating Φ and Γ. Frequently in applications where a detection filter is to be used, the sampling interval Δt will be relatively small, and when that is so, the most efficient way to find Φ is to calculate it directly from the definition of the matrix exponential:

$$\Phi = I + A\Delta t + \frac{1}{2}A^2\Delta t^2 + \cdots + \frac{1}{n!}A^n\Delta t^n + \cdots \qquad (4\text{-}10)$$

With small Δt, the number of terms required for acceptable accuracy is reasonable.[2] Alternatively, one may obtain an explicit closed-form solution by using Sylvester's Expansion Formula.[3] A third method is numerical integration of the derivative of Equation (4-7):

$$\dot{\Phi}(t) = A\,\Phi(t) \qquad (4\text{-}11)$$

Integrating from $t = 0$ to $t = \Delta t$, with $\Phi(0) = I$, yields Φ.[4]

The matrix Γ also can be computed by direct numerical integration or by series expansion, but when A is invertible, a closed-form solution

---

[2] An eighth-order model of the F100 engine required from four to six terms, depending on the size of Δt, for an accuracy of four to five decimal places.

[3] See, for instance, Schultz and Melsa [39], p.141.

[4] In contrast to the other two methods, this technique is valid even when A is not constant. In that case, Φ depends explicitly on both the initial and final times, not just the difference between them.

for Γ exists. Considering first the solution by integration, we combine (4-8) and (4-9) and differentiate the result to obtain

$$\dot{\Gamma}(t) = \Phi(t)\, B \tag{4-12}$$

Simultaneous integration of (4-12) and (4-11), beginning with $\Gamma(0) = 0$, yields $\Gamma(t)$.

Alternatively, by series expansion,

$$\Gamma = \left[I\Delta t + \frac{1}{2}A\Delta t^2 + \cdots + \frac{1}{(n+1)!}A^n\Delta t^{n-1} + \cdots\right] B$$

Supposing now that Φ can be easily determined by series expansion and that A is nonsingular, we can obtain from (4-9) and (4-11) an explicit relation for Ψ. (The F100 model fits these conditions.) The integral of (4-11) from $t = 0$ to $t = \Delta t$ is

$$\int_0^{\Delta t} \dot{\Phi}(\tau')\, d\tau' = \int_0^{\Delta t} A\, \Phi(\tau')\, d\tau'$$

or

$$\Phi(\Delta t) - \Phi(0) = A \int_0^{\Delta t} \Phi(\tau')\, d\tau' \tag{4-13}$$

where τ' is the dummy variable of integration. If we define

$$\tau \equiv \Delta t - \tau'$$

then since $d\tau' = -d\tau$ and $\Phi(0) = I$, we can write (4-13) as

$$-A \int_{\Delta t}^{0} \Phi(\Delta t - \tau)\, d\tau = \Phi - I$$

Swapping the limits of integration and multiplying by A^{-1} gives

$$\int_0^{\Delta t} \Phi(\Delta t-\tau)\, d\tau = A^{-1}[\Phi - I]$$

Using (4-9), we get

$$\Psi = A^{-1}[\Phi - I] \tag{4-14}$$

From (4-8), Γ follows immediately as the product of Ψ and B:

$$\Gamma = A^{-1}[\Phi - I]B \tag{4-15}$$

4.1.2 Detection Filter Design

A detection filter for (4-3) will have the form

$$\begin{aligned} \hat{\underline{x}}_{k+1} &= \Phi\hat{\underline{x}}_k + \Gamma\underline{u}_k + D(\underline{y}_k - \hat{\underline{y}}_k) \\ \hat{\underline{y}}_{k+1} &= C\hat{\underline{x}}_{k+1} \end{aligned} \tag{4-16}$$

The state difference vector and the residual vector are defined as before:

$$\underline{q}_k = \underline{x}_k - \hat{\underline{x}}_k \tag{4-17}$$

$$\underline{r}_k = \underline{y}_k - \hat{\underline{y}}_k \tag{4-18}$$

Just as in the continuous-time case, we seek a feedback matrix D that will constrain $\underline{r}$ to a line or to a plane when any one of a number of specified components and sensors fails. Clearly, this D will not be the same as the one that would be used if the filter were implemented with continuous measurements.

In Chapter 2, many different types of failures were demonstrated to be describable by what was called the input failure model,

$$\dot{\underline{x}}(t) = A\underline{x}(t) + B\underline{u}(t) + n(t)\underline{f} \tag{4-19}$$

The discrete-time form of this is found by the same procedure used to derive (4-3) from (4-1):

$$\underline{x}_{k+1} = \Phi\underline{x}_k + \Gamma\underline{u}_k + [\int_0^{\Delta t} \Phi(\Delta t-\tau)\cdot n(t_k+\tau)\cdot d\tau]\underline{f} \tag{4-20}$$

Whenever n(t) can be considered invariant over each sampling interval, (4-20) reduces to

$$\underline{x}_{k+1} = \Phi\underline{x}_k + \Gamma\underline{u}_k + n_k\underline{f}' \tag{4-21}$$

where

$$\underline{f}' = \Psi\underline{f} \tag{4-22}$$

When (4-21) is valid, the theory in Chapter 2 is fully applicable, with A and $\underline{f}$ replaced by Φ and $\underline{f}'$; and the procedure for calculating D is unchanged. When n(t) is not piecewise constant and (4-21) is not strictly valid, a filter does not exist that can keep $\underline{r}$ exactly unidirectional for arbitrary n(t).

Subtracting (4-16) from (4-20), we see that the dynamics of $\underline{q}$ and $\underline{r}$ are described by

$$\begin{aligned} \underline{q}_{k+1} &= [\Phi - DC]\underline{q}_k + [\int_0^{\Delta t} \Phi(\Delta t-\tau)\cdot n(t_k+\tau)\cdot d\tau)\underline{f} \\ \underline{r}_{k+1} &= C\underline{q}_{k+1} \end{aligned} \tag{4-23}$$

When n(t) is piecewise constant, these equations become

$$\begin{aligned} \underline{q}_{k+1} &= [\Phi - DC]\underline{q}_k + n_k\underline{f}' \\ \underline{r}_{k+1} &= C\underline{q}_{k+1} \end{aligned} \tag{4-24}$$

The reason there is no choice of D which makes (4-23) a detection filter is that the vector

$$[\int_0^{\Delta t} \Phi(\Delta t-\tau)\cdot n(t_k+\tau)\cdot d\tau]\underline{f}$$

is not fixed in direction, even though $\underline{f}$ is fixed. When the direction of this vector changes, so too will the direction of $\underline{r}$, regardless of what D is.

So in designing detection filters for discrete-time implementation, we can only design for failures for which n(t) either is piecewise constant or can be reasonably approximated as such. Failures that are likely to be piecewise constant are incorrect transmissions of an element of $\underline{u}$. These are easily modeled with $\underline{f}'$ equal to the appropriate column of Γ and with n equal to the deviation in the element of $\underline{u}$. Some state-independent changes in dynamics can also be modeled exactly with n(t) piecewise constant. But most changes in dynamics, particularly those involving changes in the A matrix, cannot be. Approximating n(t) as piecewise constant is reasonable whenever its change during each sampling interval is small. In practice, this may frequently be the case, for Δt is usually set so the digital controller functions well, which most often means Δt is small relative to the dominant response times of the system.

Sensor failures modeled by the measurement failure model (2-30) constitute a group of failures for which n(t) is always piecewise constant. Failures of this type are described by

$$\underline{x}_{k+1} = \Phi\underline{x}_k + \Gamma\underline{u}_k \tag{4-25a}$$

$$\underline{y}_{k+1} = C\underline{x}_{k+1} + n_k\underline{e}_j \tag{4-25b}$$

Unlike malfunctions that affect the system directly, erroneous measurements only have influence at the sampling times, so in (4-25b) n_k is inherently a discrete variable, not a continuous one.

The response of the filter (4-16) to a failure modeled by (4-25) is given by

$$\begin{aligned} \hat{\underline{x}}_{k+1} &= \Phi\hat{\underline{x}}_k + \Gamma\underline{u}_k + DC[\underline{x}_k - \hat{\underline{x}}_k] + n_j\underline{d}_j \\ \hat{\underline{y}}_{k+1} &= C\hat{\underline{x}}_{k+1} + n_{k+1}\cdot\underline{e}_j \end{aligned} \tag{4-26}$$

where $\underline{d}_j$ is again the j'th column of D. The unit vector $\underline{e}_j$ and the vector $\underline{d}_j$ are both fixed and are both uniquely associated with the j'th sensor; therefore, just as with a continuous-time filter, D can be chosen so that when the sensor fails, the residual will stay within the plane defined by $\underline{e}_j$ and $\underline{d}_j$. Furthermore, as will be shown in Section 4.3, if n_k is increasing or is steady, $\underline{r}$ will stay within just one segment of that plane.

4.1.3 Summary

The discrete-time model is

$$\begin{aligned} \underline{x}_{k+1} &= \Phi\underline{x}_k + \Gamma\underline{u}_k \\ \underline{y}_{k+1} &= C\underline{x}_k \end{aligned} \tag{4-2}$$

with Φ and Γ given by

$$\Phi = I + A\Delta t + \frac{1}{2}A^2\Delta t^2 + \cdots + \frac{1}{n!}A^n\Delta t^n + \cdots \tag{4-10}$$

$$\Gamma = A^{-1}[\Phi - I]B \tag{4-15}$$

(If A is not invertible, use Equation (4-12).)

The discrete-time detection filter is

$$\begin{aligned} \hat{\underline{x}}_{k+1} &= \Phi\hat{\underline{x}}_k + \Gamma\underline{u}_k + D[\underline{y}_k - \hat{\underline{y}}_k] \\ \hat{\underline{y}}_{k+1} &= C\hat{\underline{x}}_{k+1} \end{aligned} \tag{4-16}$$

The event vectors are computed from the continuous-time ones by using

$$\underline{f}' = A^{-1}[\Phi - I]\underline{f} \tag{4-27}$$

(This relation follows from (4-14) and (4-22).) The discrete-time event generators $\underline{g}'$ and the event spaces $\mathcal{f}'$ are found by applying the procedures given in Chapter 2, with Φ and $\underline{f}'$ in place of A and $\underline{f}$.

The feedback matrix D is then the solution of the following equations obtained from (2-64):

$$\begin{aligned} DC\underline{f}_1' &= p_{11}\underline{g}_1' + p_{12}\Phi\underline{g}_1' + \cdots + p_{1\nu_1}\Phi^{\nu_1-1}\underline{g}_1' + \Phi^{\nu_1}\underline{g}_1' \\ &\vdots \\ DC\underline{f}_m' &= p_{m1}\underline{g}_m' + p_{m2}\Phi\underline{g}_m' + \cdots + p_{m\nu_m}\Phi^{\nu_m-1}\underline{g}_m' + \Phi^{\nu_m}\underline{g}_m' \end{aligned} \tag{4-28}$$

Here, m is the number of independent measurements (it is assumed that there are m event vectors, so that D is fully specified). The eigenvalues λ' assigned to $[\Phi-DC]$ are related to the continuous-time λ's by

$$\lambda' = \exp(\lambda\cdot\Delta t) \tag{4-29}$$

In the next section a simpler version of (4-28) is derived.

4.2 A CONCISE APPROACH TO DETECTION FILTER DESIGN

For the F100 engine a single detection filter is sufficient to cover failures of all sensors and actuators and of several engine components. When the reference model is constructed in the proper form, the design of the filter is straightforward and uncomplicated. Just one filter is needed because the system is well measured--the engine's controller requires direct measurement of all of the state variables associated with the important dynamics of the engine. Therefore, the reference model in the filter has nearly as many measurements as state variables. This circumstance allows a considerable simplification in the procedure for designing the filter.

Since complex systems frequently do require many measurements for good control, the design method for the F100 detection filter may be widely applicable. For this reason, the method is detailed in this section in general terms; direct application to the F100 is deferred to Chapter 5.

4.2.1 Refining the Model

We assume that a discrete-time model has been constructed as specified in Section 4.1. Also, we require that the measurements be independent, that is, that the rows of C be linearly independent. We have, then, a model in the form of (4-2):

$$\begin{aligned} \underline{x}_{k+1} &= \Phi \underline{x}_k + \Gamma \underline{u}_k \\ \underline{y}_{k+1} &= C \underline{x}_{k+1} \end{aligned} \tag{4-2}$$

It is desirable to simplify this model by transforming the state vector so that $\underline{y}$ equals the first m state variables. That is, we would like C to be [I:0], where I is the m x m identity matrix and 0 represents an m x (n-m) matrix of zeros. Provided the measurements are independent, this tranformation can always be accomplished. Let T denote

the transformation matrix--it must be square and nonsingular--and let $\underline{x}'$ be the new state vector. The transformation has the form

$$\underline{x}' = T\underline{x} \tag{4-30a}$$

When substituted into (4-2), this gives us

$$\begin{aligned} \underline{x}'_{k+1} &= T\Phi T^{-1}\underline{x}'_k + T\Gamma\underline{u}_k \\ \underline{y}_{k+1} &= CT^{-1}\underline{x}'_{k+1} \end{aligned} \tag{4-30b}$$

If we let

$$T = \begin{bmatrix} C \\ W \end{bmatrix} \tag{4-31}$$

with W any (n-m) x m matrix that makes all the rows of T linearly independent, then

$$CT^{-1} = [I:0]$$

as desired. Accordingly, we define three new matrices Φ', Γ', and C':

$$\begin{aligned} \Phi' &= T\Phi T^{-1} \\ \Gamma' &= T\Gamma \\ C' &= CT^{-1} = [I:0] \end{aligned} \tag{4-32}$$

Equations (4-30b) then become

$$\begin{aligned} \underline{x}'_{k+1} &= \Phi'\underline{x}'_k + \Gamma'\underline{u}_k \\ \underline{y}'_{k+1} &= C'\underline{x}'_{k+1} \end{aligned} \tag{4-33}$$

Let us now partition $\underline{x}'$, Φ', and Γ' into sections of dimension m and n-m:

$$\underline{x}' = \begin{bmatrix} \underline{x}_1' \\ \underline{x}_2' \end{bmatrix} \begin{matrix} (m) \\ (n-m) \end{matrix}$$

$$\Phi' = \begin{bmatrix} \Phi_{11}' & \Phi_{12}' \\ \Phi_{21}' & \Phi_{22}' \end{bmatrix} \tag{4-34}$$

$$\Gamma' = \begin{bmatrix} \Gamma_1' \\ \Gamma_2' \end{bmatrix}$$

With this partitioning, we have

$$\underline{y} = \underline{x}_1' \tag{4-35}$$

The remainder of the state vector, $\underline{x}_2'$, is composed of arbitrary combinations of the original state variables, combinations that result from the W used in (4-31).

The choice for W can be used to simplify the model further. The submatrices Φ_{21}' and Φ_{22}' depend only on W and Φ; C has no effect on them. If the rows of W are chosen to be certain rows of the inverse of the matrix whose columns are the eigenvectors of the original Φ, then Φ_{21}' will be all zeros and Φ_{22}' will be diagonal.[5] That this is true can be seen by considering the transformation defined by a T matrix consisting of the entire inverse of the eigenvector matrix. This would transform (4-2) into

[5]This statement might not be strictly valid if Φ has repeated eigenvalues and does not have a full complement of n distinct eigenvectors; but in practice, very few systems need be modeled with such a Φ matrix. In the event that this is the case, however, Φ_{21}' can still be made zero, and Φ_{22}' can at least be made nearly diagonal, in what is called Jordan form. This is discussed in Hildebrand [22] and in Kwakernaak and Sivan [26].

$$\begin{aligned} \underline{z}_{k+1} &= \Lambda \underline{z}_k + \Gamma'' \underline{u}_k \\ \underline{y}_{k+1} &= C'' \underline{z}_{k+1} \end{aligned} \tag{4-36}$$

where Λ is a diagonal matrix comprising the eigenvalues of Φ. Appropriate rows of the inverse eigenvector matrix to use for W are those corresponding to the modes of the system that least involve the state variables that $\underline{y}$ most depends on. In other words, they are the n-m rows that are least like the rows of C.

Let these rows be denoted $\underline{w}_1, \cdots \underline{w}_{n-m}$; then

$$\underline{x}_2' = W\underline{x} = \begin{bmatrix} \underline{w}_1 \\ \underline{w}_2 \\ \cdot \\ \cdot \\ \cdot \\ \underline{w}_{n-m} \end{bmatrix} \underline{x} \tag{4-37}$$

This makes $\underline{x}_2'$ consist of n-m of the variables in $\underline{z}$. One or more of the $\underline{w}_i$'s could be complex, in which case $\underline{x}_2'$ would not be real. To avoid this, when one of the $\underline{w}_i$'s is complex we require the other member of the complex pair also be one of the $\underline{w}_i$'s. Supposing that such a pair is $\underline{w}_j$ and $\underline{w}_{j+1}$, we replace these rows of W with

$$\begin{aligned} \underline{w}_j' &= 1/2\ (\underline{w}_j + \underline{w}_{j+1}) = \mathrm{Re}(w_j) \\ \underline{w}_{j+1}' &= -1/2i(\underline{w}_j - \underline{w}_{j+1}) = \mathrm{Im}(w_j) \end{aligned} \tag{4-38}$$

When this is done with each complex pair, all elements of $\underline{x}_2'$ and Φ_{22}' will be real. The structure of Φ_{22}' will now be block diagonal, with the real parts of the eigenvalues as the diagonal elements and the imaginary parts as the immediately adjacent elements.

In summary, with T given by (4-31) and W chosen as just described, we have

$$\Phi' = \begin{bmatrix} \Phi_{11}' & \Phi_{12}' \\ 0 & \Phi_{22}' \end{bmatrix} \tag{4-39}$$

where Φ_2' is diagonal or block diagonal. An obvious benefit of this simplification is a reduction in the computation required in running the model. Another benefit, one that will not be apparent until the conclusion of the next subsection, is that a filter based on (4-39) can have all sensor failures included in the set of failures it is designed for, without increased complexity.

4.2.2 Detection Filter Design

We assume that a model of the system has been prepared with the state vector chosen so that $\underline{y}$ equals $\underline{x}_1'$, as described above. For the moment, however, we do not specify any particular choice of variables for $\underline{x}_2'$. For notational convenience, the primes are now dropped, and the model is written as

$$\begin{aligned} \underline{x}_{k+1} &= \Phi \underline{x}_k + \Gamma \underline{u}_k \\ \underline{y}_{k+1} &= [I:0]\underline{x}_{k+1} \end{aligned} \tag{4-40}$$

With the state vector partitioned appropriately, (4-40) becomes

$$\begin{bmatrix} \underline{x}_1 \\ \underline{x}_2 \end{bmatrix}_{k+1} = \begin{bmatrix} \Phi_{11} & \Phi_{12} \\ \Phi_{21} & \Phi_{22} \end{bmatrix} \begin{bmatrix} \underline{x}_1 \\ \underline{x}_2 \end{bmatrix}_k + \begin{bmatrix} \Gamma_1 \\ \Gamma_2 \end{bmatrix} \underline{u}_k \tag{4-41}$$

$$\underline{y}_{k+1} = \underline{x}_{1k+1} \tag{4-42}$$

As stated in Section 4.1, the filter will have the form

$$\begin{aligned} \hat{\underline{x}}_{k+1} &= \Phi\hat{\underline{x}}_k + \Gamma\underline{u}_k + D(\underline{y}_k - \hat{\underline{y}}_k) \\ \hat{\underline{y}}_{k+1} &= [I:0]\hat{\underline{x}}_{k+1} \end{aligned} \tag{4-43}$$

The dynamic behavior of the state difference vector $\underline{q}$ and of the residual vector $\underline{r}$ is given by the difference between (4-40) and (4-43):

$$\underline{q}_{k+1} = [\Phi - DC]\underline{q}_k \tag{4-44a}$$

$$\underline{r}_{k+1} = [I:0]\underline{q}_{k+1} \tag{4-44b}$$

In (4-44a), C is written in place of [I:0] to shorten the notation. The principal task in making the filter (4-42) be a detection filter is developing an expression that specifies D appropriately. First, the event vectors must be determined for the components the filter is to monitor.

Detection filters can only be constructed for failures that can be modeled in (4-40) by a single additive vector of fixed direction. (The magnitude of the vector may vary in any manner whatever.) This restriction does not usually inhibit the use of detection filters; most actuator and sensor failures, and many failures of other system components as well, can be characterized in this manner. Sections 2.3 and 4.1 together describe how to determine the event vectors characteristic of various failures. In determining an expression for the feedback matrix D, the failures we shall consider first are those described by the input failure model, (4-21). As shown in (4-24), they affect $\underline{r}$ through an additive term in (4-44a):

$$\begin{aligned} \underline{q}_{k+1} &= [\Phi - DC]\underline{q}_k + n_k\underline{f} \\ \underline{r}_{k+1} &= C\underline{q}_{k+1} \end{aligned} \tag{4-45}$$

The prime on the $\underline{f}'$ in (4-24) has been dropped; $\underline{f}$ now denotes a discrete-time event vector. After the event vectors have been identified, we choose from them m vectors--as many as there are measurements in $\underline{y}$--whose failure directions, $[I:0]\underline{f}_i$, are linearly independent and are as well separated as possible.[6] These vectors are made the columns of an n x m matrix F:

$$F = [\underline{f}_1 : \underline{f}_2 : \cdots : \underline{f}_m] \tag{4-46}$$

Then F is partitioned in the same manner $\underline{x}$ is:

$$F = \begin{bmatrix} F_1 \\ \\ F_2 \end{bmatrix} = \begin{bmatrix} \underline{f}_{11} & \underline{f}_{12} & & \underline{f}_{1m} \\ : & : & \cdots & : \\ \underline{f}_{21} & \underline{f}_{22} & & \underline{f}_{2m} \end{bmatrix} \begin{matrix} (m) \\ \\ (n-m) \end{matrix} \tag{4-47}$$

The columns of the square matrix F_1 are the failure directions $[I:0]\underline{f}_i$. These were required to be independent so that F_1 would be invertible.

The function of a detection filter is the generation of a continuing sequence of residual vectors in which the failure signature of any component whose event vector is one of $\underline{f}_1, \cdots \underline{f}_m$ is a sequence of vectors all lying in a single, specific direction. That direction is the direction of the column of F_1 that is associated with the particular component. The feedback matrix D can be obtained by working directly from

---

[6] One consequence of this condition, though not the primary one, is that any vector whose product with [I:0] is zero is excluded from consideration. With sampled-data systems such vectors are rare. Even if a system has a failure that would with a continuous-time reference model have an event vector with this property, when the model and the vector are integrated to their discrete-time equivalents, the vector always acquires components directly affecting $\underline{x}_1$ (and $\underline{y}$). (This is true because we only consider models that are completely observable.) On the other hand, these components of the vector may be so small the event vector is effectively excluded anyway. Also, some sampled-data systems might possibly have failures unique to themselves that have event vectors with no direct projection to y. If necessary, any vector for which [I:0]f is zero can in fact be included, but doing so requires the procedures given in Chapter 2.

this statement of the desired behavior of the filter. Suppose the i'th component--the component with event vector $\underline{f}_i$--fails at the k'th sampling time after a period of normal operation during which the filter residual has been zero. Then, according to (4-45), the residual at time k+1 is $n_k\underline{f}_{1i}$, regardless of what D is. But $\underline{q}_{k+1}$ equals $n_k\underline{f}_i$, so for $\underline{r}_{k+1}$ also to be in the direction of $\underline{f}_{1_i}$, D must be suitably chosen. For our purposes here, the best choice--sometimes the only choice--is the one that makes $\underline{f}_i$ an eigenvector of $[\Phi-DC]$:

$$[\Phi - DC]\underline{f}_i = \lambda_i\underline{f}_i \tag{4-48}$$

The eigenvalue λ_i may be any number between zero and one, this being the range of values for which the filter would be stable and well-behaved. If (4-48) is satisfied, not only $\underline{r}_{k+1}$, but all subsequent $\underline{r}$'s will lie in the direction of $\underline{f}_{1_i}$. Consequently, (4-48) is the condition on D for the filter to be a detection filter for the i'th component.

Similarly, for each of the other m-1 components of concern, choose D to satisfy (4-48). Collected together, all the resulting vector equations form a single matrix equation:

$$[\Phi - DC]F = F\Lambda \tag{4-49}$$

The matrix Λ is an m x m diagonal matrix of the λ_i's. Equation (4-49) represents mn linear equations in the mn elements of D. Because CF equals F_1, we obtain

$$DF_1 = -F\Lambda + \Phi F \tag{4-50}$$

Since F_1 is nonsingular, a unique solution for D exists.

By proceeding a few steps further, we can gain some insight into the nature of a detection filter. Partition D as we have previously partitioned Φ and F:

$$D = \begin{bmatrix} D_1 \\ D_2 \end{bmatrix} \begin{matrix} (m) \\ (n-m) \end{matrix} \tag{4-51}$$

Then rewrite (4-50) as

$$\begin{matrix} D_1 \\ D_2 \end{matrix} F_1 = -\begin{bmatrix} F_1 \\ F_2 \end{bmatrix} \Lambda + \begin{bmatrix} \Phi_{11} & \Phi_{12} \\ \Phi_{21} & \Phi_{22} \end{bmatrix} \begin{bmatrix} F_1 \\ F_2 \end{bmatrix} \tag{4-52}$$

From (4-52), we obtain two equations, one each for D_1 and D_2:

$$D_1 = -F_1 \Lambda F_1^{-1} + \Phi_{11} + \Phi_{12} F_2 F_1^{-1} \tag{4-53a}$$

$$D_2 = -F_2 \Lambda F_1^{-1} + \Phi_{21} + \Phi_{22} F_2 F_1^{-1} \tag{4-53b}$$

An important simplification results from assigning the same value to all the λ_i's. This gives

$$\Lambda = \lambda I$$

and Equations (4-53) become

$$D_1 = \Phi_{11} - \lambda I + \Phi_{12} F_2 F_1^{-1} \tag{4-54a}$$

$$D_2 = \Phi_{21} + (\Phi_{22} - \lambda I) F_2 F_1^{-1} \tag{4-54b}$$

A block diagram of a filter constructed with D_1 and D_2 as given by (4-54) is shown in Figure 4.1. A noteworthy feature of this filter is that because $\underline{r}$ contains $-\hat{\underline{y}}$ (which is $-\hat{\underline{x}}_1$), the terms $\Phi_{11}\underline{r}$ and $\Phi_{21}\underline{r}$ in the outer loop cancel $\Phi_{11}\hat{\underline{x}}_1$ and $\Phi_{21}\hat{\underline{x}}_1$ in the inner loop and replace them with $\Phi_{11}\underline{y}$ and $\Phi_{21}\underline{y}$. In effect, the reference model operates with $\hat{\underline{x}}_1$ replaced by $\underline{x}_1$: the measured values of the real state variables drive the dynamics of the model's state variables. In Figure 4.2, the block diagram of Figure 4.1 is redrawn to show the result of this cancellation. Except for the terms containing $F_2F_1^{-1}$, this decouples the variables in $\hat{\underline{x}}_1$.

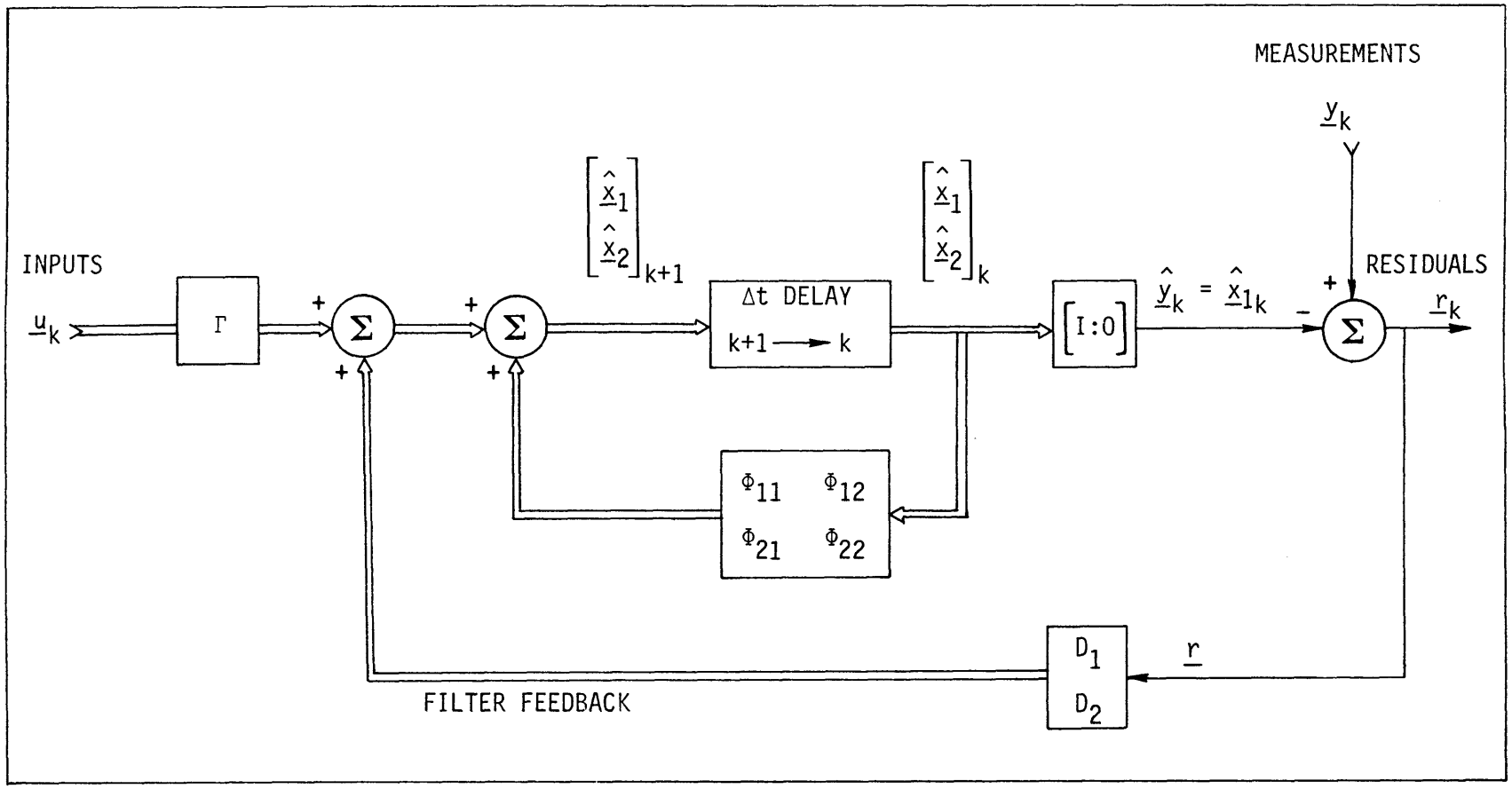

Figure 4.1. A discrete-time detection filter with partitioned state vector.

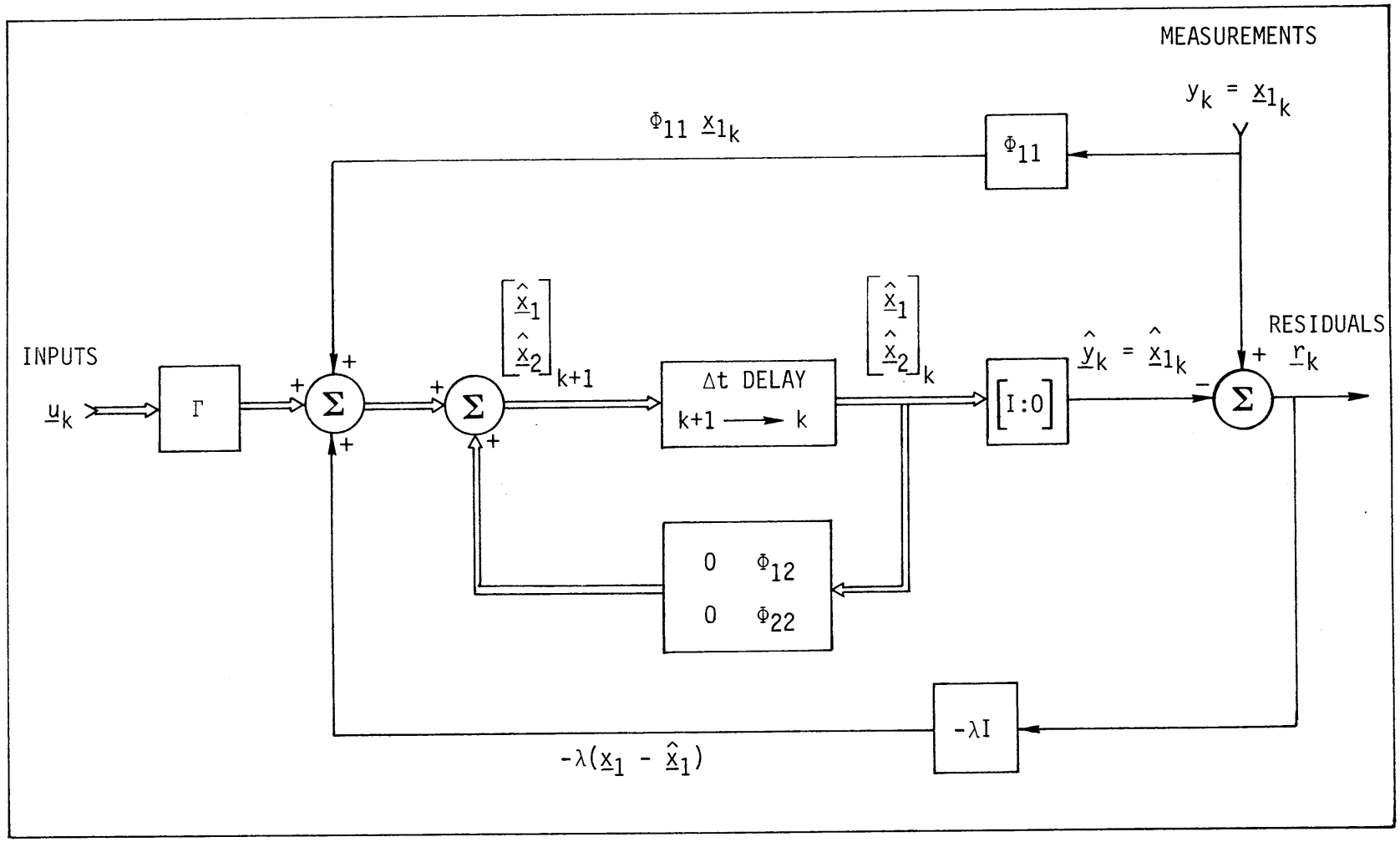

Figure 4.2. Detection filter with cancelled terms.

The filter designed for the air-turbine example in Section 2.2 is similar. There the system is fully measured, and $\hat{\underline{x}}_1$ is the entire state vector. Each dynamic section of the reference model is decoupled from the others, which prevents the residual created by a failure in one section of the system from affecting any but the corresponding section of the model. The other sections of the model, driven by the measurements from the system, respond to the failure exactly the same as the unfailed parts of the system do. Here, the concept is similar, but the unmeasured state variables complicate the decoupling. The additional terms $\Phi_{12}F_2F_1^{-1}\underline{r}$ and $[\Phi_{22}-\lambda I]F_2F_1^{-1}\underline{r}$ are necessary to complete it. Each of the m elements of the vector $F_1^{-1}\underline{r}$ corresponds to one of the components the filter is designed for. When a single component fails, only one element of $F_1^{-1}\underline{r}$ becomes nonzero; the magnitude of the element indicates the severity of the failure. Through the matrices $\Phi_{12}F_2$ and $[\Phi_{22}-\lambda I]F_2$, this information about the failure is introduced into the model to make the model respond to the failure just as the real system does. The failure signature is thereby prevented from coupling into the other elements of $F_1^{-1}\underline{r}$.

The term λI in D_1 does not contribute to the decoupling; it is a diagonal matrix and only feeds each element of $\underline{r}$ back to the corresponding element of $\hat{\underline{x}}_1$. The value selected for λ becomes m of the eigenvalues of $[\Phi-DC]$, and as such it strongly influences the behavior of the filter. It should be between zero and one, otherwise the filter will be oscillatory or unstable. Within this range, the smaller λ is, the smaller is any residual caused by a failure or some other persistent disturbance, and the sooner the residual decays to zero if the disturbance vanishes. High-frequency sensor noise enters the residual with relatively little attentuation, so λ must not be so near zero that any important failure signatures are attenuated so much they become masked by the noise. We have no general way to determine what value of λ is best for a given application, but experience so far shows that good performance is obtained when λ is chosen to make the filter somewhat

faster than the important modes of the real system.[7] This strikes a reasonable balance between the signal-to-noise ratio and the decay rate of the effects of momentary disturbances. An additional consideration when the filter is implemented in a sampled-data system is that λ should not be so small that the time constant of the filter is nearly as small as the measurement sampling interval.

The remaining n-m eigenvalues of [Φ-DC] also affect the performance of the filter. Unfortunately, there is no guarantee that these will be such that the filter is stable. They depend on both Φ and F, but not on λ.[8] If necessary, one can alter them by replacing some of the columns of F with other event vectors or by changing the system model so the failures can be modeled differently.[9] It is always possible to stabilize an unstable filter, but that requires excluding certain event vectors from F. For instance, if the event vectors can be chosen such that F_2 is all zeros, then the remaining eigenvalues will be the eigenvalues of Φ_{22}. These are likely to be suitable, but if they are not, one can alter them by changing the choice of variables in $\underline{x}_2$. When, for example, the variables are chosen to make Φ_{21} zero and Φ_{22} diagonal, the eigenvalues are the same as some of the ones of the real system, and should the system itself have unstable modes, they probably would be included in Φ_{11}, not Φ_{22}, this because unstable modes must be stabilized by the controller, and that frequently requires measurement of the state variables responsible for the instability.

Sensor failures that are modeled by the measurement failure model, (4-25), are different than the failures for which (4-54) was developed. To accommodate them in the design of the filter, we introduce the concept

---

[7] This guideline is the same as that frequently used with linear observers [30].

[8] To calculate these eigenvalues, one need not work from [Φ-DC] directly. Using (2-42) one can show that they are the eigenvalues of $[\Phi_{22}-F_2F_1^{-1}]$.

[9] A third--and more complicated--alternative is augmentation of the reference model, as described in Section 2.4.6.

called output stationarity. Although we shall use it specifically for sensor failures, it is generally applicable to other failures too. An event vector is, by definition, output stationary with the event vectors in F if its failure signature is unidirectional just as the signatures of those vectors are. Suppose $\underline{h}$ is an event vector to be tested for output stationarity. Looking back at (4-48), we see that a failure of the component for which $\underline{h}$ is the event vector will create residual vectors lying along $C\underline{h}$ if

$$[\Phi - DC]\underline{h} = \lambda\underline{h} \tag{4-55}$$

This equation will be true when $\underline{h}$ is a linear combination of $\underline{f}_1, \cdots \underline{f}_m$, the columns of F. To prove this, write

$$\underline{h} = \sum_{i=1}^{m} \alpha_i \underline{f}_i \tag{4-56}$$

and then expand $[\Phi-DC]\underline{h}$:

$$\begin{aligned}
[\Phi - DC]\underline{h} &= [\Phi - DC] \sum_{i=1}^{m} \alpha_i \underline{f}_i \\
&= \sum_{i=1}^{m} \alpha_i [\Phi - DC]\underline{f}_i \\
&= \lambda \sum_{i=1}^{m} \alpha_i \underline{f}_i \\
&= \lambda\underline{h}
\end{aligned}$$

Thus, when we use (4-54) to determine a detection filter for $\underline{f}_1, \cdots \underline{f}_m$, the filter is also a detection filter for all linear combinations of $\underline{f}_1, \cdots \underline{f}_m$--any such event vector will be output stationary.

When discussing sensor failures in Section 4.1, we noted that the residual created by a failure of sensor j will lie in the plane defined by $\underline{e}_j$ and $\underline{d}_{1j}$ (the j'th column of D_1) if the filter is a detection

filter for $\underline{d}_j$. This will be true whenever $\underline{d}_j$ is output stationary, that is, whenever (4-55) is satisfied with $\underline{h}$ equal to $\underline{d}_j$. Normally, $\underline{d}_j$ would be output stationary only by coincidence, but one can in fact design a filter in a way which guarantees that $\underline{d}_j$, and every other column of D as well, will be output stationary. This requires choosing the reference model and the event vectors so that all the elements of Φ_{21} and F_2 are either zero or negligibly small. Then (4-54) reduces to

$$\begin{aligned} D_1 &= \Phi_{11} - \lambda I \\ D_2 &= 0 \end{aligned} \tag{4-57}$$

This removes the explicit dependence on the event vectors, so with this filter, any vector in the $\underline{x}_1$ partition of the state space--any vector $\underline{f}$ with all zero elements in $\underline{f}_2$--has a unidirectional residual. And since D_2 is zero, all the $\underline{d}_j$'s fit that description. The failure signature of each sensor will lie solely in a plane uniquely associated with the sensor.

This property is a useful one--a filter designed directly from (4-57) would be suitable for any application where sensor failures are the most important consideration or where none of the important actuator or component failures have event vectors with significant $\underline{f}_2$ components. The only additional consideration is simply that Φ_{21} be zero, which can be achieved by the method advocated in Section 4.2.1. Figure 4.3 illustrates the relatively simple structure of this type of detection filter.

4.2.3 Summary

With the reference model constructed in the form

$$\begin{bmatrix} \underline{x}_1 \\ \underline{x}_2 \end{bmatrix}_{k+1} = \begin{bmatrix} \Phi_{11} & \Phi_{12} \\ \Phi_{21} & \Phi_{22} \end{bmatrix} \begin{bmatrix} \underline{x}_1 \\ \underline{x}_2 \end{bmatrix}_k \begin{matrix} (m) \\ (n-m) \end{matrix} + \begin{bmatrix} \Gamma_1 \\ \Gamma_2 \end{bmatrix} \underline{u}_k \tag{4-41}$$

$$\underline{y}_{k+1} = \underline{x}_{1_{k+1}} \tag{4-42}$$

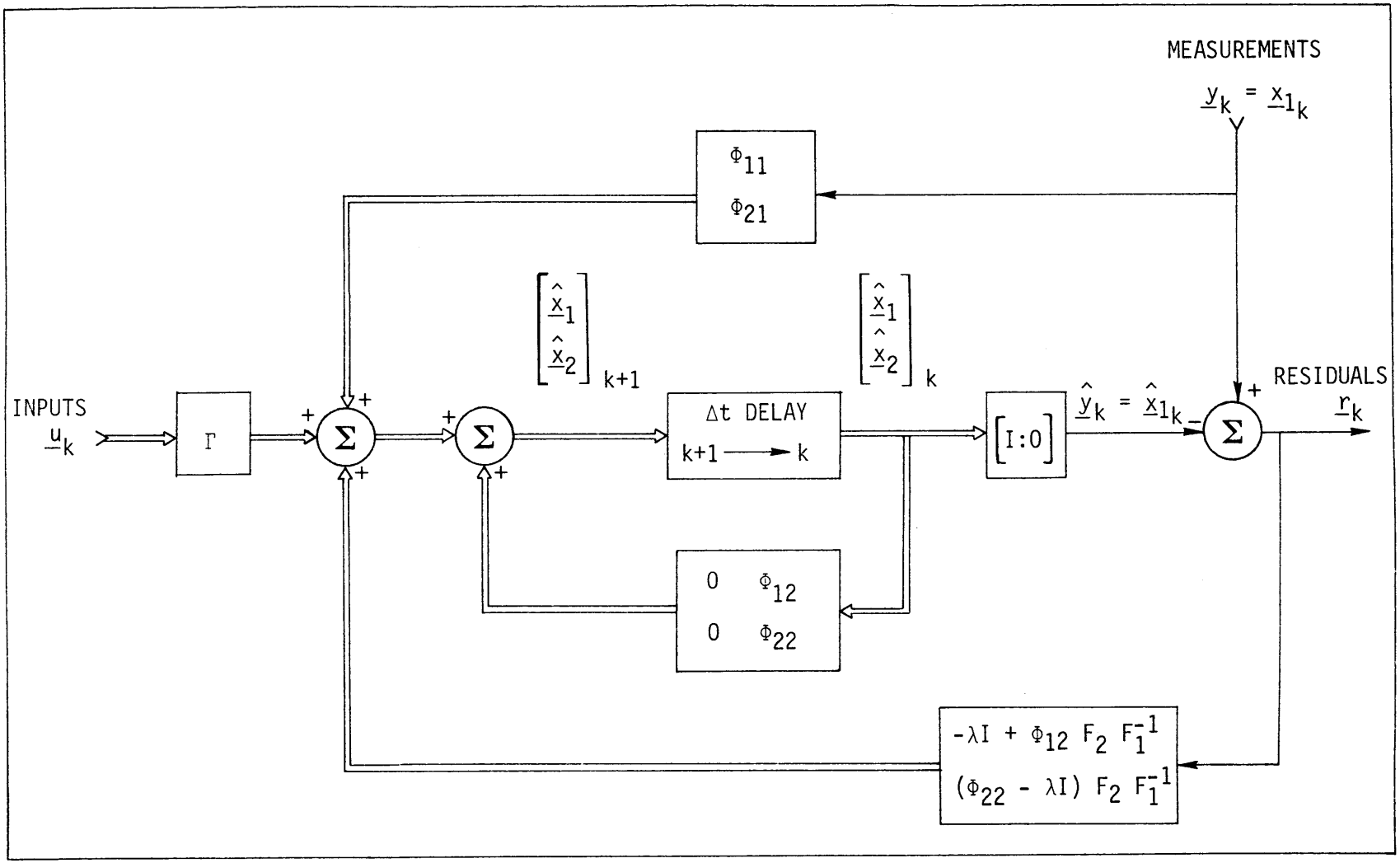

Figure 4.3. Detection filter with $\Phi_{21} = 0$ and $F_2 = 0$.

and m event vectors collected into

$$F = \begin{bmatrix} F_1 \\ F_2 \end{bmatrix}$$

(with F_1 nonsingular), the solution for D is

$$D_1 = \Phi_{11} - \lambda I + \Phi_{12}F_2F_1^{-1}$$

$$D_2 = \Phi_{21} + (\Phi_{22} - \lambda I)F_2F_1^{-1}$$

If one does not wish to assign the same value λ to m of the eigenvalues of $[\Phi-DC]$, the form of the solution given in (4-53) can be used.

If the filter is to cover sensor failures, design the reference model so Φ_{21} is zero and use D as given by

$$\begin{aligned} D_1 &= \Phi_{11} - \lambda I \\ D_2 &= 0 \end{aligned} \qquad (4\text{-}57)$$

Equation (4-57) is the expression used to design the detection filter for the F100.

4.3 FAILURE IDENTIFICATION

The failure signatures produced by detection filters are amenable to simple diagnostic techniques. As with any type of detection system using a reference model, appearance of a residual with a magnitude greater than some threshold signals a failure. Various statistical tests, many of which involve summation of successive residuals, can be used to minimize the number of false detections caused by measurement noise and modeling errors. But the special property of detection filters is not their ability to detect failures, rather it is generation of easily recognized failure signatures that are unique for each of many different components.

These signatures are, of course, the unidirectional residuals of input failures and the planar residuals of measurement failures. After

a filter has been designed, there remains the task of implementing some procedure for analyzing the filter residuals. The technique described here was developed for the filters used on the simulation of the F100 engine. With those filters, the number of failure directions and failure planes is considerably greater than the number of measurements. This means the residual vector cannot be resolved uniquely into components along each of the directions of concern, as it could be if the number of directions equalled the number of measurements. This results from using (4-57) to design the filter, because that creates two distinct directions for each sensor while also giving most of the other components specific failure directions.

At first, this situation may seem undesirable, but actually it is not, for this allows use of a single filter and a single identification algorithm. It is then easy to predict how one failure will affect the identification logic for each of the other possible failures. Should the identification task be divided among several filters, determining what effect any particular failure would have on the filters that were not designed for it would be more difficult. Consequently, a single failure might well generate indications of several. When a single identification procedure is used, simple precautions can prevent that. Also, it is readily apparent from the relative closeness of failure directions which failures are particularly difficult to discriminate between, so one can foretell which failure signatures are likely to be ambiguous.

4.3.1 Unidirectional Signatures

We shall first develop the identification procedure for unidirectional signatures. That procedure will then be extended to cover the more complicated planar signatures. The information available from a detection filter can be separated essentially into three pieces:

1. The magnitude of the residual vector.
2. The direction of the residual vector.
3. The directions of each of the possible failure signatures.

The first two are computed each sampling interval; the third is computed and stored when the filter is designed. Only the first is required for failure detection. Identification requires all the information. The identification procedure presented here works best when only one failure occurs at a time. It is designed, however, so that should simultaneous failures occur, proper identification is possible, though not certain. In general, such an approach covers all of the more probable situations without becoming unduly complex.

Figure 4.4 shows a two-dimensional residual space with three failure directions. The system has two sensors (1 and 2), and there are three components (a, b, and c) to be monitored. The unit basis vectors of the space are $\underline{e}_1$ and $\underline{e}_2$. The vectors $\underline{v}_a$, $\underline{v}_b$, $\underline{v}_c$ are the failure vectors $C\underline{f}_a$, $C\underline{f}_b$, and $C\underline{f}_c$ normalized to length one. A large bias in component a, coupled with some modeling error, might produce a residual such as indicated by $\underline{r}$. After the magnitude of $\underline{r}$ (to be written as $|\underline{r}|$) is computed, the cosines of the angles θ_a, θ_b, and θ_c between $\underline{r}$ and the three failure directions can be found by taking the dot products of the $\underline{v}$'s with $\underline{r}$ and using the relation

$$\underline{r}\cdot\underline{v} = |\underline{r}||\underline{v}|\cos\theta = |\underline{r}|\cos\theta \qquad (4\text{-}58)$$

In Figure 4.4 the residual shown is closest to $\underline{v}_a$, and $\cos\theta_a$ is the closest either to 1 or to -1. We would like a single number that measures both the severity of the failure and the likelihood the failure is actually in component a. We could use the dot product $\underline{r}\cdot\underline{v}_a$ directly, but $\cos\theta$ is a broadly peaked function and is thus not very selective of residual direction. A better measure--and one that is still easily calculated--is $\cos^N\theta_a|\underline{r}|$, where N is some positive even integer. Let us denote this measure as FS_a--the "failure signal" for component a:

$$FS_a \equiv s_a\cos^N\theta_a|\underline{r}| \qquad (4\text{-}59)$$

The symbol s_a denotes the sign of FS_a and is equal to the sign of $\cos\theta_a$. Thus we attribute to the direction $\underline{v}_a$ the fraction of $|\underline{r}|$ specified by

the weighting function $\cos^N\theta_a$. The value of N is a design parameter that determines the selectivity of this process. Larger values prevent identification of any component as failed unless the residual vector is very near a failure direction, which reduces the likelihood of making a false identification and increases the likelihood of missing a failure. $\text{Cos}^N\theta$ is graphed in Figure 4.5 for several values of N.

We do not wish to ignore the possibility of simultaneous failures or of unidentifiable failures, so we also compute failure signals for the other failure directions--otherwise we would be unaware of the relative closeness of $\underline{r}$ to the other failure directions. We begin the calculation of FS_b and FS_c just as FS_a was calculated, namely, with

$$FS_b = s_b \cos^N\theta_b |\underline{r}|$$

$$FS_c = s_c \cos^N\theta_c |\underline{r}|$$

But by this measure alone, even when $\underline{r}$ lies exactly along $\underline{v}_a$--indicating with virtual certainty that component a, and it alone has failed--there will be an indication, albeit a smaller one, that component b has failed. So, after the closest $\underline{v}$ is found, it is desirable to weight the projections of $\underline{r}$ onto the other $\underline{v}$'s in a way that reflects the knowledge of how close $\underline{r}$ is to that first $\underline{v}$. A weighting that does this is

$$FS_b \equiv s_b \frac{1 - \cos^N\theta_a}{1 - \cos^N\theta_b} \cos^N\theta_b |\underline{r}| \qquad (4\text{-}60)$$

$$FS_c \equiv s_c \frac{1 - \cos^N\theta_a}{1 - \cos^N\theta_c} \cos^N\theta_c |\underline{r}| \cdot \qquad (4\text{-}61)$$

If $\underline{r}$ lies along $\underline{v}_a$, then $FS_a = |\underline{r}|$, and FS_b and FS_c are both zero. Conversely, if $\underline{r}$ lies near the bisector of $\underline{v}_a$ and $\underline{v}_b$, then $FS_a = FS_b$.

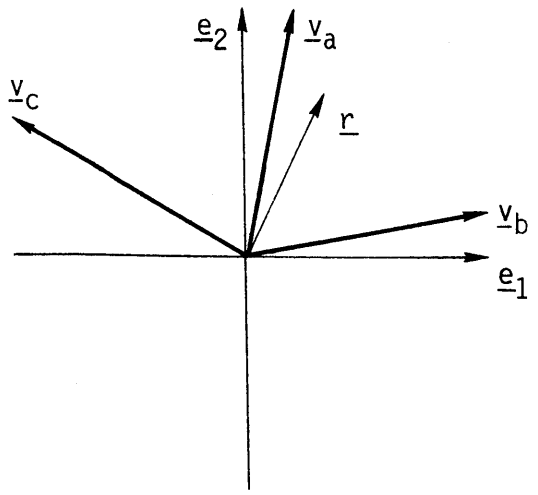

Figure 4.4. A two-dimensional residual space with three failure directions.

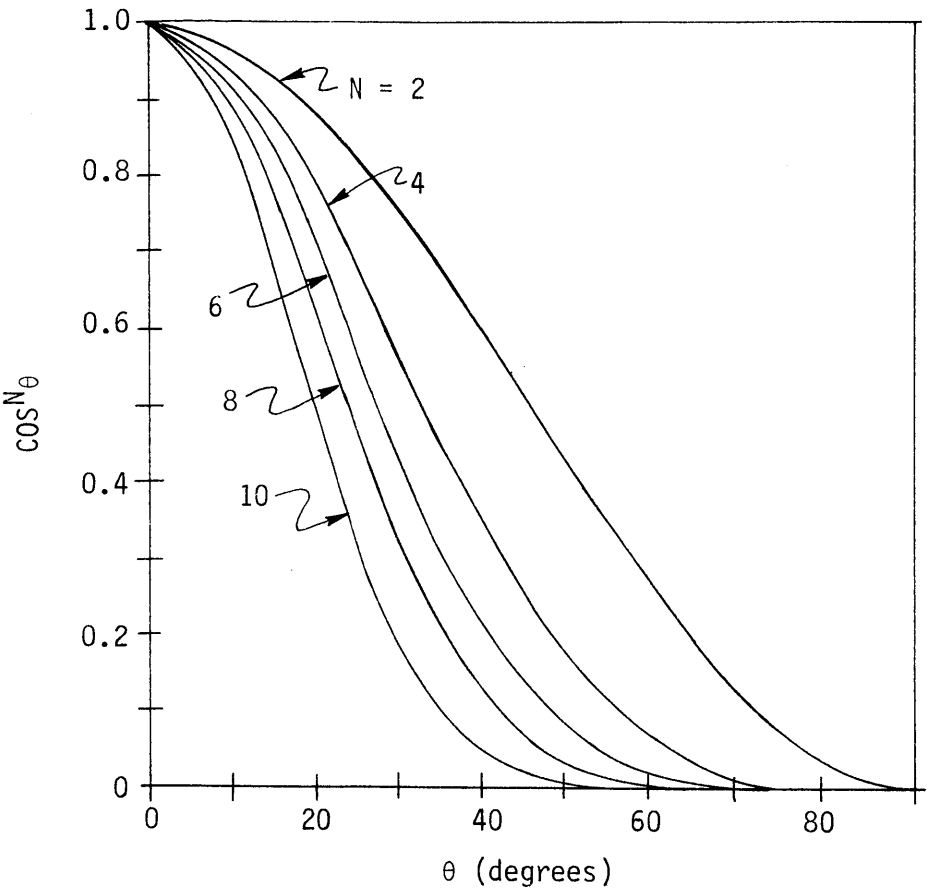

Figure 4.5. Plots of $\cos^N\theta$ for several values of N.

Thus, simultaneous failures of components a and b of comparable effects will produce equally large FS's for a and b. Should a and b fail simultaneously, with comparable type and size of malfunction, then FS_a and FS_b will be roughly equal. (This measure is not, however, complex enough to make FS_a and FS_b proportional to the magnitudes of the respective failures, whatever the relative magnitudes of those concurrent failures are.)

4.3.2 Planar Signatures

To test for a sensor failure that produces a residual constrained to a plane, we calculate a measure of the proximity of $\underline{r}$ to the expected planar signature. As demonstrated in Sections 2.4 and 4.2, a failure of the j'th sensor yields a residual that lies in the plane spanned by $\underline{e}_j$ and $C\underline{d}_j$. A closer analysis of the behavior of that residual reveals, moreover, that in most circumstances the residual stays within just a segment of that plane. This allows the identification algorithm to be more selective; a residual lying in the plane but not in the appropriate segment need not be construed as an indication of a sensor failure. This is especially useful if one or more other failure directions lie near the plane.

Consider the behavior of $\underline{r}$ when the output of sensor j suddenly becomes biased as shown in Figure 4.6. Initially, the residual is

$$\underline{r} = \Delta y_j \underline{e}_j \tag{4-62}$$

It then moves across the plane along the trajectory described by

$$\begin{aligned} \underline{q}_{k+1} &= [\Phi - DC]\underline{q}_k - \Delta y_j \underline{d}_j \\ \underline{r}_{k+1} &= C\underline{q}_{k+1} + \Delta y_j \underline{e}_j \end{aligned} \tag{4-63}$$

This result is the difference between (4-2) and (4-26), per the definitions of $\underline{q}$ and $\underline{r}$. The rate $\underline{r}$ moves is determined by the value assigned to λ in (4-57) when the filter is designed. Eventually, it settles to a specific vector, which is found by setting $\underline{q}_{k+1}$ equal to $\underline{q}_k$:

$$\underline{q}_{ss} = [\Phi - DC]\underline{q}_{ss} - \Delta y_j \underline{d}_j$$

or

$$\underline{q}_{ss} = -\Delta y_j [I - \Phi + DC]^{-1} \underline{d}_j \tag{4-64}$$

The filter is stable, so a solution for $\underline{q}_{ss}$ exists. The steady-state residual is then

$$\underline{r}_{ss} = -\Delta y_j C[I - \Phi + DC]^{-1} \underline{d}_j + \Delta y_j \underline{e}_j \tag{4-65}$$

Let $\underline{v}_j$ denote the vector $[\underline{e}_j - C[I-\Phi+DC]^{-1}\underline{d}_j]$ normalized to length one. As shown in Figure 4.7, after the onset of the bias, the trajectory of $\underline{r}$ is from $\underline{e}_j$ to $\underline{v}_j$. Thus a positive bias is evidenced by residuals lying solely in the plane segment between $\underline{e}_j$ and $\underline{v}_j$, counter-clockwise from $\underline{e}_j$ as drawn in the figure. Similarly, a negative bias produces residuals bounded by $-\underline{e}_j$ and $-\underline{v}_j$.

The residuals caused by any sensor failure characterized by Δy_j steadily increasing or steadily decreasing will also be constrained in the same manner. Only a fluctuating sensor output can drive $\underline{r}$ outside that region of the plane. Even so, if the fluctuations are relatively fast and have zero mean value, the residual will tend to stay along the $\underline{e}_j$ axis. Overall, a procedure that identifies sensor failures by looking just between $\underline{e}_j$ and $\underline{v}_j$, and between $-\underline{e}_j$ and $-\underline{v}_j$, should work well.

The relation for $\underline{r}_{ss}$ given in (4-65) can be simplified when the filter is designed from Equation (4-57). Specifically, when

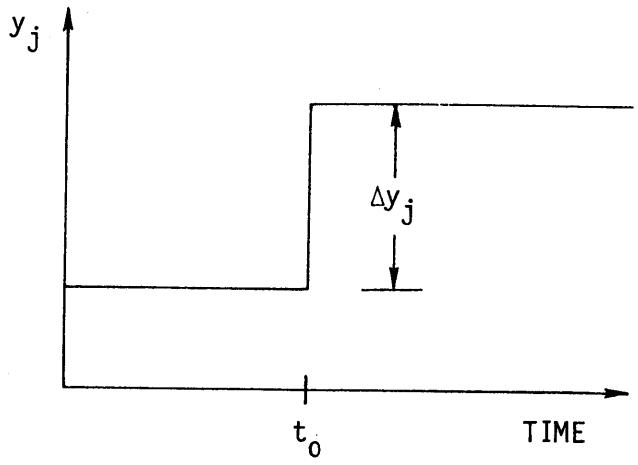

Figure 4.6. Bias suddenly appearing in the output of the j'th sensor.

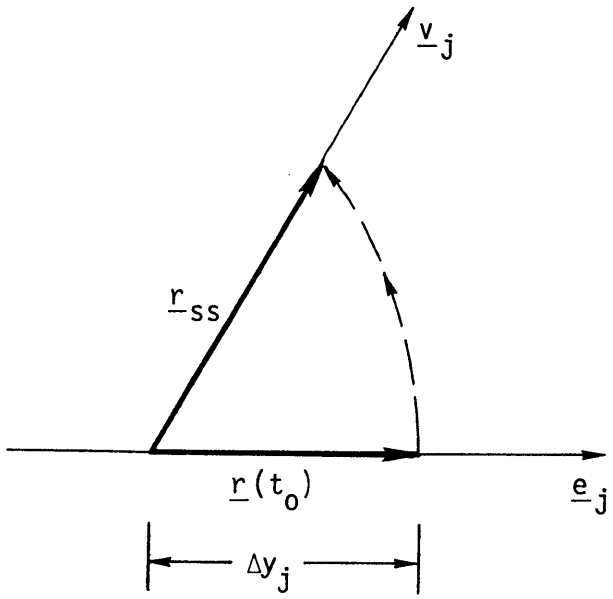

Figure 4.7. Trajectory of the residual vector caused by the biased sensor.

$$\Phi = \begin{bmatrix} \Phi_{11} & \Phi_{12} \\ 0 & \Phi_{22} \end{bmatrix} \tag{4-66}$$

$$C = [I : 0] \tag{4-67}$$

$$D = \begin{bmatrix} \Phi_{11} - \lambda I \\ 0 \end{bmatrix} \tag{4-68}$$

we have

$$[I - \Phi + DC]^{-1} = \begin{bmatrix} (1-\lambda)I & -\Phi_{12} \\ 0 & I-\Phi_{22} \end{bmatrix}^{-1}$$

$$= \begin{bmatrix} (1-\lambda)^{-1}I & (1-\lambda)^{-1}\Phi_{12}[I-\Phi_{22}]^{-1} \\ 0 & [I-\Phi_{22}]^{-1} \end{bmatrix} \tag{4-69}$$

and

$$\underline{d}_j = \begin{bmatrix} \underline{\phi}_j - \lambda \underline{e}_j \\ 0 \end{bmatrix} \tag{4-70}$$

where $\underline{\phi}_j$ is the j'th column of Φ_{11}. Substitution of these results into (4-65) yields

$$\underline{r}_{ss} = \frac{\underline{e}_j - \underline{\phi}_j}{1 - \lambda} \Delta y_j \tag{4-71}$$

Thus the vector $\underline{v}_j$ becomes simply $[\underline{e}_j - \underline{\phi}_j]$ normalized to length one.

The next step is calculation of the cosine of the angle between $\underline{r}$ and the closer of the two plane segments bounded by $\pm\underline{e}_j$ and $\pm\underline{v}_j$. Let $\underline{r}^\circ$ be the <u>orthogonal</u> projection of $\underline{r}$ onto the whole plane spanned by $\underline{e}_j$ and $\underline{v}_j$. Figure 4.8a shows a situation in which $\underline{r}^\circ$ lies between $\underline{e}_j$ and $\underline{v}_j$. We can write $\underline{r}^\circ$ as a linear combination of $\underline{e}_j$ and $\underline{v}_j$:

$$\underline{r}^\circ = \alpha\underline{e}_j + \beta\underline{v}_j \tag{4-72}$$

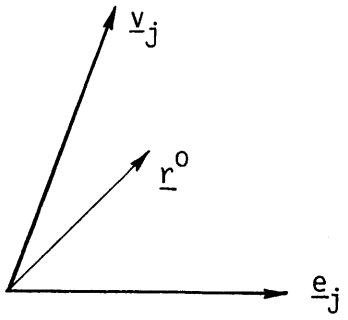

Part a.

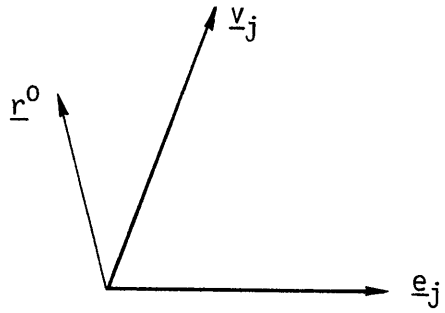

Part b.

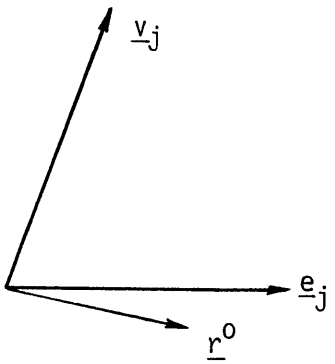

Part c.

Figure 4.8. Orthogonal projections of various residuals onto the failure plane of the j'th sensor.

Taking the dot products of $\underline{r}^\circ$ with $\underline{e}_j$ and $\underline{v}_j$, we obtain

$$\underline{r}^\circ \cdot \underline{e}_j = \alpha \underline{e}_j \cdot \underline{e}_j + \beta \underline{v}_j \cdot \underline{e}_j \tag{4-73}$$

$$\underline{r}^\circ \cdot \underline{v}_j = \alpha \underline{e}_j \cdot \underline{v}_j + \beta \underline{v}_j \cdot \underline{v}_j \tag{4-74}$$

We have that

$$\underline{e}_j \cdot \underline{e}_j = \underline{v}_j \cdot \underline{v}_j = 1$$

and it can be shown that

$$\begin{aligned} \underline{r}^\circ \cdot \underline{e}_j &= \underline{r} \cdot \underline{e}_j \\ \underline{r}^\circ \cdot \underline{v}_j &= \underline{r} \cdot \underline{v}_j \end{aligned} \tag{4-75}$$

Now, let

$$\begin{aligned} r_j &= \underline{r} \cdot \underline{e}_j \\ v_j &= \underline{v}_j \cdot \underline{e}_j \end{aligned} \tag{4-76}$$

Then, solving for α and β yields

$$\alpha = \frac{r_j - (\underline{r} \cdot \underline{v}_j) v_j}{(1 - v_j^2)} \tag{4-79}$$

$$\beta = \frac{\underline{r} \cdot \underline{v}_j - r_j v_j}{(1 - v_j^2)} \tag{4-80}$$

The magnitude of $\underline{r}^\circ$ is given by

$$\begin{aligned} |\underline{r}^\circ| &= [(\alpha \underline{e}_j + \beta \underline{v}_j) \cdot (\alpha \underline{e}_j + \beta \underline{v}_j)]^{1/2} \\ &= [\alpha^2 + \beta^2 + 2\alpha\beta v_j]^{1/2} \end{aligned} \tag{4-81}$$

Let us consider separately the three configurations of $\underline{r}^\circ$, $\underline{e}_j$, and $\underline{v}_j$ sketched in Figure 4.8:

a) Figure 4.8a and its complement (the direction of $\underline{r}^\circ$ reversed)--the sign of α is the same as the sign of β. Define a scalar number r_p as

$$r_p = \pm|\underline{r}^o| = \pm(\alpha^2 + \beta^2 + 2\alpha\beta v_j)^{1/2}$$

The sign chosen for r_p is the sign of α and β.

b) Figure 4.8b and its complement--the signs of α and β are opposite, and $|\beta| > |\alpha|$. Define r_p by

$$r_p = \underline{r}\cdot\underline{v}_j$$

c) Figure 4.8c and its complement--the signs of α and β are opposite, and $|\beta| \leq |\alpha|$. Define r by

$$r_p = \underline{r}\cdot\underline{e}_j = r_j$$

In sum, the definition of r_p is

$$r_p = \begin{cases} \pm(\alpha^2 + \beta^2 + 2\alpha\beta v_j)^{1/2}, & \text{sign}(\alpha) = \text{sign}(\beta) \\ \left.\begin{matrix} \underline{r}\cdot\underline{v}_j \\ \underline{r}\cdot\underline{e}_j \end{matrix}\right\} & \text{sign}(\alpha) \neq \text{sign}(\beta) \begin{cases} |\beta| > |\alpha| \\ |\beta| \leq |\alpha| \end{cases} \end{cases} \qquad (4\text{-}82)$$

This number can be thought of as the "dot product" of $\underline{r}$ with the plane segment $[\underline{e}_j,\underline{v}_j]$ (this notation means the segments between $\underline{e}_j$ and $\underline{v}_j$ and between $-\underline{e}_j$ and $-\underline{v}_j$ that $\underline{r}$ would traverse). We shall use it in the same manner we used the dot product of $\underline{r}$ with the vector failure directions. The cosine of the angle θ_j between $\underline{r}$ and $[\underline{e}_j,\underline{v}_j]$ is calculated from

$$r_p = |\underline{r}|\cos\theta_j \qquad (4\text{-}83)$$

To find which failure direction $\underline{r}$ is closest to, we look among all the $\cos\theta$'s from both (4-58) and (4-83) for the one closest to ± 1. Then the failure signals are calculated exactly as before, for both the vector directions and the plane segments. Continuing the example of Section 4.3.1, suppose θ_1 were the smallest of θ_a, θ_b, θ_c, θ_1, and θ_2. The failure signals for $[\underline{e}_1,\underline{v}_1]$ and $\underline{v}_a$ would be

$$FS_1 = s_1 \cos^N\theta_1 \, |\underline{r}| \tag{4-84}$$

$$FS_a = s_a \frac{1 - \cos^N\theta_1}{1 - \cos^N\theta_a} \cos^N\theta_a \, |\underline{r}| \tag{4-85}$$

Conversely, if $\underline{r}$ were closest to $\underline{v}_j$, as before, then we would have

$$FS_1 = s_1 \frac{1 - \cos^N\theta_a}{1 - \cos^N\theta_1} \cos^N\theta_1 \, |\underline{r}| \tag{4-86}$$

$$FS_a = s_a \cos^N\theta_a |\underline{r}| \tag{4-87}$$

In summary, r_p plays the same role for measurement failures as $\underline{r}\cdot\underline{v}$ does for input failures.

With the FS's, one can implement independent detection tests for failures of each component. In general, any component for which the FS gets too large would be declared failed. Conceivably, $|\underline{r}|$ could be large enough to indicate a failure without any of the FS's being large enough to do so, in which case an undiagnosed failure would be declared. Similarly, a large $|\underline{r}|$ coupled with a highly unlikely combination of FS's, all notably smaller than $|\underline{r}|$, would also indicate an undiagnosed failure. In both instances, the failure would probably be one for which the detection filter is not designed. Sometimes, though, modeling errors or simultaneous failures could disguise the signature of a failure for which the filter *is* designed. On the other hand, a large $|\underline{r}|$ coupled with a predictable combination of FS's might be interpreted as an indication of concurrent failures of two or more components.

The matter of how to decide when a scalar measure is large enough to indicate a failure is discussed in detail in the literature and will not be elaborated on here (see, for instance, Van Trees [48]). In a relatively noise-free environment, a simple threshold test may be adequate. When sensor noise is bothersome, a more sophisticated, integrative technique is needed. One relatively simple technique is the sequential probability ratio test as modified by Chien [12] and Deckert et al [13].

4.3.3 Scaling

Detection filters do not produce residuals of equal magnitude for similar failures of different components, even when the reference model and the measurements have been nondimensionalized. This is a result of the variation in the magnitudes of the event vectors and of the columns of D. We can compensate for this, but first we must clarify the meaning of "comparable failures." We require at the outset that all the variables in $\underline{x}$, $\underline{y}$, and $\underline{u}$ be normalized so they range in value from zero to one over the normal operating range of the system. This not only makes the values of the variables comparable, it also makes the magnitude of the residual a meaningful number. (Furthermore, the reference model becomes easier to understand and to implement.) Now, with this done, we define the magnitude of a failure to be the value of n_k in the input failure model (4-21) or in the measurement failure model (4-25). In other words, it is the deviation of a component's output from its nominal value, relative to its normal range. We should like each failure signal to equal in magnitude any failure of the corresponding component, if not always when the magnitude is varying, then at least when it is steady.

As usual, let us consider first those failures modeled by the input failure model. For convenience, we take as a sample failure a steady bias in the i'th input. The magnitude of the failure is written as Δu_i. The event vector is the i'th column of Γ, denoted by $\underline{\gamma}_i$. From (4-45), the response of the filter to the bias is given by

$$\begin{aligned} \underline{q}_{k+1} &= [\Phi - DC]\underline{q}_k + \Delta u_i \underline{\gamma}_i \\ \underline{r}_{k+1} &= C\underline{q}_{k+1} \end{aligned} \tag{4-88}$$

In steady state, $\underline{r}$ becomes

$$\underline{r}_{ss} = C[I - \Phi + DC]^{-1}\underline{\gamma}_i \Delta u_i \tag{4-89}$$

When the filter is designed according to Equation (4-57), the relation for $[I-\Phi+DC]^{-1}$ given in (4-69) is valid, and (4-89) reduces to:

$$\underline{r}_{ss} = \frac{1}{1-\lambda} \{I : \Phi_{12}[I-\Phi_{22}]^{-1}\} \underline{\gamma}_i \Delta u_i \tag{4-90}$$

Partitioning Γ as $\underline{x}$ was partitioned, we may write it as

$$\Gamma = \begin{bmatrix} \Gamma_1 \\ \Gamma_2 \end{bmatrix} = \begin{bmatrix} \underline{\gamma}_{11} & \underline{\gamma}_{12} & \cdots & \underline{\gamma}_{1\ell} \\ \underline{\gamma}_{21} & \underline{\gamma}_{22} & & \underline{\gamma}_{2\ell} \end{bmatrix} \tag{4-91}$$

The i'th column is then expressible as

$$\underline{\gamma}_i = \begin{bmatrix} \underline{\gamma}_{1_i} \\ \underline{\gamma}_{2_i} \end{bmatrix} \tag{4-92}$$

To be consistent with the use of (4-57) and (4-69) in obtaining (4-90), we assume $\underline{\gamma}_{2_i}$ is negligible. From (4-90), we see that this does not necessarily mean that the elements of $\underline{\gamma}_{2_i}$ are small compared to those of $\underline{\gamma}_{1_i}$, but rather that $\Phi_{12}[I-\Phi_{22}]^{-1}\underline{\gamma}_{2_i}$ is small compared to $\underline{\gamma}_{1_i}$. With this so, we have

$$\underline{r}_{ss} = \frac{\underline{\gamma}_{1_i}}{1-\lambda} \Delta u_i \tag{4-93}$$

Previously, for the event vector $\underline{f}_a$ we defined $\underline{v}_a$ to be $C\underline{f}_a$ normalized to length one; here, let $\underline{v}_i$ be $\underline{\gamma}_{1_i}$ normalized to length one (note that $\underline{\gamma}_{1_i}$ is $C\underline{\gamma}_i$). For the hypothesized bias failure, $\underline{r}$ begins at zero and simply grows in the direction of $\underline{v}_i$ until its magnitude is $|\underline{\gamma}_{1_i}|\Delta u_i$. The failure signal as defined in Section 4.3.1 becomes

$$FS_i = s_i \frac{1 - \cos^N\theta_{min}}{1 - \cos^N\theta_i} \cos^N\theta_i |\underline{r}_{ss}| \tag{4-94}$$

When there are no disturbances or errors, $\cos^N\theta_i$ and $\cos^N\theta_{min}$ equal 1, and

$$FS_i = \frac{|\underline{\gamma}_{1_i}|}{1-\lambda} \Delta u_i \tag{4-95}$$

To compensate for the term in front of Δu_i, we define a scaling factor κ_i as follows:

$$\kappa_i \equiv \frac{1 - \lambda}{|\underline{\gamma}_{1_i}|} - 1 \tag{4-96}$$

and we redefine the failure signal to be

$$FS_i = s_i w_i (1 + w_i \kappa_i) |\underline{r}| \tag{4-97}$$

where for notational simplicity, the angle-dependent weighting function is represented by w_i:

$$w_i \equiv \frac{1 - \cos^N \theta_{min}}{1 - \cos^N \theta_i} \cos^N \theta_i \tag{4-98}$$

The failure signal now has the desired magnitude, Δu_i, when $\underline{r}$ is steady and lies exactly along $\underline{v}_i$. The scaling factor is weighted by w_i to make its effectiveness dependent on how likely it appears that component i is causing $\underline{r}$. It is possible for κ_i to be considerably greater than one, in which case if it were not itself weighted by w_i, it would tend to cancel the desired overall attenuation by w_i.

We proceed now to the more difficult task of scaling the failure signals for the sensors with planar failure signatures. Consider again the sudden appearance of a bias in sensor j. From (4-71) we know that in steady state the residual becomes

$$\underline{r}_{ss} = \frac{[\underline{e}_j - \underline{\phi}_j]}{1 - \lambda} \Delta y_j \tag{4-71}$$

When the bias first occurs, however, the residual is

$$\underline{r} = \Delta y_j \underline{e}_j \tag{4-99}$$

The magnitude of $\underline{r}$ changes from Δy_j--the desired value for FS_j--to $[|\underline{e}_j-\underline{\phi}_j|/(1-\lambda)]\Delta y_j$, so we cannot simply scale FS_j by a constant factor. We must instead vary the scaling according to where $\underline{r}$ is in relation to $[\underline{e}_j,\underline{v}_j]$. In (4-82), the value of r_p was defined in three parts; similarly, the scaling factor κ_j will be defined in parts, for the same three cases. This requires the coefficients α and β used previously, so for reference, Equations (4-72), (4-79), and (4-80) describing the orthogonal projection of $\underline{r}$ onto the plane spanned by $\underline{e}_j$ and $\underline{e}_j-\underline{\phi}_j$ are rewritten here:

$$\underline{r}^\circ = \alpha\underline{e}_j + \beta\underline{v}_j \tag{4-100}$$

$$\alpha = \frac{r_j - (\underline{r}\cdot\underline{v}_j)v_j}{(1 - v_j^2)} \tag{4-101}$$

$$\beta = \frac{(\underline{r}\cdot\underline{v}_j) - r_j v_j}{(1 - v^2)} \tag{4-102}$$

We would like to define κ_j so that the failure signal for sensor j given by

$$FS_j = s_j w_j (1 + w_j\kappa_j)\ |\underline{r}| \tag{4-103}$$

will equal Δy_j when $\cos\theta_j$ is ± 1. To this end, let ρ_j be another scale factor, defined by

$$\rho_j \equiv \frac{1 - \lambda}{|\underline{e}_j - \underline{\phi}_j|} \tag{4-104}$$

Now we define κ_j by

$$\kappa_j \equiv \begin{cases} \dfrac{(\alpha^2 + (\rho\beta)^2 + 2\alpha\rho\beta v_j)^{1/2}}{(\alpha^2 + \beta^2 + 2\alpha\beta v_j)^{1/2}} - 1, & \text{sign}(\alpha)=\text{sign}(\beta) \\ \left.\begin{matrix} \rho_j - 1 \\ 0 \end{matrix}\right\} & \text{sign}(\alpha)\neq\text{sign}(\beta) \quad \begin{cases} |\beta| > |\alpha| \\ |\beta| \leq |\alpha| \end{cases} \end{cases} \tag{4-105}$$

The first part of this definition is illustrated in Figure 4.9. Part a of the figure is similar to Figure 4.8a; part b shows the effect of multiplying β by ρ_j. The vector $\underline{r}^{\circ\prime}$ is the vector whose projection onto the plane spanned by $\underline{e}_j$ and $\underline{v}_j$ is $\underline{r}'$ and whose angle to that plane is θ_j, the same angle $\underline{r}$ makes.

With κ_j defined as in (4-105), we obtain the desired result, namely that whenever w_j equals 1, Equation (4-103) reduces to

$$FS_j = \Delta y_j \tag{4-106}$$

4.3.4 Summary

The identification procedure presented in this section consists mainly of the calculation at each sampling time of a scalar quantity associated with each component. These scalars are well-suited to any of several deterministic or statistical tests for deciding whether one, or more, is large enough to indicate a failure.

The scalars are defined by

$$FS_i = s_i w_i (1 + w_i \kappa_i) \left|\underline{r}\right| \tag{4-97}$$

with

$$w_i = \frac{1 - \cos^N\theta_{min}}{1 - \cos N_{\theta_i}} \cos^N\theta_i \tag{4-108}$$

The cosines are calculated from (4-58) for unidirectional failure vectors and from (4-83) for plane segments:

$$r \cdot v_i = \left|r\right| \cos\theta_i \tag{4-58}$$

$$r_{p_i} = \left|r\right| \cos\theta_i \tag{4-83}$$

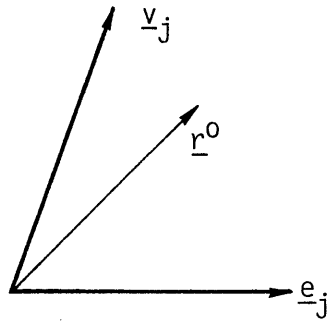

Orthogonal projection $\underline{r}^\circ$ prior to scaling of β.

Part a.

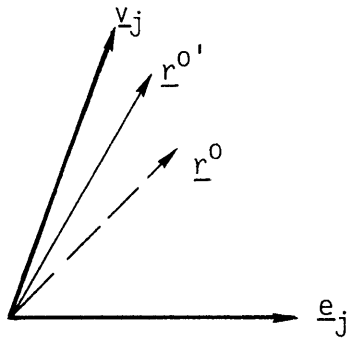

The modified projection $\underline{r}^{\circ\prime}$.

Part b.

Figure 4.9. Scaling the failure signature of a sensor.

The sign of FS_i, s_i, is the sign of $\cos\theta_i$. The number N is any positive even integer, chosen to give the calculations the desired selectivity. The angle θ_{min} is the θ for which $\cos\theta$ is closest to ± 1. For unidirectional signatures κ is given by

$$\kappa_i \equiv \frac{(1 - \lambda)}{|\underline{f}_{1_i}|} - 1 \qquad (4\text{-}107)$$

where $\underline{f}_{1_i}$ is frequently $\underline{\gamma}_{1_i}$. For planar signatures, κ is given by the lengthier expression in (4-105).

Chapter V

APPLICATION TO THE F100 ENGINE

The motivation for the analytical discussion just completed is the need for methods of failure detection, identification, and accommodation suitable for use in the controllers of modern aircraft turbine engines. One important way of increasing the performance, the overall efficiency, and the life of these engines is to use sophisticated control laws implemented in versatile and economical microprocessors. But such control requires measurement of many pressures, temperatures, and rotor speeds and requires precise regulation of fuel flow and of the positions of the fan vanes, compressor vanes, and exhaust nozzle; each sensor and actuator incorporated in the system to fulfill these needs might at some time malfunction. The more of them there are, the more likely that one will fail. But on the other hand, with many of them, when one does fails sufficient capability remains to run the engine satisfactorily, provided the controller does not act blindly on the basis of a false measurement or does not expect an inoperative actuator to move. When it knows a component has failed, it can adapt its operation to keep the engine running properly, though perhaps not with full performance.

The aim of this research was to evaluate the ability of a detection filter to detect and identify failures of most engine parts of concern--sensors, actuators, compressors, and turbines. Specifically excluded is the controller itself, for its microprocessors will do the calculations that constitute the filter. For the purposes of this study, it has been assumed that the microcomputer controller will be made reliable by other fault-accommodation techniques appropriate to it.

5.1 THE F100 ENGINE

The testbed chosen for the evaluation of the detection filter concept is a nonlinear dynamic simulation of the Pratt and Whitney F100-PW-100(3) military engine. The Pratt and Whitney Company has provided the digital simulation that that company and others have used to test new control techniques. The F100 powers the McDonnell-Douglas F15 Eagle and the General Dynamics F-16 Falcon and is currently the most advanced engine in production. It is a two-spool, low-bypass-ratio turbofan with a mixed-flow afterburner. Maximum thrust is between 25,000 and 30,000 pounds, roughly eight times its weight. The F100 is shown in Figure 5.1 with the major components labeled. Figure 5.2 shows the locations of the control measurements and inputs and of the station numbers used in the notation. The variables shown are described in Table 5.1.

The F100's control system is primarily hydromechanical, but it has an electronic supervisory unit that performs some of the logic and trims the engine for more precise operation. The F100-PW-100(3) simulation incorporates a representation of this control system. The detection filter designed for the engine is of course intended for use with an electronic controller, but its performance depends little, if any, on the control law actually used, so the simulation as it is provides a suitable test of the filter. Pratt and Whitney is developing a full-authority electronic controller for the engine, a controller that will probably use just one more measurement than the present system. That measurement is P_{t6} and is included in the reference model of the detection filter. Figure 5.3 shows the general structure of the electronic control system, with the measurements and control inputs the system is likely to have. The sensors in this system will be more accurate and more responsive than the ones in the hydromechanical system; the sensor models in the simulation have been altered to reflect this improvement. Also, a model of the P_{t6} sensor has been added. Table 5.2 lists the probable characteristics of the electronic sensors, including their dominant first-order time constants.

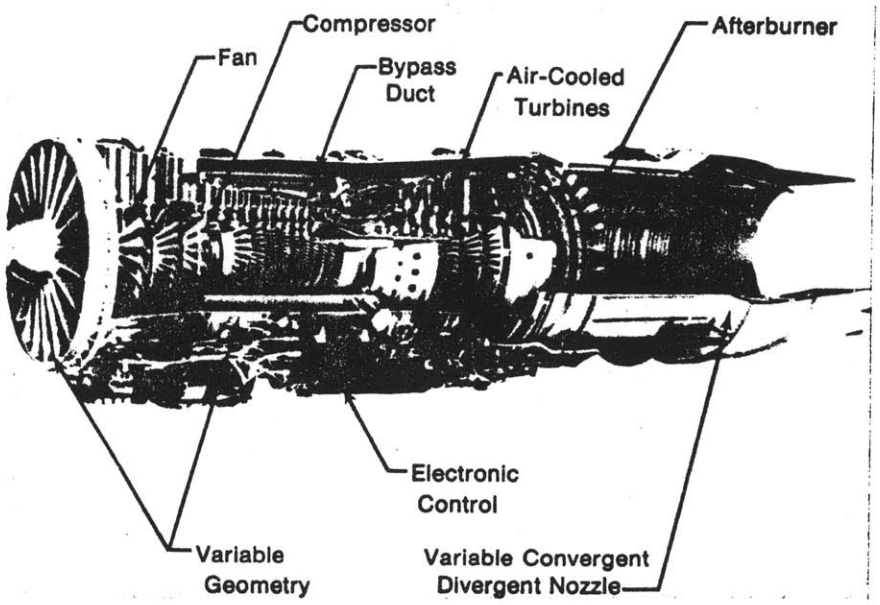

Figure 5.1. A cut-away view of the F100 turbofan.

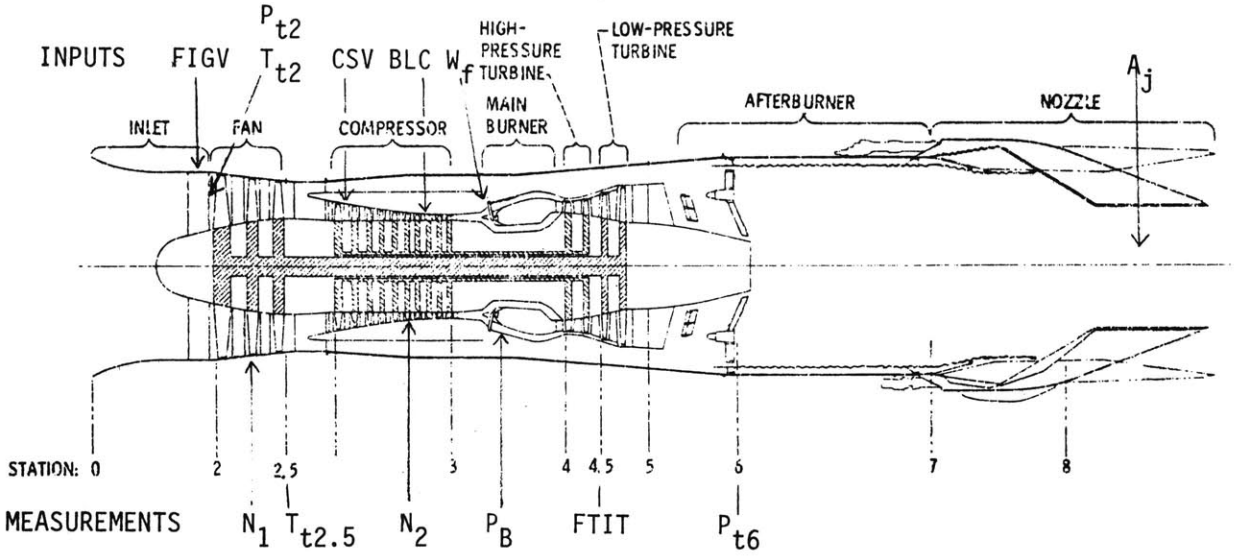

Figure 5.2. Drawing of the F100 showing the measured variables, the actuators, and the station numbers.

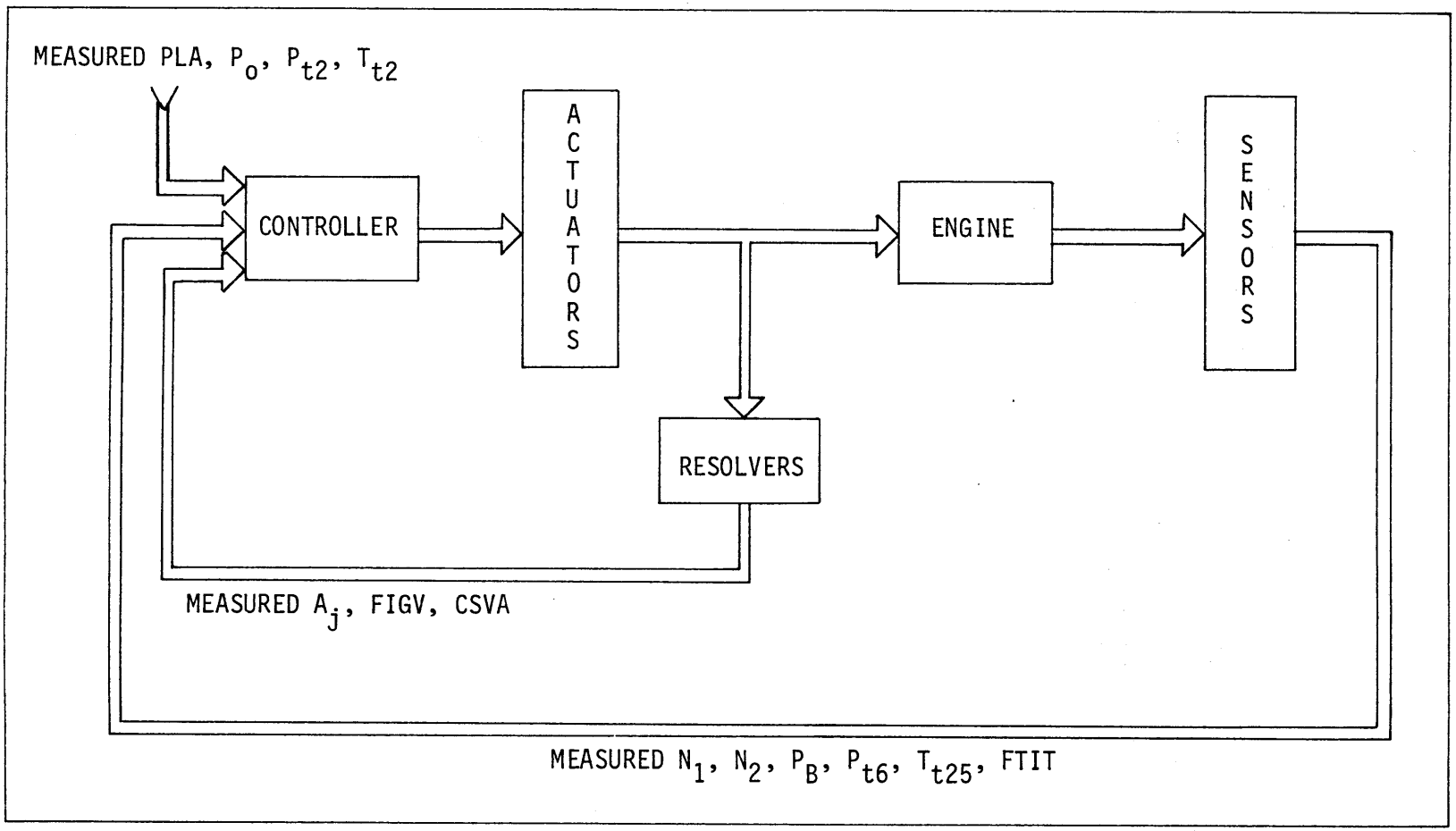

Figure 5.3. General structure of a digital electronic control system for the F100.

TABLE 5.1

Control variables.

Measured Engine Variables		Inlet Conditions	
		P_0	- Ambient static pressure
N_1	- Fan speed	P_{t2}	- Fan inlet total pressure
N_2	- Compressor speed	T_{t2}	- Fan inlet total temp.
P_6	- Burner total pressure		
P_{t6}	- Augmentor total pressure	Controlled Inputs	
T_{t25}	- Fan outer discharge total temperature	W_f	- Fuel flow, main burner
FTIT	- Low pressure turbine inlet total temperature	W_{ab}	- Fuel flow, augmentor
		A_j	- Exhaust nozzle area
		FIGV	- Fan inlet vane angle
		CSVA	- Compressor vane angle
		BLC	- Compressor bleed airflow

5.2 CONSIDERATIONS FOR THE DESIGN OF THE FILTER.

Some of the motivation and justification for using an analytical technique such as the detection filter comes from statistical data on sensors that have been in service. As the numbers in Table 5.2 indicate, about 90 percent of all sensor failures are hard failures that can be detected and diagnosed by checking for signals that go out of range or that change unreasonably rapidly. But recent studies suggest that if goals

TABLE 5.2

Sensor characteristics.

Sensor	Type	Accuracy (% of range[1])	Time Constant	Failure rate per mil. hrs.	Out-of-range %	Drift %	Noise %
N_1	Magnetic pickup	3 rpm (.04%)	.02 sec.	22	93	1	6
N_2	Alternator winding	3 rpm (.07%)	.02	58	80	10	10
P_{t2}	Vibrating cylinder	.02 psi(.09%)	.02	18	89	10	1
P_b	Vibrating cylinder	.4 psi (.07%)	.035	18	89	10	1
P_{t6}	Vibrating cylinder	.07 psi (.1%)	.02	18	89	10	1
T_{t2}	Thermocouple	3 R (1%)	0.5-2.0[2]	43	87	10	1
T_{t25}	Thermocouple	7 R (1%)	0.1-0.5[2]	43	87	12	1
FTIT	Thermocouples	12 R (1%)	0.5-6.0[3]	222	20	79	1
A_j	Resolver	-	-	25	85	10	5
FIGV	Resolver	-	-	25	85	10	5
CSVA	Resolver	-	-	25	85	10	5

[1]Range is normal operating range listed in Table A.2.
[2]Depends on how well the instrumentation can compensate for heat transfer lags.
[3]The response is best modeled by two parallel first-order lags, one with time constant of .6, the other of 5.5.

for overall reliability are to be achieved, virtually no single sensor failure can be allowed to evade detection and identification.[1] Therefore the fault-accommodation system must be able to isolate the remaining 10 percent of the sensor failures--slow, in-range drifts and excessive noise. The detection filter concept is a promising approach to meeting that challenge.

A filter will only be part of the detection system, and there are many benefits to designing it specifically to complement the rest of the system. In particular, a filter can be used in conjunction with redundant sensors to greatly enhance identification accuracy. It is likely that some of the least costly and most failure-prone sensors will be duplicated--perhaps the two speed sensors and either the T_{t2} sensor or the T_{t25} sensor. In that case, only one of each pair is connected to the detection filter. A mismatch in any pair signals a failure, and whether or not the filter also signals a failure indicates which member of the pair is faulty. Subsequently, the filter covers the second member of the pair for a possible failure. Common-mode failures of each pair would also be covered. In principle, when a detection filter is used, redundant sensors should not be necessary, at least for coverage of any single sensor failure; but in practice, some redundancy may be essential, both to enhance coverage of multiple failures and to help the filter with single failures. Some of the failure directions lie close enough together that modeling error may prevent consistent identification of which of two possible failures has occurred. Wherever potential ambiguity exists involving a sensor, a redundant sensor would resolve the problem.

For purposes of modeling sensor behavior, we categorize the sensors on the engine into two classes: those that measure important dynamics (viz. N_1, N_2, P_b, P_{t6}, T_{t25}, FTIT) and those that measure inputs (viz.

[1] The sensor data and reliability studies are presented in the progress reports of the FAFTEEC Program [31]. Similar sensor data are given in the monthly reports of the Failure Detection System Program [28].

P_{t2}, T_{t2}, A_j, FIGV, CSVA).[2] The first class is explicitly discussed in the procedures of the preceding chapters; the second is not. Nevertheless, the sensors in the second class come within the purview of the filter, for the failures of these sensors can be modeled in the same way as actuator failures. Let us consider first the P_{t2} and T_{t2} sensors.

The inlet conditions are not freely controllable in the manner the actuators are, so for purposes of control system design they are not usually considered as inputs (i.e. they are not included in the input vector $\underline{u}$). But in the reference model for a detection system they should be. The measurements of P_{t2} and T_{t2} are essential--the required fuel flow and the appropriate vane and nozzle positions depend on those quantities--so it is important to monitor the sensors for malfunction. With P_{t2} and T_{t2} included in $\underline{u}$, failures of those sensors can be treated just like actuator failures, and the failure signatures will be unidirectional. Specifically, suppose the i'th element of $\underline{u}$ represents P_{t2} and the sensor is in error by the amount Δu_i. The input failure model is applicable, so the error would be modeled by

$$\begin{aligned} \underline{x}_{k+1} &= \Phi\underline{x}_k + \Gamma\underline{u}_k + \underline{\gamma}_i \Delta u_i \\ \underline{y}_{k+1} &= [I:0]\underline{x}_{k+1} \end{aligned} \tag{5-1}$$

The event vector is $\underline{\gamma}_i$, the corresponding column of Γ.

A general note of clarification is needed here. When modeling failures in the above manner, we have implicitly considered $\underline{u}$ to be the expected inputs to the system--that is, the commanded or measured[3] positions of actuators and the measured values of uncontrolled inputs. When a failure occurs, one of the elements of $\underline{u}$ differs from the actual input to the system, and we add a term to the dynamics equation to depict the

[2] See Figure 5.3. Also, fuel flow is not measured because there is no reliable sensor that is accurate over the full range of flow rates.

[3] The measured position of an actuator can be used when the dynamics of the actuator are insignificant and the actuator's output is not made a state variable. This approach is discussed later in this section.

difference. In other words, the elements of $\underline{u}$ are specifically what the controller believes each input to be either on the basis of a command issued or a measurement received. This is not entirely consistent with the original definition of $\underline{u}$ as the "vector of inputs"--which by implication meant the actual inputs--but the shift in interpretation should cause little, if any, difficulty.

The sensors that measure A_j, FIGV, and CSVA must be considered in conjunction with the actuators. A detection system can be designed to monitor each actuation system as a unit or to look separately for failures of the actuator mechanism and of the feedback sensor. The latter approach is taken here because the detection filter provides not only the information necessary to perform the separation but also a means of controlling the actuator if the sensor fails.

The four controllable inputs--W_f, A_j, FIGV, and CSVA--are all regulated by mechanisms with inherent dynamic lags, but only one, the fuel flow, is slow enough to warrant including its dynamics in the reference model. Figure 5.4 shows approximate transfer functions for the actuators. The nozzle position and the fan and compressor vane angles are fed back in high-gain proportional control loops, which make the actuators respond rapidly. The time constants characteristic of these actuation systems range from 0.05 second to 0.02 second. The time constants of the dominant dynamic lags in the engine range from a little under 1 second down to about 0.15 second. At 0.10 second, the dominant time constant of the fuel system is comparable to some of the important time constants of the engine itself.

A simple method of failure detection can be used in conjunction with the detection filter to take advantage of the rapid responses of the three actuators that have feedback loops. Since the position of any of these actuators should never lag much behind the commanded position, a comparison of the measured position with the position commanded tells whether the actuator is functioning properly: a significant discrepancy

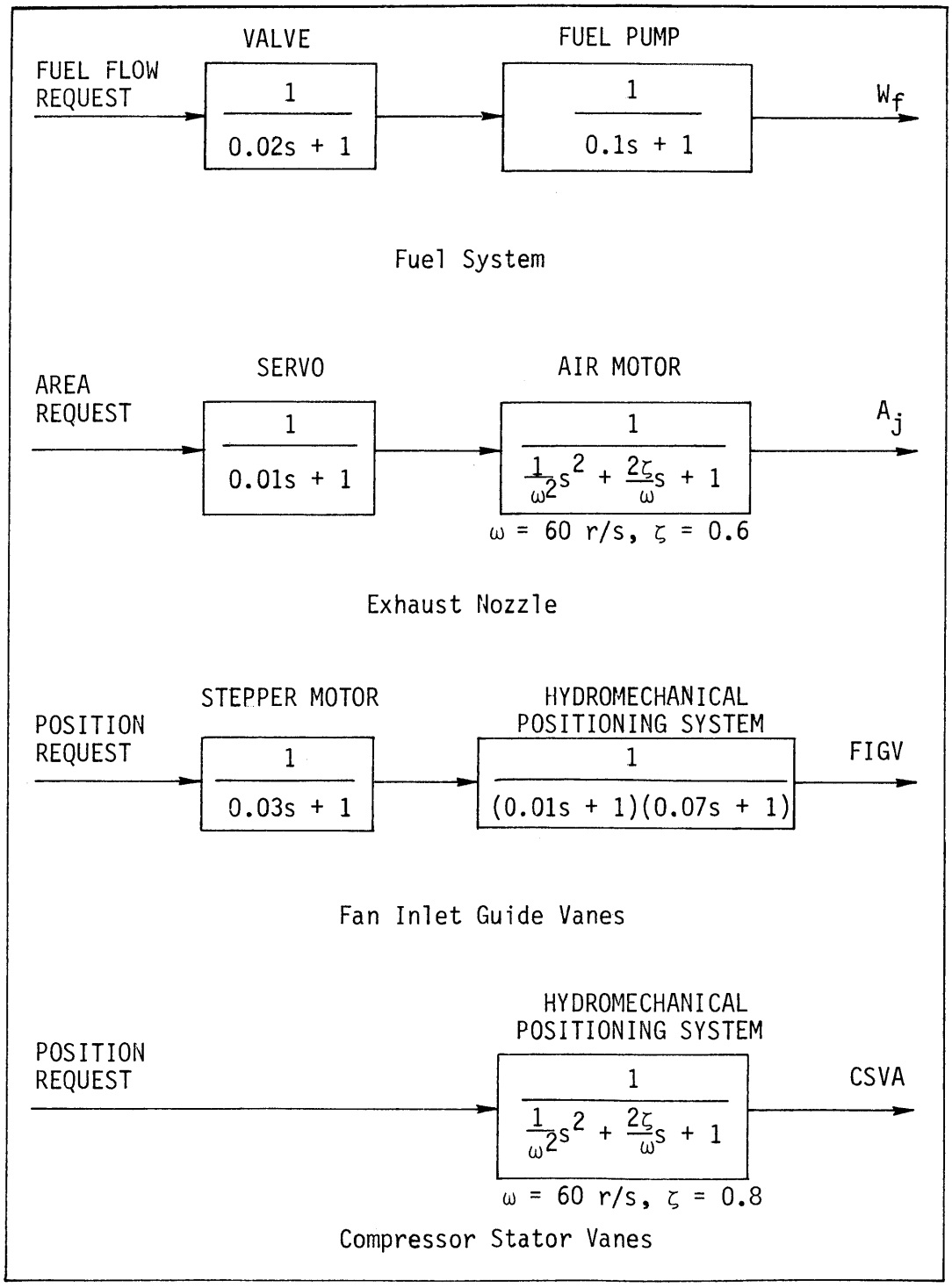

Figure 5.4. Linear characterizations of the actuation systems.

indicates malfunction.[4] The detection filter would then be designed to identify failures of the position sensors, in the same manner failures of the P_{t2} and T_{t2} sensors are to be identified. Figure 5.5 illustrates this approach. The quickness of the actuators should allow use of tight thresholds, particularly if the rate of change of the command is used to move the threshold band up or down as appropriate. Since each of the nozzle and vane control loops inherently contains integration, the difference between the measured position and the command should quickly become zero whenever the command stays constant. Just a small difference would indicate some difficulty with the actuator.

We should note that relatively rapid sensor failures could also cause the difference between the actuator commanded position and measured position to exceed the threshold. To cover the possibility that the change in sensor output is not rapid enough to be caught by the reasonableness checks, the failure identification logic must include a pause after an indication of an actuator failure to give time for the filter to generate a failure signature should the sensor be at fault.

When a position sensor does fail, it must be disconnected from the filter, and the position error signal must be disconnected from the input to the actuator. Operation of the actuator can then be partly restored by using the position command as the input to the filter and the failure signal corresponding to that input as the driver of the actuator, as shown in Figure 5.6. The failure signal is a slow-response error signal indicative of the difference between the actuator's position and the command. This substitute feedback loop must have a low gain, but however small the gain is and however slowly the actuator then moves, at least the actuator can still be used.

This idea has not been tested, nor has the proposed method of detecting actuator failures. The failure simulations that have been conducted were intended strictly for testing the ability of the detection filter and the identification procedure to produce readily

[4] This method of diagnosing actuator failures has been proposed by others as well, notably by Rock [37].

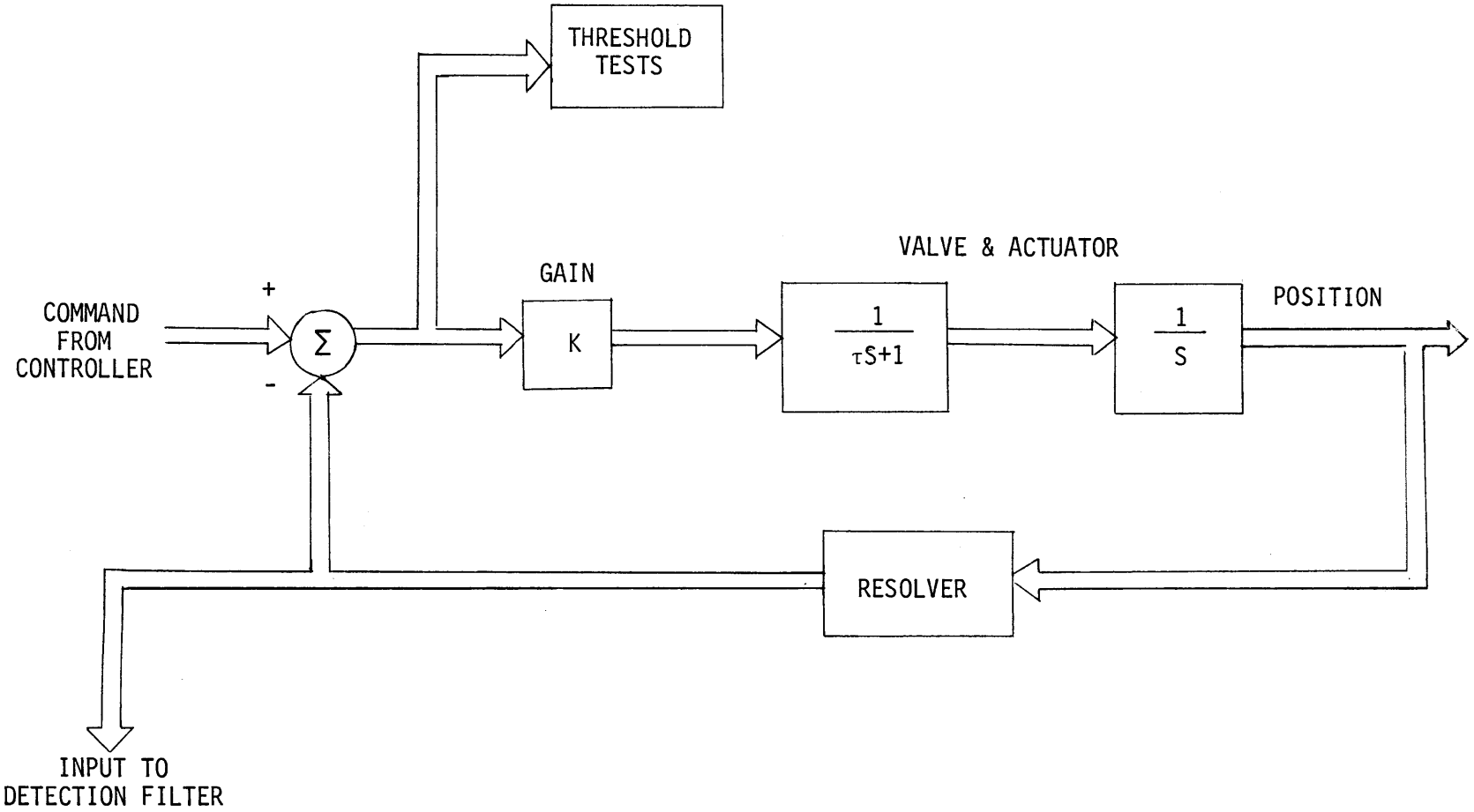

Figure 5.5. Proposed approach for separately identifying actuator failures and failures of position sensors.

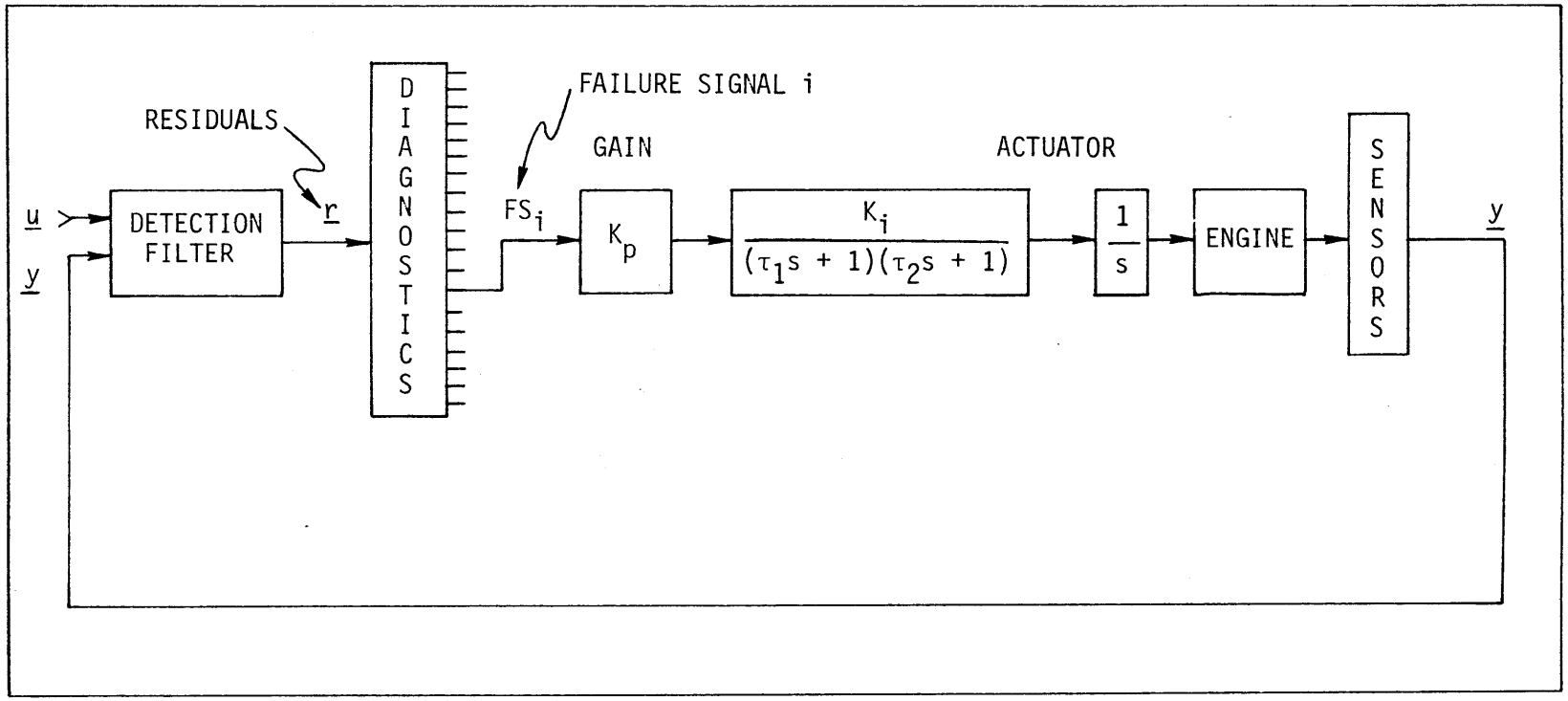

Figure 5.6. Method for accommodating a failure of a nonredundant actuator position sensor.

interpretable failure signals. Failures of the fuel system and of the position sensors for nozzle and the vanes do come within the scope of the filter, and the testing included examples of such failures. The untested procedures are mentioned to provide the rationale for designing the filter to identify failures specifically of the position sensors, not of each actuation system as a whole, and to suggest another possible use of detection filters.

In summary of this section, Table 5.3 lists the components the filter is designed for and the type of failure signature each has. Not yet mentioned are the high-pressure compressor and turbine; decreases in the efficiencies of these components were simulated to test the filter's ability to diagnose malfunctions within the engine itself.

TABLE 5.3

Components covered by the detection filter and the identification procedure.

With planar signatures	With unidirectional signatures	
1) N_1 sensor	5) T_{t25} sensor*	10) nozzle pos sensor
2) N_2 sensor	6) FTIT sensor*	11) FIGV pos sensor
3) P_{b}^{2} sensor	7) HP comp eff	12) CSVA pos sensor
4) P_{t6} sensor	8) HP turb eff	13) P_{t2} sensor
	9) Fuel system	14) T_{t2} sensor

*These sensors have unidirectional signatures because they are not included in the state vector.

5.3 LINEAR MODELS

There are many methods of constructing linear models of nonlinear systems, and several have previously been applied to turbine engines.[5] The

[5]See, for example, DeHoff and Hall [14], Edmunds [17], Merrill [32] & [33](pp.3-9), and Michael and Farrar [35].

one used in this study is a multivariable tangent-approximation method. Basically, it involves calculation of the first-order terms in the Taylor series expansion of the nonlinear dynamic relationships about a given operating point. This approach can only be used when an accurate, nonlinear mathematical representation of the system is available. For the F100 engine, the nonlinear simulation serves this purpose. In this chapter, the reference model for the filter is derived for the vicinity of just one operating point; in Chapter 6, a procedure is developed for concatenating linear models from several operating points into a single, piecewise linear model.

5.3.1 Full-order Model

The F100 nonlinear simulation contains a tangent-approximation routine for generating a 16th-order linear model at any equilibrium point. The operating point selected for initial evaluation of detection filters is full intermediate (nonaugmented) power at sea level static conditions. Only some of the dynamics of the 16th-order model are slow enough to warrant inclusion in the reference model of the filter, so the high-order model was reduced to a more easily implemented low-order model. Since detection filter theory is strictly linear, initial testing of a filter built from this linear reference model that is reasonably accurate at one operating point has verified the applicability of the concepts embodied in the theory. Morever, working with various models obtained from the 16th-order model has shown what the important dynamics of the engine are, and hence what order and what state variables the reduced-order model should have.

The 16th-order linearizations are produced in the form

$$\begin{aligned} \dot{\underline{x}}(t) &= A\Delta\underline{x}(t) + B\Delta\underline{u}(t) \\ \Delta\underline{y}(t) &= C\Delta\underline{x}(t) + D\Delta\underline{u}(t) \end{aligned} \tag{5-2}$$

The Δ's indicate deviations from the equilibrium about which the linearization is performed. The matrix D in (5-2) is unrelated to the feed-

back matrix of the detection filter, and in fact, it must be eliminated to make the model suitable for a detection filter. The linearization procedure consists of calculating approximate partial derivatives of $\dot{\underline{x}}$ and $\Delta\underline{y}$ with respect to the elements of $\underline{x}$; these derivatives become the elements of A and C. Then for a small deviation in each u_i, the respective columns of B and D are set to make $\dot{\underline{x}}$ zero and $\underline{y}$ the appropriate value for the equilibrium $\Delta\underline{x}$ corresponding to the Δu_i. Details are presented in References [14] and [21]. Table 5.4 lists all the variables of the model used in this study.

The next few pages describe the steps taken to obtain a simple linear model. Appendix A presents the numerical results. Given first in Table A.1 are the A, B, C, and D matrices of the 16th-order model. The beginning step in reducing these to a lower order is calculation of the eigenvalues of A; they determine the selection of variables for the reduced-order model. Table 5.5 lists them in sequence from least to most negative. The separation between the fifth and sixth values is the division chosen for the order reduction: all dynamics with eigenvalues less than -10 are ignored. The reduction is accomplished by identifying five state variables with the first five eigenvalues and eliminating from the model the remaining state variables.[6] From the nonlinear simulation's modeling of the mechanics and thermodynamics of the F100, one can discern which eigenvalues correspond to which energy-storing components in the engine, and hence with which state variables. The first two eigenvalues are associated with heat transfer between the gases and the heavier metal parts in the hot section; the variables are T_{t41o} and T_{t451o}. The third, fourth, and fifth correspond to couplings among the kinetic energies of the two rotors and the energy of the large volume of gas in the augmentor. They as a group are related to N_1, N_2, and P_{t7}. The energies involved in the two heat transfer processes are an order of magnitude less than those of the primary thermodynamic processes in the engine, so the variables T_{t41o} and T_{451o} could justifiably be neglected

[6]Weinberg [50] and Edmunds [17] have previously used this approach with the F100 linear models.

TABLE 5.4

Variables of the 16th-order model.

Engine State Variables

x_1 = Fan speed, N_1 - rpm
x_2 = Compressor speed, N_2 - rpm
x_3 = Compressor discharge total pressure, P_{t3} - psia
x_4 = Interturbine total pressure, P_{t45} - psia
x_5 = Augmentor total pressure, P_{t7} - psia
x_6 = Fan core discharge total temperature, T_{t25} - °R
x_7 = Fan duct discharge total temperature, T_{t25} - °R
x_8 = Compressor discharge temperature, T_{t3} - °R
x_9 = Burner exit fast-response temperature, T_{t4hi} - °R
x_{10} = Burner exit slow-response temperature, T_{t4lo} - °R
x_{11} = Burner exit total temperature, T_{t5} - °R
x_{12} = Fan turbine inlet fast-response temperature, T_{t45hi} - °R
x_{13} = Fan turbine inlet slow-response temperature, T_{t45lo} - °R
x_{14} = Fan turbine exit total temperature, T_{t5} - °R
x_{15} = Duct exit total temperature, T_{t6} - °R
x_{16} = Augmentor exit total temperature, T_{t7} - °R

Inputs

u_1 = Main burner fuel flow, W_f - lb./hr.
u_2 = Exhaust nozzle area, A_j - $ft.^2$
u_3 = Fan inlet guide vane angle, FIGV - degrees
u_4 = Compressor stator vane angle, CSVA - degrees
u_5 = Compressor bleed to aircraft, BLC - fraction of airflow
u_6 = Fan inlet total pressure, P_{t2} - psia
u_7 = Fan inlet total temperature, T_{t2} - °R

Measurements

y_1 = Fan speed, N_1 - rpm
y_2 = Compressor speed, N_2 - rpm
y_3 = Burner total pressure, P_b - psia
y_4 = Augmentor inlet total pressure, P_{t6} - psia
y_5 = Fan outside discharge total temperature, T_{t25} - °R
y_6 = Fan turbine inlet total temperature, FTIT (T_{t45}) - °R

even though their dynamics are slow. In Chapter 6, T_{t41o} and T_{t451o} are deleted from the model, but here they are retained because of the possibility their effects would, if neglected, cause false indications of small failures. The test results presented at the end of this chapter show, however, that their effects are smaller than the many modeling errors already introduced by neglecting nonlinearities and some of the dynamics.

TABLE 5.5

Eigenvalues of the 16th-order model.

1) -0.660	6,7) -18.62 ± i5.352	12) -47.52
2) -1.964	8) -19.45	13) -49.38
3) -2.732	9,10) -20.66 ± i0.921	14) -58.26
4,5) -6.102 ± i2.259	11) -39.71	15) -177.7
		16) -573.4

At some point in the construction of the reference model, the variables must be normalized. It is advantageous to do so before reducing the full-order model, for when the model is normalized one can more easily discern what elements of the model are most important. In particular, the eigenvectors of the normalized model provide confirmation of how the eigenvalues are related to particular state variables.[7] The most most meaningful normalization for purposes of failure detection is

[7] Skira and DeHoff [41] did an eigenmode analysis of the F100 linear model as part of a modal reduction of the model. This reduction procedure yields a model whose eigenvalues are selected eigenvalues of the full model. This procedure was tried in this study also, but the model obtained was not quite as good as the one obtained using the approach described above. In general, unless the deleted eigenvalues are all greatly different from the ones retained, the eigenvalues of the best low-order model do not form a subset of the eigenvalues of the full-order model. Truxal [46] (p.285) made this point in regard to single-input single-output systems.

Rock and DeHoff [37] have done an eigenmode analysis of a variable cycle engine. This provides some additional insight into the dynamic behavior of turbofan engines.

obtained by referencing each variable to its minimum realizable value and scaling it by the reciprocal of its range over all operating conditions. The normalized variables thus defined range from zero to one. (See Table A.2.) Henceforth, although the notation is unaltered, all the variables are normalized unless otherwise indicated.

5.3.2 Reduced-Order Model

We now reorder and partition the state variables to collect in a subvector $\underline{x}_1$ the variables to be retained:

$$\underline{x}_1 = \begin{bmatrix} N_1 \\ N_2 \\ P_{t7} \\ T_{t4} \\ T_{t45} \end{bmatrix} \tag{5-3}$$

With A, B, and C rearranged accordingly, the state and measurement equations of the 16th-order model take the form

$$\begin{bmatrix} \dot{\underline{x}}_1 \\ \dot{\underline{x}}_2 \end{bmatrix} = \begin{bmatrix} A_{11} & A_{12} \\ A_{21} & A_{22} \end{bmatrix} \begin{bmatrix} \underline{x}_1 \ (5) \\ \underline{x}_2 \ (10) \end{bmatrix} + \begin{bmatrix} B_1 \\ B_2 \end{bmatrix} u \tag{5-4}$$

$$\underline{y} = [C_1 \ C_2] \begin{bmatrix} \underline{x}_1 \\ \underline{x}_2 \end{bmatrix} + D\underline{u}$$

To perform the reduction, we assume the variables in $\underline{x}_2$ are always in equilibrium with respect to $\underline{x}_1$ and $\underline{u}$. Their values as functions of $\underline{x}_1$ and $\underline{u}$ are found by setting $\dot{\underline{x}}_2$ in (5-4) equal to zero:

$$\dot{\underline{x}}_2 = 0 = A_{21}\underline{x}_1 + A_{22}\underline{x}_2 + B_2\underline{u} \tag{5-5}$$

This yields

$$\underline{x}_2 = -A_{22}^{-1}[A_{21}\underline{x}_1 + B_2\underline{u}] \tag{5-6}$$

There are no zero eigenvalues of A_{22}, so the solution given in (5-6) exists. Substituting (5-6) into (5-4), we obtain the reduced-order model:

$$\dot{\underline{x}}_1 = [A_{11} - A_{12}A_{22}^{-1}A_{21}]\underline{x}_1 + [B_1 - A_{12}A_{22}^{-1}B_2]\underline{u}$$
$$\underline{y} = [C_1 - C_2A_{22}^{-1}A_{21}]\underline{x}_1 + [D - C_2A_{22}^{-1}B_2]\underline{u} \qquad (5\text{-}7)$$

To this fifth-order model must be added first-order dynamics to account for hydromechanical lags in the fuel system and heat transfer lags in the T_{t25} and FTIT sensors.[8] The primary time constants of all three components are greater than or equal to the value of 0.10 second that delineates the dynamics included in the model. The procedure used to generate the resulting eighth-order model is outlined in Appendix A.

The expansion to eighth-order leaves $\underline{y}$ unchanged, but it does, however, change the elements of $\underline{u}$ slightly. We replace the first element, W_f, by the fuel flow command, and now, having neglected the dynamics of the vane and nozzle mechanisms, we consider u_2, u_3, and u_4 to be the measured values of nozzle area, inlet vane angle, and stator vane angle, in accordance with the previously described method of separating actuator failures from failures of position sensors.

The next step in the process of putting the model in the desired form is transforming the state variables so that six of them equal the measurements and so that the remaining two are independent of those six. We do this as described in Section 4.2.1, except that it is more convenient to do so now rather than after the model is put in discrete-time form. The eight state variables are currently N_1, N_2, P_{t7}, T_{t41o}, T_{t451o}, W_f, T_{t25} sensed, and FTIT sensed. The measurement variables are the sensed values of N_1, N_2, P_b, P_{t6}, T_{t25}, and FTIT. Clearly, four of the state variables are already appropriate; the remaining four must be transformed to P_b and P_{t6} and to two independent canonical variables. The variables P_{t6} and P_{t7} differ only by the pressure drop along the augmentor duct (they have appeared separately in this model because the nonlinear simulation uses P_{t7} as the state variable, while in practice P_{t6} is the quantity measured), so transforming P_{t7} to P_{t6} presents no

[8] With the reduction procedure given by (5-7), it makes no difference whether these dynamics are added before or after the reduction is performed.

difficulty. Of the three remaining state variables, W_f is most closely related to P_b. At intermediate power, the burner pressure depends roughly one-half on P_{t6}, one-quarter on N_2, and one-quarter on T_{t4}; and in turn, T_{t4} depends strongly on W_f. Thus W_f can reasonably be replaced by P_b. The two slow-response temperatures, T_{t41o} and T_{t451o} are replaced by the two canonical variables that make the last two rows of A all zeros except for the elements on the main diagonal, which become the eigenvalues associated with the T_{t41o} and T_{t451o} (see Section 4.2.1 and Equation (4-37)).

Accordingly, beginning with the eighth-order model (with the transfer of W_f into the state vector, the $D\underline{u}$ term becomes negligible)

$$\begin{aligned} \dot{\underline{x}} &= A\underline{x} + B\underline{u} \\ \underline{y} &= C\underline{x} \end{aligned} \tag{5-8}$$

and following Section 4.2.1, we define the transformation as follows:

$$\begin{aligned} \underline{x}' &= T\underline{x} \\ T &= \begin{bmatrix} C \\ W \end{bmatrix} \\ A' &= TAT^{-1} \\ B' &= TB \\ C' &= [I:0] \end{aligned} \tag{5-9}$$

The resulting model is

$$\begin{bmatrix} \dot{\underline{x}}_1' \\ \dot{\underline{x}}_2' \end{bmatrix} = \begin{bmatrix} A_{11}' & A_{12}' \\ 0 & A_{22}' \end{bmatrix} \begin{bmatrix} \underline{x}_1' \\ \underline{x}_2 \end{bmatrix} + \begin{bmatrix} B_1' \\ B_2' \end{bmatrix} \underline{u} \tag{5-10}$$

$$\underline{y} = \underline{x}_1'$$

The variables in $\underline{x}'$, $\underline{y}$, and $\underline{u}$ are summarized in Table 5.6. The two rows of the matrix W are rows from the inverse of the matrix of A's eigenvectors, the two rows corresponding to the eigenvalues associated with

T_{t41o} and T_{t451o}. The matrices of (5-10) are listed in Table A.3., along with the eigenvalues of A'.

TABLE 5.6

The state, input, and measurement variables of the transformed eighth-order model.

$$\underline{x}_1' = \begin{bmatrix} N_1 \\ N_2 \\ P_b \\ P_{t6} \\ T_{t25} \text{ sensed} \\ \text{FTIT sensed} \end{bmatrix} \qquad \underline{u} = \begin{bmatrix} W_f & \text{command} \\ A_j & \text{sensed} \\ \text{FIGV} & \text{sensed} \\ \text{CSVA} & \text{sensed} \\ \text{BLC} & \\ T_{t2} & \text{sensed} \\ P_{t2} & \text{sensed} \end{bmatrix}$$

$$\underline{x}_2 = \begin{bmatrix} Z_1 \\ Z_2 \end{bmatrix}$$

$$\underline{y} = \begin{bmatrix} N_1 & \text{sensed} \\ N_2 & \text{sensed} \\ P_b & \text{sensed} \\ P_{t6} & \text{sensed} \\ T_{t25} & \text{sensed} \\ \text{FTIT} & \text{sensed} \end{bmatrix}$$

5.3.3 Discrete-Time Model

The continuous-time model (5-10) is in the standard linear form of (4-1), so the procedure in Section 4.1 for calculating discrete-time models applies directly. It is not yet apparent just how long the samp-

ling interval in an operational electronic controller will be, as the intervals used in experiments have ranged from about 5 ms to 50 ms or more. The interval selected for testing the detection filter is 20 ms, short enough that there is some assurance the discontinuity in the measurements will not noticeably degrade the performance of the filter, yet long enough that it is reasonably likely the required calculations can be implemented in a microprocessor.

The form of the discrete-time model derived from (5-10) is (with the primes on $\underline{x}$ omitted)

$$\begin{bmatrix} \underline{x}_1 \\ \underline{x}_2 \end{bmatrix}_{k+1} = \begin{bmatrix} \Phi_{11} & \Phi_{12} \\ 0 & \Phi_{22} \end{bmatrix} \begin{bmatrix} \underline{x}_1 \\ \underline{x}_2 \end{bmatrix}_k + \begin{bmatrix} \Gamma_1 \\ \Gamma_2 \end{bmatrix} \underline{u}_k \tag{5-11}$$

$$\underline{y}_{k+1} = \underline{x}_{1\,k+1}$$

(See Table A.4.)

5.4 DESIGNING A DETECTION FILTER

The system model (5-11) is in the form necessary for the design procedure given in Section 4.2.2. Because failures of the sensors of $\underline{y}$ must be detected, Equation (4-57) is used to compute the feedback matrix D. Specifically,

$$\begin{aligned} D_1 &= \Phi_{11} - \lambda I \\ D_2 &= 0 \end{aligned} \tag{5-12}$$

(Table A.5 lists the elements of D.) Fortunately, a filter having this D matrix is also suitable for all the other components of concern. The value selected for λ is .819, the discrete-time equivalent of -10. This value results in relatively little attenuation of the failure signatures and yet does not make the filter unduly slow. It becomes six of the

eigenvalues of [Φ-DC]; the other two are the elements of the diagonal matrix Φ_{22}, .846 and .983. These two unassignable eigenvalues are less than one and thus are acceptable.

Table 5.3 listed all the components the filter is to cover. Because it is designed by (5-12), the filter covers the six sensors of $\underline{y}$ properly, but it slightly compromises coverage of some of the other components to do so. The signatures of the others, which we would like all to be unidirectional, will deviate slightly from the desired directions. The event vectors for most of them are columns of Γ, and the elements of Γ_2 are not zero, as they must be if (4-57) is to be entirely valid for the associated components. But the two rows of Γ_2 drive the two state variables associated with the gas/metal heat transfers that do not influence the engine's behavior much. It is therefore reasonable to expect that Γ_2 can be neglected. The maximum deviations from the expected directions can be found by calculating the matrix $\Phi_{12}[I-\Phi_{22}]^{-1}\Gamma_2$ and comparing it column by column to Γ_1.[9] The deflection angles thus calculated are listed in Table A.5. The failure signature for the fuel system is the only one that should deviate noticeably, and that only by about 18 degrees. The calculated deflections of the others are less than 5 degrees. It turns out that even the predicted deflection for the fuel system signature is unnoticeable amidst the distortion caused by modeling error.

The method used for evaluating the residuals generated by the filter is exactly as specified in Section 4.3, with the parameter N equal to six (this value was found by experiment to give the desired degree of sensitivity). Using the failure vectors and scale factors listed in Table A.5, the algorithm calculates the magnitude of the residual vector, the angle the vector makes with the failure vector or plane segment nearest it, and scalar failure signals for the covered components. The test results that follow consist of plots of the residual magnitude, the angle, and the failure signals for simulations of various failures. As previously noted, the failure signals are designed so that in the

[9] Refer to Equations (4-90) to (4-93).

absence of sensor noise and modeling error, a failure causes the appropriate failure signal to become equal to the magnitude of the failure (e.g., to Δu_i or Δy_j), with the others remaining zero. With a failure of a sensor in $\underline{y}$, the failure signal immediately acquires the value Δy_j, whereas with failures of any of the other components the failure signal trails the value of Δu_i (or Δ efficiency in the case of turbine or compressor degradation) with the first-order lag associated with the 0.10-second time constant of the filter.

5.5 SIMULATION RESULTS

Sample failures induced in the full nonlinear simulation generated measurement and input data to test the detection filter on. The arrangement used in the testing is illustrated in Figure 5.7. Though the simulation and the detection filter were programmed on the same digital computer (Amdahl 470-V/8), they were run separately, with data from the simulation recorded for use by the filter. Early in each 1.8-second run of the simulation a small offset was injected into the output of the component selected to "fail" during that run. The controller compensated according to the normal control laws, unaware that a component had malfunctioned. The measurement and input data needed by the filter were recorded at 20 ms intervals, the design rate for the filter. Running the filter on these 1.8-second segments of data produced output consisting of the residuals and the failure signals. The latter appear in the results plotted on the following pages.

The responses of the filter to simulated malfunctions of four components are shown. Those components are the T_{t2} sensor, the high-pressure turbine, the fuel valve, and the P_b sensor. In addition, a fifth set of results shows the response to a sudden increase in airflow bled from the compressor. For each test, the plots appear in four groups of four. The first group gives the measured fan and compressor speeds, the fuel flow command, the magnitude of the filter residual vector, and the angle the vector makes with the failure direction it is nearest to. These plots provide information about the behavior of the

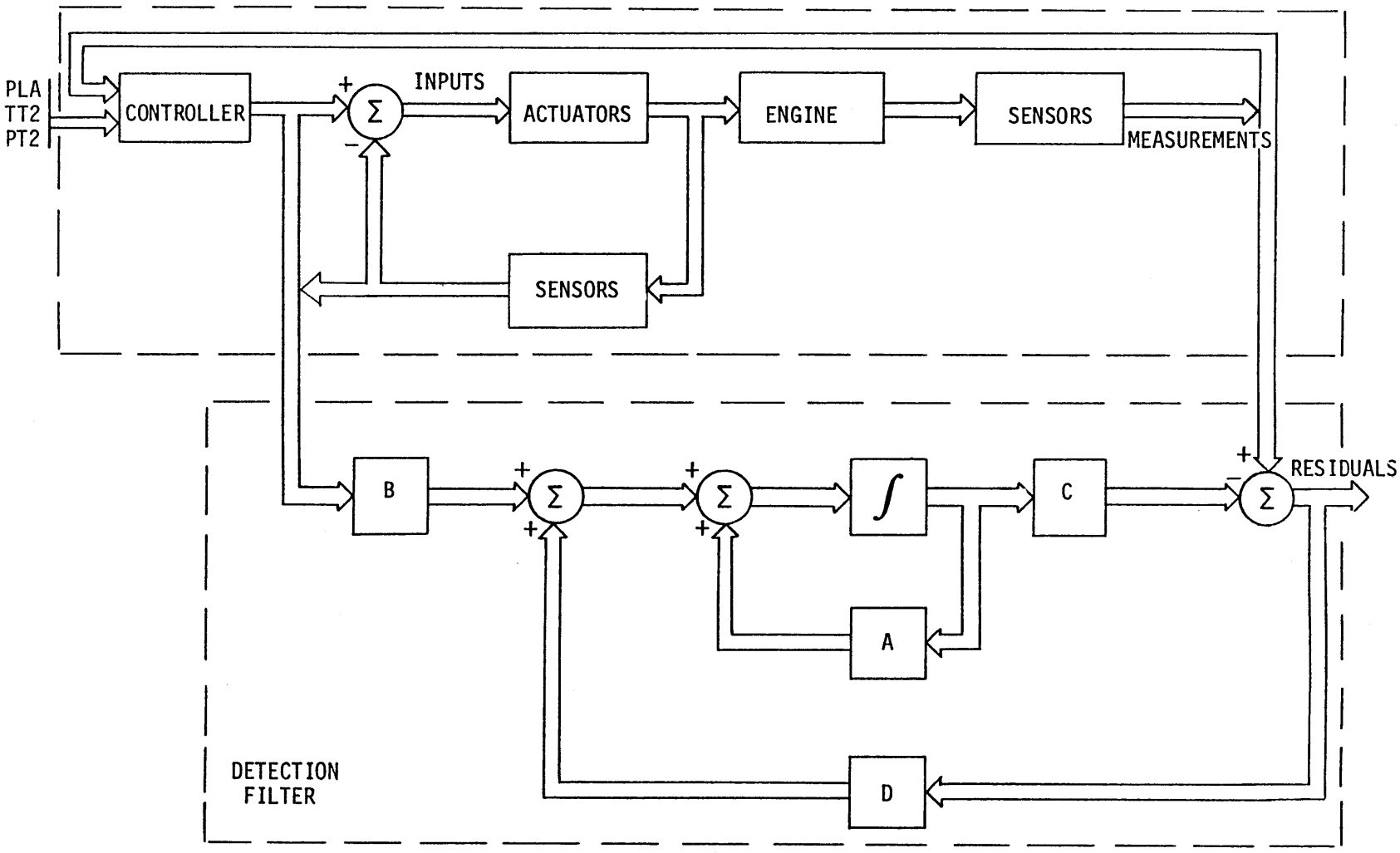

Figure 5.7. Testing the detection filter with the nonlinear F100 simulation.

F100 simulation, including the action of the controller, and about the performance of the filter in generating a residual vector of the size and direction expected for the particular malfunction. The other three groups of plots show the failure signals for 12 of the 14 components listed in Table 5.3. One of the two left out is the signal for decreases in compressor efficiency; it was not calculated during these tests. The other is the signal for the T_{t25} sensor; in each of these tests it was insignificant. Chapter 6 presents results from simulated failures of several of the components not failed in any of these examples, including the compressor and the T_{t25} sensor.

Figure 5.8 shows the results of a test in which the simulation was steady at intermediate power and then the inlet total temperature, T_{t2}, was gradually increased by 7°R, or 2 percent of range, with the T_{t2} sensor inhibited from indicating this change. The increase occurred as a linear ramp between the times of 0.1 and 1.0 second. As the graphs show, the rotor speeds eventually increased, and fuel flow command decreased slightly. Not shown is the decrease in burner pressure that caused the controller to reduce the fuel flow command. The residual from the filter increased in proportion to the increase in P_{t2}, with the slight time lag it must have because the engine does not respond instantaneously to the temperature change. As the residual became large enough to be definitive, it moved to a direction within a few degress of the failure direction for the T_{t2} sensor. The failure signal for that sensor moved negative about 2 percent, indicating that the sensor output was too low by that amount. None of the other failure signals became significant.

The results of the second example failure, an uncommanded increase in fuel flow by 200 lbs/hr, are shown in Figure 5.9. The increase represents about 1.2 percent of the maximum flow rate the fuel pump can deliver to the primary burner, and about 2 percent of the actual flow at steady state with PLA equal to 83. It caused 1 percent increases in the rotor speeds and created a residual vector with a magnitude of only 0.002. This was actually what the magnitude should have been, given the

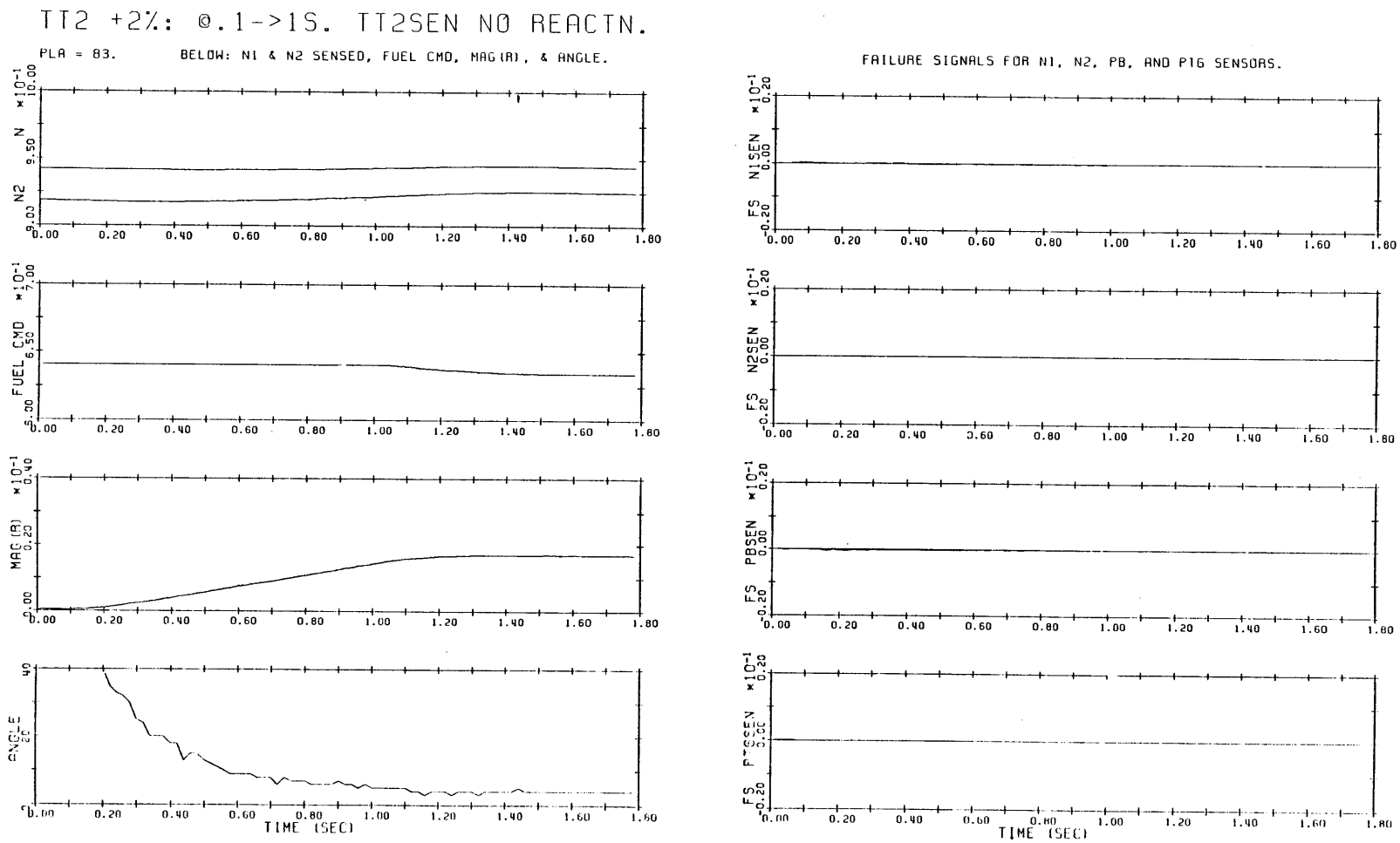

Figure 5.8. T_{t2} sensor failing to indicate a 7°R (2%) increase in T_{t2}.

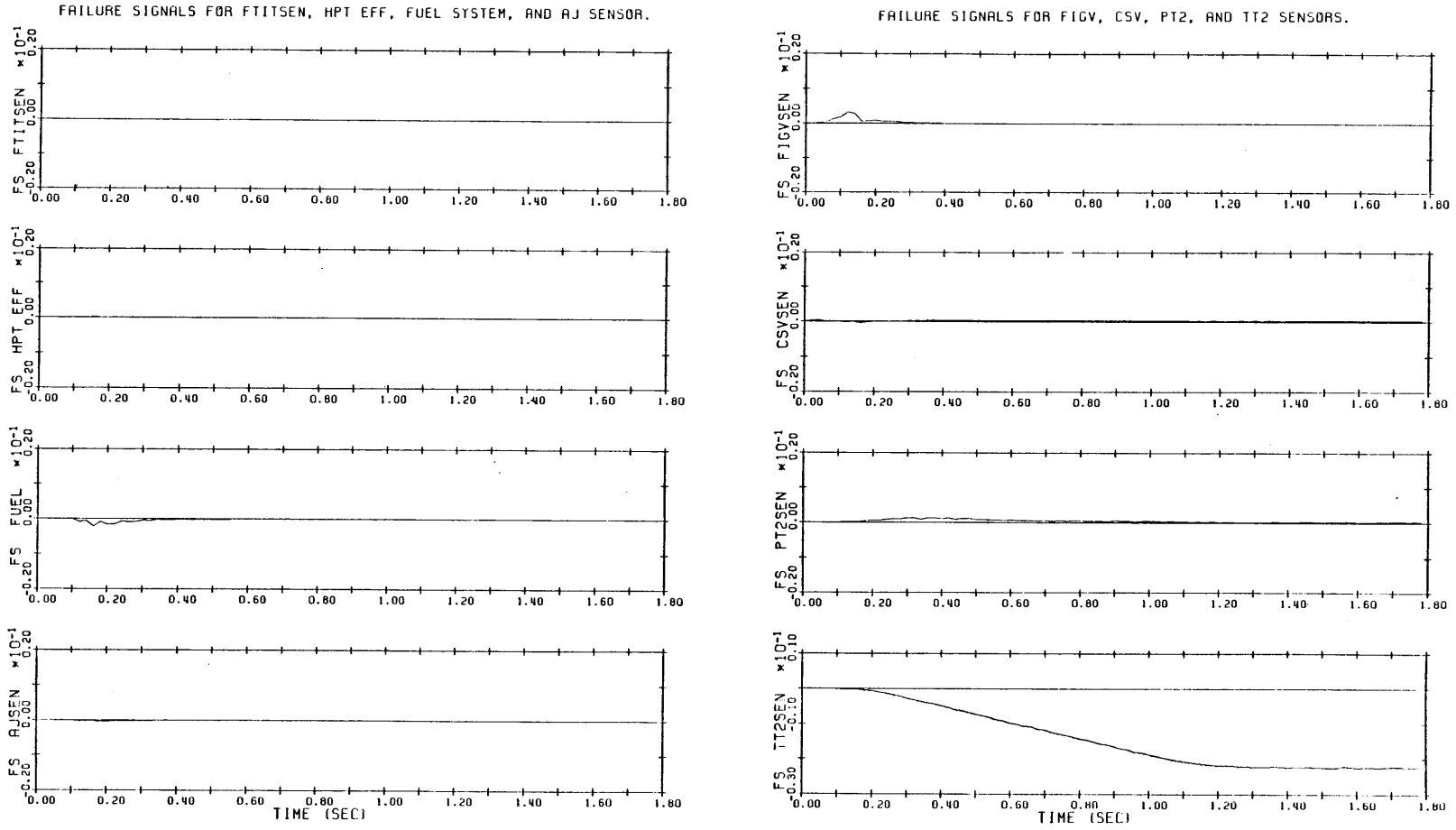

Figure 5.8, continued.

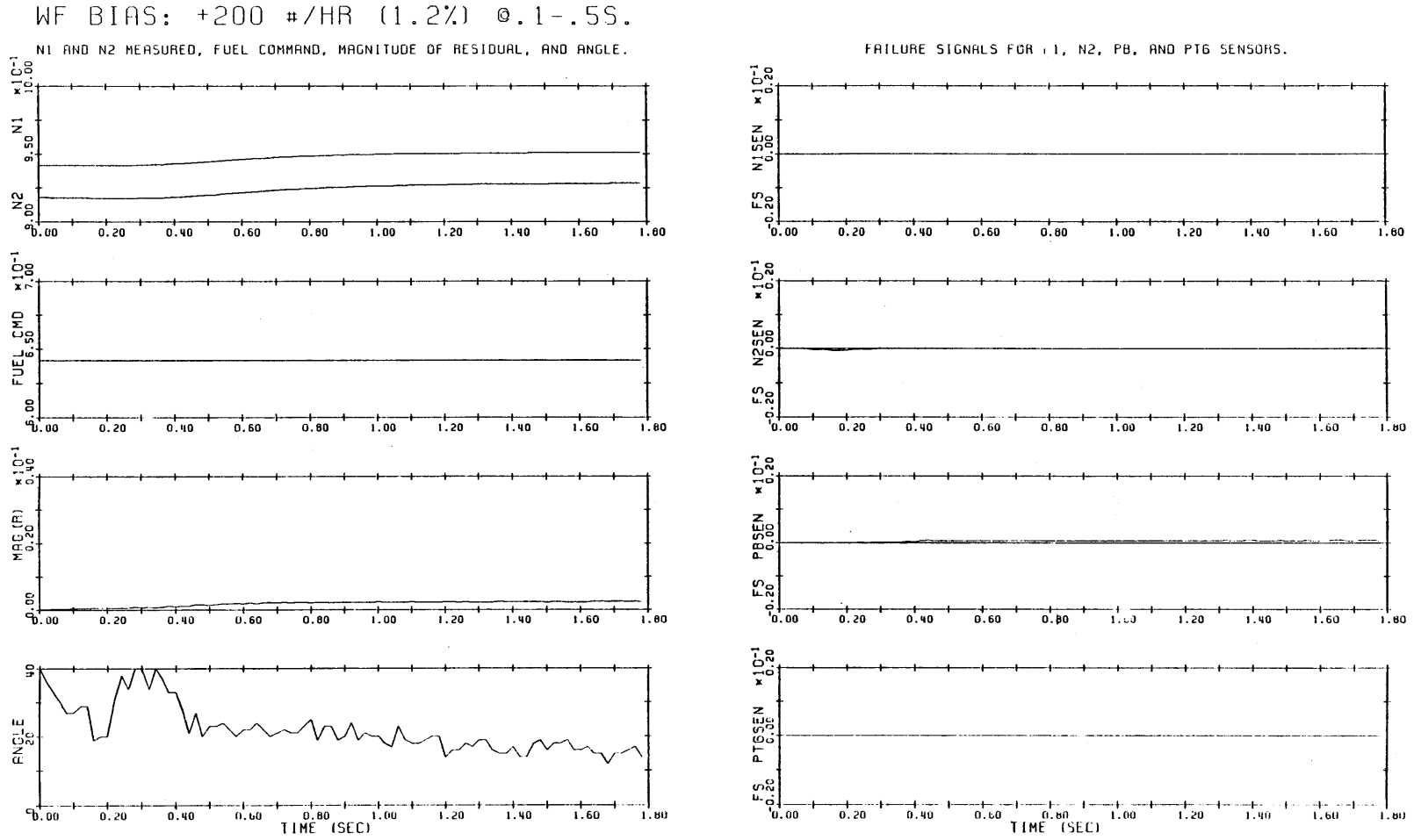

Figure 5.9. Uncommanded increase in fuel flow by 200 lbs/hr (1.2%).

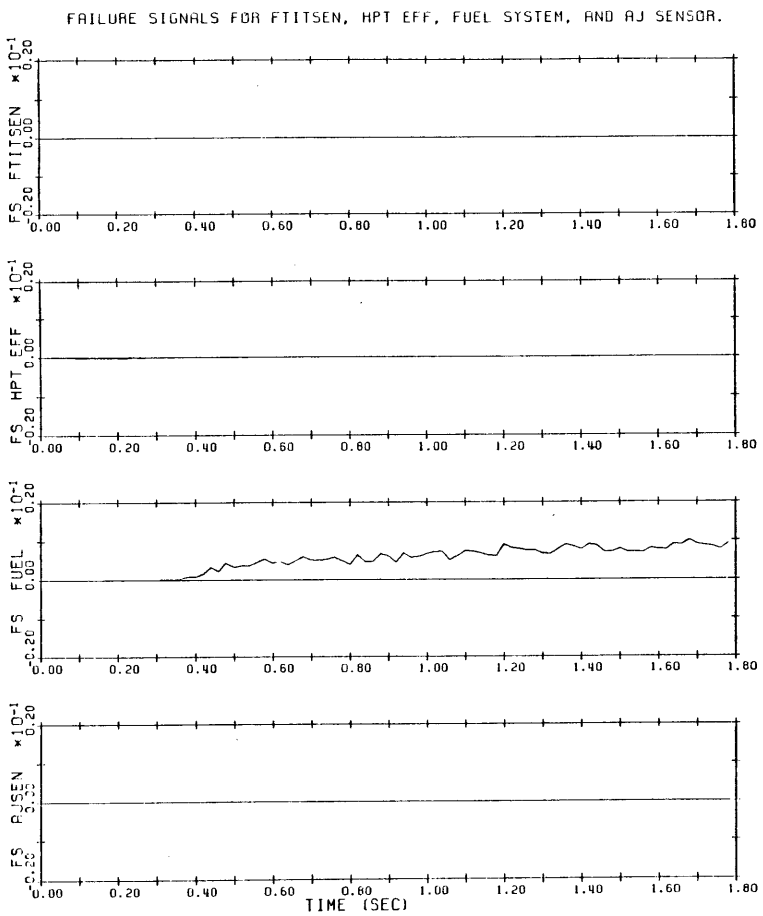

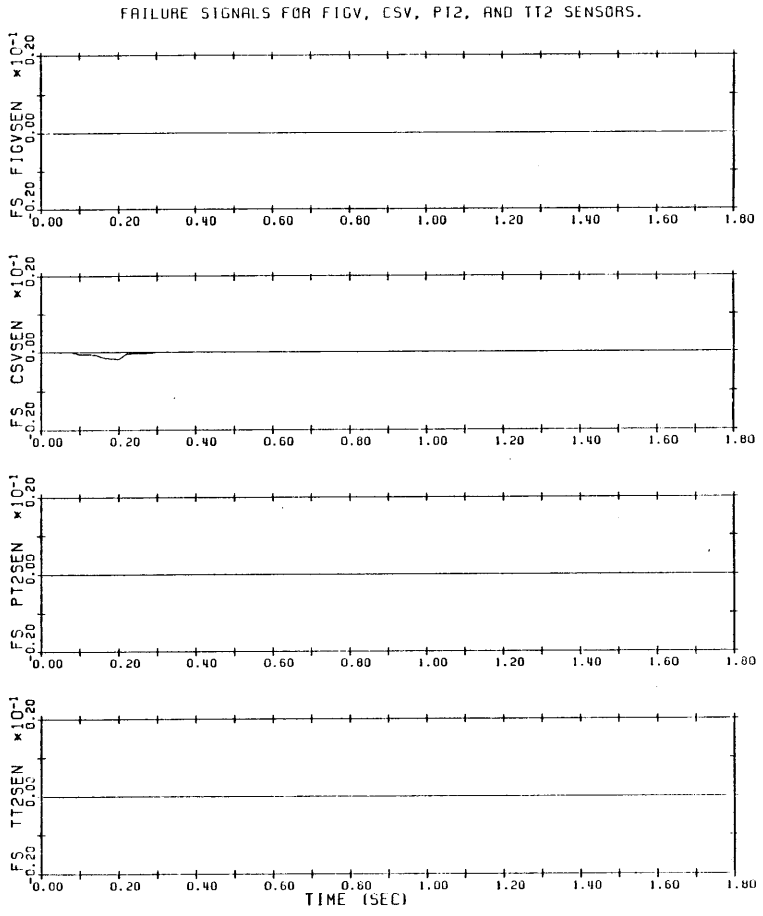

Figure 5.9, continued.

small size of the event vector for fuel system failures (the first column of Γ). The scale factor of 5 for the W_f failure signal (see Table A.5), which reflects the size of the event vector, made the failure signal as large as 0.01. If the residual vector had not been 15 to 20 degrees from the fuel failure vector, then the signal would have indicated almost exactly the 1.2 percent increase in fuel flow that had occurred.

This example was included among the test cases for the purpose of determining whether the W_f failure signature would deviate about 18 degrees as predicted in Section 5.4. Certainly it has, but examination of the residual vector reveals that the direction of the deviation is altogether different than expected--in fact, the vector is more than 20 degrees from the predicted deflected direction. It is apparent that, as mentioned in Section 5.4, the reference model is not accurate enough to warrant concern about neglecting the effects of the slow-response gas/metal heat transfers.

In any case, in spite of missing the proper direction for the residual, the filter did not generate any failure indications for any other components, and it produced a W_f failure signal of nearly the correct magnitude.

The third set of graphs, shown in Figure 5.10, show the results of a simulated decrease in the efficiency of the high-pressure turbine from about 90 percent to 88 percent. The decrease was induced suddenly at t equal to 0.1 second. The speed of the turbine dropped quickly, and the low-pressure rotor sped up momentarily, then slowed. Meanwhile, the controller increased the fuel command to compensate. The filter residual responded quickly, and at first grew in a direction very close to the failure direction for the turbine. Accordingly, the failure signal for the turbine rapidly indicated the 2 point drop in efficiency. But as the fuel command took effect beginning between 0.3 and 0.4 second, the direction of the residual vector pulled more than 20 degrees away from where it should have been. Commensurately, the failure signal declined and settled at an indication of a 1 point drop in efficiency.

One possible reason for this is that this malfunction is not correctly modeled by the input failure model, either because its effects are nonlinear or because it is a type of failure that even in a purely linear system would not fit that model. Another is that the reference model poorly tracked the effects of the 2.5 percent increase in fuel flow. Once again, in spite of difficulty with the direction of the residual, the filter indicated an anomaly in the faulty component and in no others.

In the next example, the PLA was first decreased from 83 to 75 degrees at t = 0.1 second, then at t = 0.3 second a bias of 10 psi (1.8%) was stepped into the output of the P_b sensor. Figure 5.11 shows the results. The purpose of this test was twofold: first to demonstrate that the filter can identify a sensor failure that occurs during a transient, and second to determine how well the filter does when the operating point is moved away from the PLA=83 condition. Some details to note are the sudden decreases at t = 0.3 second in the fuel command and in the failure signal for the P_b sensor. The first is the direct effect of the bias on the controller and the second is from the change the bias causes in the P_b residual. Shortly afterward, the failure signal for the P_b sensor became the largest one, and as the transient settled out, it indicated a negative bias of just over 1.8 percent, while all the others dropped nearly to zero. The only particularly apparent steady-state effect of mismodeling is the angle of about 10 degrees. When the same bias is introduced with PLA steady at 83 degrees, the angle is virtually zero.

During the transient, the filter exhibited some undesirable behavior caused by inaccurate modeling of the dynamics of the F100 simulation. The large peak in the fuel failure signal shortly after the beginning of the transient indicates once again that the reference model does not appropriately follow changes in fuel command. Also, as the graph of the angle shows, during the transient the direction of the residual wanders around some. Overall, the results of this test show that the filter functioned reasonably well inspite of the modeling

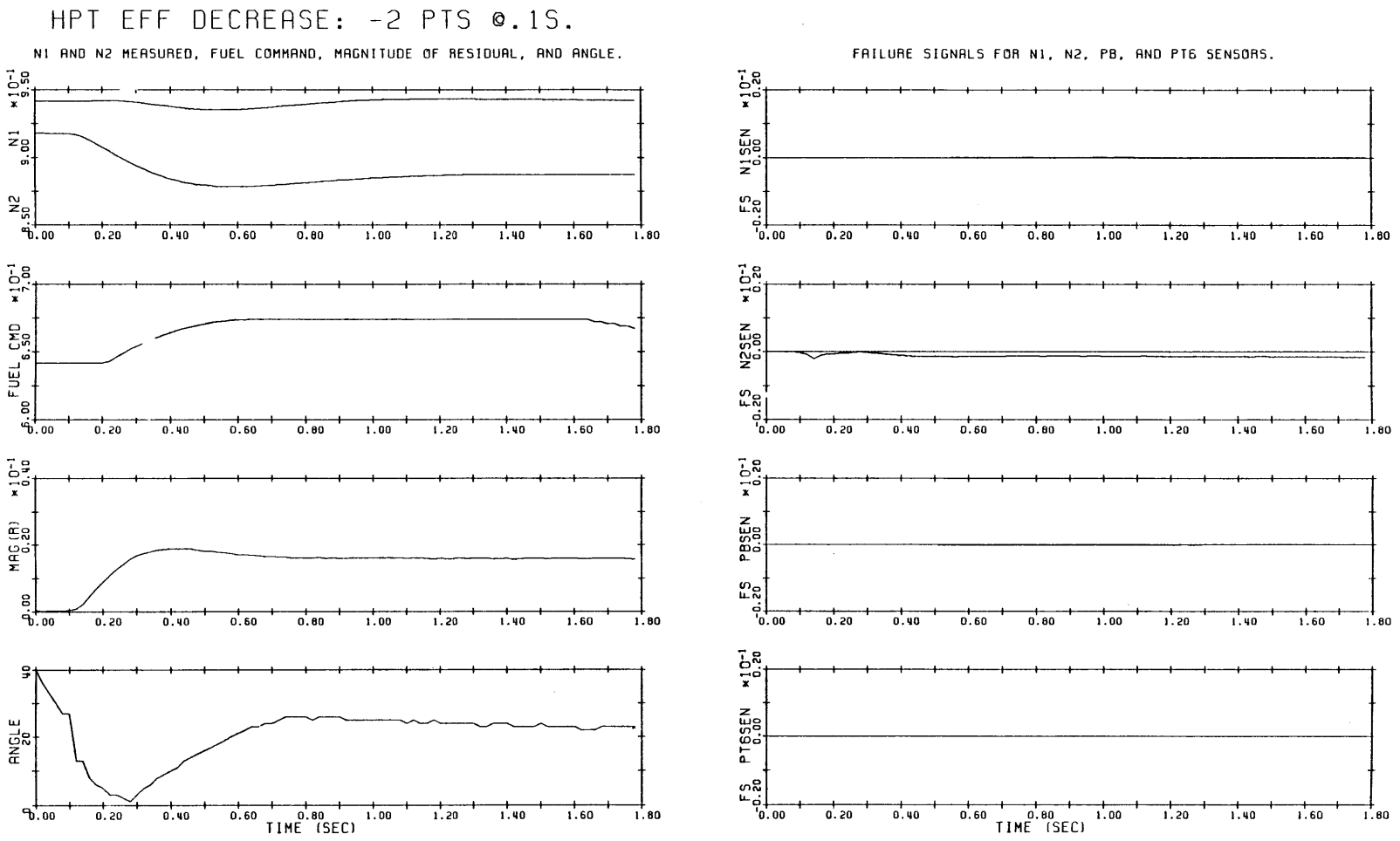

Figure 5.10. Decrease in high-pressure turbine efficiency from 90% to 88%.

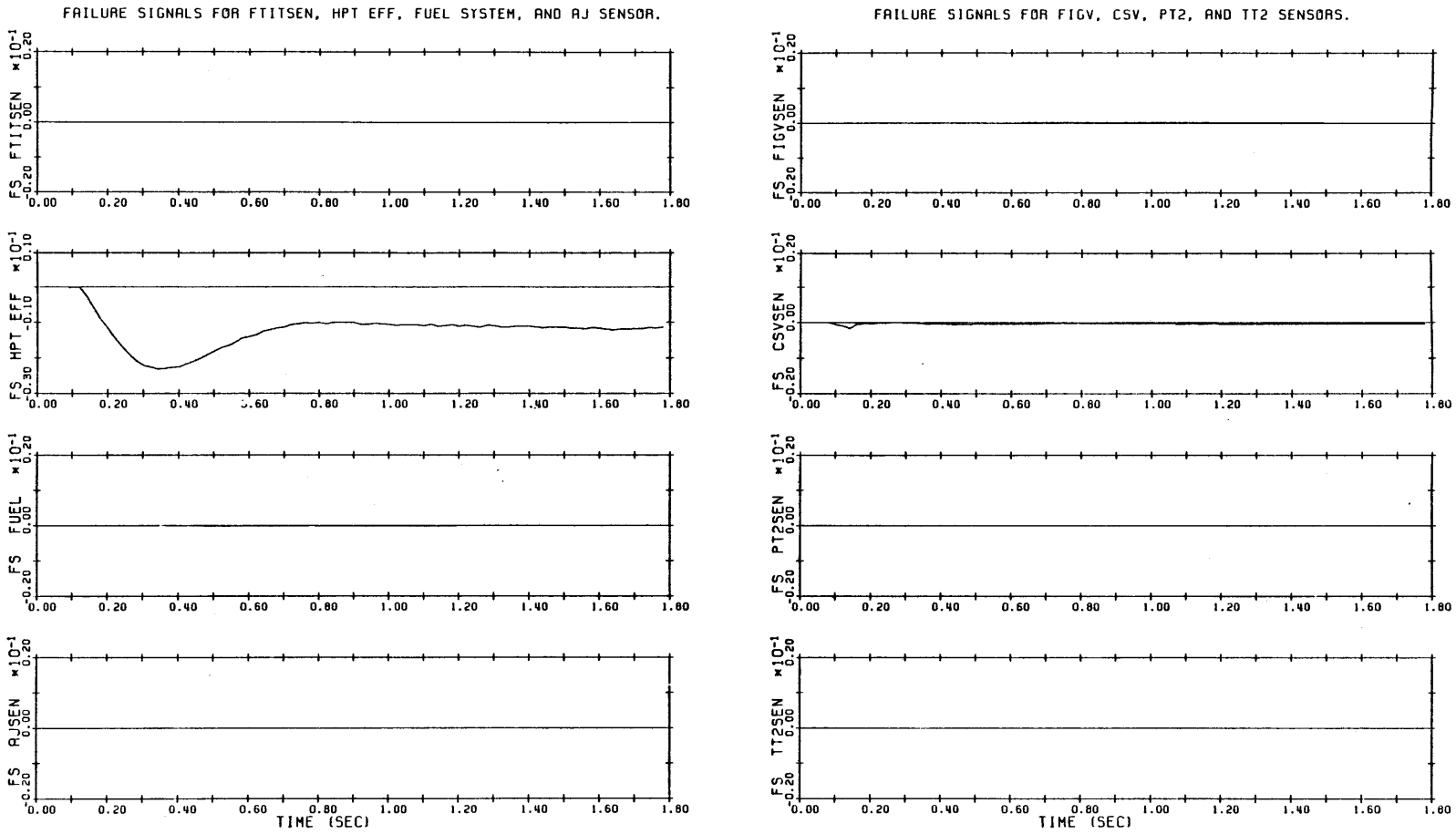

Figure 5.10, continued.

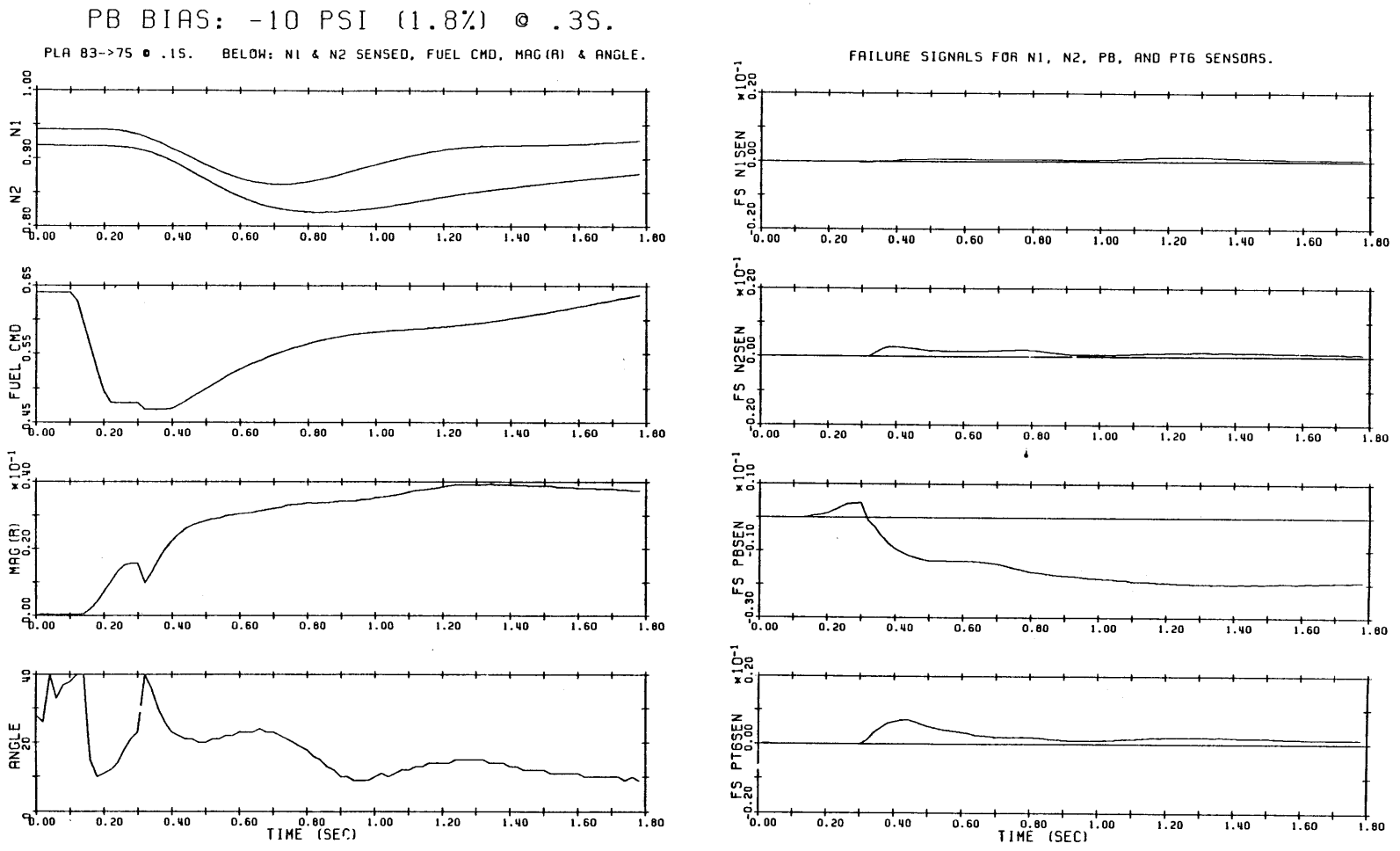

Figure 5.11. P_b sensor biased 10 psi (1.8%) during a transient from PLA=83 to PLA=75.

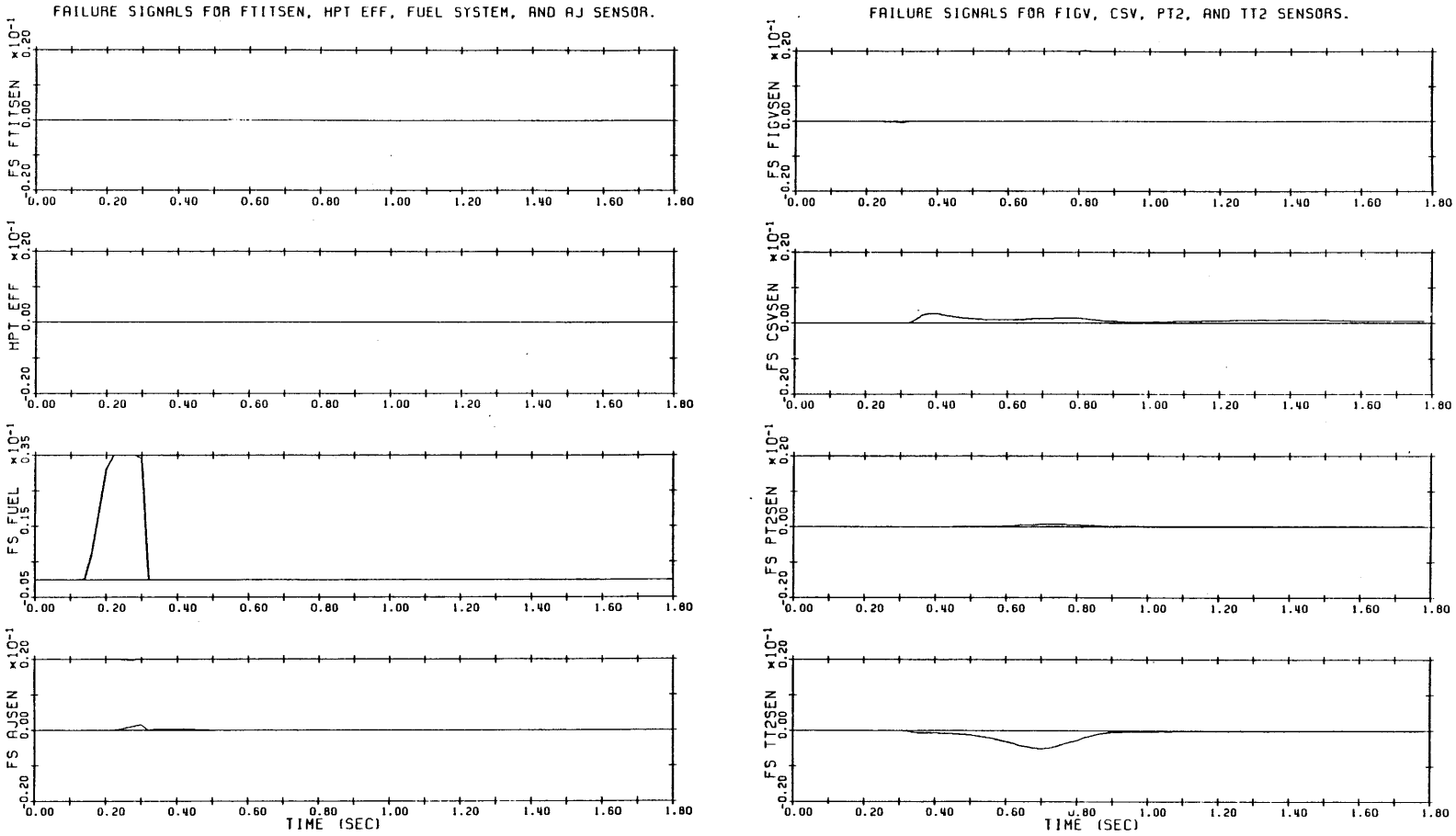

Figure 5.11, continued.

inaccuracy, yet that the modeling must be better if false indications of fuel system failures are to be avoided.

The last example, shown in Figure 5.12, is of a smaller change in power followed by an abrupt opening of the compressor bleed valve at $t = 1.0$ second. The purpose of this test was to see if the filter would correctly identify the 2 percent bleed of compressor airflow, rather than falsely indicate a failure of some component. The reference model was not informed of the command to open the valve, because most often the changes in bleed airflow are the result of varying demand from aircraft systems, with no indication of such sent to the engine controller. Except again for anomalous signals caused by the transient, the filter performed properly.

In these examples the filter performed generally as intended. As small as the malfunctions were, in each case the faulty component would have been identified, provided that short-lived peaks in the fuel failure signal are ignored. The performance of the filter together with the algorithm for computing the failure signals was mostly robust; even when the reference model was obviously not accurately duplicating the engine dynamics, the proper failure signal, and only that one, emerged and gave a useful estimate of the magnitude of the failure. The main problem encountered was the sensitivity of those failure signals that contain a large scale factor in their calculation--namely those for the fuel system, the inlet guide vanes, and the compressor stator vanes--to inaccuracies in the modeling of the dynamics. This is not unexpected, as it is bound to be difficult to distinguish modeling errors from malfunctions that cause only small residuals.

Nevertheless, the results clearly indicate that the modeling of the effects of changes in fuel flow command, both dynamic and static, must be better if a detection filter is to be practical in this application. Improved modeling is the main topic of the next chapter.

5.6 SUMMARY

The detection filter designed for the F100 operating at full intermediate power at sea level static conditions incorporates an eighth-order linear model that approximates the engine's dynamics near that operating point. The dynamics the model includes are those of the rotors, the gas volume in the augmentor, the fuel system, the T_{t25} and FTIT sensors, and the slower gas/metal heat transfers in the hot section.

The measurement sampling rate used with the filter is 50 times per second, and the time constant selected for the filter's dynamics is 0.10 second. The linear model is implemented in the filter in discrete-time form and thus has no differential equations to be integrated.

Tests results presented include simulations of decreased efficiency in the high-pressure turbine and of steady biases and ramped biases in the P_b and T_{t2} sensors and in fuel flow. The magnitudes of these simulated failures were from 1 to 3 percent of range. The results demonstrate that the filter functions properly for the engine operating condition the linear reference model was designed for, even though the model does not include any dynamics with time constants smaller than 0.10 second. A test with 2 percent of the compressor airflow suddenly bled off produced no false failure indications and demonstrated that the filter can estimate what the bleed airflow is. Experience with this filter has guided the development reported in the next chapter of a filter able to accommodate the nonlinear behavior of the engine.

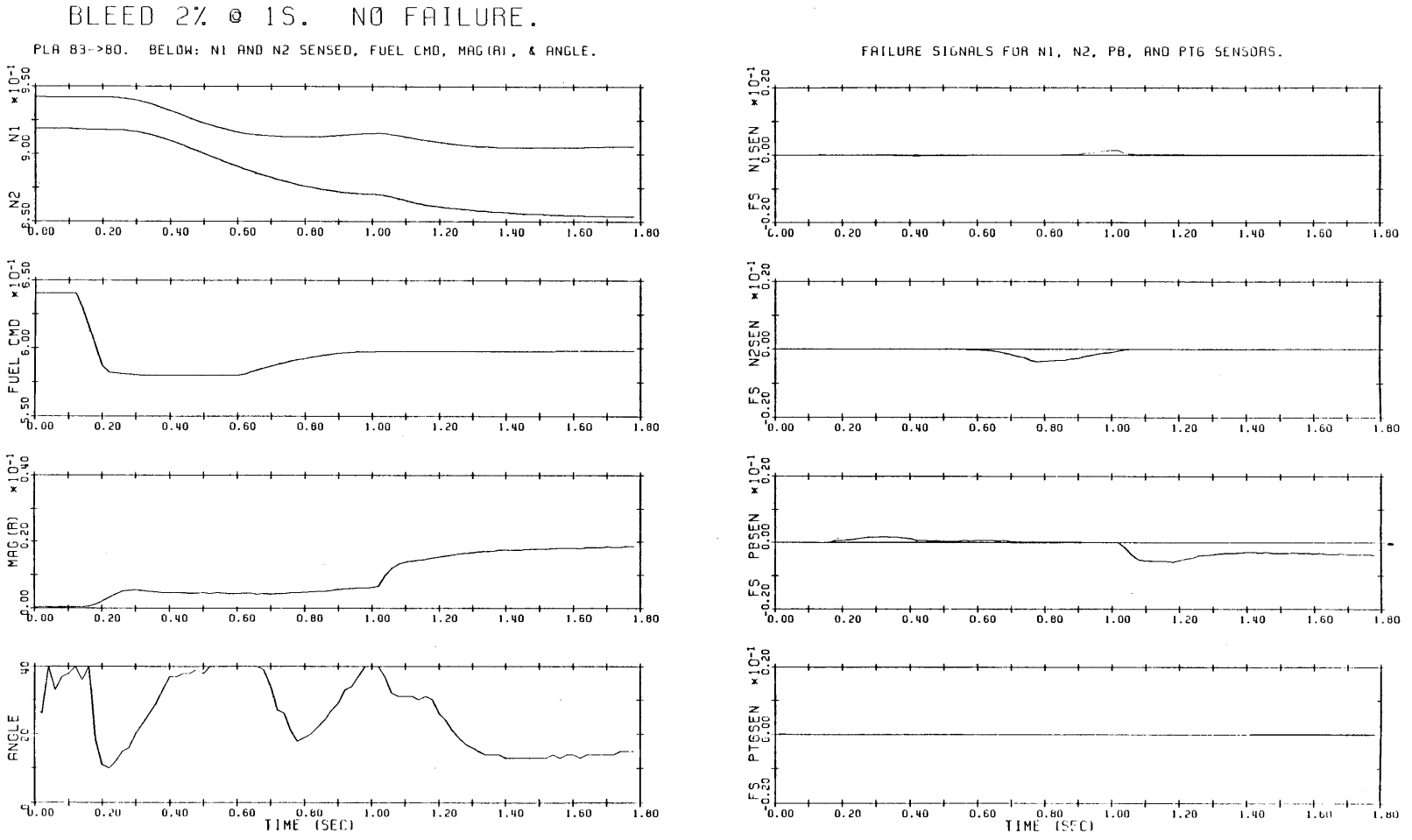

Figure 5.12. Transient from PLA=83 to PLA=80 followed by an abrupt 2% increase in compressor bleed airflow.

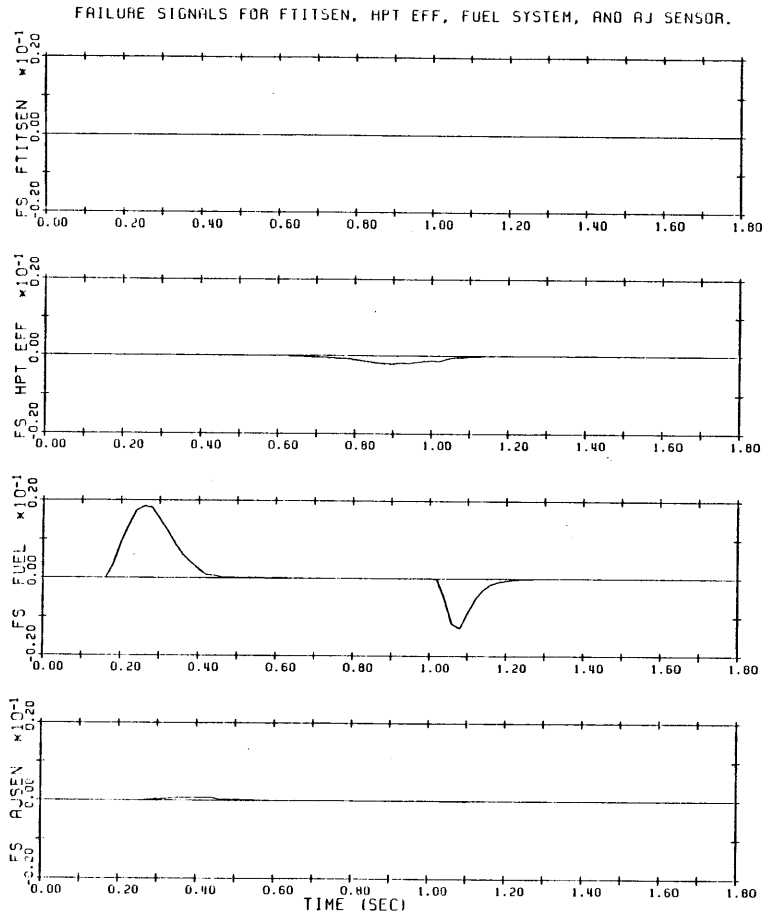

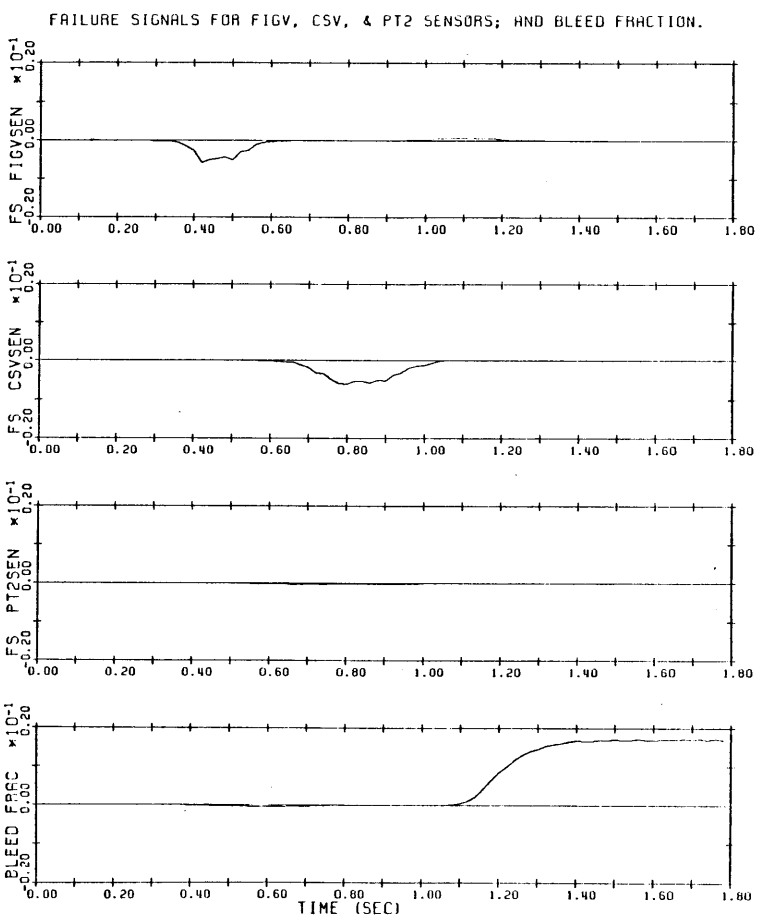

Figure 5.12, continued.

can easily be calculated as accurately as desired. Investigation of the behavior of the F100 simulation revealed that the transient responses it generated did not faithfully represent the true behavior of the physical processes incorporated in the simulation. Actually, within a restricted range of operation, the simplified linear model more accurately reflected the dynamic relationships embodied in the simulation than the simulation did.

Notable improvement resulted from inserting a more rigorous integration routine into the simulation. As anticipated, this quickened the response of the simulation. At 0.3 second following a PLA step from 83° to 60°, the compressor speed was slowed by 150 rpm more than it was in the response generated with the original integration routine. This is about 4% of the speed range of the compressor, an amount large enough to disrupt identification of the smaller in-range failures of concern. The graphs in Appendix B show the response curves for the transient just mentioned, plotted to the same scale used in Appendix A for the curves produced by the original version of the simulation.

The integration method previously used is a modified Euler method that enabled the simulation to run stably with an integration time step that normally would be too large. Unfortunately, specifying a time step small enough for the basic Euler routine to be accurate is uneconomical. With a more complex routine, though, the necessary accuracy could be attained at acceptable cost. The new routine was implemented in two parts, a simple third-order Adams "derivative predictor" procedure for the dynamics of the sensors and actuators, and, for the engine dynamics, a "backwards differentiation formula" designed by Gear [19] for use on systems that have a wide range of eigenvalues.[1]

[1]This procedure is available as part of the International Mathematical Subroutine Library.

Chapter VI

EXTENSION TO NONLINEAR OPERATION

The two preceding chapters described the methods used to derive a simplified linear model and to implement it in a filter; this chapter deals with making the dynamics of the reference model and the F100 simulation more alike. Two changes were needed to achieve the necessary improvement: replacement of the numerical integration routine in the F100 simulation and expansion of the reference model to include nonlinear effects. The new filter worked well in tests on simulated failures at a variety of power levels, both steady and varying. The focus here was on extending the validity of the reference model; no changes were made to the manner of selecting the feedback matrix of the filter or to the procedure used to analyze the residuals.

Unexpectedly, a substantial reduction in modeling error was achieved by using a different integration method in the F100 simulation. This is discussed in Section 6.1. Additional improvement resulted from linking several linear models together in the reference model to make it nonlinear, as described in Section 6.2. The simulation results given Section 6.3 show the performance of the filter constructed from that model.

6.1 NUMERICAL INTEGRATION IN THE F100 SIMULATION

The complexity of the physical processes modeled in the F100 simulation requires that sophisticated numerical integration be used if the time response of the engine is to be calculated accurately. In contrast, the F100 model used in the filter is simple enough that its dynamic response

6.2 THE NONLINEAR REFERENCE MODEL

6.2.1 Method of Incorporating Nonlinear Effects

The results given in Chapter 5 demonstrate successful operation of the detection filter with the F100 simulation operating near the equilibrium point at which the linear model was derived. Extending the range of the filter to a variety of operating conditions requires making the reference model nonlinear, but for ease of use in a detection filter a nonlinear model should have the same form as the linear model used previously. A way to construct such a model is to concatenate linear models into a single model that is nonlinear overall, but that operates linearly within small ranges of engine power and flight condition. When used in a filter, this type of model switches successively from one linear model to another as the state of the engine changes. This approach accommodates most of the nonlinear effects associated with variations in engine power and with changes in aircraft altitude and Mach number, but it does not encompass the off-equibrium nonlinear effects encountered when an engine is transitioning rapidly from one power level to another.

Figure 6.1 shows schematically how several linear models for different power levels at one flight condition would be linked together. A state variable or a combination of state variables would be selected as an approximate indicator of the state of the engine. The measured value of N_2 is the choice here. For a given flight condition, at selected values of N_2 the equilbrium values of the state varaibles and the inputs are recorded and the matrices Φ and Γ of the linear model for that point are derived. In operation, the set $\{\underline{x}_0, \underline{u}_0, \Phi, \Gamma\}_j$ whose recorded value of N_2 is closest to the measured value is used in the filter equations. At each sampling time, the filter is updated as follows:

$$
\begin{aligned}
\underline{r}_k &= \underline{y}_k - \hat{\underline{y}}_k \\
\Delta\underline{x}_k &= \underline{x}_k - \underline{x}_{0j} \\
\Delta\underline{u}_k &= \underline{u}_k - \underline{u}_{0j} \\
\\
\Delta\hat{\underline{x}}_{k+1} &= \Phi_j \Delta\hat{\underline{x}}_k + \Gamma_j \Delta\underline{u}_k + D_j \underline{r}_k \\
\hat{\underline{x}}_{k+1} &= \Delta\hat{\underline{x}}_{k+1} + \underline{x}_{0j} \\
\hat{\underline{y}}_{k+1} &= C\hat{\underline{x}}_{k+1}
\end{aligned}
\qquad (6\text{-}1)
$$

The sets $\{\underline{x}_0, \underline{u}_0, \Phi, \Gamma\}$ can be stored individually or as polynomial functions of N_2 and aircraft altitude and Mach number (or of whatever other independent variable may have been chosen). Obviously, much less memory space would be required for storing the steady-state points $\{\underline{x}_0, \underline{u}_0\}$ than for the dynamics matrices Φ and Γ. It is probably desirable, then, to record $\underline{x}_0$ and $\underline{u}_0$ at more points than Φ and Γ in order to make the stored "map" of steady-state operating points as accurate as possible. For purposes of failure identification, the dynamics part of the reference model need not be as accurate as the steady-state part; identification of small biases in components can usually wait until a period of steady-state operation.

This separation of the static model from the dynamics model is the approach used with the filter for the F100. For demonstration of the concept, at one flight condition--sea-level-static--ten $\{\underline{x}_0, \underline{u}_0\}$ pairs and two $\{\Phi, \Gamma\}$ pairs were recorded. The steady-state data spans the power range from idle to intermediate, while Φ and Γ were calculated only for PLA equal to 53° and to 83°. This is illustrated in Figure 6.2. The N_2 measurement is the independent variable. When a reference state other than either of the two with corresponding Φ and Γ is selected, approximate values for Φ and Γ are calculated by linear interpolation or extrapolation (with respect to N_2) between or from the two recorded $\{\Phi, \Gamma\}$ pairs. At each measurement sampling time, the new value of N_2 is checked to see if the reference state last used is still

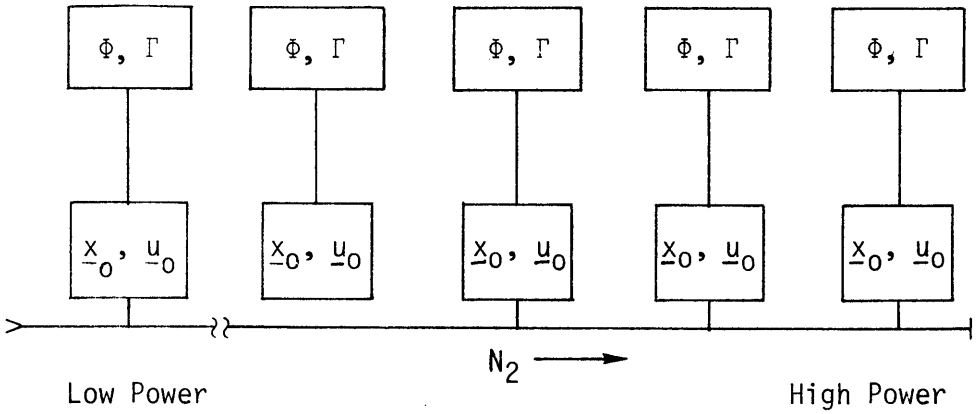

Figure 6.1. Format of a piecewise linear model.

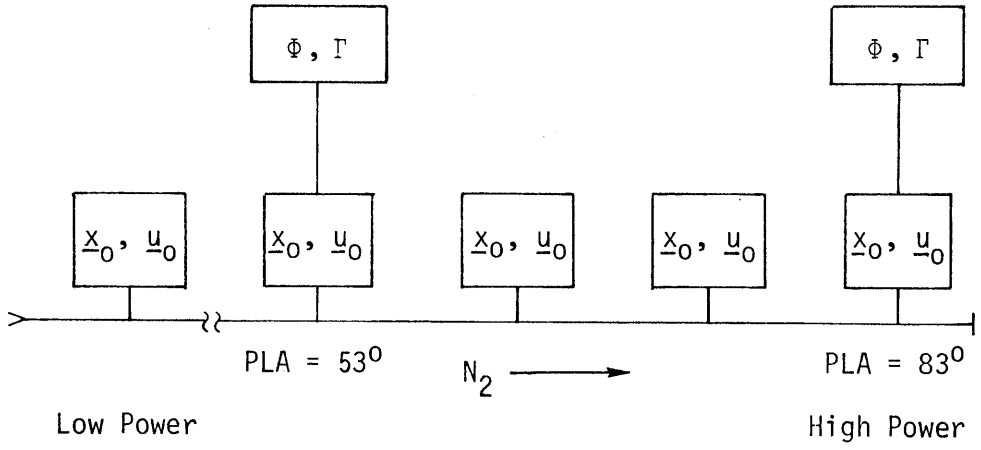

Figure 6.2. Format of the model used in the F100 filter.

the one whose N_{2_0} is closest to N_2; if not, the reference state is changed, and only at that time are Φ and Γ recomputed. Thus Φ and Γ become step functions of N_2. It was anticipated, however, that for low power settings this relation would not be quite adequate, and, indeed, the results indicate that a third $\{\Phi,\Gamma\}$ pair is needed to provide sufficient accuracy at those settings. An additional feature incorporated in the model is that when the rate of change of N_2 is small, the model determines the reference $\{\underline{x}_0,\underline{u}_0\}$ pair by interpolating between the two nearest recorded pairs.

In addition to its use in modeling for failure identification, separation of the static and dynamic parts of the reference model may also be useful in controlling the engine. For every power setting, the control system must have a set of reference values to match the measured engine variables to, and the values $\underline{x}_0$ and $\underline{u}_0$ that would be contained in the steady-state part of the model are just the values needed.

6.2.2 Designing the Filter

The two $\{\Phi,\Gamma\}$ pairs were derived slightly differently than the $\{\Phi,\Gamma\}$ pair used earlier in the linear model. The linearization procedure was modified, and after the order reduction, the two unimportant state variables were deleted, which decreased the order of the final model to six. The method of linearization, namely tangent approximation, was not changed, but the procedure was rewritten to avoid some uncertainty about its calculation of derivatives and to make the derivation of the B matrix the same as that of the A matrix. For both A and B, the revised approach consists of calculating approximations to the partial derivatives that are the first-order terms of the Taylor series expansion of $\dot{\underline{x}}$ about the chosen equilibrium reference point, $\{\underline{x}_0,\underline{u}_0\}$. For the method of nonlinear modeling described above, it is better that the B matrices, and hence the Γ matrices, be calculated to represent engine dynamics, rather than steady-state relationships as was previously the case.

For the calculation of the partial derivatives of $\dot{\underline{x}}$ and of $\underline{y}$ with respect to $\underline{x}$ and $\underline{u}$, the perturbation sizes selected were 2% of range for each element of $\underline{x}$ and 200 lbs/hr (1.3%) for fuel flow, .07 ft^2 (2%) for nozzle area, -4 degrees (16%) for fan vane angle, and -1 degree (2.3%) for compressor vane angle. For use as failure vectors, the partial derivatives of $\dot{\underline{x}}$ with respect to bleed fraction, P_{t2}, T_{t2}, compressor efficiency, high-pressure turbine efficiency, and low-pressure turbine efficiency were also calculated. The perturbations in bleed fraction and in the efficiencies were 0.02, and in P_{t2} and T_{t2} they were 2% of range.

The 16th-order linearization of the engine dynamics was augmented with first-order dynamics for the fuel system, the T_{t25} sensor, and the FTIT sensor. The resulting model was reduced to eighth order and subsequently transformed to make $\underline{x}$ equal to $\underline{y}$, as described in Chapter 5. The same state variables were retained: N_1, N_2, P_b, P_{t6}, T_{t25} sensed, FTIT sensed, and the two canonical variables for the modes associated with the slow-response metal temperatures in the turbines. The time constant used for the fuel system dynamics was 0.125 second.

Following the conversion of the continuous-time eighth-order model to discrete-time form, the two state variables for the slow-response metal temperatures were simply deleted, leaving a sixth-order, fully-measured model. As mentioned in Chapter 5, those two state variables have relatively little effect on the engine dynamics and, as expected, eliminating them from the model caused little additional modeling error.

Implementing the detection filter with the nonlinear reference model posed no difficulty. The filter was structured in the form shown in Figure 4.3 (with $\underline{x}_1$ being the entire state vector), so at each change of Φ and Γ, the corresponding change in the feedback of the filter occurred automatically. Also at each change, the majority of the failure directions became the new directions of the columns of Γ and $I-\Phi$ (see Equation (4-71)). Thus, because most of the failure vectors depend

so simply on Φ and Γ, they need not be kept in memory. The remainder were stored as adjuncts to the Γ matrix.

As before, the time constant of the filter was chosen to be 0.1 second, and the measurement sampling interval was taken as 20 ms.

6.2.3 Estimates of Memory and Computation Requirements

The filter appears simple enough to be implemented in a microcomputer engine controller. The greatest uncertainty is how much memory will be required to store a reference model that encompasses all flight conditions and power levels. Table 6.1 lists the number of arithmetic operations needed to run the three portions of the filter--the filter update, the model interpolation, and the analysis of the residuals--and estimates of the times required to perform them. The times assumed for the individual operations are 4 μs for additions and compares, 10 μs for multiplications, 20 μs for divisions, and 25 μs for square roots. The total times shown are double the sums of the operation times and thus should not be unduly optimistic.

The 3 ms listed for the filter update allows for calculation of the magnitude of the residual vector. Presumably, failure detection would be based on this, and the identification routine would be called only after a failure is detected. The time requirements for that are, as shown, 12 ms for the first sample time--the failure directions must be determined--and 6 ms for each subsequent sample time at which the model does not change.

Also listed in the table are estimates of the memory requirements for a sixth-order model with six inputs (including P_{t2} and T_{t2}) and four additional vectors (directions for the compressor and turbine efficiencies and compressor bleed). It was assumed that for each flight condition five to ten sets of ten numbers (six variables and four inputs) will be needed for the steady-state part of the model and three sets of Φ and Γ and the additional vectors will be needed to model the dynamics. The number of flight conditions at which the model must be explicitly recorded was assumed to be between 20 and 40. The memory requirement,

TABLE 6.1

Estimates of computation and memory requirements.

Computation Time

Filter update and failure detection:

Frequency - every 20 to 50 ms

Number of operations - additions and compares 80

- multiplications 80

Total time - 3 ms

Change coefficients of the model:

Frequency - every .1 to .2 sec

Number of operations - additions 120

- multiplications 186

Total time - 5 ms - (univariate -- N_2)

10 ms - (bivariate -- N_2 and flight condition)

Identification:

Frequency - on demand

Number of operations - additions and compares 270

- multiplications 300

- divisions 40

- square roots 20

Total time - 12 ms on first call and following each subsequent model change.

- 6 ms each other sample time.

Memory Space
(16-bit words)

	Min	Max
Steady-state model	500	4000
Dynamics model	4,500	16,000
Total	5,000	20,000

then, might be as low as 5,000 words or as high as 20,000 words. Achieving the lower figure would require storing the elements of the model as polynomial functions.

6.3 SIMULATION RESULTS

We proceed now to discussion of the performance of the nonlinear filter on six sample failures. The data sequences for these tests were generated by the F100 simulation with the new integration routine. The first five examples involve malfunctions in the T_{t25} sensor, the P_{t2} sensor, the fuel pump, the compressor, and the P_b sensor. The sixth shows an acceleration from idle to intermediate power without a malfunction. The simulated failures varied in magnitude from 2% to 10% of range, and they were introduced at various transient and static conditions between part power and intermediate power. The graphs are presented in the same format as before, except that only four failure signals are plotted--in each case the four most prominent ones. To supplement to these six examples, Appendix C presents, without discussion, several other examples.

6.3.1 Bias in the T_{t25} Sensor

The plots from the first test of the nonlinear filter, shown in Figure 6.3, give the responses of the F100 simulation and the filter to a step bias of 50°F (10% of range) in the T_{t25} measurement. The bias was introduced at T = .5 second, following a rapid increase in PLA from 60° to 70° and during a gradual decrease in PLA from 70° back to 60°. (Recall that the axis labels on the plots on the left indicate the measured fan and compressor speeds, the fuel flow command, the length of the residual vector, and the angle that that vector makes with the failure vector it happens to be closest to.) At the moment of the malfunction, the residual vector and failure signal for the T_{t25} sensor both jumped to the appropriate magnitudes. Subsequently, these magnitudes were maintained, and no other failure indication appeared.

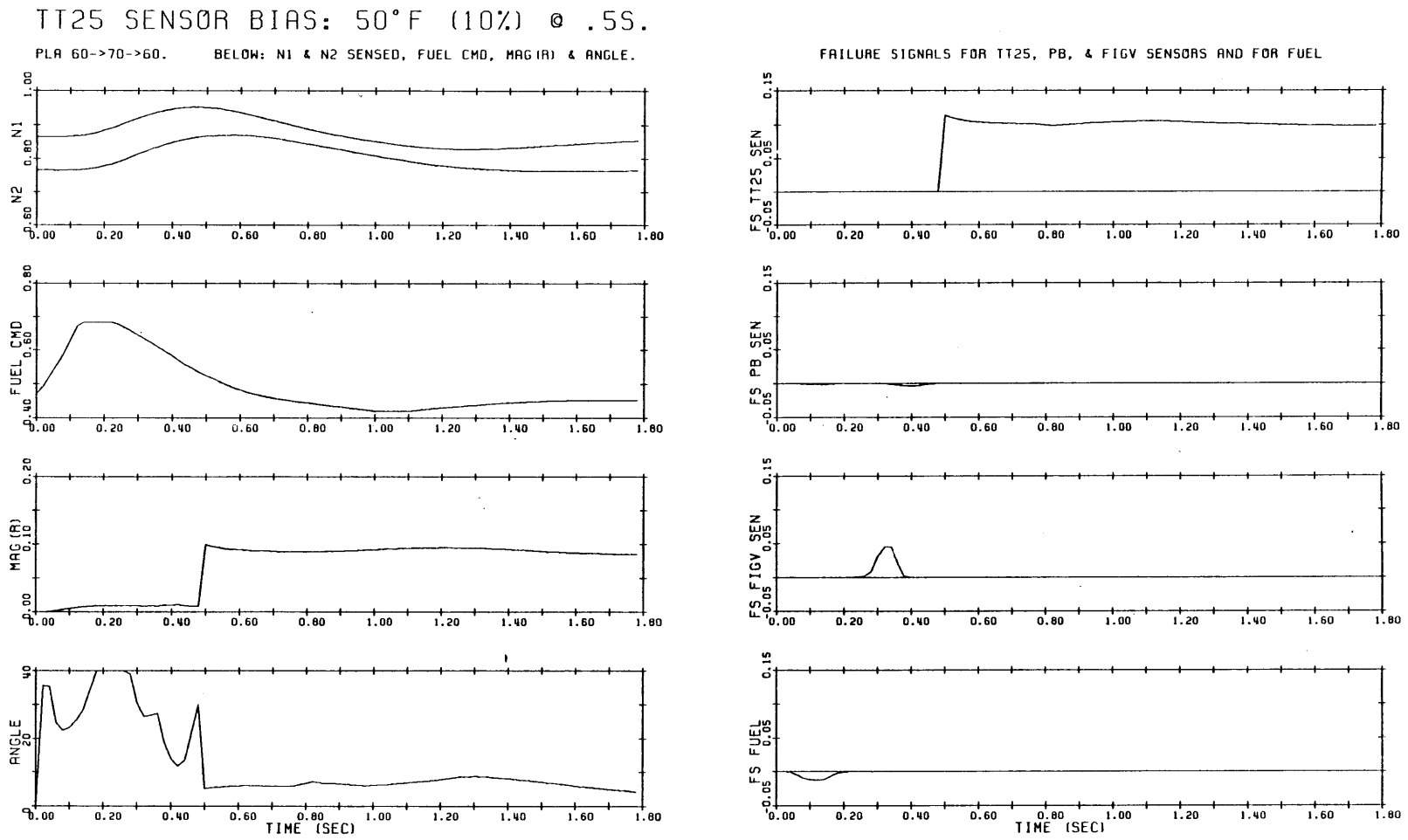

Figure 6.3. Bias in the T_{t25} sensor.

Prior to the malfunction, the transient in engine power caused brief failure signals for the fuel system and the FIGV sensor. Notably, the fuel signal is insignificant compared to what it is in the examples in Chapter 5. The FIGV signal, which indicates a momentary one degree mispositioning of the inlet guide vanes, is of small concern because the failure threshold for that signal would be large, commensurate with the minor effect that deflection of the vanes has on the engine.

6.3.2 Bias in the P_{t2} Sensor

The second example is of a bias in the P_{t2} sensor. Figure 6.4 shows the results. Part way through an acceleration commanded by a ramped increase in PLA from 60° to 83°, the measurement of P_{t2} was abruptly decreased by 2 psi (6% of range) while P_{t2} remained constant. The residual vector soon lengthened, and the failure signal for the P_{t2} sensor increased to the proper magnitude. The increase was not immediate as in the previous example because P_{t2} is an input to the engine, whereas T_{t25} is an output. An erroneous measurement of P_{t2} must propagate through the reference model before it affects the residuals.

In addition to the signal for the P_{t2} sensor, we see a short-lived signal for the T_{t2} sensor. This arose because mismodeling of the transient in engine speed deflected the residual vector by 10 to 15 degrees. In part, the mismodeling is due to the 10% overshoot in engine speed, because that put the engine state in a region beyond where the last step in the reference model is accurate. Probably this is correctable by including in the model another step, an equilibrium point at a (nonafterburning) power level higher than that at PLA=83°. (At such a point, one or more operating limits would be exceeded).

A deflection of 10 to 15 degrees would in many other circumstances be inconsequential, but the physical effects of changes in P_{t2} and T_{t2} are closely related, so in this case the deflection caused some uncertainty. The influence of P_{t2} and T_{t2} on the engine occurs, in essence, through their effects on the corrected mass flow,

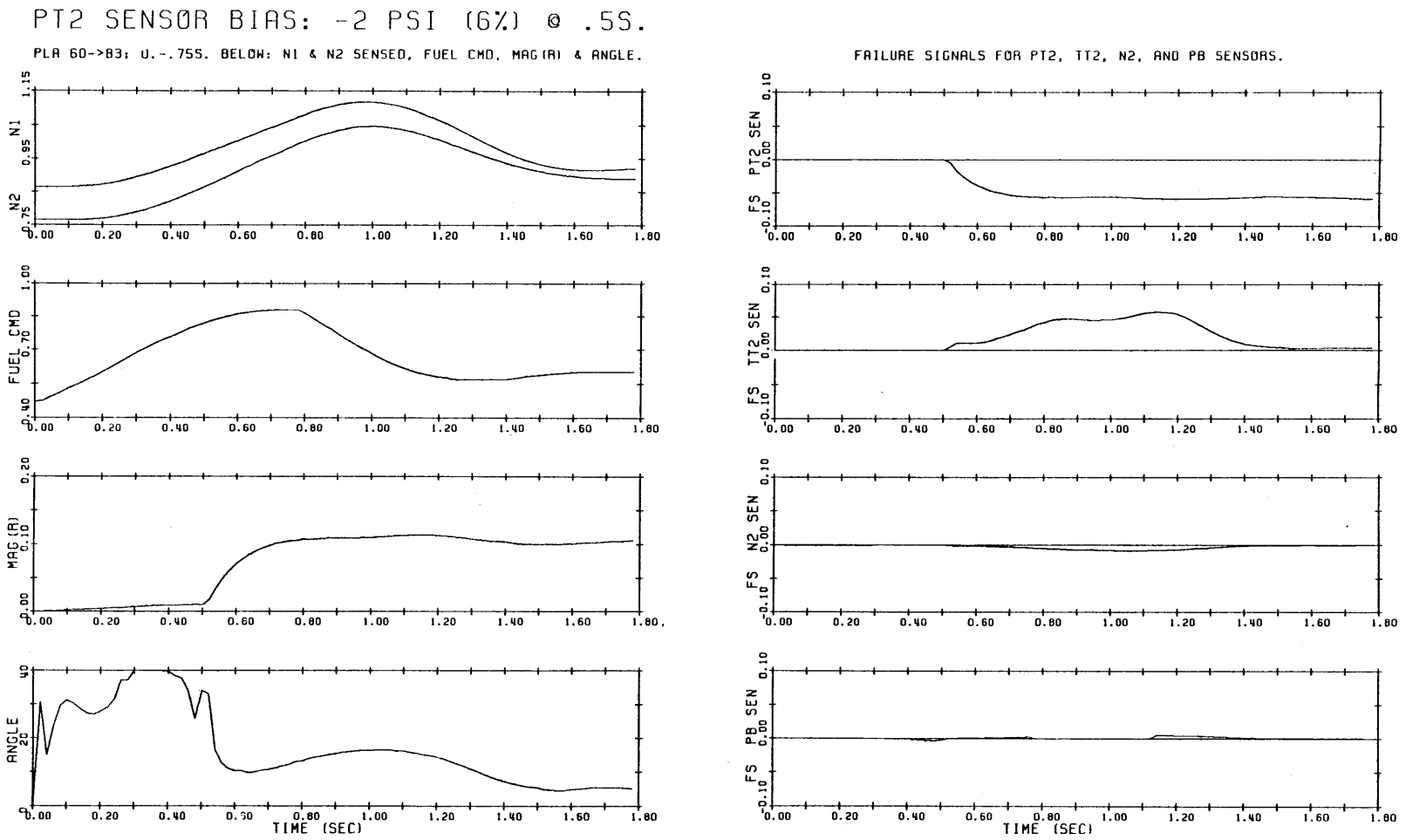

Figure 6.4. Bias in the P_{t2} sensor.

$\frac{\dot{m}_{air}\sqrt{T_{t2}/T_{ref}}}{P_{t2}/P_{ref}}$, and on corrected speed, $N/\sqrt{T_{t2}/T_{ref}}$. To first order, P_{t2} and T_{t2} have inverse effects on the mass flow, so the failure vectors associated with them lie near each other and have opposite signs.

6.3.3 Uncommanded Increase in Fuel Flow

This example, Figure 6.5, is of a malfunction in the fuel system that resulted in a fuel flow that was 2000 lbs/hr (12% of range) more than the amount commanded. First an increase in PLA from 50° to 65° over the interval from zero to 0.5 second began an acceleration, and then, during the next quarter of a second, the extra fuel flow was introduced. The filter produced a clear failure signal for the fuel system, but the signal was less than half as large as it should have been. This was due to the 30-degree angle between the residual vector and the failure vector for the fuel system. This, in turn, was a consequence of the small magnitude of the residual vector, little more than twice the magnitude before the malfunction. The modeling errors were thus able to skew the direction of the vector considerably.

As mentioned in Chapter 5, the small size of the residual vector reflects the small size of the first column of the Γ matrix (see Appendix B, Table B.2). Unfortunately, the only remedy for that is a sensor that directly measures fuel flow. Burner pressure is now the measured variable most directly dependent on fuel flow, and that dependence is at most only 20% to 25% . Therein lies the difficulty: the detection filter is designed to let only the direct effects of a malfunction in a system input show up in the residuals; that is how it keeps the residual vector fixed in direction. If a suitable flow meter were available and were used in the system, then 100% of any change in fuel flow (assuming negligible sensor dynamics) would appear immediately in a measurement.

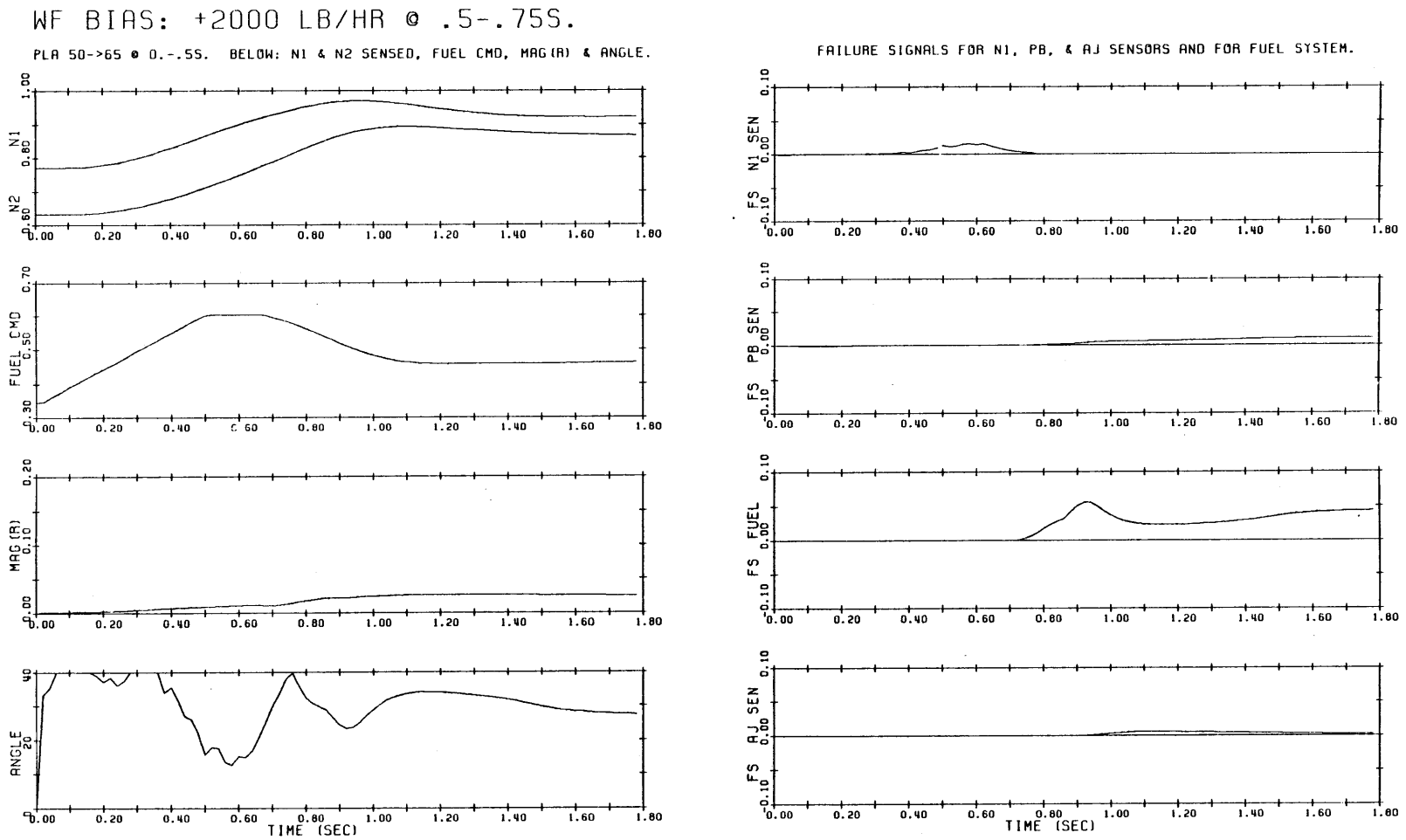

Figure 6.5. Uncommanded increase in fuel flow.

A similar difficulty hinders identification of malfunctions in the nozzle actuation system, as illustrated by the example in Appendix C that shows results from a simulated malfunction in the A_j sensor. Although a measured variable, P_{t6}, is strongly dependent on nozzle area, the rate of change of P_{t6} is relatively slow, and, consequently, the second column of Γ, the one for nozzle area, is not much larger than the first.[2] And two more inputs, FIGV angle and CSV angle, have columns (the 3rd and 4th) that are even smaller. In sum, the foregoing observations point to this conclusion: In this application of a detection fiter, it is exceedingly difficult to detect and identify small malfunctions in the actuation of the four control inputs.

This example of the fuel-flow malfunction brings up another, unrelated point, one that is perhaps better illustrated by the examples in Appendix C of a decrease in LPT efficiency and of a bias in the A_j sensor. There is some indication in Figure 6.5 that the P_b sensor had become biased, and, under these same circumstances, when the fuel flow bias is smaller, the signal for the P_b sensor is about the same size as the one for the fuel system. Such ambiguity is avoidable, though, because the failure vector for a steady bias in the P_b sensor is well separated from the one for a fuel flow malfunction. The problem is that a portion of the plane segment associated with the P_b sensor is relatively close to the failure vector for the fuel system. With some additional computation, the algorithm that calculates the failure signals could discriminate between the transient and steady effects of sensor malfunctions. A steady residual vector would then be compared only to the steady-state failure directions for sensors, not to the entire plane segments.

---

[2]The reason a fuel flow sensor would make the first column larger, while, even with a sensor for A , the second column is not large, is that fuel flow is a state variable of the reference model and nozzle area is not.

6.3.4 Decrease in Compressor Efficiency

This example is intended to demonstrate what capability the filter may have in detecting a consequence of rotating stall, namely a significant drop in efficiency of the compressor. The results are plotted in Figure 6.6. In the first half-second, an increase in PLA from 50° to 60° initiated an acceleration, and during the next tenth of a second the compressor efficiency was dropped by 10 points.[3] Subsequently, the compressor speed dropped sharply, and in compensation the fuel command increased. Concurrently, the failure signal for compressor efficiency grew, and for a while it was the only significant signal. But then the direction of the residual vector changed 5 degrees, causing indications of failures in three more components: the N_2 sensor, the CSV sensor, and the high-pressure turbine. This sharp sensitivity to the direction of the residual vector is due to the small angles between the failure vectors of concern here (see the tables of angles in Appendix B). Once again, similarity of physical effect is the reason for this. Reduced efficiency in either the compressor or the turbine makes N_2 decrease and the pressures increase, and, further, one of the most noticeable effects of mispositioning the stator vanes is a drop in compressor efficiency. Note how much deflection of the vanes is indicated in this example--some 20 to 25 degrees. This occurs because the immediately measurable effects (measurable with the given sensor set) of movement of the stator vanes, like those of the fan vanes, are relatively small (provided they are not moved far enough to induce a surge), and conversely, even a small residual vector can indicate substantial movement of the vanes. One of the examples in Appendix C is of a malfunction of the CSV sensor; it illustrates the difficulty of trying to identify a problem in the stator-vane actuation system.

---

[3] A 10-point decrease was selected as one that was not likely to cause a surge and hence cause the simulation to fail. Also, the ramping of the decrease over a tenth of a second avoided a sharp change that could make the simulation integrate improperly.

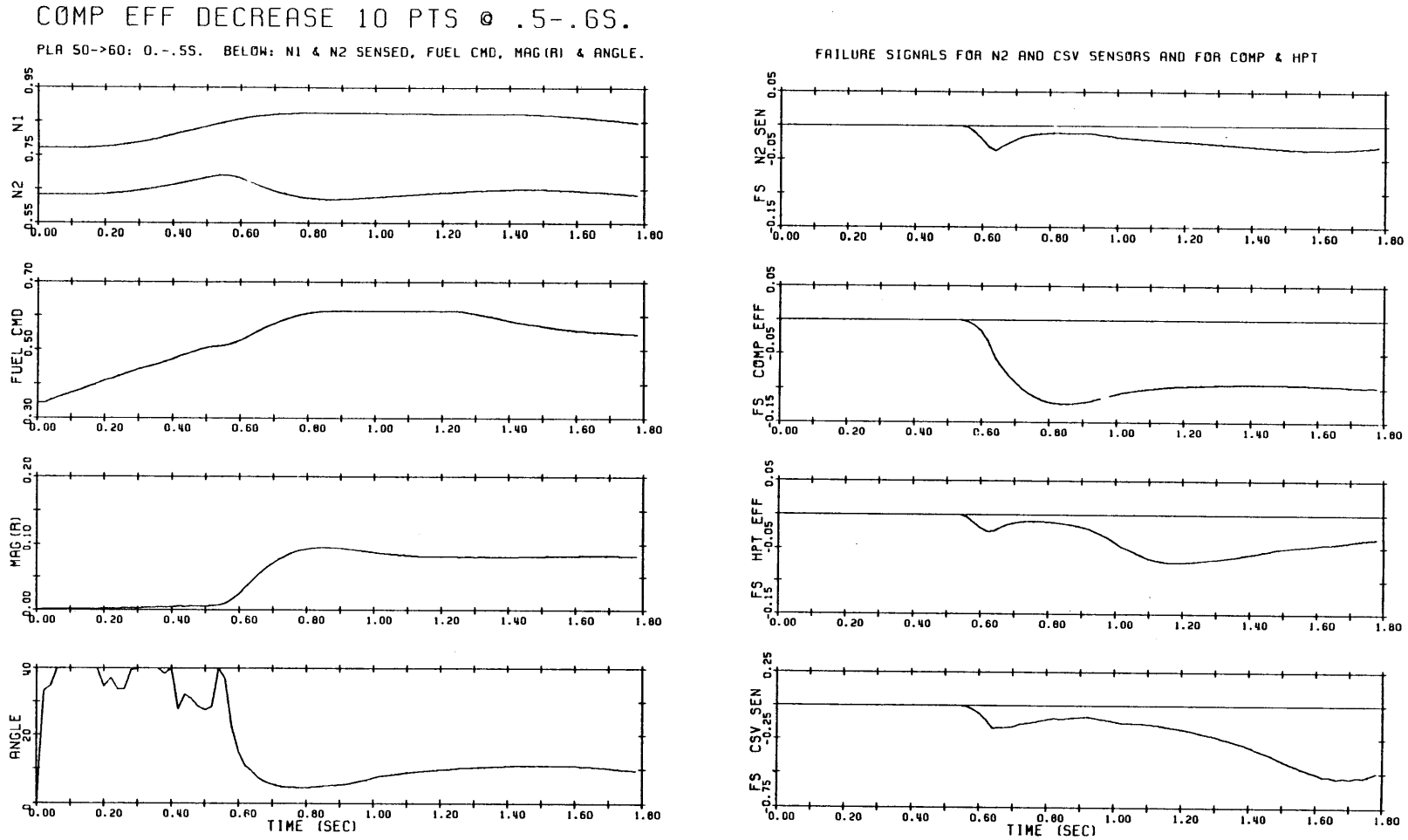

Figure 6.6. Decrease in compressor efficiency.

6.3.5 Change in the Scale Factor of the P_b Sensor

The results of this example are shown in Figure 6.7. The scale factor of the P_b sensor was changed from 1.0 to 1.1 over the interval 0.5 to 0.75 second, during an acceleration from low power to cruise power. The change caused a small but noticeable increase in fuel command. The rise in scale factor resulted in a P_b measurement that was about 30 psi (6% of range) too high, an error that the failure signal for the P_b sensor soon showed. Indication of the malfunction was delayed slightly by modeling errors encountered at low power levels, apparently because the reference model lacked the third pair of Φ and Γ necessary to model the dynamics at those power levels sufficiently accurately.

6.3.6 Acceleration from Idle to Intermediate Power without a Malfunction

This test demonstrated that the filter suppresses failure indications when there is no failure, even during a sharp transient. In Figure 6.8, the eight most significant failure signals are given, showing that no signals of concern appeared. Again, the brief peaks in the signals for the FIGV and CSV sensors are below what the thresholds for those components would be.

Of more concern is the failure signal that toward the end of the test indicated a possible 90°F error in the FTIT measurement. The reason for this is that the sensor is characterized in the reference model by only one state variable, whereas the sensor actually exhibits two prominent thermal lags that act in parallel rather than in series. One is associated with the thermocouple itself and has a time constant of about 0.5 second. The other is due to the thermal capacity of the casing and support of the sensor and has a time constant of approximately 5 seconds. For the purposes of this study, using a single lag with a compromise time constant of 1.7 second proved to be adequate, but in a real application, probably both of the lags would have to be included in the

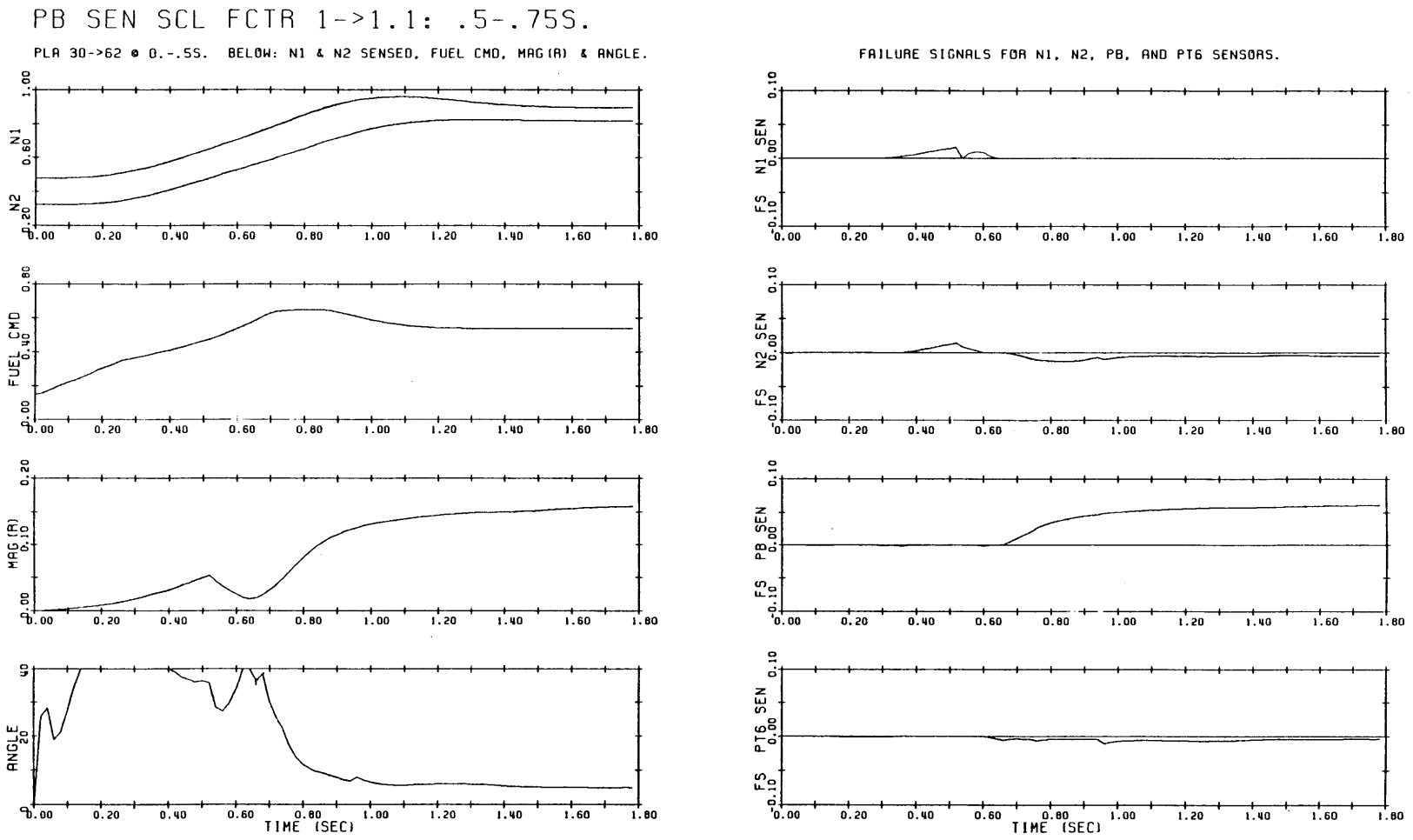

Figure 6.7. Increase in the scale factor of the P_b sensor.

reference model. An additional complication is that the time constants of a real sensor vary with mass flow and pressure.

Regarding sensor dynamics, a consideration worth noting here is that the slower a sensor is, the less its output contributes to the failure signatures generated by a detection filter for malfunctions of other components. This suggests that if a slow sensor can be modeled well, the model should not be used in the filter itself but in a separate compensator that improves the dynamic response of the measurement. The representation in the filter should be of the compensated measurement, as this would further separate the failure vectors. With the FTIT sensor, for example, dynamic compensation would be quite helpful.

The good performance of the filter during the first part of the acceleration seems to indicate that the modeling at low power settings is adequate, but other examples indicate otherwise. In particular, in Appendix C are results from a deceleration from intermediate power to idle that show erroneous failure signals when the rotor speeds get small. This evidence supports the conjecture made in Section 6.3.5 that a third $\{\Phi,\Gamma\}$ pair is needed to improve the modeling at low power settings.

This concludes both the discussion of the examples and the presentation of the research undertaken during this project. Chapter 7 summarizes the results and then presents several conclusions.

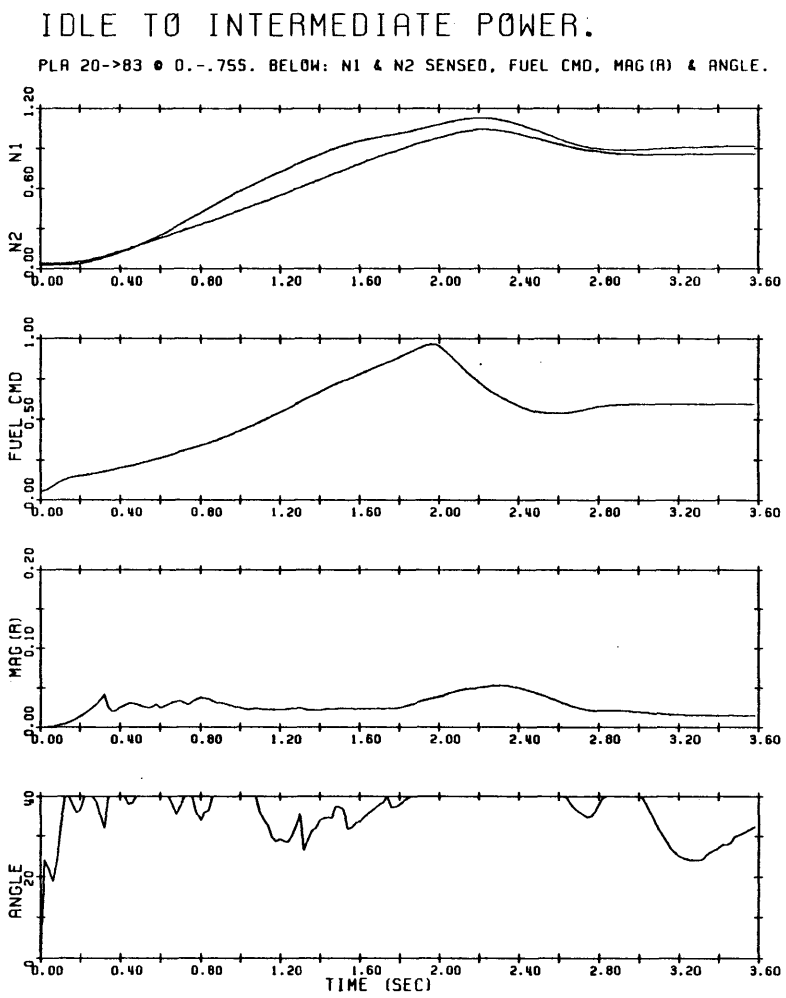

Figure 6.8. Acceleration from idle to intermediate power without a malfunction.

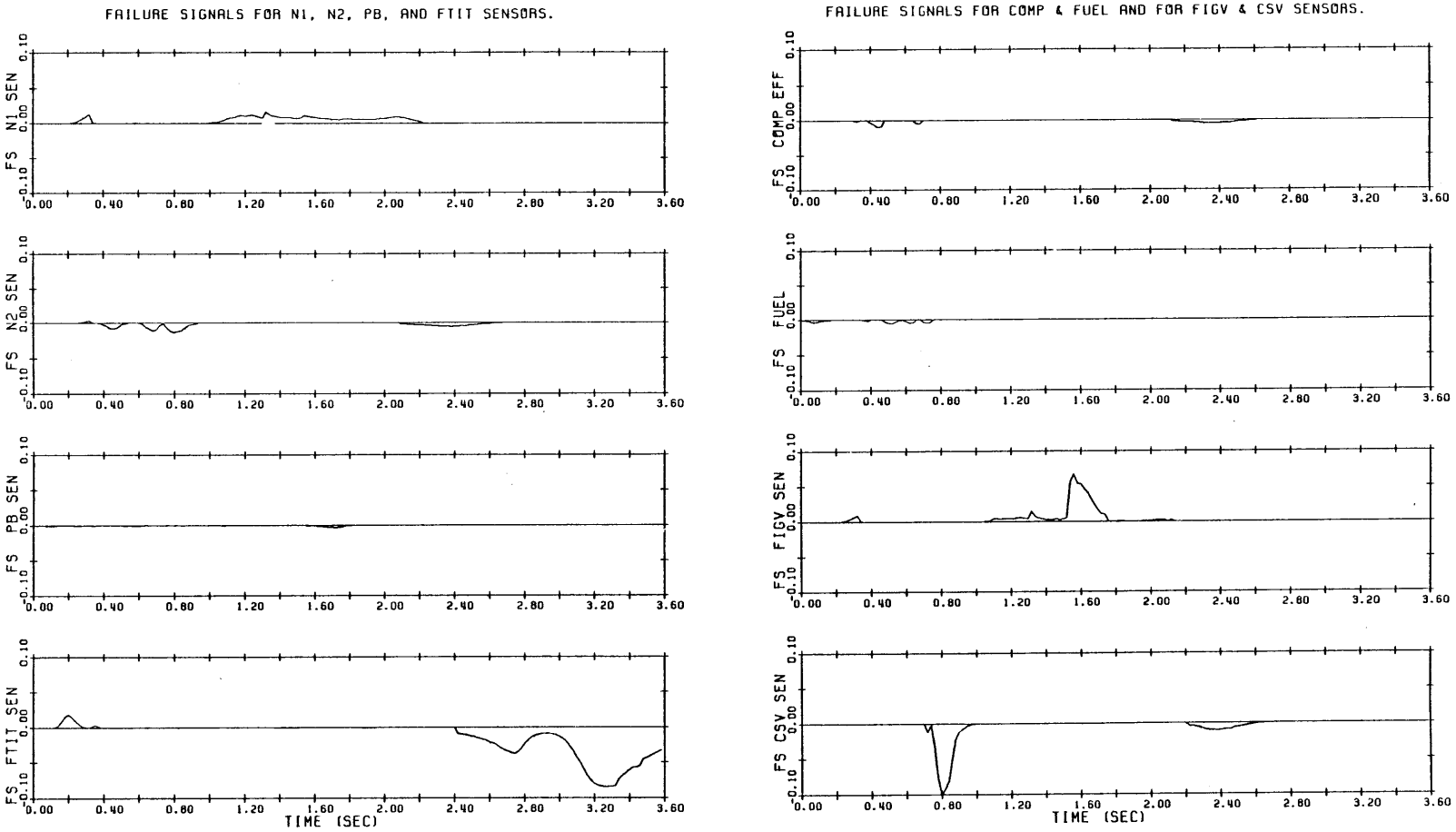

Figure 6.8, continued.

Chapter VII

SUMMARY AND CONCLUSIONS

7.1 SUMMARY

The results of this research establish that the detection filter is a viable approach to failure detection and identification in the control of advanced turbofan engines. Although detection filter theory is strictly applicable only to linear systems, it has been shown to be useful in the design of a filter for a highly nonlinear system, the F100 engine. Tests on a full simulation of that engine have demonstrated successful operation of the filter and, in the process, have shown that the filter need not be highly complex in order to function well.

Only a few of the many dynamic modes of the engine must be represented by the reference model contained in the filter, and an approximate and undetailed representation of the nonlinear characteristics of the engine apparently is sufficient. Specifically, the reference model used is only sixth order. Of the six state variables, three represent the dynamics of the rotors and of the pressure in the afterburner duct, one the hydromechanical lag in the fuel system, and two the thermal lags in the T_{t25} and FTIT sensors. The model has the simple structure of a linear model, but it is nonlinear in that the coefficients vary as step functions of the compressor speed. All the testing was conducted for one flight condition: sea level static. To be suitable for other flight conditions, the model must also vary with aircraft altitude and Mach number.

In tests on simulated failures, the filter was able to monitor fifteen components: the inlet sensors, the sensors on the engine, the fuel system, the nozzle and vane actuation systems, and the high- and low-pressure turbines. It was also able to identify changes in compressor bleed and thereby avoid falsely indicating a malfunction. The measurements used by the filter are the same ones likely to be used by the electronic controllers now under development, namely the outputs N_1, N_2, P_b, P_{t6}, T_{t25}, and FTIT, plus the inputs P_{t2}, T_{t2}, nozzle area, fan vane position, and compressor vane position. As it was designed to do, the filter constrained the failure signatures of the monitored components to characteristic directions in the vector space of filter residuals. The technique developed for discerning which, if any, of the fifteen failure directions the residual vector lies close to consistently yielded "failure signals" that correctly indicated the failed component and the magnitude of the failure. These signals are scalar numbers to which one can easily apply deterministic or statistical threshold tests.

Malfunctions of some components have similar effects on engine performance--for example, decreases in compressor efficiency and high-pressure turbine efficiency--and, as a result, occasionally the correct failure signal was accompanied by one or more other failure signals. In some cases it may not be possible, and perhaps not necessary, to resolve this difficulty; then the filter will only be able to indicate that one of two or more related components has malfunctioned--not which one. Another difficulty the tests showed lay in obtaining correct failure signals for the positions of the fan and compressor vanes. Movements of the vanes normally have such small effects that a malfunction must cause a deflection of at least 10 to 20 degrees to produce a residual vector that might be identifiable.

Generally, aside from vane deflections, any malfunction that altered the output of the affected component by 10% or more of the range of the component was almost always identifiable even during a sharp transient in engine power. With some components, even 5% deviations in

output were distinguishable, and when engine power was steady, deviations of 2% could be correctly attributed. These results are summarized in Table 7.1.

TABLE 7.1

Summary of the performance of the filter.

- Detection: 2% to 5% change in one or more output measurements

- Identification:

Engine state:	Minimum failure size: Steady	Unsteady
Output sensors	2%	5-10%
Inlet sensors	2%	5-10%
Fuel system, exhaust nozzle	5-10%	10-20%
Compressor vanes, fan vanes	10-30%	20-60%
Rotor efficiencies	2%	5-10%

The method used to design the filter is much simpler than the design procedure devised from the full theory of detection filters. The complete procedure and the condensed one have been described in detail in separate sections. Also, an algorithm was developed for analyzing the residuals the filter generates. Although the condensed design procedure and the diagnostics algorithm were both developed for use with the F100, they are described in general terms without reference to any attributes of the F100, and, therefore, they may be useful for failure detection and identification in other complicated systems as well.

7.2 CONCLUSIONS

The results obtained lead to these conclusions:

1. The detection filter is a viable approach to the task of failure detection and identification in the control of advanced

gas turbine engines. Tests with a full simulation of the F100 turbofan engine have demonstrated that the concept works well even when many approximations are made in implementing it.

2. Only three of the dynamic modes of the F100 engine need be represented in the mathematical model contained in the filter. Of the dynamics in the sensors and actuators, only the hydromechanical lag in the fuel pump and the thermal lags in the temperature sensors are important.

3. The detection filter concept works with nonlinear systems. The reference model must be nonlinear, but when it is, the filter is robust: identification accuracy is good, and in failure-free circumstances, indications of failures are well suppressed.

4. Contrary to early expectations, the filter does just as well, and frequently better, with failures in the sensors that measure state variables as with failures in the actuator subsystems. The larger magnitudes of the residuals produced by the sensor failures outweighed the greater difficulty of identifying residual vectors constrained only to a plane segment rather than to a single direction.

5. The computation time and the memory space needed to implement the filter apparently are reasonable. Estimates are that when the filter designed in this study is implemented in a microcomputer, it would require 3 ms of computation every sampling cycle (every 20 to 50 ms), plus 5 to 10 ms every fourth or fifth cycle for determining the coefficients of the model. When called on, the diagnostics will need 6 and 12 ms, respectively. Estimates of the memory required for the reference model range from 4,000 to 20,000 16-bit words.

7.3 SUGGESTIONS FOR FURTHER WORK

This research has developed the detection filter from a theoretical concept to a potentially practical method for diagnosing failures in a complicated system, but it is yet a long way from application. Some suggestions follow for both further analytical research and further development.

Theoretical investigation is needed of the behavior of filters containing nonlinear reference models. An analytical description of how the direction of the residual vector is influenced by nonlinearities would be helpful in developing methods for including nonlinearities in the model. Regarding the algorithm for analyzing the residuals, better selectivity is possible by making the algorithm sensitive to the transient behavior of the residual vectors that are caused by sensor malfunctions.

For the application to turbine engines, the range of the nonlinear model must be extended to encompass the entire flight envelope. Also, the accuracy of the filter could be improved by including in the model the major nonlinearities associated with nonequilibrium states. Further, the possibility of storing and executing the reference model in terms of nondimensional and corrected parameters should be explored. Use of such a model would undoubtably reduce the number of parameters that the model's coefficients depend on and would thereby make the storage of the model much more compact. On the other hand, the corrected parameters must be converted to physical variables for comparison with the measurements, so additional computation would be required. On the whole, modeling in terms of corrected parameters would probably be beneficial, but more investigation is needed to demonstrate this.

And in conclusion, none of the possible auxiliary uses of the filter have been explored. One of the important capabilities of a detection filter is that when a nonredundant sensor fails, the filter can provide to the controller an estimated substitute for the lost measure-

ment. And, generally, as filtering concepts are further developed and are applied in conjunction with other techniques, other ways a detection filter can help with fault accommodation may arise. It is through the combination and interlinking of separate techniques of failure detection, identification, and accommodation that a truly fault-tolerant engine control system will evolve.

Appendix A

NUMERICAL DATA OF THE LINEAR MODEL REFERENCE

This appendix contains tables of the matrices of the full- and reduced-order linear models of the F100 at full intermediate (PLA=83) power. Also included are listings of the feedback matrix and the failure vectors of the detection filter.

Table A.1 contains the matrices of the 16th-order model produced by the linearization routine built into the nonlinear simulation. The variables of the model are listed in Table 5.4. The perturbation sizes used in the linearization are 2 and 3 percent of the equilibrium values of the elements of $\underline{x}$ and $\underline{u}$ respectively, except for FIGV, which was perturbed by 5 degrees, and CSVA, perturbed by 2 degrees. These perturbation sizes give a model which, compared to other models that were generated with different perturbation sizes, appears least inaccurate for a transient from 100 percent intermediate power to 75 percent (PLA=60) and back to 90 percent (PLA=75).

The method used to normalize the variables and matrices is given in Table A.2. The resulting nondimensional model was reduced to fifth order by the procedure given in Section 5.3.2. To this model were added first-order dynamics representative of the fuel system and the T_{t25} and FTIT sensors. Fuel flow is the first element of $\underline{u}$, so the first columns of the normalized and reduced B and D matrices become the sixth columns of the new A and C matrices. The elements A_{66} and B_{16} become respectively the negative and positive reciprocals of the fuel system time constant; the remainders of the first column of B and the sixth row of A become zero, as does the entire first column of D. The dominant time

constant of the fuel system is 0.10 second (see Figure 5.4), but using 0.15 second in the model yields better results, as that helps account for some of the neglected lags. The measurements T_{t25} and FTIT are the fifth and sixth elements of $\underline{y}$. To make them state variables, we divide the fifth and sixth rows of C and D by the respective time constants and juxtapose them with D_{15} and D_{16} to make up most of the the seventh and eighth rows of A and B. The values of A_{77} and A_{88} are the negative reciprocals of the time constants, and A_{78} and A_{87} are zero. Those rows of C and D become zero, except for C_{55} and C_{66}, which of course take the value one.

The variables of the resulting eighth-order model were transformed to the variables listed in Table 5.6. The model that this tranformation produced is listed in Table A.3. Conversion to discrete-time form resulted in the model given in Table A.4. In Table A.5 appear the D matrix (computed from Equation (5-12)) for the detection filter, and the associated failure vectors and scale factors used in the identification algorithm. (The vectors are all normalized to length one.) The failure vectors shown for the four sensors that have planar signatures point in the steady-state directions of the signatures. Also shown are the maximum deflections that neglecting Γ_2 should cause in the failure signatures. Table A.6 lists the angles between the failure directions. For the four failure signatures that are plane segments, the direction the angles are measured from is the steady-state failure direction.

Finally, in Figure A.1 is shown a comparison of the responses of the F100 nonlinear simulation and the linear model given in Table A.4 to two changes in PLA, from 83 to 60 degrees, and from 60 to 75 degrees. On the left appear the measured values of N_1, N_2, P_b, P_{t6}, T_{t25}, and FTIT, then the fuel command and the nozzle and FIGV positions, all from the simulation. On the right are the differences between the six measurements from the simulation and the measurements from the linear model. The model received the same inputs in fuel command and nozzle and vane positions as the simulation did. The model did not have the feedback loop of the detection filter.

TABLE A.1

Matrices of the 16'th-order F100 linear model.

$$A = \begin{bmatrix}
-4.469 & .1470 & 4.951 & 400.5 & -738.6 & -2.686 & 1.032 & -1.032 \\
-.4250 & -5.205 & 127.7 & -232.6 & -431.3 & 32.62 & 2.193 & -2.505 \\
1.032 & 5.050 & -166.9 & -5.294 & 1029. & -91.40 & -5.343 & 5.036 \\
.5187 & -.1842 & 131.8 & -574.9 & 110.2 & -9.623 & -.5772 & -2.117 \\
.1057E-1 & -.1198E-1 & .9341E-1 & 1.694 & -9.657 & .2355 & .7577E-2 & -.1275E-1 \\
.8638 & -.9928E-2 & .6168E-1 & -.3056 & 42.19 & -19.75 & -.2048 & .1288E-2 \\
.6643 & -.7697E-2 & .1113 & .3369 & 78.32 & .2572 & -20.35 & .1288E-2 \\
-.1023 & .9729 & 17.42 & .5101 & -97.27 & 29.75 & .5288 & -20.00 \\
-.9134E-2 & -.7251E-2 & .1765 & .3008E-1 & -8.583 & .7823 & .4089E-1 & 6.547 \\
-.1352E-3 & -.1078E-3 & .2607E-2 & .4011E-3 & -.1273 & .1159E-1 & .6082E-3 & .9700E-1 \\
-1.265 & -5.435 & 26.86 & 6.389 & -1246. & 115.1 & 6.560 & 36.49 \\
-.2681E-1 & -.4216 & -52.19 & 198.8 & -26.60 & 2.572 & .1510 & 9.672 \\
-.1191E-2 & -.1874E-1 & -2.320 & 8.837 & -1.182 & .1143 & .6700E-2 & .4299 \\
-.1299 & -.2245 & -23.82 & 24.12 & 149.9 & 1.852 & .1085 & 4.435 \\
-.1279E-1 & .2556E-1 & -.1183 & -.2406E-1 & 5.796 & -.4824 & 19.81 & .1270 \\
-1.696 & 1.528 & -3.864 & 113.8 & 343.7 & -29.71 & -1.763 & -.4543
\end{bmatrix}$$

$$\begin{bmatrix}
1.038 & 1.098 & -4.030 & 9.540 & 9.560 & -.6664 & -.1530 & .0 \\
11.38 & 11.40 & -3.989 & .4990E-2 & .1123E-1 & .4010E-2 & -.4090 & .0 \\
-.3380E-1 & -.1056 & 5.634 & -.1497E-1 & -.8982E-1 & -.9357E-2 & 1.002 & .0 \\
-2.920 & -2.978 & 5.858 & -.9356E-2 & -.7859E-1 & -.5347E-2 & .8741E-1 & .0 \\
.7029E-2 & -.8075E-2 & -.3617E-1 & -.2485E-2 & -.2282E-1 & .4136E-1 & .2091E-1 & -.3508E-2 \\
-.2253E-2 & -.5915E-2 & .3783E-2 & -.3743E-3 & -.4491E-2 & -.2674E-3 & .5120E-1 & .0 \\
-.3474E-2 & -.1014E-1 & .1674E-1 & -.9980E-3 & -.5614E-2 & -.4010E-3 & .5932E-1 & .0 \\
.2535E-2 & .2535E-2 & -.9337E-2 & .3743E-3 & .0 & .0 & -.1011 & .0 \\
-50.00 & -.4225E-2 & 39.42 & -.2183E-2 & .1403E-1 & -.3342E-3 & -.8585E-2 & .0 \\
-.6667 & -.6667 & .5841 & -.3327E-4 & .1871E-3 & -.4456E-5 & -.1353E-3 & .0 \\
.3568E-1 & .8450E-1 & -47.86 & .1123E-1 & .5614E-1 & .4010E-2 & -1.244 & .0 \\
-9.620 & -9.603 & 38.39 & -50.00 & .6175E-1 & .1337E-2 & -.2419E-1 & .0 \\
-.4275 & -.4268 & 1.706 & -2.000 & -1.997 & .5347E-4 & -.1093E-2 & .0 \\
-4.416 & -4.413 & 17.61 & -3.122 & -3.089 & -19.78 & -.3715E-1 & .0 \\
-.2816E-3 & -.8450E-3 & .1956E-1 & -.1248E-3 & .0 & .0 & -19.99 & .0 \\
.5896 & .5894 & -2.323 & .3119E-3 & .3930E-1 & 30.82 & 20.05 & -50.00
\end{bmatrix}$$

Eigenvalues of A:

-0.660	-1.964	-2.732	-6.102 ± i2.259		-18.62 ± i5.352	-19.45
-20.66 ± i.9212		-39.71	-47.52	-49.38	-58.26	-177.7	-573.4

TABLE A.1 continued

$$B = \begin{bmatrix}
.7976E-1 & -488.7 & -121.9 & 2.707 & -2235. & -554.5 & 24.39 \\
-.2038 & -1055. & .9591 & -89.78 & 8343. & -268.6 & -5.987 \\
.7882 & 1977. & 4.701 & 89.97 & -.7859E5 & 616.4 & -9.704 \\
.1632 & 212.9 & .1114 & 9.412 & 584.1 & 89.80 & 1.604 \\
.5816E-3 & -103.4 & .8520 & -.2008 & -5.820 & 12.22 & -.3455 \\
-.1217E-1 & 72.71 & 8.942 & -.1999 & 341.1 & -142.9 & 21.13 \\
-.3931E-2 & 74.68 & 9.684 & -.1376 & 37.90 & -266.0 & 22.87 \\
-.1073 & -93.08 & -1.432 & 13.27 & 2396. & -104.7 & .2060 \\
.4868E-1 & 3.567 & -.2836 & -.7813 & -6699. & -34.83 & -1.722 \\
.7220E-3 & .5113E-1 & -.4173E-2 & -.1154E-1 & -99.28 & -.5158 & -.2552E-1 \\
5.349 & -2273. & -4.258 & -108.5 & .9977E5 & -691.1 & 10.43 \\
.1247 & 16.56 & -.6889 & -2.392 & -6178. & -54.17 & -1.450 \\
.5542E-2 & .7278 & -.3053E-1 & -.1063 & -274.7 & -2.407 & -.6444E-1 \\
.4374E-1 & 41.49 & .3919 & -1.752 & -1683. & -26.66 & -.3746 \\
.2755E-2 & 13.40 & -1.075 & .5007 & -45.68 & -14.29 & .4961 \\
.2279 & 629.3 & -114.8 & 30.02 & -2686. & -1704. & 50.92
\end{bmatrix}$$

$$C = \begin{bmatrix}
1.000 & .0 & .0 & .0 & .0 & .0 & .0 & .0 \\
.0 & 1.000 & .0 & .0 & .0 & .0 & .0 & .0 \\
-.5445E-3 & -.2402E-2 & 1.048 & .2767E-2 & -.5466 & .4763E-1 & .2831E-2 & -.1146E-1 \\
.8644E-4 & -.1121E-3 & .1210E-2 & .2335E-1 & .9367 & .2624E-2 & .1740E-3 & -.1232E-3 \\
.0 & .0 & .0 & .0 & .0 & .0 & 1.000 & .0 \\
-.5955E-3 & -.9370E-2 & -1.160 & 4.418 & -.5911 & .5715E-1 & .3350E-2 & .2149 \\
.0 & .0 & .0 & .0 & .0 & .0 & .0 & .0 \\
.0 & .0 & .0 & .0 & .0 & .0 & .0 & .0 \\
.0 & .0 & .9135E-3 & .0 & .0 & .0 & -.5307E-3 & .0 \\
.1203E-3 & .1347E-3 & -.4600E-3 & .0 & .0 & .7348E-3 & .3307E-3 & .0 \\
.0 & .0 & .0 & .0 & .0 & .0 & .0 & .0 \\
-.2138 & -.2134 & .8532 & .0 & .0 & .0 & .0 & .0
\end{bmatrix}$$

$$D = \begin{bmatrix}
.0 & .0 & .0 & .0 & .0 & .0 & .0 \\
.0 & .0 & .0 & .0 & .0 & .0 & .0 \\
-.3011E-3 & -1.098 & -.2606E-2 & -.4793E-1 & 40.16 & -.3284 & .5294E-2 \\
-.3149E-4 & .2832E-2 & .7632E-2 & -.2327E-2 & .6998 & .1103 & -.3536E-2 \\
.0 & .0 & .0 & .0 & .0 & .0 & .0 \\
.2778E-2 & .4064 & -.1552E-1 & -.5317E-1 & -136.9 & -1.207 & -.3217E-1
\end{bmatrix}$$

TABLE A.2

Values used to normalize the variables in the F100 model.

$$x_{i\,norm} = (x_i - x_{i\,min}) / x_{i\,range}$$
$$u_{i\,norm} = (u_i - u_{i\,min}) / u_{i\,range}$$
$$y_{i\,norm} = (y_i - y_{i\,min}) / y_{i\,range}$$

$$A_{ij\,norm} = A_{ij} * x_{j\,range} / x_{i\,range}$$
$$B_{ij\,norm} = B_{ij} * u_{j\,range} / x_{i\,range}$$
$$C_{ij\,norm} = C_{ij} * x_{j\,range} / y_{i\,range}$$
$$D_{ij\,norm} = D_{ij} * u_{j\,range} / y_{i\,range}$$

State Variables	Minimum	Range	Units
N1	3700	7000	rpm
N2	9000	4500	rpm
PT3	30	570	psia
PT45	5	155	psia
PT7	2	65	psia
TT25H	500	500	deg R
TT25C	500	500	deg R
TT3	880	820	deg R
TT4hi	1350	1305	deg R
TT4lo	150	145	deg R
TT4	1550	1500	deg R
TT45hi	990	990	deg R
TT45lo	110	110	deg R
TT5	960	900	deg R
TT6C	500	450	deg R
TT7	730	2920	deg R

Inputs	Minimum	Range	Units
Wf	300	16000	lbs/hr
AJ	2.8	3.6	sq.ft.
FIGV	0	25	degrees
CSVA	4	44	degrees
BLC	0	1	fraction
PT2	1	35	psia
TT2	400	350	deg R

Measurements	Minimum	Range	Units
N1sen	3700	7000	rpm
N2sen	9000	4500	rpm
PBsen	30	550	psia
PT6sen	2	65	psia
TT25Csen	500	500	deg R
FTITsen	1100	1100	deg R

TABLE A.3

Normalized, continuous-time, reduced-order linear model of the F100 operating at sea level static conditions with PLA = 83.

Equilibrium values of the state variables:

	N1	N2	PB	PT6	TT25sen	FTITsen	Z1	Z2	
$\underline{x}$ =	0.9416	0.9182	0.6174	0.6457	0.5523	0.9768	1.0701	1.2646	

$$A = \begin{bmatrix} -2.730 & -1.788 & 14.598 & -10.527 & 0.0 & 0.0 & -0.065 & 0.151 \\ 2.550 & -5.567 & 10.869 & -7.236 & 0.0 & 0.0 & 0.394 & -0.004 \\ 1.242 & -0.053 & -3.904 & -1.283 & 0.0 & 0.0 & 0.080 & -0.050 \\ 2.597 & -1.241 & 5.279 & -9.347 & 0.0 & 0.0 & -0.052 & -0.047 \\ 3.759 & 0.039 & -0.256 & 4.479 & -8.333 & 0.0 & 0.0 & 0.0 \\ 1.194 & -1.079 & 4.073 & -2.630 & 0.0 & -0.833 & -0.026 & 0.0 \\ 0.0 & 0.0 & 0.0 & 0.0 & 0.0 & 0.0 & -0.661 & 0.0 \\ 0.0 & 0.0 & 0.0 & 0.0 & 0.0 & 0.0 & 0.0 & -1.957 \end{bmatrix}$$

N1, N2, PB, PT6, TT25sen, FTITsen, Z1, Z2

Eigenvalues:

-0.661 -0.833 -1.957 -3.033 -5.975 ± 11.8806 -6.667 -8.333

Equilibrium values of the inputs:

	WF	AJ	FIGV	CSVA	BLC	PT2	TT2	
$\underline{u}$ =	0.6418	0.0085	-0.0859	0.0	0.0	0.3913	0.3391	

$$B = \begin{bmatrix} 0.0 & -0.577 & -0.346 & -0.239 & 0.547 & -4.891 & 3.506 \\ 0.0 & -0.909 & 0.160 & -1.001 & 0.366 & -5.752 & 3.929 \\ 1.770 & -2.545 & 0.235 & -0.022 & -0.447 & 4.648 & -1.792 \\ 0.090 & -5.549 & 0.394 & -0.175 & 0.081 & 5.696 & -0.212 \\ 0.0 & 0.225 & 0.185 & 0.006 & -0.010 & -7.871 & 6.627 \\ 0.0 & -0.261 & 0.058 & -0.184 & 0.379 & -2.174 & 1.951 \\ 0.959 & 0.509 & -0.040 & -0.012 & 0.067 & -1.345 & 0.686 \\ 3.690 & 2.109 & -0.165 & -0.021 & 0.241 & -4.868 & 2.321 \end{bmatrix}$$

N1, N2, PB, PT6, TT25sen, FTITsen, Z1, Z2

$$C = \begin{bmatrix} 1 & 0 & 0 & 0 & 0 & 0 & 0 & 0 \\ 0 & 1 & 0 & 0 & 0 & 0 & 0 & 0 \\ 0 & 0 & 1 & 0 & 0 & 0 & 0 & 0 \\ 0 & 0 & 0 & 1 & 0 & 0 & 0 & 0 \\ 0 & 0 & 0 & 0 & 1 & 0 & 0 & 0 \\ 0 & 0 & 0 & 0 & 0 & 1 & 0 & 0 \end{bmatrix}$$

N1sen, N2sen, PBsen, PT6sen, TT25sen, FTITsen

TABLE A.4

Discrete-time linear model of the F100 operating at sea level static conditions with PLA=83.
(Time interval for sampling of measurements is 0.02 second.)

Equilibrium values of the state variables:

	N1	N2	PB	PT6	TT25sen	FTITsen	Z1	Z2
$\underline{x}$ =	0.9416	0.9182	0.6174	0.6457	0.5523	0.9763	1.0701	1.2646

State transition matrix:

Φ =	0.9444	-0.0307	0.2595	-0.1876	0.0	0.0	-0.0011	0.0028	N1
	0.0460	0.8953	0.1976	-0.1319	0.0	0.0	0.0076	0.0	N2
	0.0226	-0.0011	0.9268	-0.0247	0.0	0.0	0.0015	-0.0009	PB
	0.0466	-0.0222	0.0968	0.8251	0.0	0.0	-0.0010	-0.0008	PT6
	0.0693	-0.0014	0.0094	0.0680	0.8465	0.0	-0.0001	0.0001	TT25sen
	0.0222	-0.0201	0.0762	-0.0494	0.0	0.9835	-0.0005	0.0	FTITsen
	0.0	0.0	0.0	0.0	0.0	0.0	0.9869	0.0	Z1
	0.0	0.0	0.0	0.0	0.0	0.0	0.0	0.9616	Z3

Equilibrium values of the inputs:

	WF	AJ	FIGV	CSVA	BLC	PT2	TT2
$\underline{u}$ =	0.6418	0.0085	-0.0859	0.0	0.0	0.3913	0.3391

Input transfer matrix:

Γ =	0.0047	-0.0069	-0.0069	-0.0040	0.0092	-0.0919	0.0625	N2
	0.0036	-0.0151	0.0028	-0.0189	0.0062	-0.1096	0.0727	N1
	0.0340	-0.0477	0.0043	-0.0004	-0.0085	0.0870	-0.0337	PB
	0.0034	-0.1037	0.0072	-0.0031	0.0012	0.1074	-0.0049	PT6
	0.0002	-0.0005	0.0035	-0.0002	0.0002	-0.1440	0.1243	TT25sen
	0.0013	-0.0043	0.0010	-0.0034	0.0072	-0.0423	0.0374	FTITsen
	0.0191	0.0101	-0.0008	-0.0002	0.0013	-0.0267	0.0136	Z1
	0.0724	0.0414	-0.0032	-0.0004	0.0047	-0.0955	0.0455	Z3

Measurement matrix:

C =	1	0	0	0	0	0	0	0	N1sen
	0	1	0	0	0	0	0	0	N2sen
	0	0	1	0	0	0	0	0	PBsen
	0	0	0	1	0	0	0	0	PT6sen
	0	0	0	0	1	0	0	0	TT25sen
	0	0	0	0	0	1	0	0	FTITsen

TABLE A.5

Filter feedback matrix and failure vectors.

Feedback matrix: $D =$

0.1256	-0.0307	0.2595	-0.1876	0.0	0.0
0.0460	0.0766	0.1976	-0.1319	0.0	0.0
0.0226	-0.0011	0.1081	-0.0247	0.0	0.0
0.0466	-0.0222	0.0968	0.0064	0.0	0.0
0.0693	-0.0014	0.0094	0.0680	0.0278	0.0
0.0222	-0.0201	0.0762	-0.0494	0.0	0.1648
0.0	0.0	0.0	0.0	0.0	0.0
0.0	0.0	0.0	0.0	0.0	0.0

Failure vectors:	N1sen	N2sen	PBsen	PT6sen	TT25sen	FTITsen	Fuel
	0.4844	0.2713	-0.7283	0.6224	0.0	0.0	0.1353
	-0.4004	0.9252	-0.5544	0.4376	0.0	0.0	0.1025
	-0.1968	0.0094	0.2054	0.0821	0.0	0.0	0.9800
	-0.4060	0.1965	-0.2716	0.5803	0.0	0.0	0.0968
	-0.6034	0.0128	-0.0263	-0.2256	1.0	0.0	0.0044
	-0.1933	0.1775	-0.2137	0.1637	0.0	1.0	0.0383
Scale factors:	1.579	1.603	0.5086	0.6013	1.181	10.97	5.219
Deflection angles:	-	-	-	-	0	0	18

Failure vectors:	AJsen	FIGVsen	CSVAsen	BLEED	PT2sen	TT2sen	HPT eff
	0.0600	0.58554	0.2037	0.5825	0.3690	-0.3792	-0.1220
	0.1307	-0.23736	0.9507	0.3925	0.4399	-0.4409	0.9306
	0.4136	-0.36765	0.0214	-0.5407	-0.3492	0.2042	0.3338
	0.8982	-0.60996	0.1558	0.0767	-0.4310	0.0296	-0.0514
	0.0046	-0.29340	0.0093	0.0154	0.5778	-0.7536	-0.0064
	0.0373	-0.08661	0.1726	0.4563	0.1698	-0.2267	-0.0706
Scale factors:	1.570	15.34	9.132	1.1524	0.7276	1.312	1.333
Deflection angles:	3.0	2.4	0.2	2.6	3.0	2.5	-

TABLE A.6

Angles between the failure directions.

	N1sen	N2sen	PBsen	PT6sen	TT25sen	FTITsen	FUEL	AJsen	FIGVsen	CSVAsen	BLEED	PT2sen	TT2sen	HPT EFF
N1sen	0	-69	-90	-89	-53	-79	-77	61	-27	67	84	82	-64	-63
N2sen	-69	0	-37	44	89	80	80	-71	78	-5	52	-63	56	36
PBsen	-90	-37	0	-30	-89	-78	89	74	80	41	-29	59	-52	-71
PT6sen	-89	44	-30	0	-77	81	74	-49	86	-49	53	-88	75	71
TT25sen	-53	89	-89	-77	0	90	90	-90	73	-90	89	-55	41	90
FTITsen	-79	80	-78	81	90	0	88	-88	85	-80	63	-80	77	-86
FUEL	-77	80	89	74	90	88	0	-59	68	-80	-67	74	-85	66
AJsen	61	-71	74	-49	90	-88	-59	0	-46	73	87	-64	89	78
FIGVsen	-27	78	80	86	73	85	68	-46	0	-77	-69	71	88	-68
CSVAsen	67	-5	41	-49	90	-80	-80	73	-77	0	-55	63	-58	32
BLEED	84	52	-29	53	89	63	-67	87	-69	-55	0	-51	52	86
PT2sen	82	-63	59	-88	-55	-80	74	-64	71	63	-51	0	-27	75
TT2sen	-64	56	-52	75	41	77	-85	89	88	-58	52	-27	0	-74
HPT EFF	-63	36	-71	71	90	-86	66	78	-68	32	86	75	-74	0

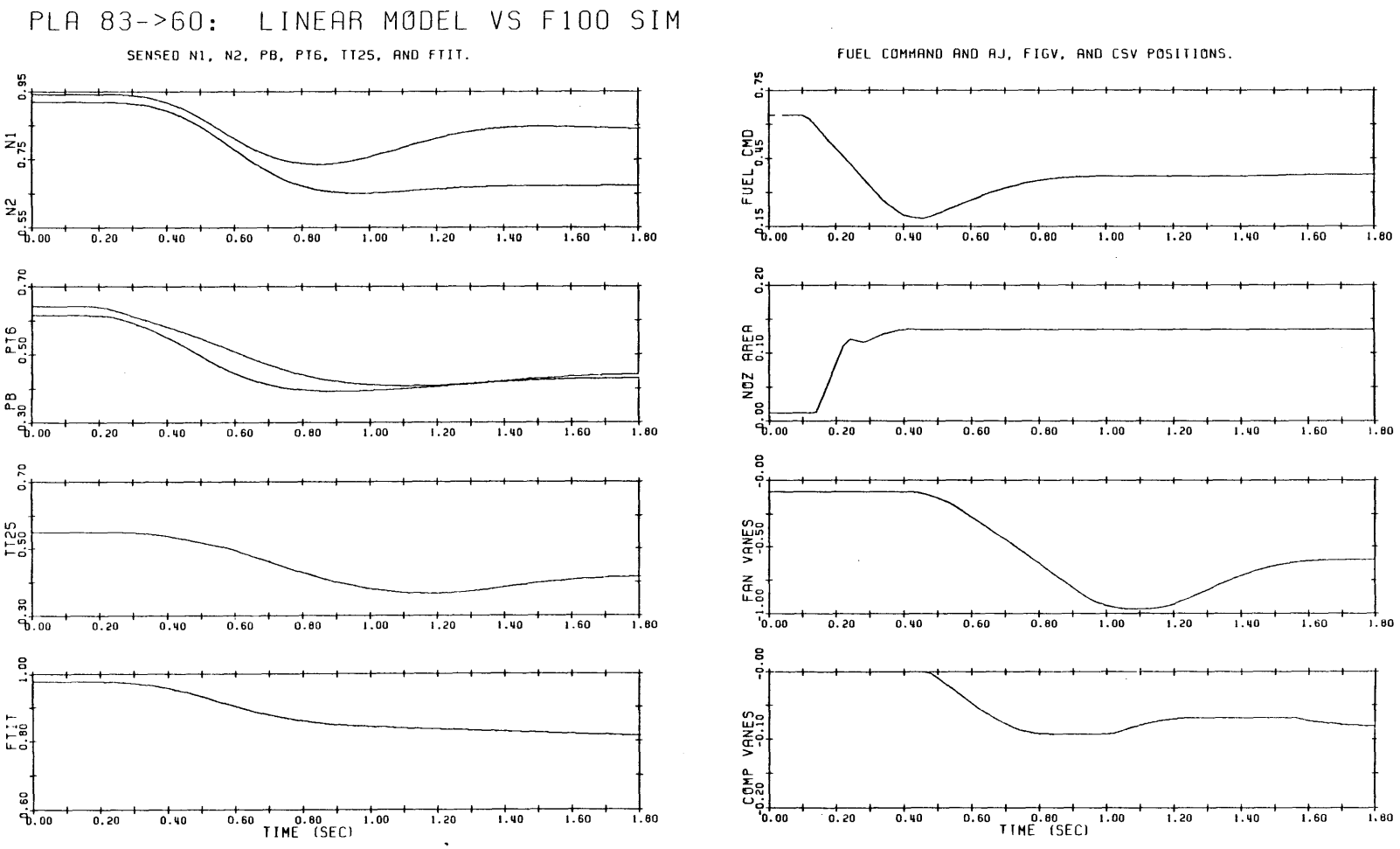

Figure A.1. Comparison of the responses of the simulation and the linear model to a change in PLA from 83° to 60°. Above: response of the F100 simulation.

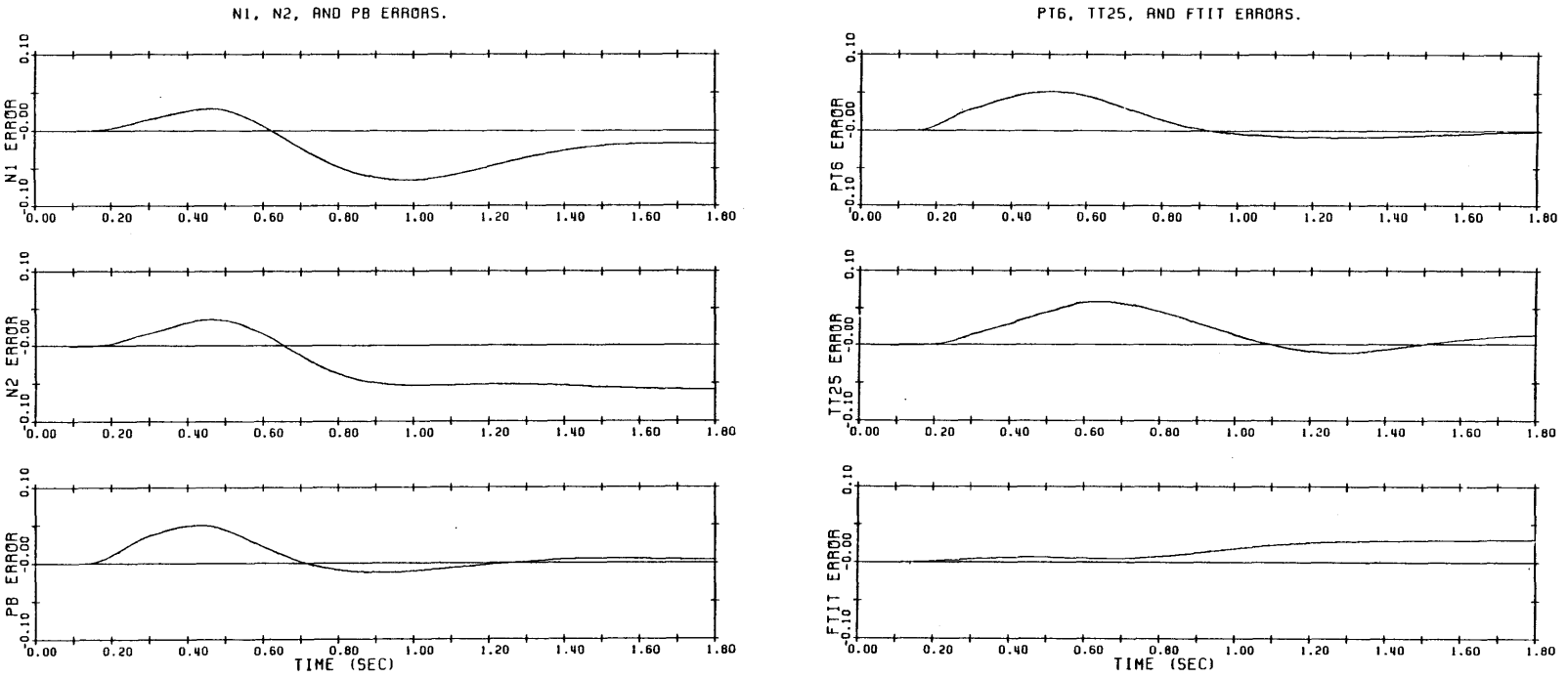

Figure A.1, continued. Differences between the F100 simulation and the linear model.

TABLE B.1

Sea-level-static equilibrium points used in the reference model.

PLA	N1	N2	Pb	Pt6	Tt25	FTIT	Wf	AJ	FIGV	CSV
83	0.94152	0.91774	0.61734	0.64569	0.55227	0.97724	0.64176	0.00850	-0.08593	0.00000
70	0.93808	0.91119	0.60732	0.63083	0.54429	0.97377	0.63135	0.00000	-0.07006	0.00000
62	0.88161	0.79355	0.51761	0.54847	0.47055	0.81944	0.49963	0.05555	-0.37138	-0.02950
53	0.80226	0.67297	0.42798	0.47361	0.40451	0.66150	0.38000	0.05555	-0.75998	-0.08285
43	0.68115	0.53394	0.32880	0.38473	0.33628	0.49823	0.26657	0.05555	-1.00000	-0.18271
35	0.56382	0.41841	0.25652	0.32545	0.28151	0.37347	0.19306	0.05555	-1.00000	-0.31164
30	0.48026	0.32464	0.20717	0.29146	0.23982	0.28089	0.14716	0.05555	-1.00000	-0.42392
26	0.33462	0.23229	0.15487	0.25894	0.19168	0.17624	0.10256	0.05555	-1.00000	-0.51645
23	0.17804	0.13945	0.11083	0.23644	0.15359	0.11282	0.07276	0.05555	-1.00000	-0.63476
20	0.02755	0.04368	0.07302	0.22075	0.12048	0.08353	0.05165	0.05555	-1.00000	-0.78068

Appendix B

NUMERICAL DATA OF THE NONLINEAR REFERENCE MODEL

TABLE B.2

Discrete-time model for PLA=83.

$$\underline{x} = \begin{bmatrix} N1 \\ N2 \\ Pb \\ Pt6 \\ Tt25sen \\ FTITsen \end{bmatrix} \qquad \Phi = \begin{bmatrix} 0.94415 & -0.04777 & 0.29633 & -0.20019 & 0.00000 & 0.00000 \\ 0.05313 & 0.84133 & 0.33139 & -0.19418 & 0.00000 & 0.00000 \\ 0.01914 & -0.00657 & 0.94621 & -0.01994 & 0.00000 & 0.00000 \\ 0.03134 & -0.01975 & 0.06827 & 0.87462 & 0.00000 & 0.00000 \\ 0.07597 & -0.00231 & 0.01042 & 0.06570 & 0.84649 & 0.00000 \\ 0.01902 & -0.03218 & 0.09511 & -0.05772 & 0.00000 & 0.98831 \end{bmatrix}$$

$$\underline{u} = \begin{bmatrix} Wf\ cmd \\ Aj \\ FIGV \\ CSV \\ Bleed \\ Pt2 \\ Tt2 \end{bmatrix} \qquad \Gamma = \begin{bmatrix} 0.00419 & 0.00217 & -0.00683 & -0.00361 & 0.10626 & -0.13813 & 0.06413 \\ 0.00474 & 0.00122 & 0.00235 & -0.02545 & 0.12030 & -0.20419 & 0.11644 \\ 0.02757 & -0.03732 & 0.00324 & -0.00421 & -0.06658 & 0.07410 & -0.01769 \\ 0.00289 & -0.07422 & 0.00478 & -0.00152 & 0.00939 & 0.08535 & -0.00648 \\ 0.00015 & -0.00294 & 0.00309 & -0.00035 & 0.00483 & -0.16349 & 0.12657 \\ 0.00132 & 0.00042 & 0.00072 & -0.00204 & 0.06950 & -0.06149 & 0.03604 \end{bmatrix}$$

	N1sen	N2sen	Pbsen	Pt6sen	Tt25sen	FTITsen	Fuel	Ajsen
	0.48207	0.28083	-0.64007	0.62822	0.00000	0.00000	0.14711	-0.02614
	-0.45860	0.93284	-0.71579	0.60935	0.00000	0.00000	0.16638	-0.01471
Failure	-0.16520	0.03863	0.11619	0.06259	0.00000	0.00000	0.96861	0.44876
Directions:	-0.27048	0.11609	-0.14745	0.39344	0.00000	0.00000	0.10143	0.89243
	-0.65568	0.01360	-0.02250	-0.20618	1.00000	0.00000	0.00542	0.03540
	-0.16412	0.18919	-0.20544	0.18113	0.00000	1.00000	0.04648	-0.00509
Scale factors:	1.5646	1.0657	0.39153	0.56883	1.1808	15.506	6.3670	2.1795

	FIGVsen	CSVsen	Bleed	Pt2sen	Tt2sen	Comp eff	HPT eff	LPT eff
	0.69916	0.13792	0.56688	0.42820	-0.34110	0.04291	-0.12638	0.98600
	-0.24010	0.97235	0.64175	0.63298	-0.61934	0.97297	0.94655	-0.00811
Failure	-0.33108	0.16088	-0.35517	-0.22970	0.09410	0.22684	0.29054	-0.15539
Directions:	-0.48857	0.05795	0.05012	-0.26460	0.03445	0.00492	-0.03630	-0.04078
	-0.31589	0.01350	0.02576	0.50682	-0.67326	0.00101	-0.00515	0.04389
	-0.07372	0.07810	0.37079	0.19062	-0.19168	0.00332	-0.04818	-0.00070
Scale factors:	18.554	6.9240	0.96703	0.56194	0.96420	0.94480	0.89947	2.46190

TABLE B.3

Discrete-time model for PLA=53.

$$\underline{x} = \begin{bmatrix} N1 \\ N2 \\ Pb \\ Pt6 \\ Tt25sen \\ FTITsen \end{bmatrix} \qquad \Phi = \begin{bmatrix} 0.92110 & -0.04189 & 0.32002 & -0.18161 & 0.00000 & 0.00000 \\ -0.02419 & 0.86096 & 0.32969 & -0.11624 & 0.00000 & 0.00000 \\ 0.00437 & -0.00785 & 0.98843 & -0.03266 & 0.00000 & 0.00000 \\ 0.02451 & -0.02764 & 0.11370 & 0.87867 & 0.00000 & 0.00000 \\ 0.04740 & -0.01242 & 0.01025 & 0.08232 & 0.84649 & 0.00000 \\ -0.00433 & -0.03403 & 0.11931 & -0.03810 & 0.00000 & 0.98831 \end{bmatrix}$$

$$\underline{u} = \begin{bmatrix} Wf\ cmd \\ Aj \\ FIGV \\ CSV \\ Bleed \\ Pt2 \\ Tt2 \end{bmatrix} \qquad \Gamma = \begin{bmatrix} 0.00490 & 0.00276 & -0.00881 & -0.00217 & 0.08738 & -0.15751 & 0.07127 \\ 0.00517 & 0.00068 & -0.00505 & -0.01646 & 0.08765 & -0.24306 & 0.13012 \\ 0.03061 & -0.01593 & 0.00085 & -0.00236 & -0.02935 & 0.02293 & -0.00395 \\ 0.00460 & -0.05678 & 0.00266 & -0.00130 & 0.02838 & 0.01517 & 0.02094 \\ 0.00023 & -0.00267 & 0.00344 & -0.00061 & 0.00097 & -0.09123 & 0.13891 \\ 0.00183 & 0.00012 & -0.00173 & -0.00164 & 0.05905 & -0.08902 & 0.05105 \end{bmatrix}$$

	N1sen	N2sen	Pbsen	Pt6sen	Tt25sen	FTITsen	Fuel	Ajsen
	0.80126	0.27489	-0.65527	0.68394	0.00000	0.00000	0.15392	-0.04663
	0.24563	0.91236	-0.67509	0.43775	0.00000	0.00000	0.16251	-0.01149
Failure	-0.04442	0.05154	0.02369	0.12299	0.00000	0.00000	0.96208	0.26958
Directions:	-0.24895	0.18136	-0.23280	0.45693	0.00000	0.00000	0.14470	0.96072
	-0.48142	0.08148	-0.02099	-0.31000	1.00000	0.00000	0.00736	0.04517
	0.04394	0.22328	-0.24431	0.14349	0.00000	1.00000	0.05750	-0.00199
Scale factors:	1.8409	1.1894	0.37117	0.68264	1.1808	15.506	5.6985	3.0672

	FIGVsen	CSVsen	Bleed	Pt2sen	Tt2sen	Comp eff	HPT eff	LPT eff
	0.78573	0.12814	0.61068	0.49589	-0.33834	0.04132	-0.13258	0.99803
	0.45021	0.97342	0.61260	0.76523	-0.61776	0.97990	0.96065	-0.00861
Failure	-0.07576	0.13932	-0.20510	-0.07218	0.01876	0.19505	0.22982	0.04475
Directions:	-0.23751	0.07661	0.19833	-0.04776	-0.09942	0.00006	-0.05863	-0.03165
	-0.30649	0.03629	0.00676	0.28721	-0.65948	-0.00616	-0.00802	0.02911
	0.15443	0.09712	0.41272	0.28026	-0.24238	0.00285	-0.05701	-0.00092
Scale factors:	16.170	10.720	1.2669	0.57069	0.86061	1.3343	1.2542	3.4720

TABLE B.4

The angles between the failure directions.

Matrix of angles for PLA = 83:

	N1sen	N2sen	Pbsen	Pt6sen	Tt25sen	FTITsen	Fuel	Ajsen	FIGVsen	CSVsen	Bleed	Pt2sen	Tt2sen	COMPeff	HPTeff	LPTeff
N1sen	0	-67	82	-88	-50	-77	-76	-69	31	-63	-83	-69	54	-62	-59	61
N2sen	-67	0	-25	33	89	75	73	83	-82	14	34	44	-44	23	34	76
Pbsen	82	-25	0	-22	-89	-73	-79	-86	-80	-37	-19	-40	43	-46	-57	-52
Pt6sen	-88	33	-22	0	-78	75	70	69	84	43	35	61	-61	51	61	56
Tt25sen	-50	89	-89	-78	0	90	90	88	-72	89	89	60	-49	90	-90	87
FTITsen	-77	75	-73	75	90	0	86	-90	-84	84	60	74	-75	90	-86	-90
Fuel	-76	73	-79	70	90	86	0	59	-71	68	-88	-89	-83	67	66	-89
Ajsen	-69	83	-86	69	88	-90	59	0	-52	83	-85	-72	87	84	85	-83
FIGVsen	31	-82	-80	84	-72	-84	-71	-52	0	-76	77	81	83	-73	-67	42
CSVsen	-63	14	-37	43	89	84	68	83	-76	0	47	49	-48	9	20	84
Bleed	-83	34	-19	35	89	60	-88	-85	77	47	0	37	-44	56	66	55
Pt2sen	-69	44	-40	61	60	74	-89	-72	81	49	37	0	-19	54	62	61
Tt2sen	54	-44	43	-61	-49	-75	-83	87	83	-48	-44	-19	0	-53	-60	-68
COMPeff	-62	23	-46	51	90	90	67	84	-73	9	56	54	-53	0	11	-90
HPTeff	-59	34	-57	61	-90	-86	66	85	-67	20	66	62	-60	11	0	-80
LPTeff	61	76	-52	56	87	-90	-89	-83	42	84	55	61	-68	-90	-80	0

Matrix of angles for PLA = 53:

	N1sen	N2sen	Pbsen	Pt6sen	Tt25sen	FTITsen	Fuel	Ajsen	FIGVsen	CSVsen	Bleed	Pt2sen	Tt2sen	COMPeff	HPTeff	LPTeff
N1sen	0	68	-51	46	-61	86	84	-72	18	72	54	62	-84	74	82	38
N2sen	68	0	-26	46	85	72	71	80	53	15	31	24	-37	26	37	75
Pbsen	-51	-26	0	-28	-89	-70	-73	-79	-37	-38	-16	-24	41	-48	-59	-52
Pt6sen	46	46	-28	0	-72	78	67	65	42	54	36	52	-66	61	71	49
Tt25sen	-61	85	-89	-72	0	90	90	87	-72	88	90	74	-50	-90	-90	88
FTITsen	86	72	-70	78	90	0	85	-90	77	82	57	67	-71	90	-85	-90
Fuel	84	71	-73	67	90	85	0	67	83	69	82	78	-78	69	70	79
Ajsen	-72	80	-79	65	87	-90	67	0	-73	84	83	-86	-84	87	90	-86
FIGVsen	18	53	-37	42	-72	77	83	-73	0	58	39	44	-68	62	72	40
CSVsen	72	15	-38	54	88	82	69	84	58	0	46	34	-45	11	22	83
Bleed	54	31	-16	36	90	57	82	83	39	46	0	26	-43	56	67	56
Pt2sen	62	24	-24	52	74	67	78	-86	44	34	26	0	-26	42	52	61
Tt2sen	-84	-37	41	-66	-50	-71	-78	-84	-68	-45	-43	-26	0	-53	-60	-70
COMPeff	74	26	-48	61	-90	90	69	87	62	11	56	42	-53	0	12	88
HPTeff	82	37	-59	71	-90	-85	70	90	72	22	67	52	-60	12	0	-83
LPTeff	38	75	-52	49	88	-90	79	-86	40	83	56	61	-70	88	-83	0

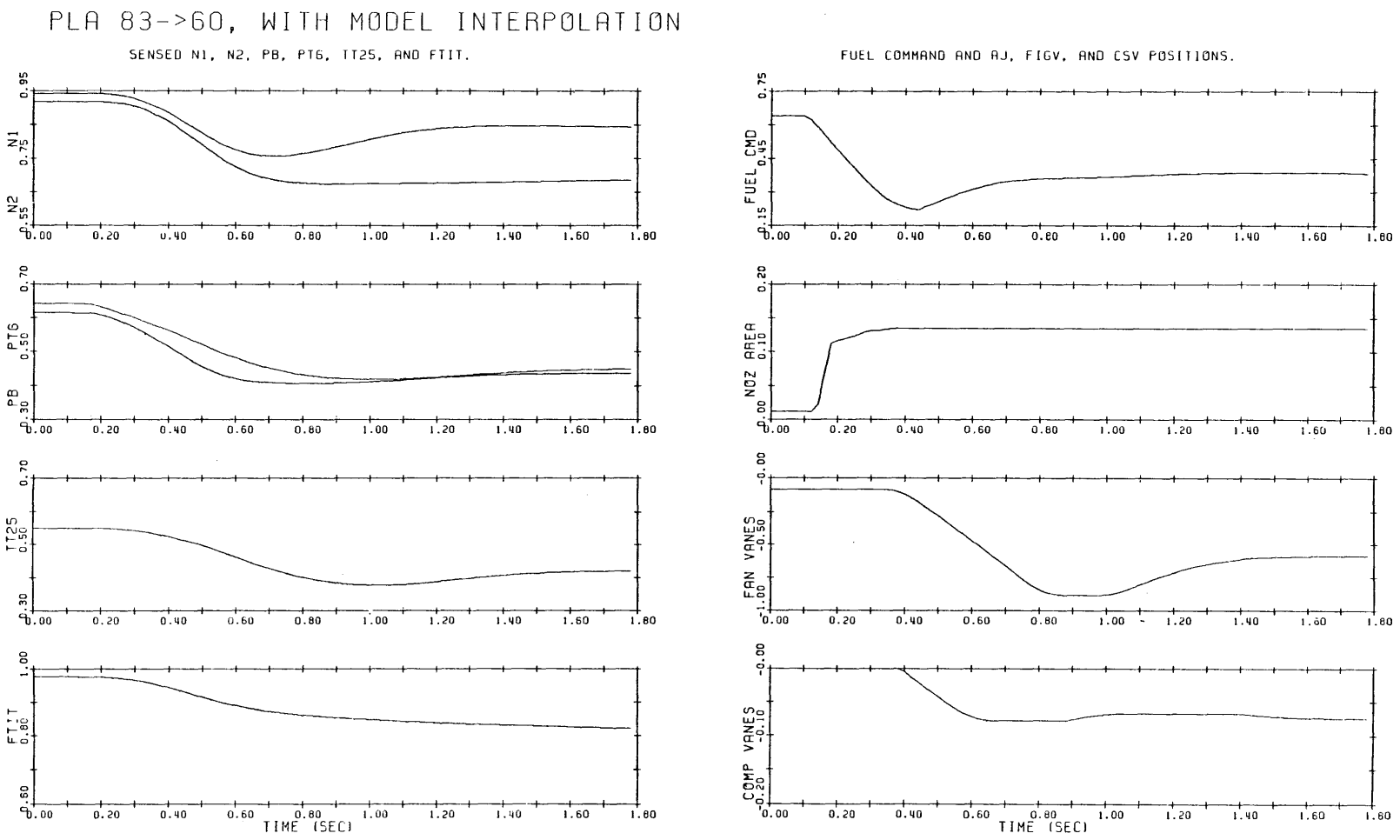

Figure B.1. Comparison of the nonlinear model and the F100 simulation for a deceleration from PLA=83° to PLA=63°. Above: response of the F100 simulation.

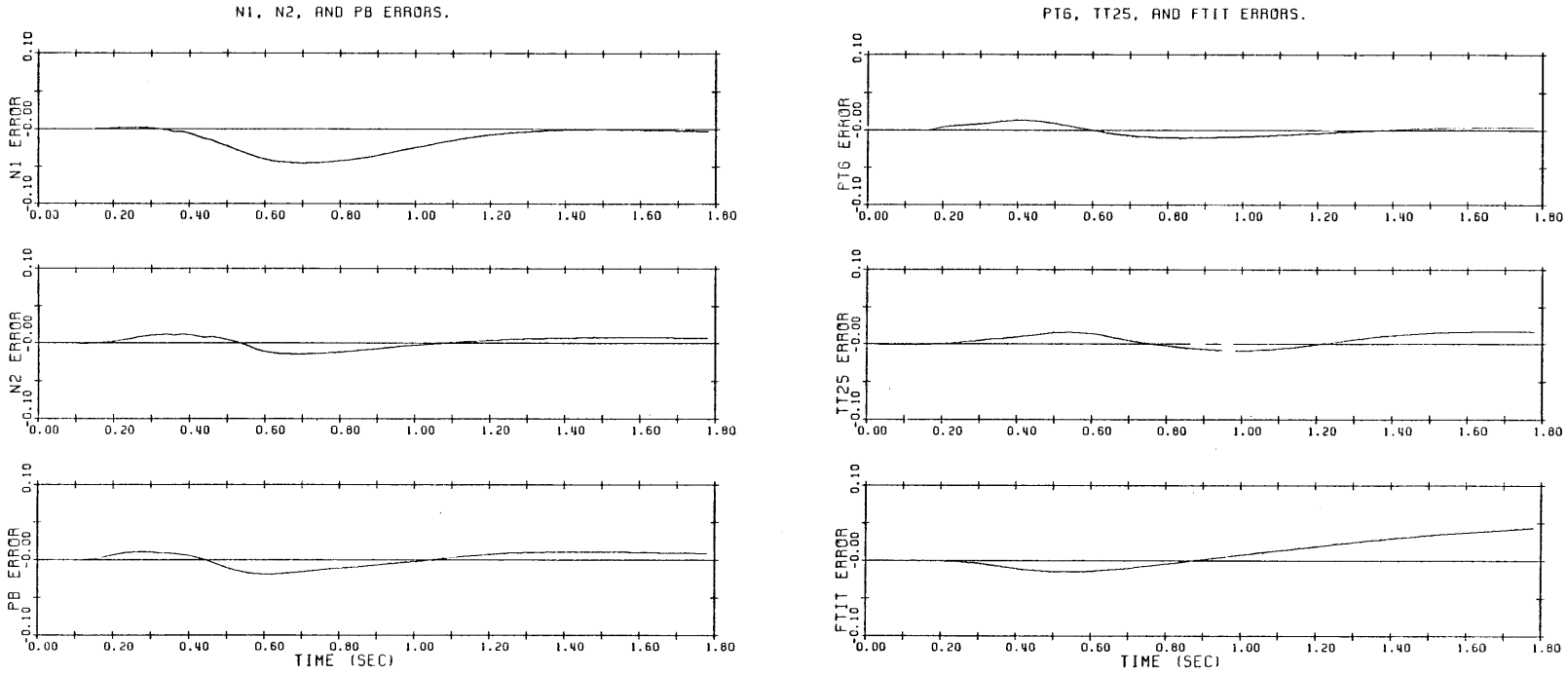

Figure B.1, continued. Differences between the responses of the F100 simluation and the model.

Appendix C

ADDITIONAL TESTS OF THE NONLINEAR FILTER

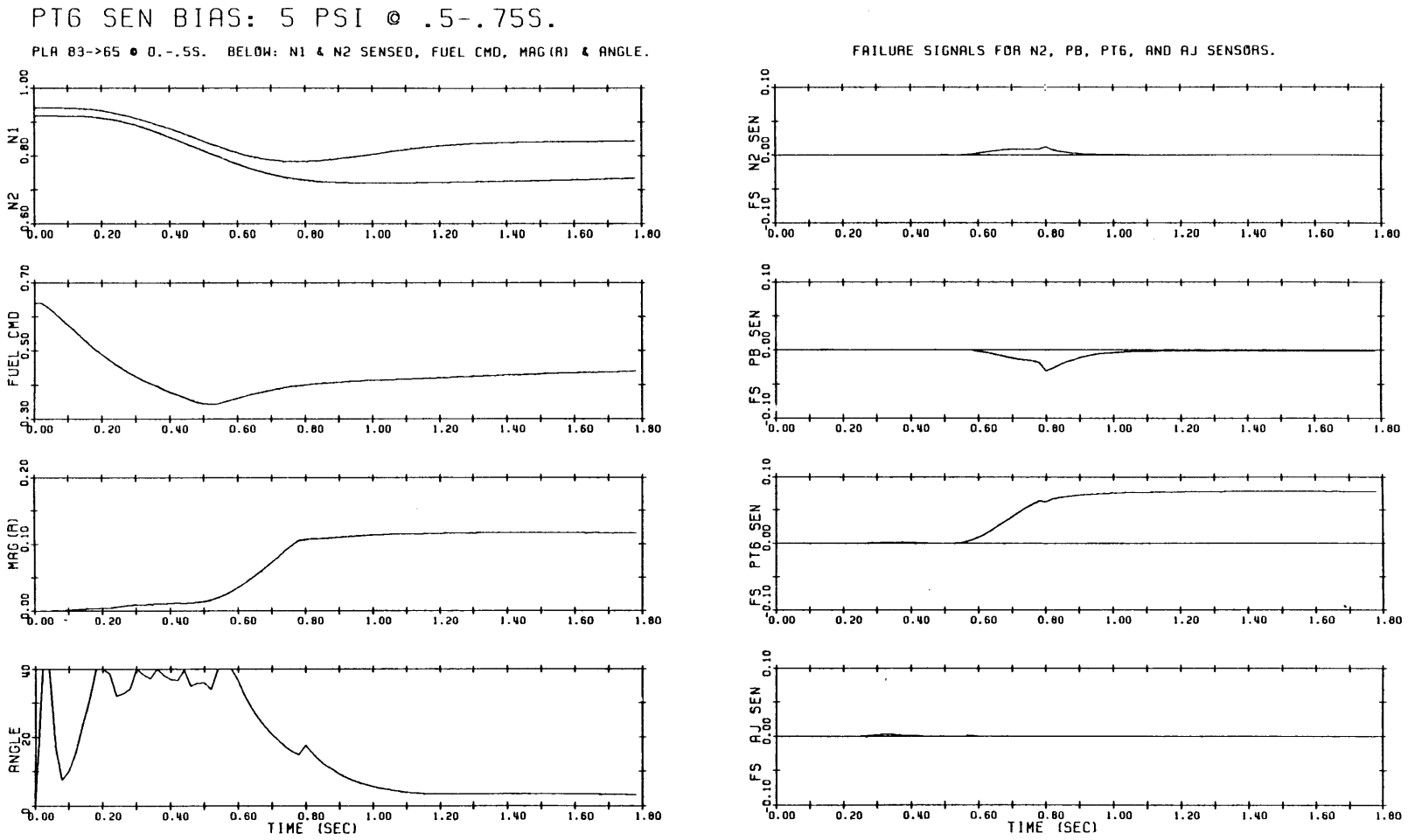

Figure C.1. Bias in the P_{t6} sensor.

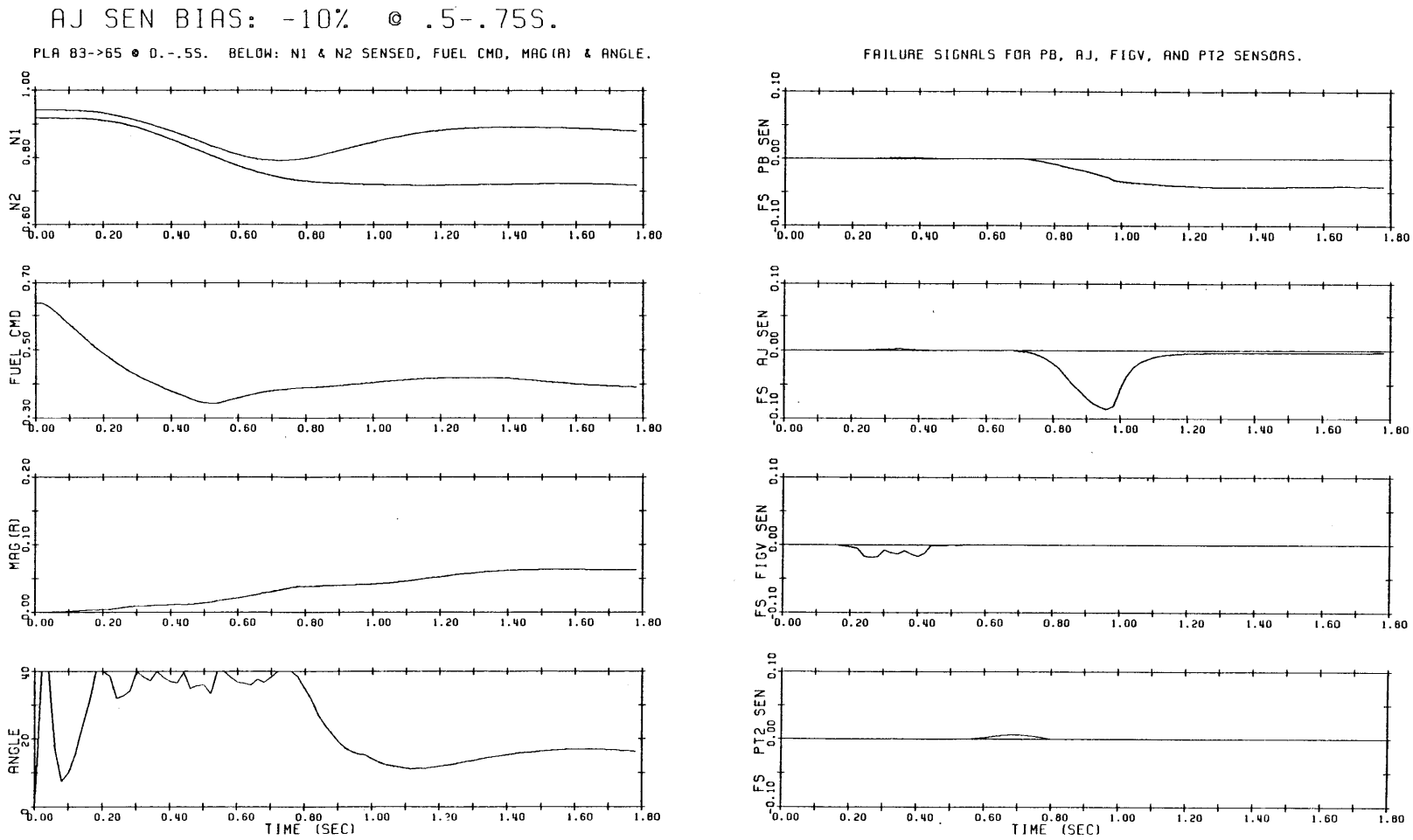

Figure C.2. Bias in the A_j sensor.

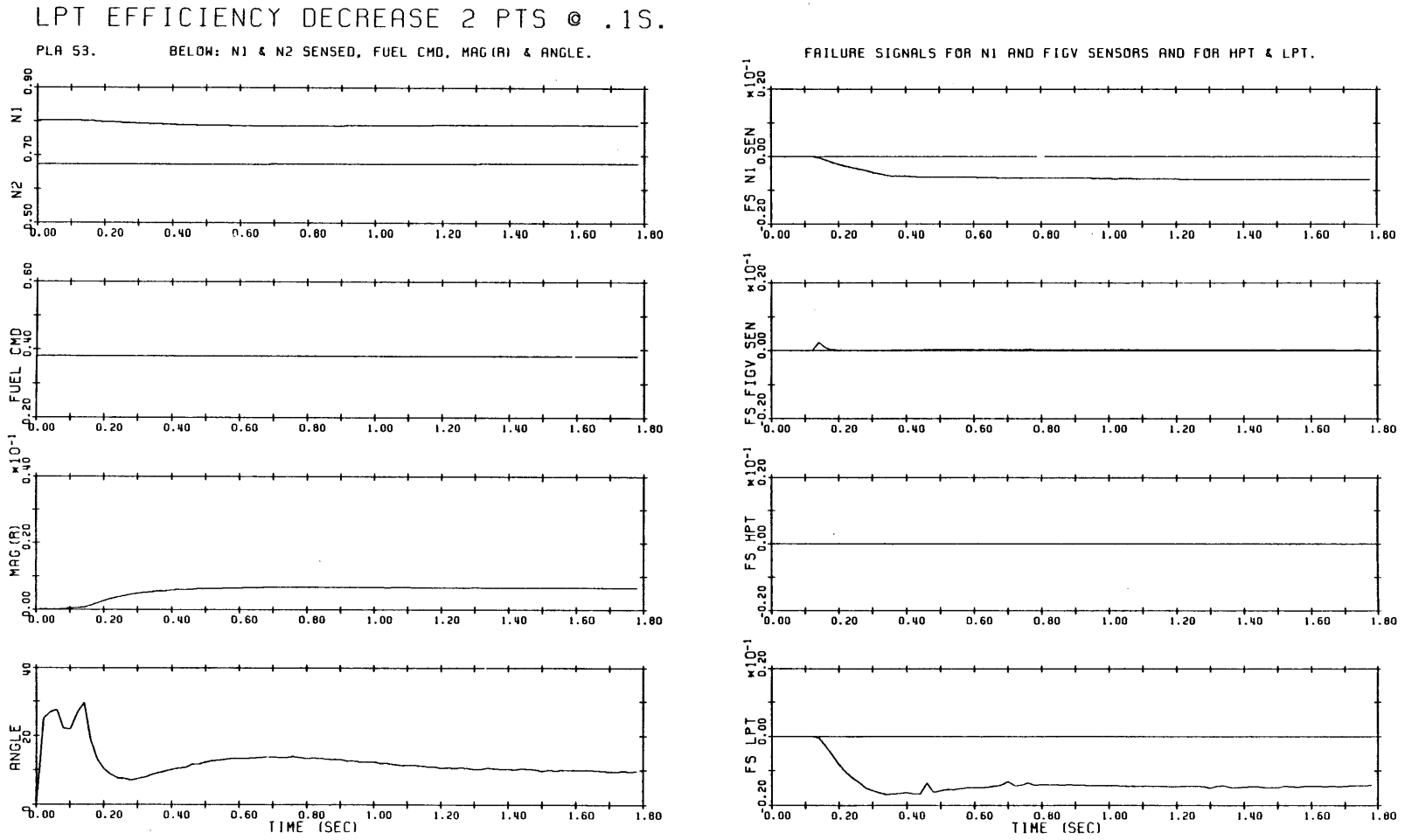

Figure C.3. Decrease in LPT efficiency.

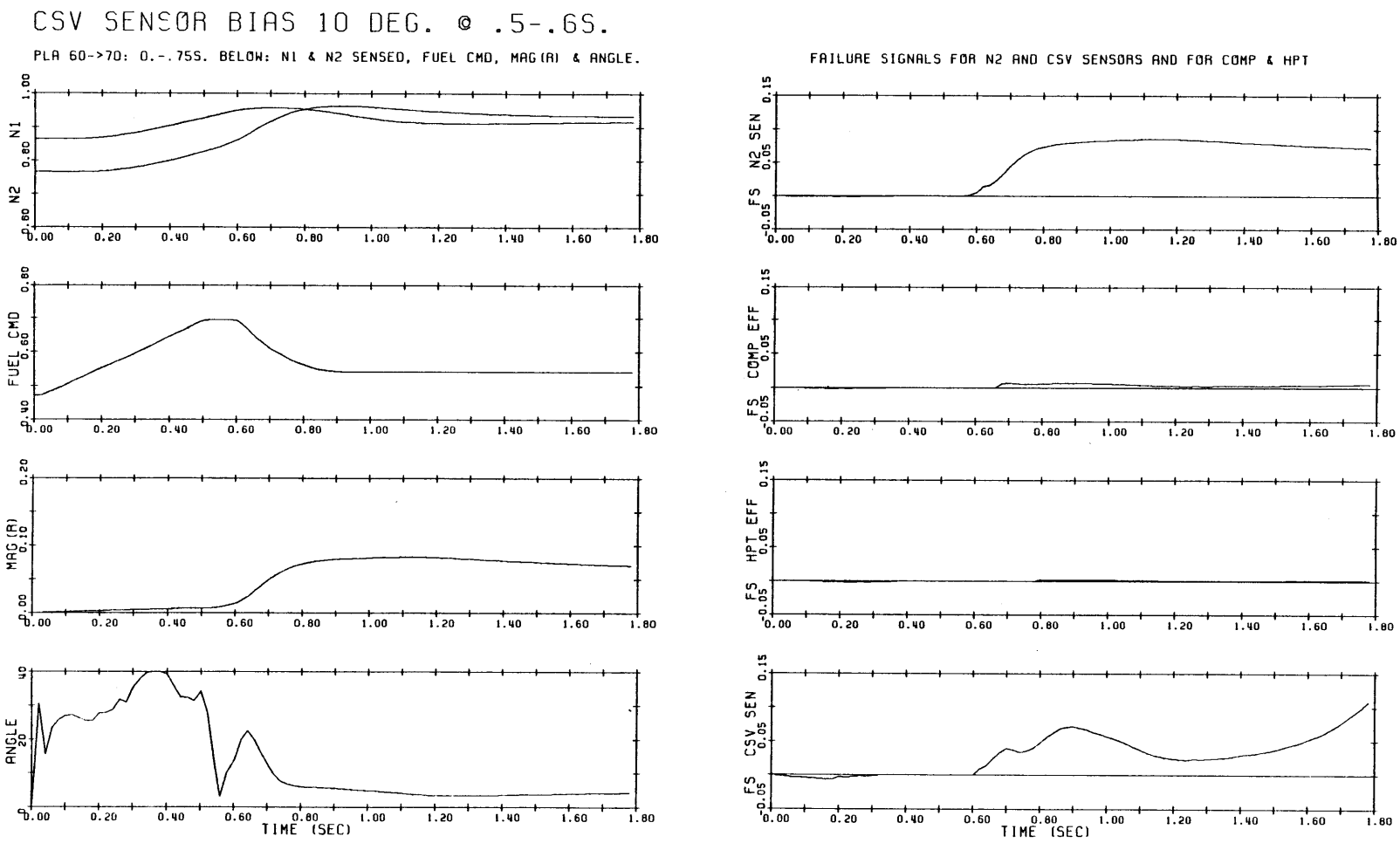

Figure C.4. Bias in the CSV sensor.

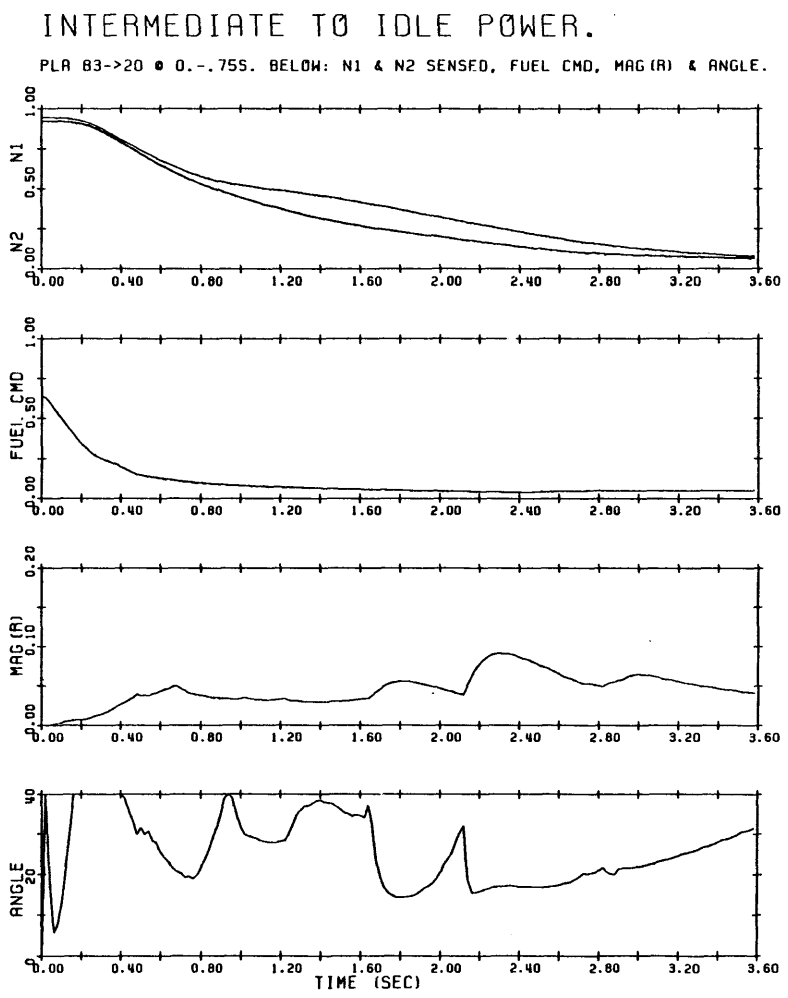

Figure C.5. Decleration from intermediate to idle without a malfunction.

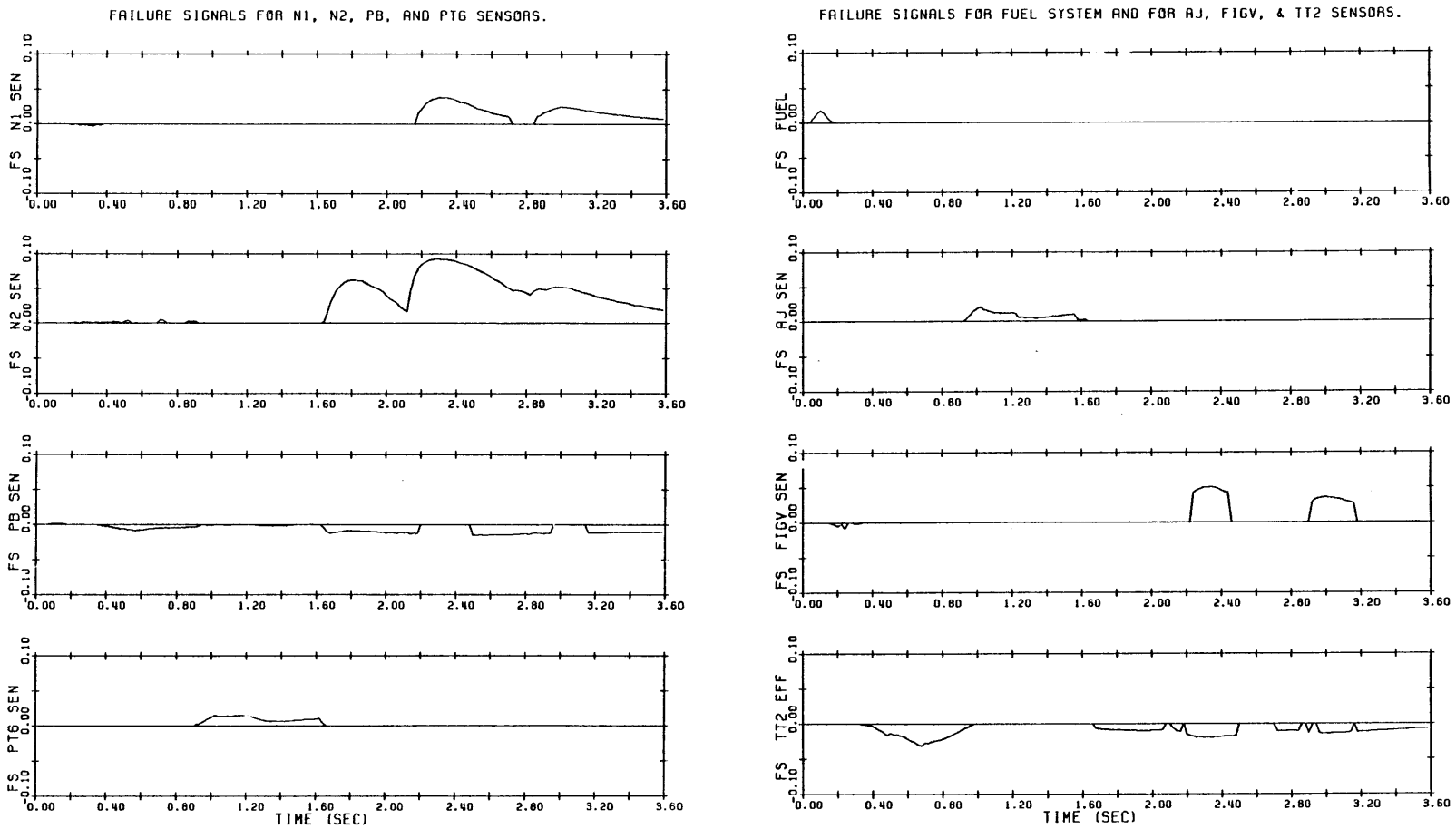

Figure C.5, continued.

BIBLIOGRAPHY

1. Adams, R.J., DeHoff, R.L. and Hall, W.E.,Jr., "Modeling and Instrumentation Requirements for Multivariable Control of an Advanced Turbofan Engine," AIAA/SAE Thirteenth Propulsion Conference, AIAA Paper 77-834, July 1977.

2. Barclay, B.A. and Richards, J.C., "Preliminary Design Overview for Variable Cycle Engine Control," AIAA/SAE Thirteenth Propulsion Conference, AIAA Paper 77-837, July 1977.

3. Barclay, B.A., Lenox, T.G. and Bosco, C.J., "Full Authority Digital Electronic Control--Highlights of Next Generation Propulsion Control Technology," ASME Paper 78-GT-165, April 1978.

4. Beard, R.V., "Failure Accommodation in Linear Systems Through Self-Reorganization," Ph.D. Thesis, Dept of Aeronautics and Astronautics, M.I.T., Cambridge, MA., February 1971.

5. Beattie, E.C., "Control Mode Studies for Advanced Variable Geometry Turbine Engines," Final report under contract F33657-73-C-0619, Report AFAPL-TR-75-7, November 1974.

6. Beattie, E.C., Carlisle, L.B., Katzer, T.J. and Spock, W.R., "Attitude Control/Engine Control Systems," Final report under contract N00019-72-C-0612, Report PWA-5275, December 1975.

7. Beattie, E.C. and Howlett, R.A., "Integrated Control Systems for Advanced Supersonic Engines," AIAA/SAE Fourteenth Propulsion Conference, AIAA Paper 78-1050, 1978.

8. Beattie, E.C. and Spock, W.R., "Application of Multivariable Optimal Control Techniques to a Variable Area Turbine Engine," Proc. 1976 Joint Automatic Control Conference, July 1976.

9. Behbehani, K. "Sensor Failure Analysis and Multivariable Control for Airbreathing Propulsion Systems," NASA Contractor Report 159791, March 1980.

10. Bentz, C.E. and Zeller, J.R., "Integrated Propulsion Control System Program," SAE Paper 730359, April 1973.

11. Burcham, F. and Batterton, P., "Flight Experience with a Digital Integrated Propulsion Control System on an F-111E Airplane," AIAA Paper 76-653, 1956.

12. Chien, T.T., "An Adaptive Technique for a Redundant-Sensor Navigation System," Draper Laboratory Report T-560, Cambridge, MA., February 1972.

13. Deckert, J.C., Desai, M.W., Deyst, J.J.,Jr. and Willsky, A.S., "Reliable Dual-Redundant Sensor Failure Detection and Identification for the NASA F-8 DFBW Aircraft," Draper Laboratory Report R-1077, Cambridge, MA., May 1977.

14. DeHoff, R.L. and Hall, W.E.,Jr., "System Identification Procedures Applied to Multivariable Control Synthesis of the F100 Turbofan Engine," Proc. of 1977 Joint Automatic Control Conference, pp.1007-1011.

15. DeMott, L.R., "TF41-A-2/A7E Inflight Engine Condition Monitoring System (IECMS)," 1978 AIAA Aircraft Systems and Technology Conference, AIAA Paper 78-1472.

16. Desai, M.N., Deckert, J.C. and Deyst, J.J,Jr., "Dual-Sensor Failure Identification Using Analytic Redundancy," J. Guidance and Control, Vol.2, No.3, May 1979.

17. Edmunds, D.B., "A Multivariable Control for a Variable Turbine Engine," USAF Report ASD-TR-77-59, August 1977.

18. Ellis, S.H., "Self-Correcting Control for a Turbofan Engine," Proc. of Third International Symposium on Air-Breathing Engines, Munich 1976; or Pratt and Whitney Aircraft Report PWA-FR-6778, 1975.

19. Gear, C.W., Numerical Initial Value Problems in Ordinary Differential Equations, Prentice-Hall, Englewood Cliffs, New Jersey, 1971.

20. Gerard, J.P., "Application of Detection Filter Theory to Longitudinal Control of Guideway Vehicles," M.S. Thesis, Dept. of Aeronautics and Astronautics, M.I.T., Cambridge, MA., June 1978.

21. Hackney, R.D., Miller, R.J. and Small, L.L., "Engine Criteria and Models for Multivariable Control System Design," Proc. of International Forum on Alternatives for Multivariable Control, National Engineering Consortium, Chicago, 1977.

22. Hildebrand, F.B., Methods of Applied Mathematics, Prentice-Hall, 1965.

23. Hrach, F.J., Arpasi, D.J. and Braton, W.M., "Design and Evaluation of a Sensor Fail-Operational Control System for a Digitally Controlled Turbofan Engine," Lewis Research Center, NASA TMX-3260.

24. Jones, H.L., "Failure Detection in Linear Systems," Ph.D. Thesis, Dept. of Aeronautics and Astronautics, M.I.T., Cambridge, MA., August 1973.

25. Kerrebrock, J.L., Aircraft Engines and Gas Turbines, MIT Press, Cambridge, MA., 1977.

26. Kwakernaak, H. and Sivan, R., Linear Optimal Control Systems, John Wiley & Sons, 1972.

27. Lampard, G.W.N. and Batka, J.J., "Development of an Integrated Propulsion Control System," AIAA Paper 75-1178, 1975.

28. LaPrad, R.F. and Beattie, E.C., "Sensor Failure Detection System Program," Monthly Progress Reports for NASA Contract NAS3-22481, Reports No. PWA5736-2 to 10, May 1980 to January 1981.

29. Lehtinen, B., DeHoff, R.L. and Hackney, R.D., "Multivariable Control Altitude Demonstration on the F100 Turbofan Engine," AIAA/SAE Fifteenth Propulsion Conference, AIAA Paper 79-1204, 1979; also J. of Guidance and Control, Vol.4, No.1, February 1981, pp.50-58.

30. Luenberger, D.G., "An Introduction to Observers," IEEE Trans. on Automatic Control, Vol.16, No.6, pp.596-602, December 1971.

31. McGlone, M.E., Davies, W.J. and Miller, R.J., "Digital Electronic Control System Reliability," Interim Report for AFAPL Contract F33615-79-C-2082, Pratt and Whitney Aircraft Report FR-13028, April 1980.

32. Merrill, W.C., "The Application of the Routh Approximation Method to Turbofan Engine Models," Proc. 1977 Joint Automatic Control Conference, pp.1019-1025.

33. Merrill, W.C., chairman, Propulsion Controls 1979, NASA Conference Publication 2137, Lewis Research Center, Cleveland, May 1979.

34. Michael, G.J. and Farrar, F.A., "Development of Optimal Control Modes for Advanced Technology Propulsion Systems," United Technologies Research Center Report N911620-2, March 1974.

35. Michael, G.J. and Farrar, F.A., "Identification of Multivariable Gas Turbine Dynamics from Stochastic Input-Output Data," ONR TR-R941620, Contract N00014-73-C-0281, March 1975.

36. Powell, M.J.D., "An Efficient Method for Finding the Minimum of a Function of Several Variables Without Calculating Derivatives," The Computer Journal, Vol.7, No.2, p.155, July 1964.

37. Rock, S.M. and DeHoff, R.L., "Variable Cycle Engine Multivariable Control Synthesis," Air Force Aero-Propulsion Lab Interim Report AFAPL-TR-79-2043, February 1979.

38. Sain, M.K., Peczkowski, J.L. and Melsa, J.L., eds., Proc. of International Forum on Alternatives for Multivariable Control, National Engineering Consortium, Chicago, October 1977; Available as a proceedings and as a book.

39. Schultz, D.G. and Melsa, J.L., State Functions and Linear Control Systems, McGraw-Hill, 1967.

40. Sellers, J.F. and Daniele, C.J., "Dyngen--A Program for Calculating Steady-State and Transient Performance of Turbojet and Turbofan Engines," NASA TN D-7901, April 1975.

41. Skira, C.A. and DeHoff, R.L., "A Practical Approach to Linear Model Analysis for Multivariable Turbine Engine Control Design," International Forum on Alternatives for Multivariable Control, 1977 Proceedings, NEC, Chicago, 1977.

42. Spang, H.A. and Corley, R.C., "Failure Detection and Correction for Turbofan Engines," General Electric Company Report 77CRD159, June 1977.

43. Szuch, J.R., "Application of Real-Time Engine Simulations to the Development of Propulsion System Controls," AIAA/SAE Eleventh Propulsion Conference, and NASA TMX-71764, September 1975.

44. Szuch, J.R., Seldner, K. and Cwynar, D.S., "Development and Verification of Real-Time, Hybrid Computer Simulation of F100-PW-100(3) Turbofan Engine," Lewis Research Center, NASA Technical Paper 1034, September 1977.

45. Szuch, J.R., Skira, C. and Soeder, J.F., "Evaluation of an F100 Multivariable Control Using a Real-Time Engine Simulation," AIAA/SAE Thirteenth Propulsion Conference, and NASA TMX-73648, July 1977.

46. Truxal, J.G., Control System Synthesis, McGraw-Hill, 1955.

47. Vander Velde, W.E., "Application of Failure Detection Filter Theory to Reliable Longitudinal Control of Guideway Vehicles," Report for U.S. Dept. of Transportation Contract No. DOT-TSC-1445, M.I.T., Cambridge, MA., March 1979.

48. Van Trees, H.L., Detection, Estimation, and Modulation Theory, Part I, John Wiley & Sons, 1971.

49. Wallhagen, R.E. and Arpasi, D.J., "Self-Teaching Digital Computer Program for Fail-Operational Control of a Turbojet Engine in a Sea-Level Test Stand," NASA TMX-3043, April 1974.

50. Weinberg, M.S. and Adams, G.R., "Low-Order Linearized Models of Turbine Engines," USAF Report ASD-TR-75-24, 1975.

51. Weinberg, M.S., "A Multi-Variable Control for a Turbofan Operating at Sea Level Static," ASME Paper 76-GT-71, or USAF Report ASD-TR-75-28, 1975.

52. Willsky, A.S., "A Survey of Design Methods for Failure Detection in Dynamic Systems," Automatica, Vol.12, 1976, pp.601-611.

BIOGRAPHY

The author was born in Englewood, NJ, and grew up in Burlington, VT. After attending Phillips Academy in Andover, MA, he went to Princeton University, where he received his Bachelor's degree in 1973. He then entered graduate school at Cornell University and obtained a Master's degree in Mechanical and Aeronautical Engineering. Subsequently he worked in research and development at Unimation, Inc. in Danbury, CT, and then matriculated at MIT. In 1980 he married Peggy Martindale, a native of Manhasset, Long Island and a graduate of Wells College in Aurora, NY. They currently live in Needham, MA.